Tellurium and selenium precipitation from copper sulphate solutions

by

Yusuf Bello

Thesis presented in partial fulfillment of the requirements
for the Degree

of

MASTER OF ENGINEERING
(CHEMICAL ENGINEERING)

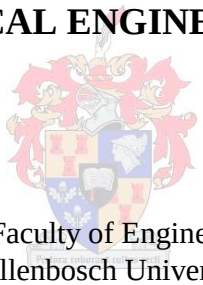

in the Faculty of Engineering
at Stellenbosch University

Supervisor:
Dr. C.Dorfling

December 2014

Declaration

By submitting this thesis electronically, I declare that the entirety of the work contained therein is my own, original work, that I am the sole author thereof (save to the extent explicitly otherwise stated), that reproduction and publication thereof by Stellenbosch University will not infringe any third party rights and that I have not previously in its entirety or in part submitted it for obtaining any qualification.

Date: November 20, 2014

Abstract

The copper sulphate leach solutions produced during the final pressure leach stages in base metal refinery processes contain low concentrations of other precious metals (OPMs, namely Rh, Ru and Ir) and impurities in addition to the base metals (BMs) of interest. Se and Te impurities, in particular, must be removed from the leach solution before it is fed to copper electrowinning because these species have adverse effects on electrowinning efficiency.

Currently, these elements are being precipitated from the leach solution with sulphurous acid. Se precipitation is satisfactory but Te removal still proves challenging. Previous studies have shown that tellurium can either be precipitated as cuprous telluride from copper sulphate solutions by reduction with sulphurous acid alone, or by the addition of SO_2 as a precipitating agent and metallic copper as an additional precipitating agent.

The objective of this study was to evaluate the effects of different process variables on Te and Se recovery in order to propose operating conditions at which increased tellurium precipitation can be achieved with minimal co-precipitation of base metals of interest (notably Cu and Ni). This would also aid in the development of a better understanding of tellurium and selenium precipitation mechanisms in $CuSO_4$-H_2SO_4 medium.

Batch precipitation tests were performed by bubbling SO_2 through an industrial $CuSO_4$ leach solution in a Buchi Polyclave Type 3 reactor with a working volume of 1 L. The temperature was varied between 65 ^oC and 95^oC for SO_2 flow rates of 4.4 cm^3/min and 5.8 cm^3/min and agitation rates of 250 rpm and 500 rpm. Metallic copper was added as powder (1g/L and 2g/L) or as plates (202.5 mm^2/L and 405 mm^2/L).

The effects of process variables on Te precipitation were similar for the tests performed without any copper addition and those with Cu plate addition. At 65^oC, better precipitation was achieved by increasing the SO_2 flow rate and decreasing the agitation speed, while copper plate addition also increased Te precipitation from 77% to 83%. Increasing the agitation speed and the SO_2 addition rate had no significant effect on the Te precipitation at 95^oC; 92% and 94% Te precipitation were obtained on average for the tests performed with and without Cu plate addition respectively.

When adding Cu in the form of powder, temperature was the only process variable that had an effect on the Te removal rate. The addition of Cu powder resulted in 93% Te precipitation

on average. It was concluded that the large specific surface area of the metallic copper in this instance allowed tellurium precipitation to proceed mainly by reaction with the added metallic copper; metallic copper formation as a result of SO_2 addition did not significantly influence the tellurium precipitation. The tellurium precipitation kinetics achieved when using copper powder as precipitation enhancing agent were noticeably faster than for the other precipitation processes.

The co-precipitation of the base metals was low at all the investigated conditions including when high Te precipitation was achieved. The optimum operating condition for tellurium recovery was determined to be: 85-95^{o}C, 4.4 cm^{3}/min SO_2 addition rate, 250 rpm agitation speed and 1 g/L copper powder addition.

A mineralogical examination of the precipitates obtained after the completion of the respective experiments, revealed the presence of amorphous structure and crystal structure in the precipitates produced from the tests conducted at 65 and 95^{o}C, respectively. The dominant phases found in the solid samples obtained include CuS, Cu_2O and Cu crystals. Cu_2(Se,Te) and OPMs were also found as minute inclusions in most of the solid samples.

Opsomming

Die kopersulfaat logingsoplossing wat gedurende die finale druklogingstadia in basis metaal raffinaderye produseer word bevat, behalwe vir die basis metale van belang, ook lae konsentrasies ander edelmetale (AEM, naamlik Rh, Ru, en Ir) sowel as onsuiwerhede. Se en Te onsuiwerhede, in die besonder, moet vanuit die logingsoplossing verwyder word voordat die oplossing na die koper elektrowinning gevoer word omdat hierdie spesies negatiewe effekte op die elektrowinning effektiwiteit het.

Hierdie elemente word tans met swaweligsuur vanuit die logingsoplossing gepresipiteer. Se presipitasie is voldoende, maar die Te verwydering bly steeds problematies. Vorige studies het getoon dat tellurium as kuprotelluried vanuit kopersulfaat oplossings presipiteer kan word deur middel van reduksie met swaweligsuur alleen, of met die byvoeging van SO_2 as presipiteermiddel en metallieke koper as addisionele presipiteermiddel.

Die doelwit van hierdie studie was om die effekte van verskillende prosesveranderlikes op Te en Se presipitasie te ondersoek ten einde bedryfstoestande voor te stel wat verbeterde tellurium presipitasie toelaat met minimale kopresipitasie van basis metale van belang (hoofsaaklik Cu en Ni). Dit sal ook bydra tot die ontwikkeling van ’n beter begrip van die tellurium en selenium presipitasie meganisme in ’n $CuSO_4$-H_2SO_4 medium.

Enkellading presipitasie toetse is uitgevoer deur SO_2 deur ’n industriële $CuSO_4$ logingsoplossing te borrel in ’n Buchi Polyclave Tipe 3 reaktor met ’n bedryfsvolume van 1 L. Die temperatuur is tussen 65°C en 95°C gevarieer vir SO_2 vloeitempo’s van 4.4 cm^3/min en 5.8 cm^3/min en roerdertempo’s van 250 rpm en 500 rpm. Metallieke koper is as poeier (1 g/L en 2 g/L) of as plate (202.5 mm^2/L en 405 mm^2/L) bygevoeg.

Die effekte van prosesveranderlikes op Te presipitasie was soortgelyk vir die toetse wat uitgevoer is sonder enige koper byvoeging en die toetse waartydens koper plate bygevoeg is. By 65°C is beter presipitasie behaal deur die SO_2 vloeitempo te verhoog en die roerdertempo te verlaag, terwyl die byvoeging van Cu plate ook die Te presipitasie van 77% na 83% laat toeneem het. Veranderinge in die roerderspoed en die SO_2 vloeitempo het geen effek op Te presipitasie gehad vir toetse wat by 95°C uitgevoer is nie. By hierdie temperatuur is gemiddelde Te presipitasie van 92% en 94% behaal vir die toetse wat uitgevoer is met die byvoeging van Cu plaat en sonder enige Cu byvoeging, onderskeidelik.

Toe Cu in die vorm van poeier bygevoeg is, was temperatuur die enigste prosesveranderlike wat ŉ effek op die Te presipitasietempo gehad het. Die byvoeging van Cu poeier het ŉ gemiddelde Te presipitasie van 93% tot gevolg gehad. Daar is afgelei dat die groot spesifieke oppervlak van die metallieke koper in hierdie geval toegelaat het dat tellurium presipitasie hoofsaaklik deur reaksie met die bygevoegde metallieke koper verloop; metallieke koper formasie as gevolg van SO_2 byvoeging het nie die tellurium presipitasie beduidend beïnvloed nie. Die tellurium presipitasie kinetika was beduidend vinniger vir die proses waar koper poeier as presipitasie verbeteringsagent gebruik is as vir die ander presipitasie prosesse.

Die kopresipitasie van die basis metale was laag by al die toestande wat ondersoek is, insluitend die toestande waar hoë Te presipitasie behaal is. Die volgende toestande is as optimaal vir tellurium presipitasie bepaal: 85-95°C, 4.4 cm^3/min SO_2 voertempo, 250 rpm roerderspoed, en 1 g/L koper poeier byvoeging.

Mineralogiese analises het in die algemeen getoon dat die presipitaat wat by 65°C gevorm het ‘n amorfe struktuur het, terwyl die presipitaat wat tydens toetse by 95°C gevorm het oor meer kristallyne eienskappe beskik. Die dominante fases wat in die vastestof monsters gevind is sluit CuS, Cu_2O, en Cu kristalle in. $Cu_2(Se,Te)$ en AEM is ook as klein insluitings in die meerderheid vastestof monsters gevind.

Acknowledgements

First and foremost, I am very grateful to my creator Allah (SWT) for the support that I received from Him while I was working on this project. I am also grateful to my parents (the Bello family) for their encouragement.

To my love Kenny, for her support.

To my supervisor Dr. Christie Dorfling, for his mentorship and guidance since I began this project up to this moment.

To Lonmin group, for its financial and material support.

To the Department of Processs Engineering, for providing the platform for this research.

To all the staff of the Department of Process Engineering, for their contributions in one way or the other towards the successful completion of this project.

Thank you all for the love and support that I received from you. I love you all.

Table of contents

List of figures

List of tables

Chapter 1 : Introduction

1.1. Background

The Western Platinum Ltd. Base Metals Refinery (BMR) employs a hydrometallurgical process route for the treatment of platinum group metal (PGM) bearing Ni-Cu converter matte. The BMR process aims to selectively remove and recover base metals from the converter matte to produce a PGM-rich solid residue suitable for PGM refining in downstream processes. The hydrometallurgical process achieves this aim by multiple leaching stages, as illustrated in figure 1.1.

Converter matte is milled before being fed to the first stage atmospheric leach for the dissolution of nickel and the precipitation of copper and PGMs. Leaching occurs in the presence of oxygen and at a temperature of 85-90^{o}C (Bircumshaw, 2008; Lamya, 2007). The slurry is fed to a thickener that yields a nickel sulphate leach solution from which $NiSO_4.6H_2O$ crystals are produced, while the underflow slurry is fed to the second and third stage pressure leach in a horizontal autoclave where most of the remaining Ni and Cu are dissolved (Lamya, 2007). Leaching is achieved at an operating condition of 6 bar and 115-140^{o}C.

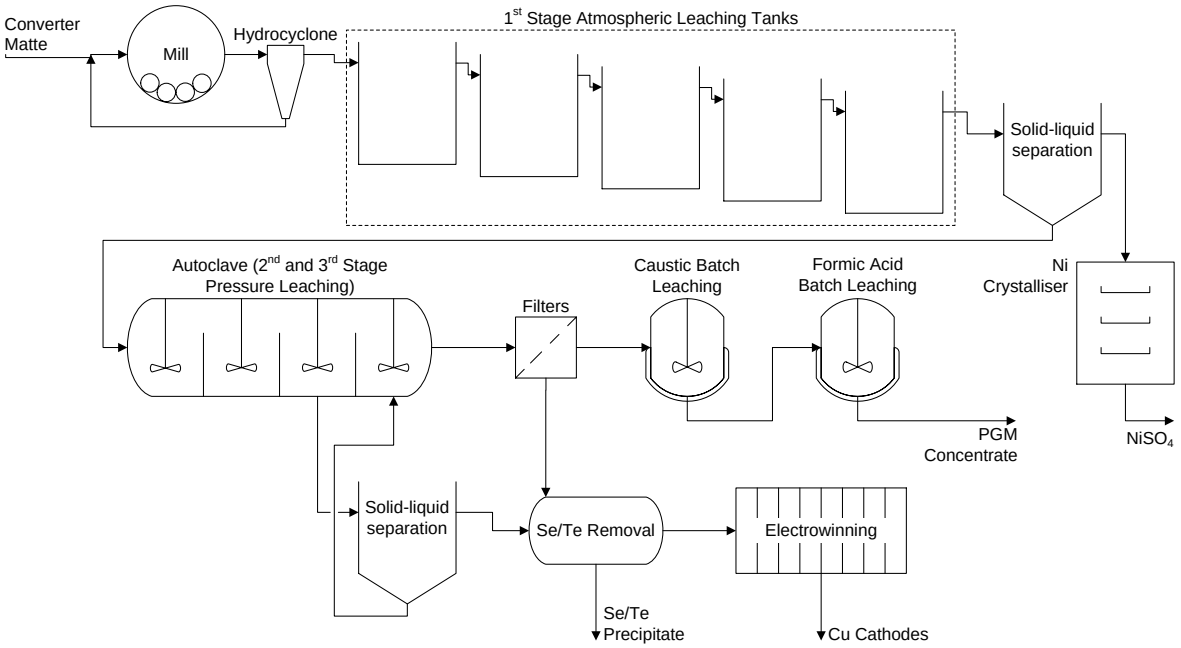

Figure 1.1: Process flow diagram of a typical base metal refinery process showing Se/Te removal section (Redrawn from (Bircumshaw, 2007))

The slurry from the pressure leach is sent to a separation unit where solid residue is separated from the copper sulphate leach solution. The solid residue is sent to a high pressure caustic leaching process to upgrade the PGM residue, where after it is sent to a formic acid leaching process to dissolve the remaining nickel and iron left in PGM concentrate (Bircumshaw, 2008). The copper sulphate leach solution recovered as filtrate is sent to the selenium removal section where selenium and tellurium impurities are precipitated using sulphurous acid as precipitation reagent. The solution from the selenium removal section is fed to copper electrowinning for the recovery of copper as copper cathodes.

Dissolved Te and Se impurities, other precious metals and base metals are the species commonly found in the $CuSO_4$-H_2SO_4 electrolyte. These species are passed from the selenium removal section to copper electrowinning. The maximum concentration of selenium and tellurium permissible in the solution fed to Cu-electrowinning is at most 1 mg/L (Weir *et al*., 1980).

1.2. Problem statement

The presence of selenium and tellurium impurities in the pregnant leach solution being sent to copper electrowinning has an adverse effect on the electrowinning performance and copper cathode quality. Therefore, these species must be removed from the leach solution prior to electrowinning. This is currently achieved by precipitating Se and Te with sulphurous acid in the selenium removal section. The current process configuration guarantees the reduction of selenium concentration in the copper sulphate solution to 1 mg/L, but Te removal by precipitation still remains problematic.

1.3. Objectives and research questions

The primary objective of this study is to evaluate the effects of the key operating variables on selenium and tellurium precipitation from a copper sulphate leach solution, so as to maximise Te precipitation while minimising the co-precipitation of base metals of interest.

The research questions which were identified include:

- What are the various process routes for Te and Se precipitation from aqueous copper sulphate solutions?
- What process variables influence Te and Se precipitation from the pregnant copper sulphate leach solution?
- What are the effects of these factors on the precipitation behaviour of the base and precious metals, and what information about the precipitation reactions can be derived from the observed effects?

- What effects do the process variables have on the characteristics of precipitates produced during tellurium and selenium precipitation?
- At what operating conditions will optimal Te and Se precipitation be achieved?

Attempting to find an entirely new process route for high Te and Se recovery from acidic copper sulphate leach solutions falls outside the scope of this research.

1.4. Thesis layout

Section 2.1 focuses on the explanation of precipitation theory and concepts which is followed by the discussion of the various types of precipitation typically found in hydrometallurgical operations (section 2.2). The properties of selenium and tellurium are reviewed in section 2.3 which leads to an overview of the different methods of Te and Se precipitation found in the literature. The effects of tellurium precipitation on other precious metals and base metals are presented in sections 2.5 and 2.6, respectively.

The information regarding the most important process variables presented in the literature review was used to plan the experimental work; details about the experimental design, equipment, and experimental procedure are provided in section 3. The results and discussion that summarized the work done are given in section 4. This includes the statistical analysis of the experimental data and the characterization of the precipitates.

The appendices include: sample calculations (Appendix A), experimental design (Appendix B), operating procedures (Appendix C), experimental data (Appendix D), statistical data (Appendix E), and supplementary experimental data (Appendix F). The repeatability analysis of the experiments performed and the nomenclature are also presented in appendix G and H, respectively, while appendix I summarizes the publications originating from this project.

Chapter 2 : Literature Review

2.1. Precipitation theory

Precipitation can be best described as reactive crystallization (Demopoulos, 2009; Sohnel and Garside, 1992). This concept is more acceptable than the conventional definition that emphasizes the removal of metal ions during precipitation reactions, because it stresses the creation of solid species by a chemical reaction (Demopoulos, 2009). Precipitation, in essence, is the crystallization of sparingly soluble species from aqueous solutions (Sohnel and Garside, 1992).

It has been shown that a solid precipitates out of the solution by the principle of crystallization thermodynamics if the following conditions are met (Demopoulos, 2009; Mohan and Myerson, 2002):

$$\Delta G = -RT\ln (a/ a_o) < 0 \qquad (2.1)$$

Where ΔG is the change in molar Gibbs free energy during crystal formation, R is the universal gas constant, T is the absolute temperature, a is the activity of solute at a given temperature, and a_o is the activity of solute in solution under equilibrium . The term a/a_o represents the saturation ratio denoted by S (Demopoulos, 2009).

On assumption of ideal solution, the activity of solute will be approximately equal to the concentration of solute (Sohnel and Garside, 1992). Under this condition:

$$S = a / a_o \approx C/C_{eq} \qquad (2.2)$$

Where C is the solute concentration, and C_{eq} is the equilibrium solubility. An ideal solution is a solution in which there is no interaction between the solvent and the solute. The relationship between an ideal and a real solution is given as (Sohnel and Garside, 1992):

$$a = C\gamma \qquad (2.3)$$

Where γ is the activity coefficient (a term that represents a departure from an ideal condition)

The value of ΔG will be negative (i.e. $\Delta G < 0$), if S is greater than unity ($S > 1$, $a > a_o$ or $C > C_{eq}$). This is the condition that must be fulfilled for a solution to become supersaturated (Demopoulos, 2009). The supersaturation ratio is given as:

$$(C- C_{eq})/ C_{eq} = (S – 1) = S_p \qquad (2.4)$$

From this analysis, it can be inferred that supersaturation is the driving force of every crystallisation process (Demopoulos, 2009). However, this analysis only holds for precipitation that does not

require a chemical reaction. If a chemical reaction is involved, then the saturation ratio should be expressed as a function of the solute concentration and the solubility product, K_{sp} (Dirksen and Ring, 1991).

$$A_{(aq)} + B_{(aq)} \rightarrow AB_{(s)} \quad (2.5)$$

For a chemical reaction described by equation 2.5, the saturation ratio is given by (Demopoulos, 2009):

$$S = \frac{[A][B]}{Ksp} \quad (2.6)$$

Mangere *et al*. (2010) also proposed equation 2.7 for the dissociation of Cu_2Se in acidic copper sulphate solution at 95^{o}C, and equation 2.8 as a relationship between the solubility product of Cu_2Se and the reacting species present in the solution.

$$Cu_2Se = 2Cu^{+}(aq) + Se^{2-}(aq) \quad (2.7)$$

$$K_{sp} = [Cu^{+}]^2[Se^{2-}] = \exp(-\Delta G/RT) \quad (2.8)$$

Where:

$K_{sp} = 10^{-57.7}$ while ΔG^{o} refers to the change in Gibbs free energy of reaction.

However, the precipitation of a solid product from an aqueous solution usually occurs in a stepwise process. For this reason, the next section of this study was devoted to exploring the different mechanisms of precipitation in an aqueous medium.

2.1.1. Mechanism of precipitation

The first step in a precipitation process is the establishment of a supersaturated condition which determines the precipitation rate. This is immediately followed by the nucleation of particles that result in the formation and growth of crystals, which later become visible in size, and eventually precipitate out of the solution as solids (Mullin, 1993; Sohnel and Garside, 1992).

The steps which are common to every precipitation reaction, irrespective of types, are illustrated in figure 2.1. They can occur in series, or in parallel, depending on the peculiarity of the precipitation process (Sohnel and Garside, 1992).

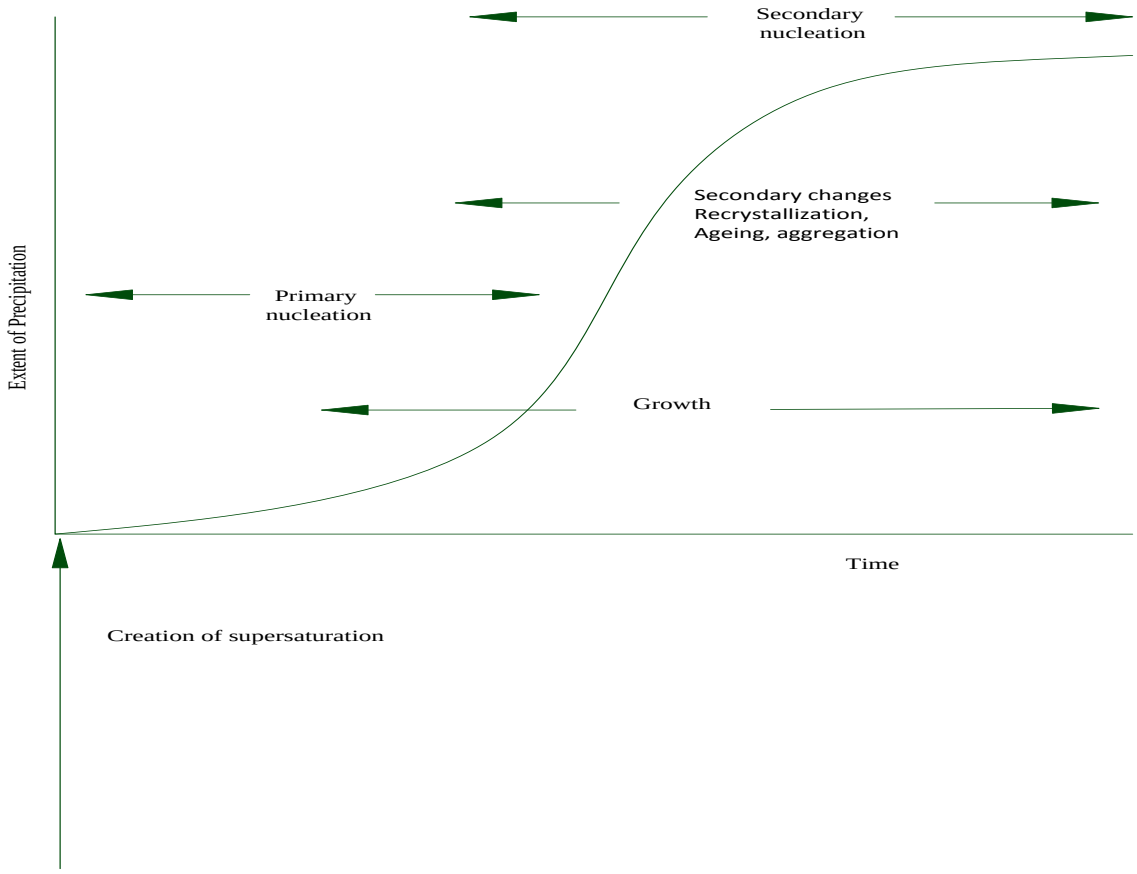

Figure 2.1: Diagrammatic illustration of steps involved in a typical precipitation process (Redrawn from Sohnel and Garside, 1992)

2.1.2. Nucleation process

Nucleation is the formation of nuclei of particles. This precipitation step usually precedes the growth of crystals. There are different nucleation mechanisms, depending on reaction conditions and the system physical properties (Sohnel and Garside, 1992).

The three major ones are:

- Homogenous nucleation that is described as the primary creation of a nucleus of a precipitating species without the presence of a surface.
- Heterogeneous nucleation that involves the primary creation of a nucleus of a precipitating species on a foreign surface.
- Surface nucleation which is described as the secondary creation of a nucleus of a precipitating species on the surface of that species itself (Dirksen and Ring, 1991; Sohnel and Garside, 1992).

The time interval between the onset of supersaturation and the detection of first crystals of the solid product formed is known as the induction period (Mullin, 1993).

2.1.3. Crystal growth

Crystal growth can be described as the speed with which a specified surface is displaced perpendicularly to the crystal face (Sohnel and Garside, 1992). The crucial steps involved in the growth of crystals during a reactive crystallization include (Dirksen and Ring, 1991):

- The migration of dissolved species onto the crystal surface from the bulk solution
- The adsorption of species onto the crystal face
- The diffusion of species over the crystal surface
- Surface reaction
- The diffusion of crystallizing species from the surface
- The release of heat of crystallization

Among these steps, the surface reaction and the migration of solute onto the crystal surface play the most crucial roles during crystal growth. The transport of solute onto the crystal surface can be achieved either by convection or diffusion or by both processes. If the rate of surface reaction is faster than the migration of dissolved species, the crystal growth rate will be governed by the mass transport mechanism. In contrast, if the rate of surface reaction is slower than the migration of dissolved species, then the rate of growth of crystals will be determined by the surface reaction (Sohnel and Garside, 1992).

Additionally, temperature and agitation are the two principal parameters that influence the rate of crystal growth and the morphology of precipitates produced during precipitation processes. The rate of crystal growth, for example, is usually governed by the mass transport mechanism at an elevated temperature while the surface reaction governs the growth of crystal at relatively low temperature condition (Sohnel and Garside, 1992).

It has also been established that high temperature speeds up the rate of crystallization, and that precipitates consisting of crystal structures are typically produced at an elevated temperature. However, amorphous structures are typically found in precipitates obtained from precipitation reactions carried out at low temperature condition (Demopoulos, 2009).

On the other hand, improved agitation reduces induction time and speeds up particle formation thereby promoting crystal growth. It has also been established that agitated solutions usually produce much larger crystals than solutions left unstirred (Sohnel and Garside, 1992).

Recent studies have also shown that selenium can be precipitated as either amorphous or crystalline solid product depending on the reagent used and the temperature involved in the precipitation process. It was found that when selenium was precipitated from aqueous solution using SO_2 at 84^{o}C, amorphous selenium precipitates were first noticed prior to the occurrence of more stable crystals of selenium atoms (Haranczyk *et al*., 2002). No literature currently explores the effects of these process variables on the morphology and crystallinity of tellurium precipitates.

2.2. Types of precipitation

2.2.1. Physical precipitation

Physical precipitation does not involve the addition of reagent to bring about precipitation. It is otherwise known as crystallization. Crystals are usually produced at a specific temperature and concentration depending on the salt being precipitated (Habashi, 1999; Sohnel and Garside, 1992). These crystals are characterized by water of crystallization. Since a reducing agent is required for tellurium and selenium precipitation from the copper sulphate medium, physical precipitation will not be suitable for this operation (Wang *et al*., 2003).

Apart from this, the crystallization process of physical precipitation method does not involve chemical reaction (Habashi, 1999; Sohnel and Garside, 1992), while chemical reactions are required (Jennings *et al.*, 1969) to bring about the crystallization which results in tellurium and selenium precipitation.

2.2.2. Chemical precipitation

Chemical precipitation involves the use of a suitable reagent to effect precipitation. This precipitation method can be divided into ionic precipitation, hydrolysis, substitution and reduction (Habashi, 1999).

2.2.2.1. Ionic precipitation

Ionic precipitation involves the reaction between cations and anions to form chemical compounds. Reaction 2.9 describes ionic precipitation in aqueous solution (Habashi, 1999).

$$yM^{x+} + xA^{y-} \rightarrow M_yA_x \qquad (2.9)$$

A typical example of ionic precipitation can be found in the precipitation of copper sulphide from cupric and sulphide ions. This precipitation reaction is given as (Habashi, 1999; Lewis, 2010):

$$Cu^{2+} + S^{2-} \rightarrow CuS \quad (2.10)$$

2.2.2.2. Hydrolysis

This kind of precipitation is typically employed in the removal of metals as oxides, hydroxides or hydrated salts. The hydrolysis of metal ion to form its hydroxide is given by (Habashi, 1999).

$$M^{x+} + xH_2O^{-} \rightarrow M(OH)_x + xH^{+} \quad (2.11)$$

No literature that describes tellurium and selenium precipitation by hydrolysis could be found.

2.2.2.3. Substitution

Here, metal ions of interest are extracted from aqueous medium with the use of organic solvents. This type of precipitation is represented by the following equations (Habashi, 1999):

$$H_2(g) = H_2(org) \quad (2.12)$$

$$RM\ (org) + H_2(org) \rightarrow RH_2(org) + M(s) \quad (2.13)$$

Where:

RM represents organic solvent

M represents a divalent metal

M(s) is the metal extracted from the organic solvent.

To the author's knowledge, no literature that describes the extraction of tellurium and selenium with organic solvent is available.

2.2.2.4. Reduction

Reduction is a type of precipitation that involves a redox reaction. This precipitation method can be divided into homogenous and heterogeneous reduction (Habashi, 1999; Jackson, 1986).

a. Homogeneous reduction

Homogenous reduction requires the addition of a reducing agent for the removal of dissolved species from aqueous medium. This reducing agent can be either ionic or non-ionic.

i. Homogeneous reduction involving ionic reducing agent

Homogenous reduction involving an ionic reducing agent is given by equation 2.14 (Habashi, 1999; Jackson, 1986):

M^{x+} + Reduced species → M + Oxidized species (2.14)

Where:

M represents the metal

M^{x+} represents the metal ion in solution

A typical example of homogenous reduction where an ionic reducing agent is used is the removal of selenium from H_2SeO_3 with sulphite ion (Wang *et al.*, 2003). Here, SO_2 dissolves in water to produce SO_3^{2-} (sulphite ion) which acts as ionic reducing agent in aqueous solution. The formation of sulphite is given by (Habashi, 1999):

$SO_2 + H_2O \rightarrow H_2SO_3 \rightarrow SO_3^{2-} + 2H^+$ (2.15)

The application of this type of precipitation to this study is discussed extensively in section 2.4.2.

ii. Homogeneous reduction involving non-ionic reducing agent

Homogenous reduction involving non-ionic reducing agent, on the other hand, is often represented as (Habashi, 1999; Jackson, 1986):

$M^{n+} + ne^- \rightarrow M$ (2.16)

The examples of non-ionic reducing agents include: hydrogen, carbon monoxide and hydrazine (Habashi, 1999;). For this study, no non-ionic reducing agent was found suitable for the removal of tellurium and selenium species from the copper sulphate solution. The selection criteria adopted in this study for choosing the reducing agents used for the precipitation of Se and Te impurities from the solution are discussed in section 2.4.

b. Heterogeneous reduction

Heterogeneous reduction involves electron transfer on the surface of solid in solution of its salt containing other ions (Habashi, 1999; Jackson, 1986). This precipitation method can be divided into electrochemical and electrolytic reduction.

i. Electrochemical reduction

Here, the solid (usually more reactive than other metal ions in the solution) acts as a reducing agent. The general form of electrochemical reduction is given as (Habashi, 1999; Jackson, 1986):

$M^{n+} + X \rightarrow M + X^{n+}$ (2.17)

Where:

M in this case represents the less reactive metal displaced from aqueous solution.

X represents the more reactive metal

n^+ stands for the valence state of those metals involved in reduction reaction

An example of electrochemical reduction is the displacement of copper by iron in copper sulphate solution. This reduction reaction is given by (Habashi, 1999; Jackson, 1986):

$$Cu^{2+} + Fe \rightarrow Cu + Fe^{2+} \quad (2.18)$$

ii. Electrolytic reduction

This involves the recovery of metal from its aqueous solution by the passage of direct current into the solution. This type of reduction is given by equation 2.19 (Habashi, 1999; Jackson, 1986; Schlesinger *et al*., 2011), and is usually employed during the electrowinning of copper (Schlesinger *et al*., 2011).

$$M^{x+} + xe^- \rightarrow M \quad (2.19)$$

Where:

M represents the metal removed from aqueous medium and x^+ represents the valence state of the metal in the solution prior to reduction

c. Cementation reactions

This involves the reduction of ions by a different metal on the interface of that metal (Jackson, 1986). A typical example of this type of precipitation is described in section 2.4.2, where the reduction of tellurium ions by cementation on the sufaces of metallic copper is discussed.

d. Disproportionation reactions

This is a special case of reduction that occurs when a metal ion acts as both an oxidizing agent and a reducing agent in aqueous medium (Habashi, 1999; Jackson, 1986). A typical example is the disproportionation of cuprous ion. Here, cuprous ion donates an electron and become oxidized to cupric ion while accepting an electron to become reduced to elemental copper (Habashi, 1999; Wang *et al.*, 2003). The reactions that describe the disproportionation of cuprous are provided in section 2.4.1, where this type of precipitation is further discussed.

Figure 2.2 shows the different types of precipitation which can be found in hydrometallurgical operations. The understanding of the properties of Se and Te is often exploited to suggest suitable reducing agents for the precipitation of these impurities from the solutions containing them. For this reason, the next section was devoted to exploring the properties of selenium and tellurium species in aqueous medium.

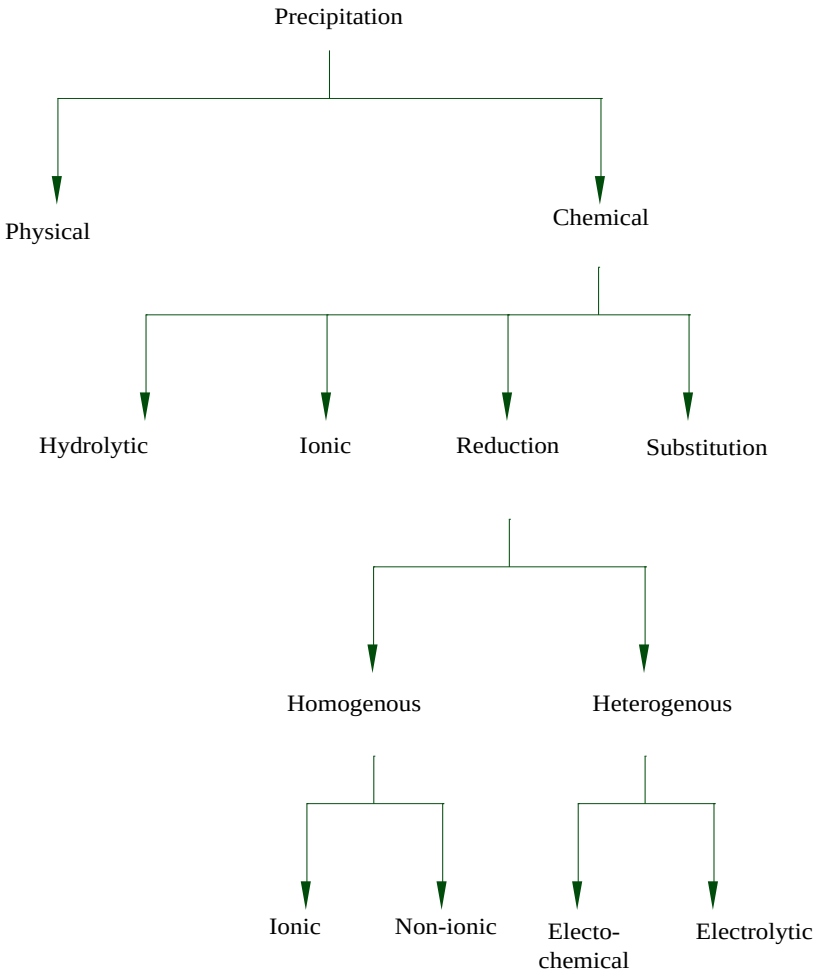

Figure 2.2: Different types of precipitation employed in hydrometallurgical operations (Redrawn from Habashi (1999))

2.3. Properties of selenium and tellurium

The chemical properties of selenium and tellurium are the main properties that influence the precipitation behaviour of these elements from the solutions containing them. Both Se and Te exhibit similar chemical properties. They are insoluble in water and highly soluble in sulphuric acid medium (Hoffman *et al.*, 2011). These species have variable oxidation states, namely, -2, 0, +4 and +6. They also belong to the same group (6) of the periodic table of elements, and this explains why Se and Te possess similar characteristics.

The redox potential of the aqueous medium in which these species are found determines their oxidation states (Seby *et al*, 2001). Selenium, for example, exists as selenate (Se^{6+}) in a medium where the redox potential is high, while selenite (Se^{4+}) is found in aqueous medium of normal redox potential. Elemental selenium (Se^{0}), on the other hand, can be found in medium where reduction is favoured. Selenide (Se^{2-}) will only be present in a highly reducing aqueous medium, and this

explains why selenium is commonly precipitated as selenides of various metals (Seby *et al*, 2001). Since selenium and tellurium exhibit similar characteristics in aqueous medium, it is very likely that tellurium behaves similarly as selenium in the same medium. No literature that describes the variation of tellurium oxidation states in various aqueous medium could be found.

Selenium and tellurium impurities are commonly present as tetravalent and hexavalent ions in the acidic copper sulphate leach solutions (Hofirek, 1983). These facts are used to suggest a suitable reducing agent to precipitate them. Moreover, tellurium must be reduced to its tetravalent state before it can be recovered as Cu_2Te (Jennings *et al.*, 1969), while selenium ions can either be reduced directly to a valence state of 0, or removed as Cu_2Se from copper sulphate solutions in its tetravalent state (Wang *et al*., 2003).

The possible selenium and tellurium species present in the copper sulphate solution to be used for this study are shown in table 2.1. At typical operating conditions (65-95^{o}C) for Te and Se removal (Wang *et al*, 2003), the dominant aqueous species of selenium and tellurium impurities present in this solution are selenious (IV) acid (H_2SeO_3), tellurious (IV) acid (H_2TeO_3) and orthotelluric acid (H_6TeO_6). This was found using OLI Analyser version 3.0.

Table 2.1: Possible Se and Te species found in the process solution supplied by Lonmin Plc (Derived from (OLI Analyser version 3.0)).

Se species	**Te species**
H_2SeO_3	H_2TeO_3
H_2SeO_4	H_2TeO_4
$NiSeO_3$	H_6TeO_6
$NiSeO_4$	H_2Te
H_2Se	
$CuSeO_4$	
$CuSeO_3$	
$CuSeO_3.2H_20$	
$Fe_2O_3.3SeO_2.H_20$	
$Fe_2O_3.2SeO_2$	
$Fe_2O_3.SeO_2$	

2.4. Reagent consideration for Se and Te precipitation

2.4.1. Te precipitation with SO_2 only

Several reagents have been proposed for the removal of dissolved Te and Se from copper sulphate solutions by different investigators. Hofirek (1983) investigated the reduction of selenium ions with sulphur dioxide in an agitated autoclave using a copper sulphate solution whose composition is summarised in table 2.2. This operation was carried out at an operating condition of 140^{o}C and about 350 kPa. The pH of the solution and the duration of the experiment were not explicitly stated. Neither was the agitation speed nor reactions that describe the precipitation process provided.

An excess of 7-100 mol of SO_2 gas per dissolved mol of Se ions was used to precipitate Se. The precipitates of cuprous selenide formed were removed from the acidic leach solution, after which oxygen was introduced in order to oxidise the cuprous ions generated during reaction to cupric copper. It was furthermore observed that Se^{4+} and Se^{6+} ions were reduced from 5 and 30 mg/L to 0.1 and 1 mg/L respectively upon the completion of the experiment. The concentration of tellurium was not given, neither was the Te precipitation achieved discussed.

Table 2.2: Chemical composition of copper sulphate solution used by Hofirek (1983)

Species	Mass concentrations (mg/L)
Cu	60000
Ni	50000
Se^{4+}	5
Se^{6+}	30
Te	-
H_2SO_4	10000

Lottering (2011) studied Se and Te precipitation with thiosulphate, formaldehyde, formic acid, thio urea and sulphurous acid using a leach solution with a composition as shown in table 2.3. Precipitation tests were conducted at temperatures ranging from 80 ^{o}C to 150 ^{o}C in a pressure vessel. It was found that at a temperature of 80 ^{o}C, none of the reagents resulted in noticeable Te precipitation.

At 115^{o}C and higher temperatures, thiourea and sulphurous acid achieved comparable Te precipitation; however, almost 100 % selenium precipitation was achieved at temperatures of 80 ^{o}C and 115^{o}C, irrespective of the percentage excesses of sulphurous acid added to the leach solution. The fast Se precipitation kinetics observed during the tests is in agreement with the findings of Haranczyk *et al*. (2002).

It was also found that sulphurous acid precipitated tellurium significantly at different investigated conditions. At 80°C, about 90 % Te precipitation was achieved in 40 minutes for the percentage excesses of sulphurous acid used. This was followed by the dissolution of tellurium-containing precipitate into the copper sulphate medium after about 60 minutes of the experiments, involving the addition of 80%, 110% and 140% excesses of sulphurous acid into the said solution (Lottering, 2011). This dissolution of tellurium-containing precipitate was also observed at 115 and 150°C respectively, regardless of the sulphurous acid added, but was most pronounced at 150°C.

Table 2.3: Chemical composition of copper sulphate solution used by Lottering (2012)

Species	**Mass concentrations (mg/L)**
Cu	70760
Fe	615.1
Ni	51910
Rh	32.7
Ru	144.4
Se	58.4
Te	32.5

Western Platinum Ltd BMR also utilizes SO_2 for the removal of Se and Te from the copper sulphate solution in the selenium removal section of the base metals refinery. This precipitation method is based on the Sherritt Gordon Mines (1983) technology.

As discussed in section 1.2, the current process conditions achieve significant Se precipitation. Selenium concentration in the solution fed to electrowinning is reduced to at least 1mg/L, but tellurium precipitation still proves challenging. The possible reactions for selenium and tellurium precipitation via this method are given by equations 2.20 and 2.21 (Sherrit Gordon Mines, 1983); however, typical chemical analysis of the precipitate produced during Te and Se precipitation via this method includes 65% Cu, 25% Se and 3% Te (Sherritt Gordon Mines, 1983). The outstanding 7% was not provided in the process description. This chemical analysis clearly revealed that larger amount of selenium than tellurium was precipitated from the solution.

$$CuSeO_3 + CuSO_4 + 4H_2SO_3 + H_2O \rightarrow Cu_2Se + 5H_2SO_4 \quad (2.20)$$

$$CuTeO_3 + CuSO_4 + 4H_2SO_3 + H_2O \rightarrow Cu_2Te + 5H_2SO_4 \quad (2.21)$$

Similar results for Te precipitation by sulphurous acid addition was also reported by Wang *et al.* (2003), who indicated that the reductive precipitation of Te from a sulphuric acid solution by sulphurous acid addition alone is unlikely. It was observed that any Te precipitation was likely to be because of a secondary cementation reaction between dissolved Te and metallic copper in contact

with the solution. Metallic copper can be produced by the disproportionation of cuprous brought about by the reduction of cupric ions by SO_2 (Wang *et al*., 2003).

Crundwell *et al.* (2011) also reported that the primary role of SO_2 in Se precipitation is the formation of cuprous ion. Cuprous sulphate acts as a reducing agent that precipitates Te and Se, from copper sulphate solution, as cuprous telluride and selenide respectively. Reaction 2.22 describes the reduction of cupric to cuprous sulphate, while reactions 2.23 and 2.24 describe the removal of dissolved Se as cuprous selenide. Both reactions occur at 90^{o}C in a pipe reactor under atmospheric condition (Crundwell *et al*., 2011).

$$2CuSO_4 + H_2SO_3 + H_2O \rightarrow Cu_2SO_4 + 2H_2SO_4 \quad (2.22)$$

$$4Cu_2SO_4 + H_2SeO_3 + 2H_2SO_4 \rightarrow Cu_2Se + 6CuSO_4 + 3H_2O \quad (2.23)$$

$$5Cu_2SO_4 + H_2SeO_4 + 3H_2SO_4 \rightarrow Cu_2Se + 8CuSO_4 + 4H_2O \quad (2.24)$$

However, the cuprous sulphate produced, may disproportionate to form cupric ions and elemental copper, as the temperature of the solution is raised to 90°C. Wang *et al*. (2003) described the disproportionation reaction of cuprous ion by reaction 2.25. Alternatively, it can be described by reaction 2.26.

$$2Cu^{+} = Cu^{2+} + Cu^{0} \quad (2.25)$$

$$Cu_2SO_4 \rightarrow CuSO_4 + Cu \quad (2.26)$$

It was thus concluded that the addition of metallic copper would be necessary to enhance tellurium precipitation, and that temperatures above 92°C are required if Te precipitation were to occur without any copper addition (Wang *et al*., 2003).

2.4.2. Te precipitation with SO_2 and metallic copper

Tellurium can be precipitated satisfactorily from the acidic leach solution with SO_2 and metallic copper (Jennings *et al.*, 1968; Wang e*t al.*, 2003). In this case, SO_2 plays the role of a reducing agent, while metallic copper acts as either a precipitation enhancing reagent or an alternative reducing agent. Tellurium is precipitated as cuprous telluride from the copper sulphate solution via this process route. Various reactor configurations and stirring patterns have been adopted for this precipitation process; examples of these include rotating drum reactors (Jennings *et al.*, 1969), fixed bed reactors (Shibasaki *et al.*, 1992) and the use of a tank containing suspended copper plates (Sugawara *et al.*, 1992).

The secondary cementation reaction between metallic copper and tellurium are described by reactions 2.27 and 2.28, while the reductive precipitation of selenium ions by metallic copper in copper sulphate medium is given by reaction 2.29 (Wang *et al*, 2003).

$$4Cu + H_2TeO_3 + 2H_2SO_4 \rightarrow Cu_2Te + 2CuSO_4 + 3H_2O \quad (2.27)$$

$$5Cu + H_6TeO_6 + 3H_2SO_4 \rightarrow Cu_2Te + 3CuSO_4 + 6H_2O \quad (2.28)$$

$$4Cu + H_2SeO_3 + 2H_2SO_4 \rightarrow Cu_2Se + 2CuSO_4 + 3H_2O \quad (2.29)$$

Mokmeli *et al*. (2012) also studied the formation of cuprous ions in H_2SO_4-$CuSO_4$ medium with the addition of metallic copper. Experiments were performed using solutions containing 50-110 g/L Cu^{2+} ions and 10-200 g/L sulphuric acid, at temperatures ranging from 50 to 95°C. The production of cuprous ions by this method is also described by reaction 2.25. It was found that cuprous ions increased progressively and significantly with increase in temperature. It was also observed that the largest amount of cuprous ion was obtained at a temperature above 90°C and that the acid concentration did not have a significant effect on cuprous formation.

Additionally, it has also been shown that tellurium can be precipitated from copper sulphate solutions with the addition of powdered copper (Sugawara *et al*., 1992) or copper shots (Jennings *et al*., 1969) or copper chopping (Shibasaki *et al.*, 1992) or with the use of both SO_2 and Cu chips (Wang *et al.*, 2003).

Jennings *et al.* (1969) investigated the kinetics of tellurium precipitation reaction using a copper sulphate solution whose composition is given in table 2.4. The solution was introduced into a batch reactor and heated to desired temperatures (70, 93, 101 and 103°C) with different masses of copper shots ranging from 95 to 7500 g added per 1L of solution depending on the experimental conditions. Various amounts of sulphuric acid ranging from 47 to 143 g/L were also used prior to the beginning of each experimental run, with the objective of investigating the effect of the acid variation on the Te precipitation reaction kinetics. The solution was agitated after copper addition, by rotating the reactor throughout the experiment. The precipitation of tellurium via this method was proposed to proceed by reaction 2.28.

Table 2.4: Chemical composition of the copper sulphate solution used by Jennings *et al.* (1969)

Species	**Mass concentration (g/L)**
Cu	105
H_2SO_4	51.6
Total Te conc.	15.25
Te^{4+} conc.	0.39
Se	0.10

It was found that temperature plays a key role in tellurium precipitation kinetics and that the Te precipitation has an activation energy of 125.574 kJ/mol. It was furthermore experimentally proven that that the rate of Te precipitation reaction is first order with respect to tellurium concentration in the leach solution, and that the effect of agitation is minimal (Jennings *et al*., 1969). It was also shown that there was a decrease in the acid concentration where fast Te precipitation was observed, and that about 50 g/L of sulphuric acid would be consumed before the precipitation of 15 g/L of tellurium could be achieved (Jennings *et al*., 1969). For the solution pertinent to this study, the ratio of sulphuric acid to tellurium (as shown in table 3.4 of section 3.2) is too large. Therefore, no significant reduction of sulphuric acid is expected for the removal of tellurium from this solution.

The kinetics of tellurium precipitation has also been studied in a fixed-bed reactor filled with copper choppings of small and medium sizes with specific surface areas of 3560 and 638.7 m^2/m^3, respectively (Shibasaki *et al*., 1992), where specific surface area refers to the surface area of the copper choppings used per unit volume of the reactor column. 500 ml of the leach solution was passed from the bottom of the reactor (having a depth of 0.5 m and an internal diameter of 0.05 m) upwards such that there was an intimate contact between the solution and the copper choppings. The copper sulphate solution used contained 3.50 g/L of Te but the concentrations of Se and other species of interest to this project were not specified. The pH of the solution was also not specified. This solution was introduced into the reactor column with a linear velocity of 8.9 cm/s, when the column was filled with small-sized copper choppings and with a linear velocity of 6.3 cm/s when copper choppings of medium sizes were used for the experiments (Shibasaki *et al*., 1992).

These experiments were, however, carried out at a temperature range of 60-90^oC for 400 seconds with the objective of investigating the influence of specific surface areas of copper choppings used on tellurium precipitation reaction (Shibasaki *et al.*, 1992). The equation of reaction that described this process was also given by reaction 2.28, while the outcomes of the study are summarised in table 2.5.

Table 2.5: The influence of specific surface area of copper choppings on tellurium precipitation kinetics (Adapted from Shibasaki *et al*. (1992))

Types of copper choppings used	Specific surface area of choppings (m^2/m^3)	Linear velocity (cm/s)	Reaction rate constant (per second)
Small (a)	3560	8.9	5.72×10^{-3}
Medium (b)	638.7	6.3	1.01×10^{-3}
Ratio a/b	5.6		5.7

As seen in table 2.5, the ratios of the rate constants and the specific surface areas of the two kinds of copper choppings used were almost equal. This indicates that the rate of tellurium precipitation reaction varies with the specific surface areas of the copper choppings (Shibasaki *et al.*, 1992). However, this observation only holds on condition that the influence of the linear velocities on the reaction was not considered (Shibasaki *et al.*, 1992).

When different values of log (C/Co) were plotted against those of reaction time, a linear relationship was observed between the two sets of values. Where C represents the concentration of Te at a desired time during the experiment and Co represents the concentration of Te prior to the commencement of the experiment. Thus, it was concluded that tellurium precipitation reaction is a first order chemical reaction with respect to the Te concentration in the copper sulphate leach solution (Shibasaki *et al.*, 1992). This observation is in line with previous study conducted by Jennings *et al*. (1969) on tellurium precipitation

Sugawara *et al.* (1992) also showed that tellurium can be precipitated with copper powder using an acidic leach solution with a chemical composition as shown in table 2.6. The reaction was carried out at a temperature of 70^{o}C on a batch scale for a duration of 12 hours. 500 ml of the solution was introduced into the reactor, after which copper powder of 7 g or 15 g or 22 g, depending on experimental conditions, was added in order to study the tellurium precipitation behaviour in copper sulphate medium. Further details of the experiment were not provided.

Table 2.6: Chemical composition of the copper sulphate solution used by Sugawara *et al*. (1992)

Species	**Mass concentration (g/L)**
Cu	65
H_2SO_4	196
Te	14.5

The results of the experiment are summarized in table 2.7. From this table, it can be observed that increasing the quantity of copper powder added into the solution, resulted in the corresponding reduction of Te concentrations found in the solution. This increase in the amount of copper used also resulted in an increase in the quantity of tellurium-containing precipitates that formed, but the relative concentrations of Te/Cu in the precipitates formed significantly declined (Sugawara *et al.*, 1992).

Table 2.7: Effects of copper addition on Te precipitation (Adapted from Sugawara *et al*. (1992))

Copper powder addition (g)	7	15	22
Te conc. after 12 hours (g/L)	4.8	1.0	0.8
Mass of precipitates formed (g)	7.1	14.9	22.8
%Te present in the precipitate	60.3	42.5	28.7
%Cu present in the precipitate	29.0	43.9	61.4

It seems increasing the amount of copper powder added without a corresponding increase in the agitation speed, resulted in the formation of deposits of copper telluride on the surfaces of this copper powder (Sugawara *et al.*, 1992). These copper telluride particles may form mud on the surfaces of the copper powder during the precipitation process. For this reason, the precipitates obtained may contain significant amount of copper in its elemental form due to poor agitation. The tellurium content of precipitate will significantly increase with improved agitation condition.

Another test was conducted with 25 g of copper powder using a slightly different solution composition with the objective of investigating the effect of increasing the residence time on Te recovery (Sugawara *et al.*, 1992). The chemical composition of the solution that was used and the results obtained are provided in tables 2.8 and 2.9 respectively.

Table 2.8: Chemical composition of the solution used by Sugawara *et al*. (1992) for the 2nd test involving copper powder addition

Species	**Mass concentration (g/L)**
Cu	56
Te	15.8
H_2SO_4	199

Table 2.9: Result of the experiment conducted by Sugawara *et al*. (1992) for the 2nd test with the use of copper powder

Reaction time (hours)	6	12	18	24
Tellurium concentration (g/L)	0.72	0.12	0.10	0.02
Mass of precipitates obtained (g)	25	25	24	23
% Te found in the precipitate	28.5	32.0	32.0	32.5
% Cu found in the precipitate	59.0	62.0	57.5	60.0

The outcome of this experiment clearly revealed that increasing the residence time brought about the reduction of significant Te concentrations in the solution when the experiments were conducted for 12, 18 and 24 hours respectively. Though, the tellurium contents of the precipitates obtained were low for all the observations. A possible explanation for this trend is that larger amounts than necessary of copper powder were lost in order to achieve significant tellurium precipitation. This excessive loss of copper powder can be minimised by investigating the amount of copper powder required, the agitation speed of the solution and the desired operating temperature, that will not only reduce the Te concentration in the solution but will also improve the tellurium content of the precipitate obtained significantly.

Wang *et al*. (2003) also studied the selenium and tellurium precipitation kinetics with SO_2 and metallic copper; the chemical composition of the copper sulphate solution used by Wang *et al.* (2003) is summarized in table 2.10.

Table 2.10: Chemical compositions of the solution used by Wang *et al*. (2003)

Species	**Mass concentration (g/L)**
H_2SO_4	26.8-112.0
Cu	68.9-98.2
Se	0.197-4.00
Te	3.18-4.70

To illustrate this process, experiments were conducted in a beaker equipped with a gas sparger, a stirrer and a thermocouple. Sulphur dioxide gas was sparged into the solution from a reagent cylinder connected to a flow meter that regulated the SO_2 flow rate. The SO_2 flow rate was not specified. Prior to the tests, predetermined quantities of H_2SO_4 and copper chips were added into the solution. This was done so as to ensure that the Cu-H_2SO_4 stoichiometric ratio was in line with reactions 2.27 and 2.28. The experiments were carried out for at most 11 hours at different temperatures ranging from 65^{o}C to 95^{o}C (Wang *et al.*, 2003).

The reductive precipitation of Se and Te by SO_2 was first investigated in the copper sulphate medium at low temperatures (65^{o}C to 73^{o}C), before the precipitation mechanisms of both impurities were further studied at high temperatures (92^{o}C to 95^{o}C) with the addition of metallic copper as a precipitation enhancing reagent; metallic copper was added in the form of copper chips (Wang *et al*., 2003).

With SO_2 only as a reducing agent, Se exhibited faster precipitation kinetics than Te at low temperatures; approximately 10 % Te and 80 % Se precipitation were achieved after 60 minutes (Wang *et al.*, 2003). Selenium continued to exhibit faster precipitation kinetics than tellurium until the fifth hour of the experiment, when metallic copper was added into the leach solution at a temperature of 92^{o}C. The addition of metallic copper at that temperature resulted in a significantly faster Te precipitation rate for the remaining experimental period. The extents of Te and Se precipitation were, however, comparable after the completion of the tests; approximately 87 % Te and 90 % Se precipitation were achieved after 6 hours (Wang *et al.*, 2003). The reduction of selenium ions to elemental Se was described as follows (Wang *et al.*, 2003):

$$H_2SeO_3\ (aq) + 2SO_2\ (g) + H_2O \rightarrow 2H_2SO_4\ (aq) + Se\ (s) \qquad (2.30)$$

It was observed that deposits of copper powder were formed on the walls of the vessel during the experiments. The formation of these deposits was explained to be as a result of a disproportionation reaction, that involved the decomposition of cuprous sulphate to cupric sulphate and the copper powder formed (Wang *et al.*, 2003). Consequently, the copper powder obtained reacted with the dissolved Se and Te to further precipitate these species as Cu_2(Se, Te) via the secondary cementation process.

It was also noticed that the formation of cuprous telluride and selenide precipitates on the surfaces of both the copper powder (obtained during Te/Se precipitation), and the copper chips (used as an additional reducing agent), could prevent further cementation reactions between these elemental copper and the dissolved Te and Se present in the copper sulphate solution (Wang *et al.*, 2003). For this reason, a stirrer was used to strip off the cuprous telluride and selenide deposits from the surfaces of the copper powder and chips during the experiments (Wang *et al.*, 2003). It can be inferred that metallic copper addition, temperature, and stirring rate are the major factors that influence tellurium precipitation using this method.

The recovery of tellurium with powdered copper is preferable to Te removal with other kinds of copper pieces discussed in this section, because the former presents a larger surface area than the latter for cementation reaction with tellurium in the solution. One major drawback of this tellurium precipitation method is the formation of cuprous telluride deposits on the surfaces of copper powder or pieces. These deposits prevent the further cementation reaction of copper with Te in the solution (Sugawara *et al.*, 1992).

Sugawara *et al.* (1992) proposed a method of tellurium precipitation with the use of at least a suspended copper plate in an acidic leach solution, thereby enabling tellurium to deposit on a metallic copper plate as cuprous telluride. The cuprous telluride formed can be removed from the surface of the suspended copper plates by means of agitation, after which the precipitate can be filtered off. This process may be modified such that several baths of the leach solutions can be arranged in series, with each bath containing two suspended copper plates and an agitator. The leach solution is passed from bath to bath in a countercurrent fashion.

This technique was first illustrated in a batch operation with the use of 1.5 m^3 copper sulphate solution containing 19 suspended copper plates. The operation was carried out at 60^oC for a duration of 36 hours. No information was provided about the pH and the agitation speed. Though, the solution was mixed slowly throughout the operation while the plates were continuously vibrated. The composition of the solution is summarised in table 2.11.

Table 2.11: Chemical composition of the copper sulphate solution used by Sugawara *et al.* (1992) in a batch operation to precipitate tellurium

Species	**Mass concentration (g/L)**
Cu	50
H_2SO_4	180
Te	8

It was found that tellurium concentration of the solution was reduced considerably to 20 mg/L by the end of the operation, and that the weight of the precipitate recovered was 23 kg (Sugawara *et al.*, 1992). The precipitate consisted of 52% Te and 47% Cu. The outstanding 1% could most likely be a species which was not relevant to that study.

The technique was further illustrated in a cascade operation using the same solution, with similar operating condition, but with different solution composition. The chemical composition of this solution is summarised in table 2.12. Here, four tanks were used with each tank containing 19 suspended copper plates, and the solution being introduced into the first tank at a flow rate of 3 L/min for 72 hours (Sugawara *et al.*, 1992). The solution was allowed to overflow to the other tanks arranged in series while the copper sulphate solution from the last tank was re-introduced into the first tank upon the complete removal of its precipitate (Sugawara *et al.*, 1992).

Table 2.12: Chemical composition of the copper sulphate solution used by Sugawara *et al*. (1992) in a cascade operation to precipitate tellurium

Species	**Mass concentration (g/L)**
Cu	53
H_2SO_4	190
Te	7.5

It was found that the tellurium concentration in the solution was reduced to 30 mg/L at the end of the cascade operation. The amount of precipitate recovered was 264 kg while the Te and Cu contents of the precipitate were 53% and 45%, respectively (Sugawara *et al*., 1992).

Shibasaki *et al*. (1992) also studied the recovery of tellurium on the surfaces of copper choppings using the same solution, similar reactor configuration and experimental conditions as those previously discussed. The experiment was carried out with the objective of finding the optimum temperature that would guarantee the effective removal of precipitates formed from the surfaces of metallic copper, and that would result in significant reduction of Te concentration in the solution (Shibasaki *et al.*, 1992). The results of this experiment are summarised in table 2.13.

Table 2.13: Experimental result showing quantities of precipitates removed from the surfaces of copper choppings at desired temperatures (Adapted from Shibasaki *et al*. (1992))

Temperature (^oC)	Te conc. (g/L)	Mass of Te (g)	Precipitates removed from copper surfaces	
			Mass of precipitate (g)	Mass of Te present (g)
Initial condition	3.50	1.75	-	-
60	3.49	1.74	0.0052	0.0026
70	3.37	1.69	0.133	0.0665
80	2.42	1.21	1.12	0.562
90	1.88	0.94	1.08	0.539

It was found that high recovery of tellurium was achieved and easy removals of precipitates were observed at 80^{o}C and 90^{o}C (Shibasaki *et al.*, 1992). This observation is also illustrated in table 2.13. As shown in this table, tellurium concentrations of the solution declined significantly as the temperature increased progressively from 60^{o}C to 80^{o}C. The amounts of precipitates removed from the surfaces of the copper choppings also increased with every rise in temperature, except for a slight deviation seen when the temperature was increased from 80^{o}C to 90^{o}C. This deviation was not explained. Thus, it was concluded that a temperature range of 80-90^{o}C would favour Te precipitation kinetics via this method (Shibasaki *et al*., 1992).

2.5. Effects of Te precipitation on other precious metals (OPMs)

Although the primary objective of this research is the precipitation of tellurium, it is worthwhile to investigate the influence of the reagent employed for Te removal, on the other precious metals present in the acidic leach solution. The other precious metals in the selenium removal section of the BMR process are rhodium (Rh), ruthenium (Ru) and iridium (Ir).

Lottering *et al*. (2012) showed that the precipitation of these precious metals depends on temperature and percentage excesses of reagent added. Rhodium and ruthenium precipitation were reported to be poor at 80^{o}C and 115^{o}C for all percentages of sulphurous acid added into the solution. At 80^{o}C, only about 10 % Rh and Ru precipitation were achieved irrespective of reagent addition, while there was much improved precipitation of these species at 115^{o}C with close to 25 % precipitation realised. A maximum percentage of 50 % rhodium and ruthenium precipitation was achieved at 150^{o}C when 140 % excess of sulphurous acid was added into the copper sulphate solution (Lottering *et al*., 2012). The poor precipitation of Rh by SO_2 was attributed to the fact that insufficient copper was present in the H_2SO_4-$CuSO_4$ medium to bring about cationic substitution that would result in Rh precipitation (Lottering *et al*., 2012).

2.6. Effects of Te precipitation on base metals

The precipitation of tellurium has a marked influence on the concentrations of the base metals and those of other dissolved species present in the acidic leach solution. Lottering (2011) also studied the precipitation of copper, nickel and iron using a copper sulphate solution with a composition as specified in table 2.3. Precipitation tests were performed under similar investigated conditions to that of Te and Se precipitation discussed in that section, with the base metals precipitation being the focus. It was found that these base metals exhibit similar precipitation trends when SO_2 was used as a reducing agent, and that increasing the temperature resulted in a larger amount of Cu, Ni and Fe precipitating regardless of the quantities of reagent added (Lottering, 2011). The maximum precipitation of copper achieved at 80^{o}C (for 80, 110 and 140 percentage excesses of sulphurous acid added) was almost 10 % while close to 15 % of iron and nickel precipitation were realised under the same experimental conditions. There was no remarkable difference in the amount of base metals precipitated as the temperature of the system was increased from 80^{o}C to 115^{o}C irrespective of the percentage excesses of SO_2 used (Lottering, 2011).

Whereas there was a significant increase in the amount of base metals precipitation observed when the temperature was increased from 115 to 150^{o}C, with about 20 % Cu and Ni precipitation achieved even with a low percentage excess of sulphurous acid added. Wang *et al.* (2003) also

reported a gradual decline of copper concentration in the leach solution used to study tellurium and selenium precipitation; it was observed that Cu concentration reduced remarkably as significant Se and Te precipitation was achieved even at a temperature as low as 75^{o}C, thereby prompting the addition of more copper chips to enhance tellurium precipitation. For example, it was noticed that Se concentration was reduced from 2.78 to 0.74 g/L, while Te concentration was reduced from 4.64 to 4.20 g/L in 1 hour, after a loss of about 21.5 g/L of Cu concentration was noticed during the experiment (Wang *et al*., 2003). It is not clear why there was a significant reduction in copper concentration at this low temperature.

As discussed in section 2.4.1, this observation could be attributed to cupric reduction and the subsequent precipitation of Cu, Te, and Se from the solution as Cu_2Te and Cu_2Se respectively by cuprous ions. Considering the ratio of copper concentration to either selenium or tellurium concentration present in the solution used for that study, significantly large amount of cuprous ion would be required in order to achieve high tellurium and selenium precipitation. Table 2.10 shows the copper and tellurium concentrations present in the copper sulphate solution used for the tests performed by Wang *et al*. (2003). The concentrations of tellurium and selenium species present in the solution used for this study are approximately 2 orders of magnitude smaller than that used by Wang *et al*. (2003). Therefore, excessive copper precipitation is not expected for the removal of Te and Se species from this solution at such low temperature.

However, iron (Fe^{3+}) is the first to react with SO_2 gas (Sherritt Gordon Mines Limited, 1983) because it has a higher oxidising power than the base metals and the other dissolved species in the acidic leach solution. It has also been observed that iron consumes a larger amount of the reagent added into the solution than the other reacting species. Therefore, its reaction with reducing agents is often used as a basis for estimating the reagent amount required, for the removal of the dissolved species from the copper sulphate solutions (Lottering *et al.*, 2012). The reaction of Fe with SO_2 is given by (Sherritt Gordon Mines Limited, 1983):

$$Fe_2(SO_4)_3 + H_2SO_3 + H_2O \rightarrow 2FeSO_4 + 2H_2SO_4 \qquad (2.31)$$

2.7. Summary

From the literature, two process routes were identified for the precipitation of tellurium and selenium, namely:

- Te/Se recovery with SO_2 only which is also regarded as experimental method 1
- Te/Se recovery with SO_2 and metallic copper.

The second process route can be divided into 2 experimental methods, namely:

- Te/Se recovery with SO_2 and copper plate which is also regarded as experimental method 2.
- Te/Se recovery with SO_2 and copper powder which is also regarded as experimental method 3.

It is also clear that the factors that influence tellurium and selenium precipitation from the copper sulphate solutions include (Wang *et al*., 2003; Jennings *et al.*, 1969; Shibasaki *et al*., 1992):

- Temperature
- Agitation speed
- SO_2 flow rate
- Copper addition (only for process route 2)

Acid variation was not considered as a process variable because it does not have a pronounced effect on the formation of cuprous sulphate (Mokmeli *et al.*, 2012). As discussed in section 2.4, cuprous sulphate is an intermediate species which acts as a reducing agent for Se and Te precipitation via cementation process (Ladriere, 1973).

Chapter 3 : Experimental

3.1. Experimental design

For both process routes, 65 and 95^{o}C were selected as the two levels of temperature for the factorial experiments. This is because these values are very close to the temperature values of 65, 70, 80 and 92^{o}C used in similar experiments conducted by Wang *et al.* (2003) for Te and Se precipitation.

One gram and two grams of copper powder were chosen as the two levels of copper powder addition for experiment method 3. These masses of copper powder are much smaller than the total mass of 50 g of copper chips used in the experiments performed by Wang *et al.* (2003). This difference stems from the fact that there is a disparity between the Te concentrations found in the process solutions supplied by Lonmin Plc, and that considered byWang *et al*. (2003) and Sugawara *et al*. (1992) for similar experiments. The Te and Se concentrations in the process solution that was used by Wang *et al*. (2003), for example, is about 2 orders of magnitude greater than that of the solution supplied by Lonmin Plc. Copper powder was chosen in preference to the other copper pieces because it offers the largest surface area among all the copper pieces considered in this study.

Furthermore, 10 x 7.5 x 1.5 mm was used as the dimension of the small copper plate while 2 of these plates were considered as a larger plate for experiment method 2. The surface areas of the small and large copper plates were estimated to be 202.5 and 405 mm^2 respectively.

An excess of SO_2 ranging from 5 to 200 mol per 1 mol of selenium ions present in the process solution was used as the basis for determining the percentage excess of SO_2 (Hofirek, 1983). This was done because the primary role of SO_2 gas in the leach solution is to precipitate Se and not Te (Wang *et a*l., 2003), although sulphurous acid also reduces the cupric copper present in the solution to cuprous copper (Crundwell *et al*., 2011).

Based on this analysis, the low and high levels of SO_2 flow rates for all the experiments, irrespective of routes/methods, were estimated to be 4.4 cm^3/min and 5.8 cm^3/min respectively. Details of this calculation can be found in appendix A.2. Stirring rates of 250 rpm and 500 rpm were also selected as low and high levels of agitation speed in order to investigate the effect of stirring intensity on Te and Se precipitation (Jennings *et al*., 1969; Sugawara *et al*., 1992; Wang *et al.*, 2003).

The same process variables were adopted for the two process routes except that copper addition was not used for the first process route. The rationale behind using similar process variables for the two process routes is to compare the Te and Se precipitation achieved via these chosen routes.

Table 3.1: Process variables for Te and Se precipitation with SO_2 only

Te precipitation with SO_2 only		
Temperature (^oC)	SO_2 flow rate (cm^3/min)	Agitation speed (rpm)
65	4.4	250
95	5.8	500

Table 3.2: Process variables for Te and Se precipitation with SO_2 and copper powder

Te precipitation with SO_2 and copper powder			
Temperature (^oC)	SO_2 flow rate(cm^3/min)	Agitation (rpm)	Copper powder addition (g/L)
65	4.4	250	1
95	5.8	500	2

Table 3.3: Process variables for Te and Se precipitation with SO_2 and Cu plate

Te precipitation with SO_2 and copper plates			
Temperature (^oC)	SO_2 flow rate (cm^3/min)	Agitation (rpm)	Surface area of Cu plate (mm^2/L)
65	4.4	250	202.5
95	5.8	500	405.0

Thus, the factors and levels of the 3 experimental methods are summarised in table 3.1, 3.2 and 3.3. These factors and levels were used to prepare a 2^3 factorial experimental design for experimental method 1, and a 2^4 factorial experimental design each for experimental methods 2 and 3. Details of the factorial experimental designs can be found in appendix B. The outcomes of these experiments were used to investigate the principal process variables that influence tellurium and selenium yield via the proposed experimental methods.

Additionally, regression models that describe the relationships between Te and Se yield and the process factors which influence their yield were developed using Design Expert. These models were used to investigate the combination of parameters that would result in optimal tellurium and selenium yield for each experimental method.

3.2. Materials required

The second stage leach solution fed to the selenium removal section of the BMR was provided by Lonmin Plc. This solution was analysed using inductively coupled plasma atomic emission spectrometry (ICP-AES) in order to obtain its chemical composition, and this analysis was done in the Geological Department, Stellenbosch University. Table 3.4 gives the chemical composition of this solution.

Table 3.4: Chemical analysis of 2nd stage leach solution provided by Lonmin Plc with species of interest highlighted.

Species	Concentration (mg/L)
Cu	**71500**
Fe	598.0
Ni	**40300**
Rh	37.9
Ru	175.2
Se	**45.1**
Te	**27.6**
Ir	31.2
H_2SO_4	**25000**

Copper powder (45 μm particle size and 99.9% purity) was supplied by Sigma Aldrich. The specific surface area of the copper powder was determined to be 0.623 m^2/g using BET analysis. A 1.5 mm thick copper sheet was cut into pieces with the dimensions of 10 mm by 7.5 mm to be used in the tests utilizing copper plates. Sulphur dioxide gas (of 99.9% purity) was also supplied by Afrox in a reagent cylinder. This gas was used for all the methods of tellurium and selenium precipitation.

3.3. Equipment specification

All the experiments were performed in a Buchi Polyclave Type 3 pressure vessel manufactured from Hastelloy with a volumetric capacity of two litres. This vessel was equipped with certain devices in order to facilitate its operation and control. These devices and the functions they perform are described in table 3.5. The anchor and the blade stirrers are the two kinds of stirrer which were provided by the manufacturer of the vessel. The blade stirrer was used for all the experiments because it results in better gas dispersion and solids suspension. Sampling was done through the drain valve situated at the bottom of the vessel.

Table 3.5: Functions of devices incorporated into Buchi Polyclave Type 3

S/N	Devices	Functions
1	Cyclone 300 magnetic stirrer	Guarantees agitation speed of up to 2000 rpm during operation
2	Stirrer controller	Ensures that agitation speed is constant
3	Stirrer	Guarantees mixing of the solution in the pressure vessel
4	Pressure gauge	Indicates the pressure of the system
5	Thermocouples	Measure the jacket and reactor temperatures
6	Programmable controller	Set the temperature to a desired value
7	Bottom drain valve	For sampling
8	Bleed valve	Helps to purge the pressure vessel of impurities
9	Switch relay valve	Regulates cooling water flowing through the reactor shell
10	Electric heating elements	Regulates reactor temperature together with switch relay valve

A variable area flow meter manufactured by Aalborg was also connected to the SO_2 cylinder as shown in figure 3.1. This variable area flow meter was equipped with a needle valve, which was used to regulate the flow of gas into the capillary tube. This device measures the gas flow rate with a precision of ±5%. The flow rates of SO_2 for the 3 experimental methods were calculated in appendix A.2.

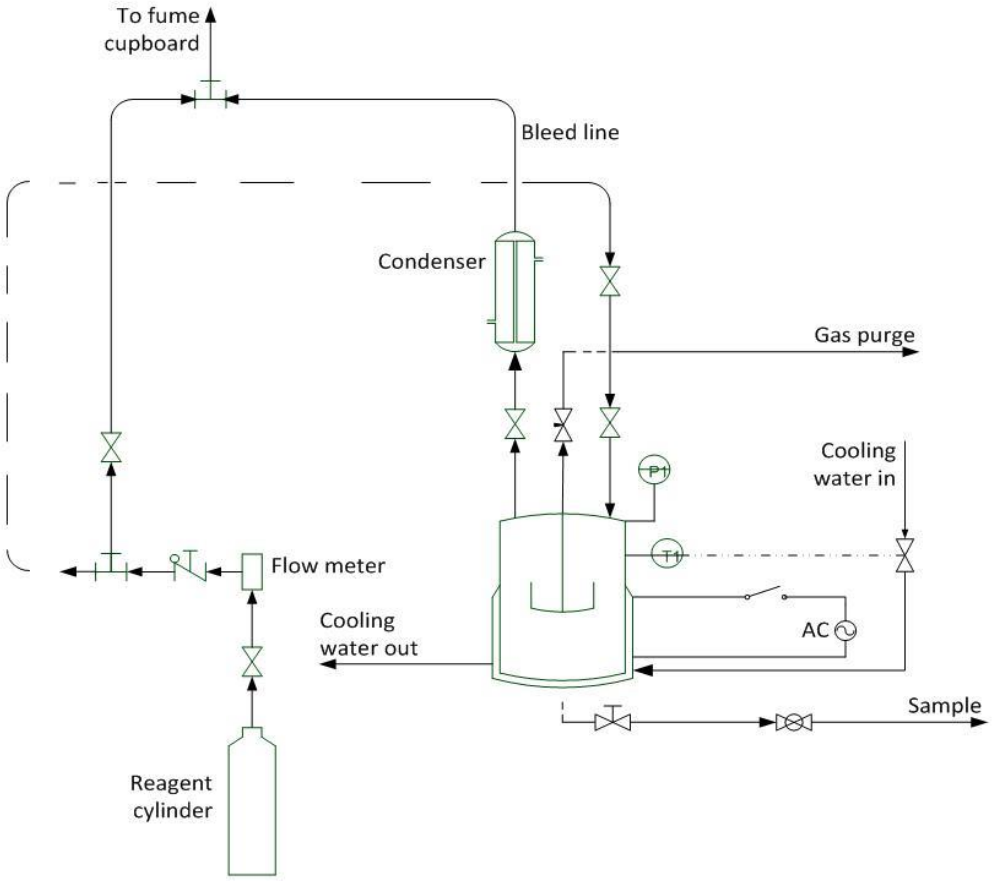

Figure 3.1: Schematic diagram of the equipment (Buchi Polyclave Type 3) used for all the experiments.

3.4. Methodology

A detailed description of the operating procedures for the 3 experimental methods can be found in appendix C. Only a brief explanation of the experimental method is provided in this section.

One liter of the process solution was introduced into the reaction vessel, where after the vessel was sealed, the stirrer switched on, and the solution heated to the desired temperature. Once the solution had reached the desired temperature, a sample of the solution was taken to confirm the initial solution composition. For tests that investigated the effect of copper addition, the copper was added to the vessel. The continuous flow of sulfur dioxide into the vessel was initiated directly after copper addition and maintained by purging gas through a bleed valve. The sulfur dioxide was bubbled into the solution for 3 hours via a dip tube connected to the reactor cover plate and held vertically within the pressure vessel.

Samples were taken at the following intervals (in minutes) after the sulfur dioxide flow had been initiated: 0, 10, 20, 30, 60, 120, 240, 360, 480. All samples were analyzed using inductively coupled plasma atomic emission spectroscopy (ICP-AES), and the percentage metal precipitation calculated by mass balance.

The autoclave was shut down upon the completion of every experiment according to the shutdown procedure provided in appendix C. The solution left in the vessel after the experiment was filtered (using a filter paper) while the residue was water washed and dried. The solution samples were submitted for ICP analysis while the solid samples were forwarded for SEM analysis.

Chapter 4 : Results and Discussion

4.1. Effects of factors on precipitation with SO_2 only

4.1.1. Selenium precipitation

Figure 4.1 shows the effect of agitation on selenium precipitation for the test performed at 65˚C and at a SO_2 flow rate of 4.4 cm³/min. As shown in this figure, increasing the agitation speed from 250 to 500 rpm resulted in a slight improvement in the selenium removal rate, though the extents of Se precipitation achieved for the two agitation conditions are comparable (96% Se precipitation on average).

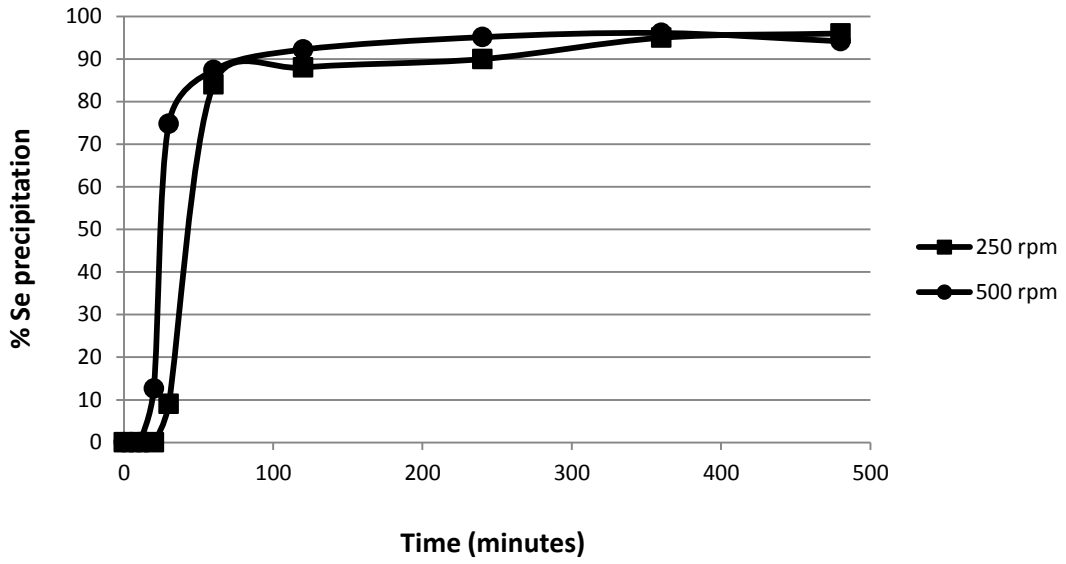

Figure 4.1: Effect of agitation on Se precipitation via SO_2 - based experimental method

Similar observations were made for the tests performed at other process conditions in that the extents of Se precipitation are comparable for the tests performed at identical temperatures and SO_2 flow rates but with different agitation rates. Increasing the agitation rate from 250 to 500 rpm, however, did not result in faster rate of Se precipitation at early period (0-60 minutes) for all the tests (figures 4.4 a and b).

For the tests performed at 65 and 95˚C and at an agitation rate of 250 rpm, increasing the SO_2 flow rate resulted in significantly faster selenium precipitation kinetics. Figure 4.2 shows the result of the test performed at 65˚C and at an agitation rate of 250 rpm as an illustration of a typical Se precipitation behaviour observed when the SO_2 flow rate was increased. One can observe from this figure that higher SO_2 flow rate allowed Se precipitation to proceed at an earlier point in time; 66% Se precipitation was achieved in 10 minutes when the SO_2 flow rate was increased from 4.4 to

5.8 cm³/min. By comparing figure 4.4 a with figure 4.4 b, one can also see the effects of increasing the SO_2 flow rate on Se precipitation for all the tests performed using this experimental method.

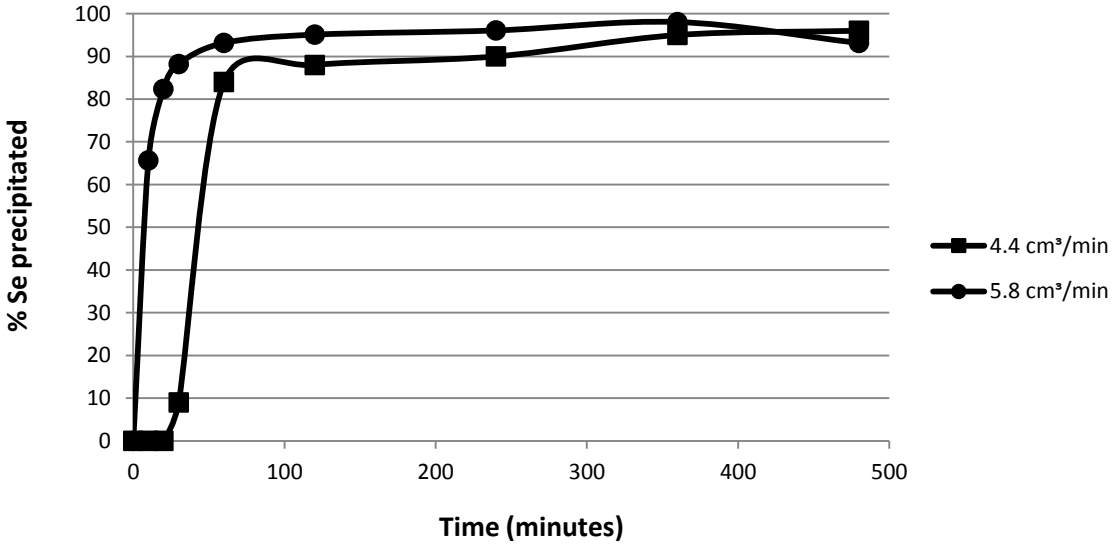

Figure 4.2: Effect of SO_2 flow rate on Se precipitation via SO_2 - based experimental method

The fast precipitation kinetics noticed for Se with improved SO_2 flow rate is in agreement with the observations of Weir *et al*. (1982), Haranzcyk *et al*. (2002), Wang *et al*. (2003) and Lottering (2012), and could be attributed to the fact that SO_2 has the capability of precipitating selenium ions (irrespective of their valencies) as elemental Se (reaction 2.30) or as Cu_2Se (equations 2.23 and 2.24) provided the copper sulphate solution used contains at least 10 g/L of cupric copper (Weir *et al*., 1982) which is the case for this study.

The presence of Cu_2Se as a major phase in the solid samples analysed, after the completion of the tests performed with high SO_2 flow rate, is an indication that larger amount of Se ions present in the solution were precipitated from the solution as cuprous selenide. This observation is illustrated in table 4.7 of section 4.3 where the mineralogical examination of precipiates obtained for this experimental method is discussed in more detail.

The effect of temperature on the rate of selenium precipitation is less profound than the effect of SO_2 flow rate; increasing the temperature from 65 to 95˚C generally resulted in slightly faster Se precipitation during the first 60 minutes (figures 4.4 a and b). The only exception was the test performed with a SO_2 flow rate of 5.8 cm^3min^{-1} at an agitation rate of 500 rpm. A typical example of Se precipitation behaviour with increase in temperature is illustrated in figure 4.3 for the test performed at an agitation rate of 250 rpm and a SO_2 flow rate of 4.4 cm³/min. As shown in this

figure, increasing the temperature from 65 to 95˚C did not result in any significant improvement in selenium precipitation achieved at early period (0-60 minutes) for this test, though there was an increase in the extent of Se precipitation observed at elevated temperature; 96% and 99% Se precipitation were achieved after 8 hours for the tests performed at 65 and 95˚C, respectively.

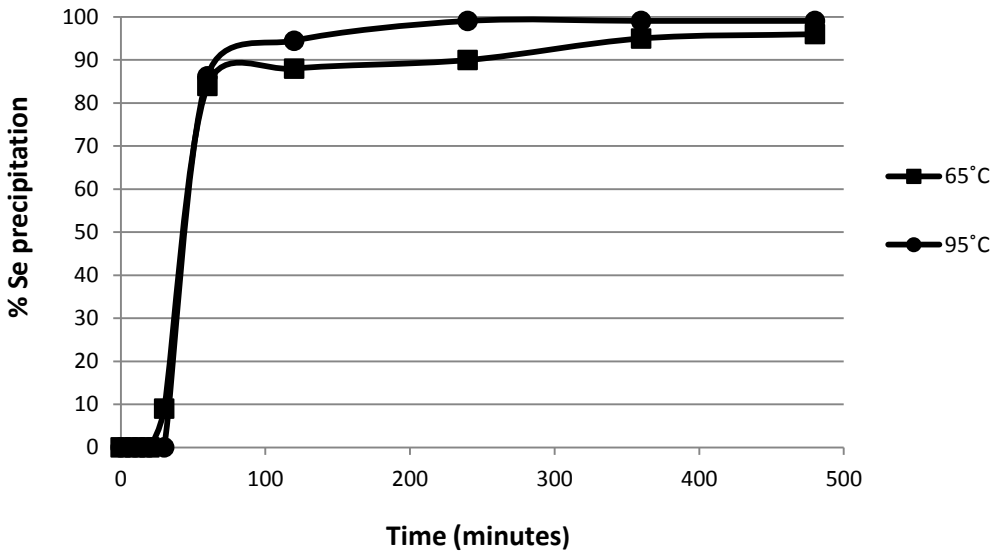

Figure 4.3: Effect of temperature on Se precipitation via SO_2 - based experimental method

It is not clear why higher temperature did not result in a faster Se removal rate for the first 60 minutes; the increased Se precipitation noticed at high temperature could, however, be attributed to the cupric reduction and the subsequent elemental copper formation (according to reactions 2.22 and 2.25) which enhances selenium precipitation from copper sulphate solution as Cu_2Se (equation 2.29).

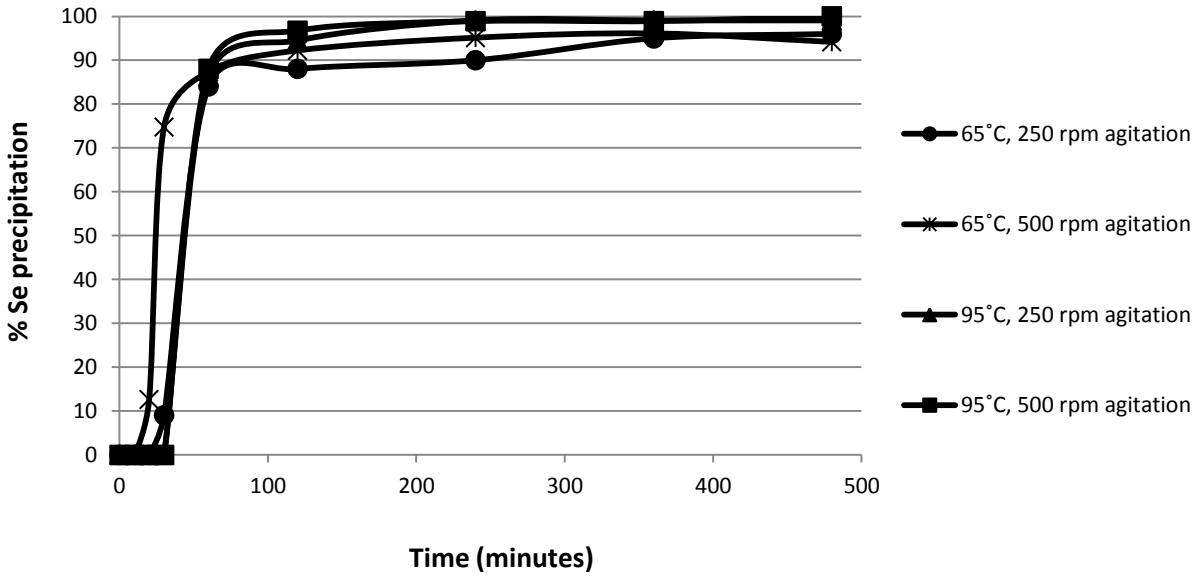

a)

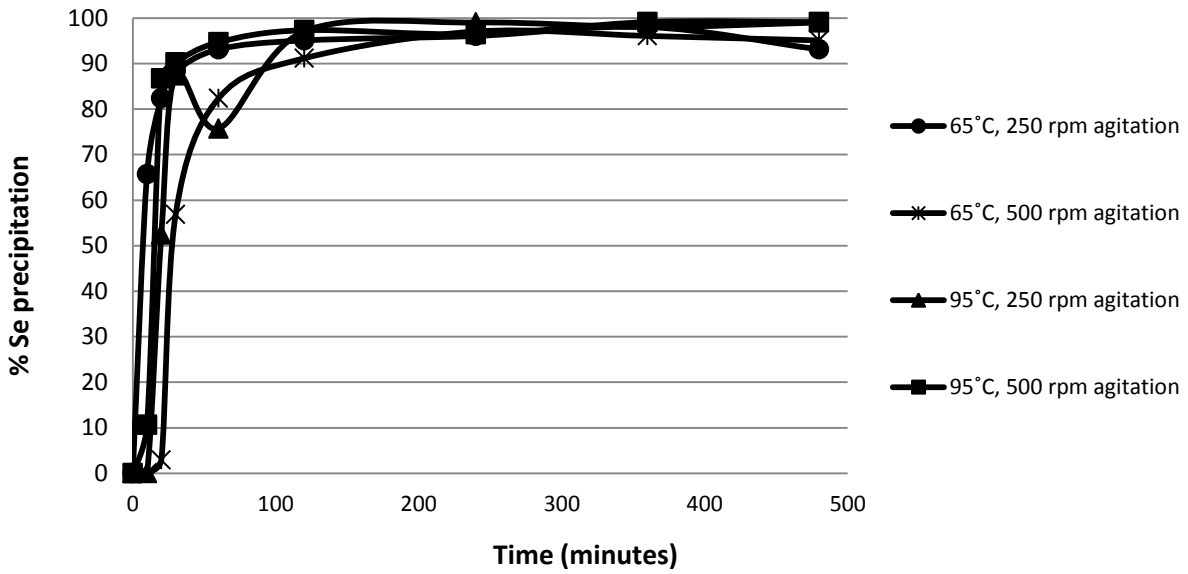

b)

Figure 4.4: Percentage Se precipitation achieved with: a. 4.4 cm³/min SO_2 flow rate b. 5.8 cm³/min SO_2 flow rate at typical operating conditions

4.1.2. Tellurium precipitation

In the case of the tests performed at 65°C with this experimental method, the tests performed at lower agitation rates achieved higher percentages Te precipitation after eight hours (80 % Te precipitation on average) than the tests performed at higher agitation rates (73 % Te precipitation on average). The results for the test performed at 65˚C and a SO_2 flow rate of 4.4 cm³/min are shown in figure 4.5 as an illustration of the typical Te precipitation behaviour observed.

At 95˚C, the agitation rate did not significantly influence the percentage Te precipitation achieved after eight hours; 93 % and 95 % Te precipitation on average were observed for the tests performed at low and high agitation rates respectively (figures 4.8 a and b).

It is not clear why increasing the agitation rate from 250 to 500 rpm resulted in lower Te precipitation after eight hours for all the tests performed at 65˚C. It seems as if the Te precipitation reactions had not attained equilibrium after eight hours for the tests described by the graphs shown in figure 4.5. The high Te precipitation achieved at lower agitation could possibly be due to the effect of localized supersaturation which is higher at low agitation rates and temperatures resulting in high nucleation rates. The slight improvement noticed in Te precipitation rate at initial period (0-240 minutes) with increase in agitation rate, for the test performed at 65˚C and a SO_2 flow rate of 4.4 cm³/min, could however be ascribed to high nucleation rate which is typical of every precipitation process that involves a high rate of stirring (Sohnel and Garside, 1992).

As was the case for the effect of the agitation rate on Te precipitation behaviour, the effect of SO_2 flow rate was also significant for the tests performed at a temperature of 65˚C regardless of the agitation conditions. For these tests, the percentage tellurium precipitation achieved after eight hours increased from 69 % to 84 % (on average) as the SO_2 flow rate was increased from 4.4 to 5.8 cm^3/min.

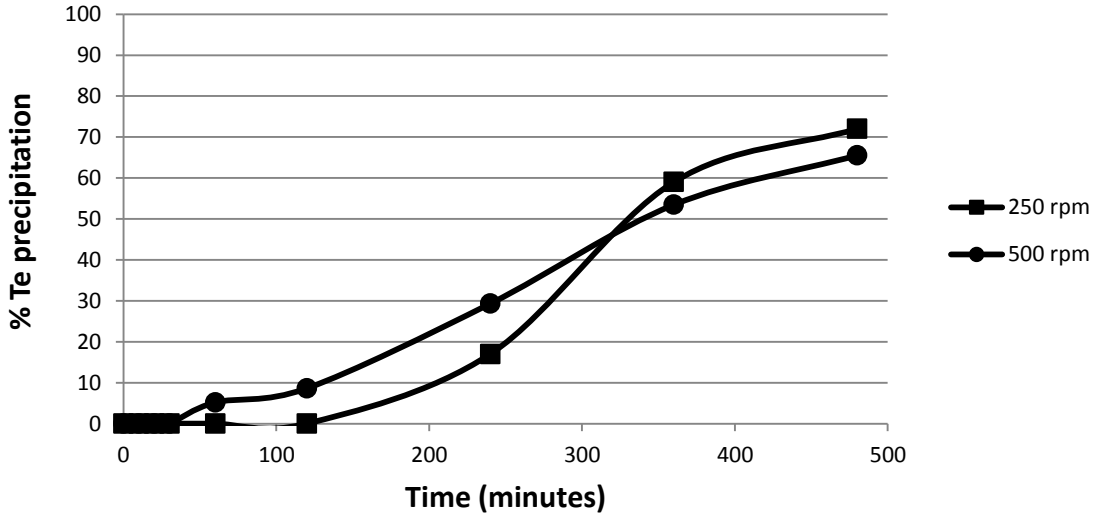

Figure 4.5: Effect of agitation on Te precipitation via SO_2 - based experimental method

The results achieved for the test performed at 65˚C at an agitation rate of 250 rpm are shown in figure 4.6 for illustrative purposes, while the results achieved via this experimental method at other process conditions are shown in figures 4.8 a and b. By comparing figure 4.8 a with figure 4.8 b, one can see the effects of increasing the SO_2 flow rate from 4.4 to 5.8 cm^3/min on Te precipitation at those process conditions. From these figures, it can be observed that higher SO_2 flow rate also contributed to faster precipitation reaction kinetics and allowed the precipitation to proceed at an earlier point in time.

It is likely that the increase in the SO_2 flow rate enhanced the rate of reduction of cupric ions to cuprous ions according to equation 2.22. As a result, the formation of elemental copper according to equation 2.25 and, subsequently, the precipitation of tellurium (equations 2.27 and 2.28) proceeded at a faster rate (Wang *et al.*, 2003).

As discussed before, the rate of cupric reduction and the subsequent elemental copper formation also appeared to increase as the temperature was increased. As a result, the rate of tellurium precipitation was noticeably faster at 95˚C than at 65˚C for the tests perfomed using this experimental method. An example of the faster precipitation kinetics observed is illustrated in

figure 4.7 for the test performed at an agitation rate of 250 rpm and a SO_2 flow rate of 4.4 cm^3/min. As shown in this figure, the percentage Te precipitation achieved for this test was higher at 95°C; 72% and 92% Te precipitation were achieved at 65 and 95˚C repectively.

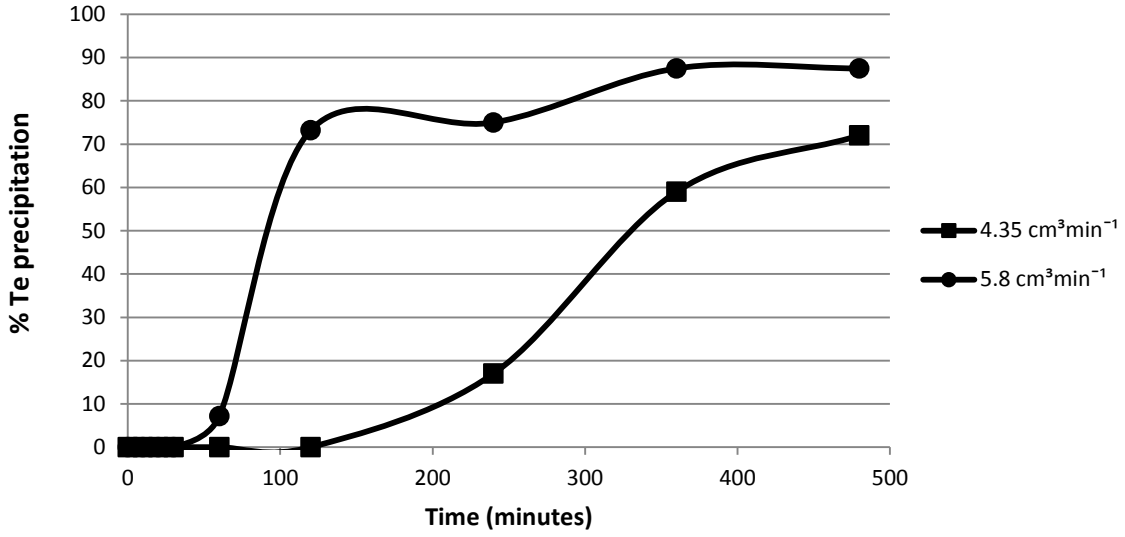

Figure 4.6: Effect of SO_2 flow rate on Te precipitation via SO_2 - based experimental method

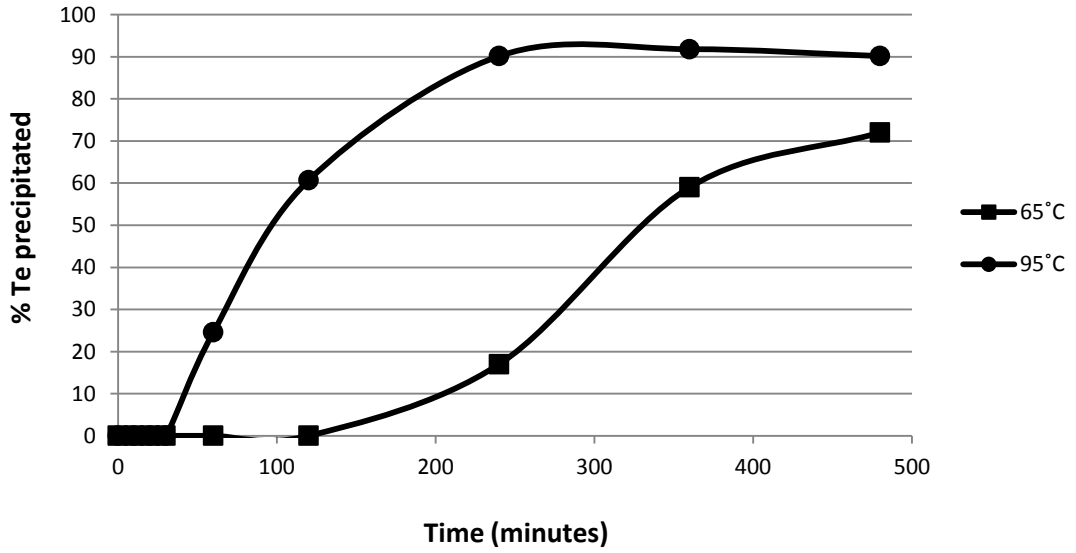

Figure 4.7: Effect of temperature on Te precipitation via SO_2 - based experimental method

Similar observations were made for the tests performed at other process conditions (figures 4.8 a and b). In general, for all the tests performed using this experimental method, the percentage tellurium precipitation increased from 77 % to 94 % on average as the temperature was increased from 65 to 95˚C.

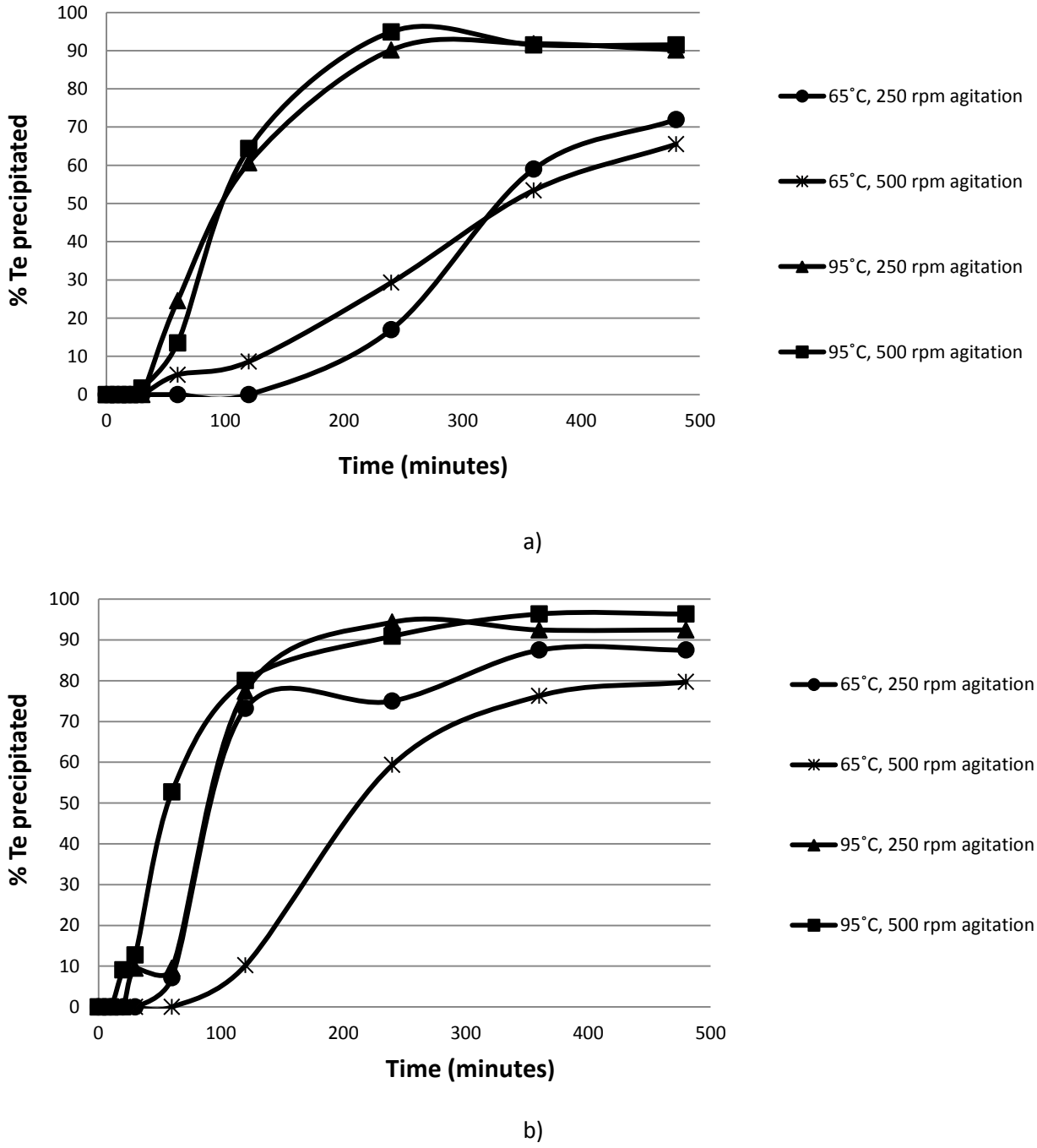

Figure 4.8: Percentage Te precipitation achieved with: a. 4.4 cm³/min SO_2 flow rate b. 5.8 cm³/min SO_2 flow rate at typical operating conditions

4.1.3. Base metal precipitation

Tables 5.4 through 5.11 (appendix D) show the changes observed in copper, iron and nickel concentrations during tellurium and selenium precipitation at different operating conditions. As shown in these tables, no significant precipitation of these base metals was observed for the various tests.

As discussed in section 2.6, the the ratio of copper concentration to tellurium concentration (present in the solution used for this study) is much larger than the ratio of copper concentration to Te concentration found in the leach solution used by Wang *et al.*(2003). This explains why a large decrease in Cu concentration was not observed for the tellurium precipitation achieved at any of the investigated experimental conditions, unlike the result presented by Wang *et al.*(2003). For clarity, the concentrations of copper and tellurium found in the solution used by Wang *et al.* (2003) and those used for this study are provided in tables 2.10 and 3.4, respectively.

4.1.4. OPM precipitation

The primary objective of this project was not to investigate the precipitation of other precious metals. It is, however, worthwhile to investigate the effects that the Te and Se removal methods (including the SO_2-based method) have on the co-precipitation of other precious metals which are also present in the copper sulphate solution used for this study.

Tables 5.4 through 5.11 also show the changes observed in Ru, Rh and Ir concentrations at different operating conditions, during tellurium and selenium precipitation via this experimental method. As shown in these tables, the co-precipitation of these precious metals was poor at all investigated conditions including when the SO_2 addition rate and the temperature were increased. Though slight improvements were seen in the recovery of Ru and Rh, in particular, when more SO_2 was added into the solution and when high temperature was used (tables 5.8 through 5.11). In general, a maximum of 15 % percentage OPMs precipitation was achieved for all the tests performed using this processing technique.

4.2. SO_2 only: Statistical analysis

The maximum Te and Se yield were considered as the responses for the three experimental methods in order to realize the primary objective of maximizing the precipitation of these impurities. Figure 4.9 graphically illustrate the maximum Te and Se yield observed for the eight experimental runs involving the use of SO_2 only, while the treatment combinations of these experimental runs and their respective responses are summarised in table 4.1.

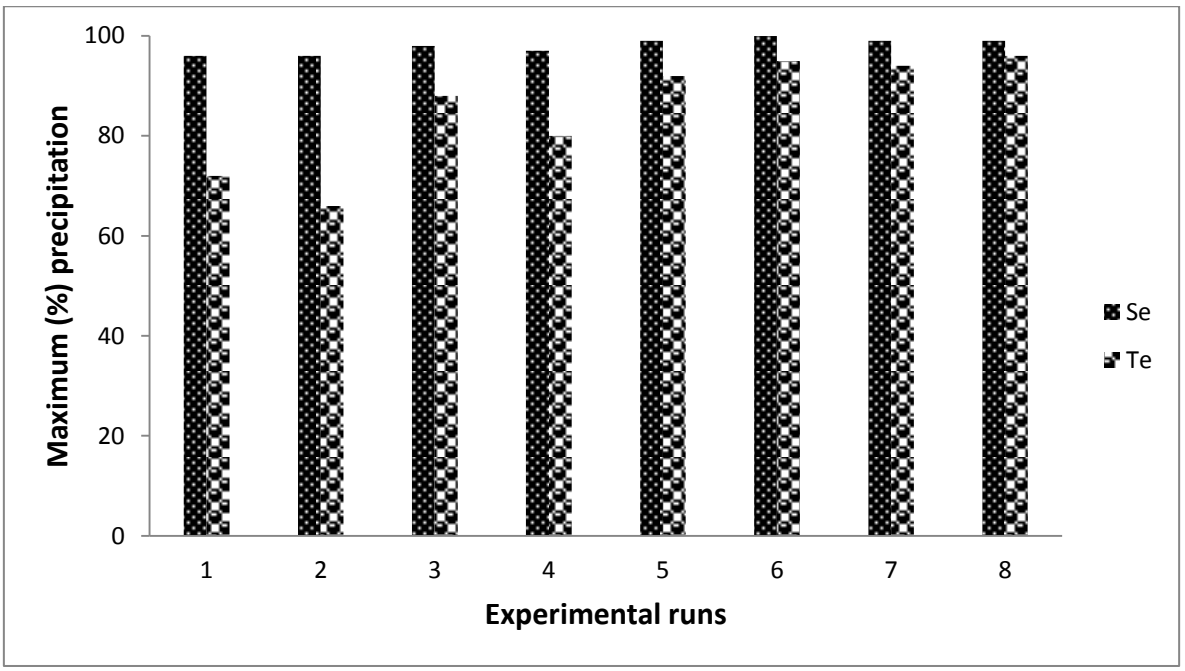

Figure 4.9: Observed maximum Se and Te precipitation for the eight runs of the SO_2-based experimental method

Table 4.1: Summary of the treatment combinations and their observed responses for the SO_2-based experimental method

Runs	Factors and Levels			Responses	
	A	B	C	x	y
1	65	4.4	250	72	96
2	65	4.4	500	66	96
3	65	5.8	250	88	98
4	65	5.8	500	80	97
5	95	4.4	250	92	99
6	95	4.4	500	95	100
7	95	5.8	250	94	99
8	95	5.8	500	96	99

Where:

A represents temperature (^oC)

B represents SO_2 flow rate (cm^3/min)

C represents agitation speed (rpm)

x represents the maximum tellurium precipitation observed for the SO_2-based experimental method

y represents the maximum selenium precipitation observed for the SO_2-based experimental method.

The values of the responses noticed for these treatment combinations were, however, used to determine the process variables that have the main effects on Te and Se yield via this experimental method.

4.2.1. Analysis of variance

Analysis of variance was used to investigate the model terms and the major interactions that have significant effects on the maximum Te and Se yield. The model terms, their p-values and the R^2 values obtained for the two responses are summarised in tables 4.2 and 4.3. The full factorial models that include the sum of squares, the predicted sum of squared errors and the other relevant statistical terms can be found in appendix E.

Table 4.2: ANOVA table (Derived from Design Expert) showing the effects of significant model terms on the maximum Te precipitation achieved via the SO_2-based experimental method

Model Terms	Coefficient Estimates	p-value
Intercept	**85.38**	
A- Temperature (^oC)	**8.88**	**0.001**
B –SO_2 addition rate (cm^3/min)	**4.13**	**0.0093**
C- Agitation speed (rpm)	-	0.0704
AB	**-3.38**	**0.0162**
AC	**2.37**	**0.0409**
BC	-	0.2048
		R-squared = 0.9876
		Adj R-squared = 0.9710

Table 4.3: ANOVA table (Derived from Design Expert) showing the effects of significant model terms on the maximum Se precipitation achieved via the SO_2-based experimental method

Model Terms	Coefficient Estimated	p-value
Intercept	**98**	
A - Temperature (^oC)	**1.25**	**0.0013**
B - SO_2 addition rate (cm^3/min)	-	0.3081
C – Agitation (rpm)	-	1.0000
AB	**-0.5**	**0.0493**
AC	-	0.2929
BC	-	0.2929
		R-squared = 0.9062
		Adj R-squared = 0.8687

The p-values of less than 0.05 for temperature and SO_2 flow rate, as shown in table 4.2, indicate that these process variables have more statistically significant effects on maximum Te yield than any other variable. The small p-values of temperature-SO_2 flow rate interaction and temperature-agitation interaction also indicate that these model terms have significant effects on the maximum Te yield. The p-value of 0.0013 for temperature, as shown in table 4.3, indicates that this process

variable has more statistically significant effect on the maximum Se yield than the other process variables, while the p-value of 0.0493 for temperature-SO_2 flow rate interaction indicates that this interaction has more statistically significant effect on the maximum Se yield than any other interaction.

These observations are in agreement with the qualitative analysis of the experimental data presented in section 4.1.1 and 4.1.2, where it was shown that temperature and SO_2 flow rate are the most influential factors that result in high tellurium and selenium precipitation. The insignificant model terms and interactions were not included in the models, but are shown in tables 4.2 and 4.3 for clarity.

Figures 4.10 a through f graphically illustrate the effects of second order interactions on the maximum Te and Se yield achieved via the SO_2-based experimental method. As seen in these figures, the temperature-SO_2 flow rate interaction indicates that SO_2 flow rate has a major positive effect on the maximum Te yield at a low level of temperature but has a mild effect at high level of temperature (fig. 4.10 a). The temperature-agitation interaction indicates that agitation has a negative effect on the maximum Te yield at a low level of temperature but has no profound effect at high level of temperature (fig 4.10 b). The temperature-SO_2 flow rate interaction also indicates that SO_2 flow rate has a major positive effect on the maximum Se yield at a low level of temperature but has a mild effect at a high level of temperature (fig 4.10 d).

Based on the statistical analysis performed in this section, the regression models (given in terms of actual factors) that determine the maximum Te and Se yield are thus given as follows:

$$\textbf{Maximum Te yield} = -123.16 + 2.26 \times \text{Temperature } (^{\circ}C) + 31.61 \times SO_2 \text{ flow rate } (cm^3/min) - 0.32 \times \text{Temperature } (^{\circ}C) \times SO_2 \text{ flow rate } (cm^3/min) - (6.57 \times 10^{-5}) \times \text{Temperature } (^{\circ}C) \times \text{Agitation } (rpm) \quad (4.1)$$

$$\textbf{Maximum Se yield} = 91.33 + 0.070 \times \text{Temperature } (^{\circ}C) + (2.70 \times 10^{-3}) \times \text{Temperature } (^{\circ}C) \times SO_2 \text{ flow rate } (cm^3/min) \quad (4.2)$$

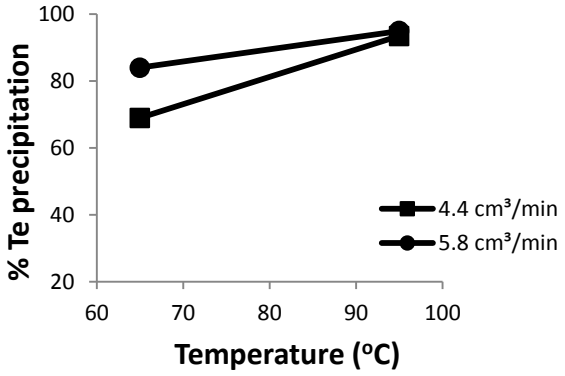

a. Effect of temperature – SO_2 flow rate interaction on Te yield

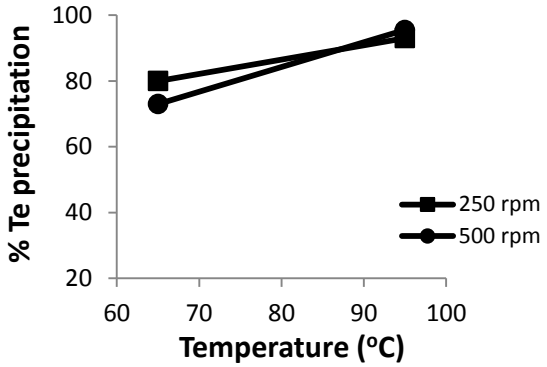

b. Effect of temperature – agitation interaction on Te yield

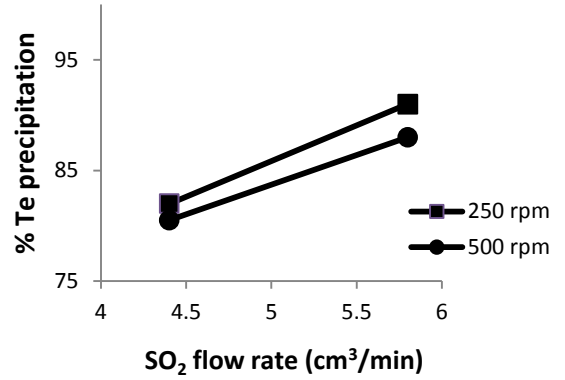

c. Effect of SO_2 flow rate – agitation interaction on Te yield

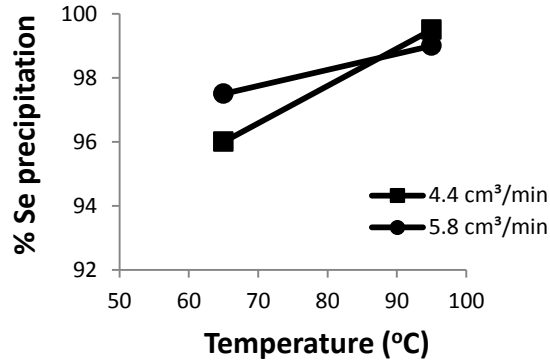

d. Effect of temperature – SO_2 flow rate interaction on Se yield

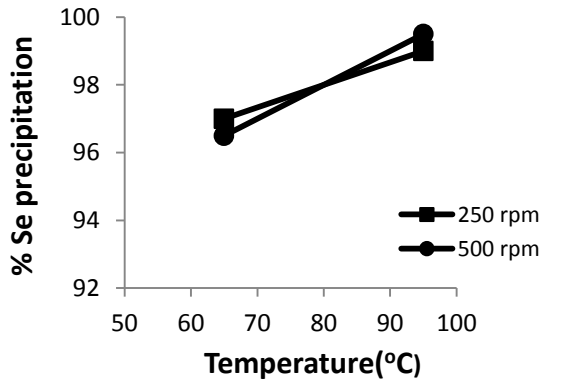

e. Effect of temperature – agitation interaction on Se yield

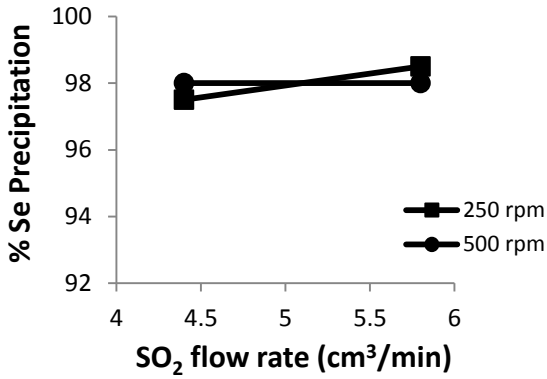

f. Effect of SO_2 flow rate – agitation interaction on Se yield

Figure 4.10: Effects of 2-order factor interactions on maximum Te and Se yield via the SO_2-based experimental method

4.2.2. Optimizing Te yield

As illustrated in the regression models presented in section 4.2.1, the process variables that influence the Te yield also result in significant improvement in the recovery of selenium. Also,

given the fact that Se recovery is satisfactory at current operating conditions, the focus of this study was therefore shifted to optimising Te recovery from the solution via this method.

Contour plots were generated using Design Expert in order to determine the regions of operability that favour high Te yield via this experimental method. This was done by keeping the agitation speed constant while varying the levels of temperature and the SO_2 addition rate along the x and y axes. The agitation speed was kept constant because it has a minimal influence on the tellurium yield at high temperature. As illustrated in figure 4.11, the regions that guarantee improved tellurium yield, point in the direction of high SO_2 additon rate and high temperature condition (the upper right corner of the plots).

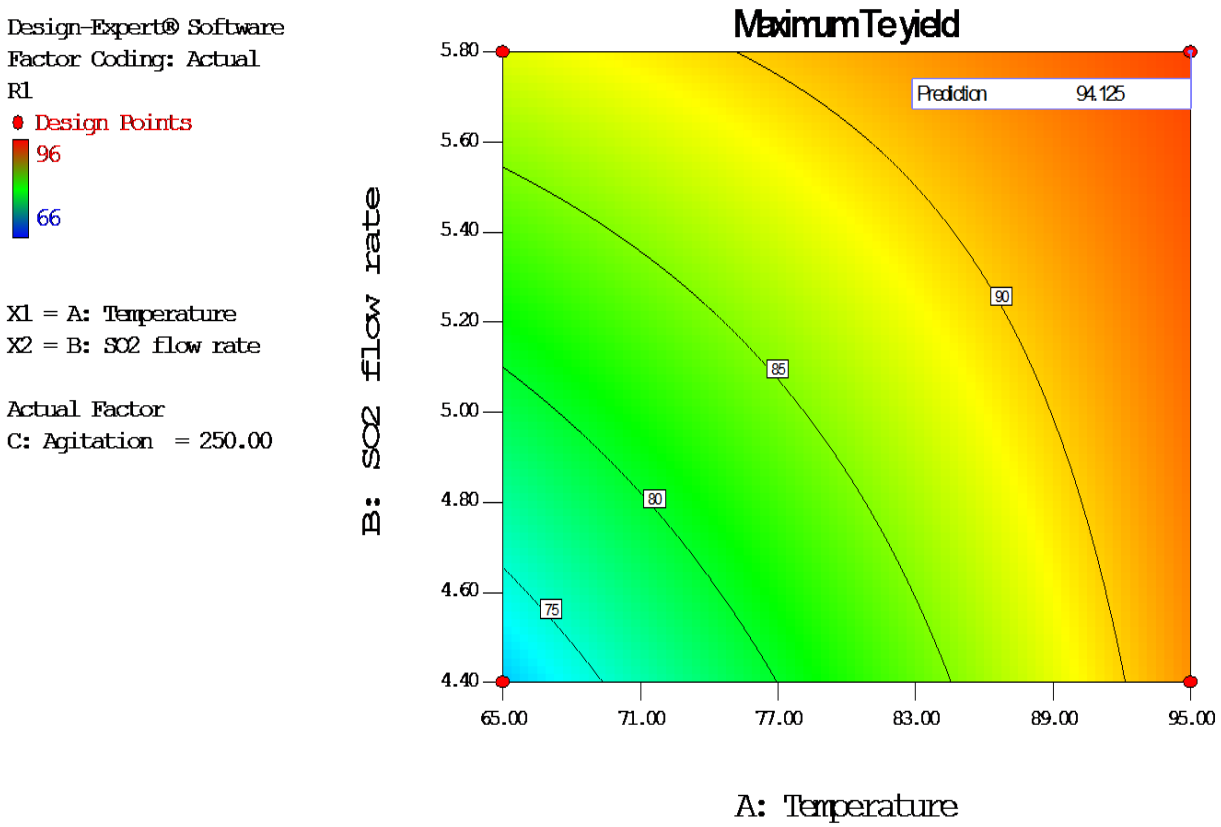

Figure 4.11: Contour plot showing the region that favours maximum Te yield via the SO_2-based experimental method (Derived from Design Expert)

The Design Expert software was also used to find the optimum solutions for the optimum criteria specified in table 4.4 using the desirability method suggested by Derringer and Suich (1980). The optimum solutions obtained for this experimental method also indicate that operating at high SO_2 flow rate and high temperature will result in the highest Te precipitation.

Table 4.4: Selection of optimum criteria for Te yield via the SO_2-based experimental method (Derived from Design Expert)

Name	Goal	Lower value	Upper values	Importance
A: Temperature (°C): factor	In range	65	95	3
B: SO_2 flow rate (cm^3/min): factor	In range	4.4	5.8	3
C: Agitation (rpm): factor	In range	250	500	3
Maximum Te yield, x (%): Response	Maximise	66	96	3
Maximum Se yield, y (%): Response	Maximise	96	100	3

4.3. SO_2 only: Precipitate analysis

As discussed in section 2.1.3, the two main factors that determine the morphology and crystallinity of the precipitates obtained during precipitation processes are temperature and stirring intensity. In this section, the effects of the investigated variables on the precipitate characteristics and the formation of phases were investigated.

The first experimental run in table 4.1 was considered the normal experimental condition,the second, third and fifth experimental runs were regarded as the experimental conditions involving improved agitation condition, high SO_2 addition rate and high temperature condition, respectively. The quantitative EDX analyses of the precipitates obtained after the completion of the tests performed at other process conditions using this experimental method are summarized in tables 5.96 through 5.99 (Appendix F), while the SEM images that show the particle morphologies and crystallinities of these precipitates are provided in figures 5.7 a through d.

4.3.1. Effect of agitation

Figures 4.12 a and b show the SEM images of the precipitates formed during the experiment performed at normal and at improved agitation conditions. As illustrated in these figures, the samples analysed consist of irregularly-shaped amorphous structures which are typically found in precipitates produced via precipitation reactions carried out at a low temperature (Demopoulos, 2009).

Quantitative EDX analyses of the solid samples obtained for both experimental conditions were also performed with the outcomes summarised in tables 4.5 and 4.6 respectively. As shown in these tables, only minute traces of elemental selenium were observed in the samples for the two experimental conditions. One can also see that there is no significant increase in the concentrations

of Se and Te found in the solid samples as the agitation rate was increased from 250 to 500 rpm. This observation is in agreement with the earlier discussion in sections 4.1.1 and 4.1.2, where it was shown that increasing the agitation rate did not result in significant increase in the extents of selenium and tellurium precipitation achieved for this processing technique. By comparing table 4.5 with table 4.6, one can also observe that larger Ni and S concentrations in the solid sample for the test performed at high agitation than for the test performed at low agitation. The relatively larger sulphur and nickel content seen in table 4.6 is as a result of the presence of Ni_3S_2 phase as a significant inclusion in the precipitate produced during the test performed at that operating condition. No copper crystals were, however, found in the precipitates obtained after the completion of the tests performed at both experimental conditions

Additionally, a mineralogical examination of these samples revealed the presence of copper sulphide phases (Cu_2S phase for the experiment carried out at normal condition and CuS phase for the experiment performed with improved agitation condition). Little traces of Ni-Pb-Cu oxide phases and minute inclusions of PGMs and Cu_2Te phase were also detected in both samples.

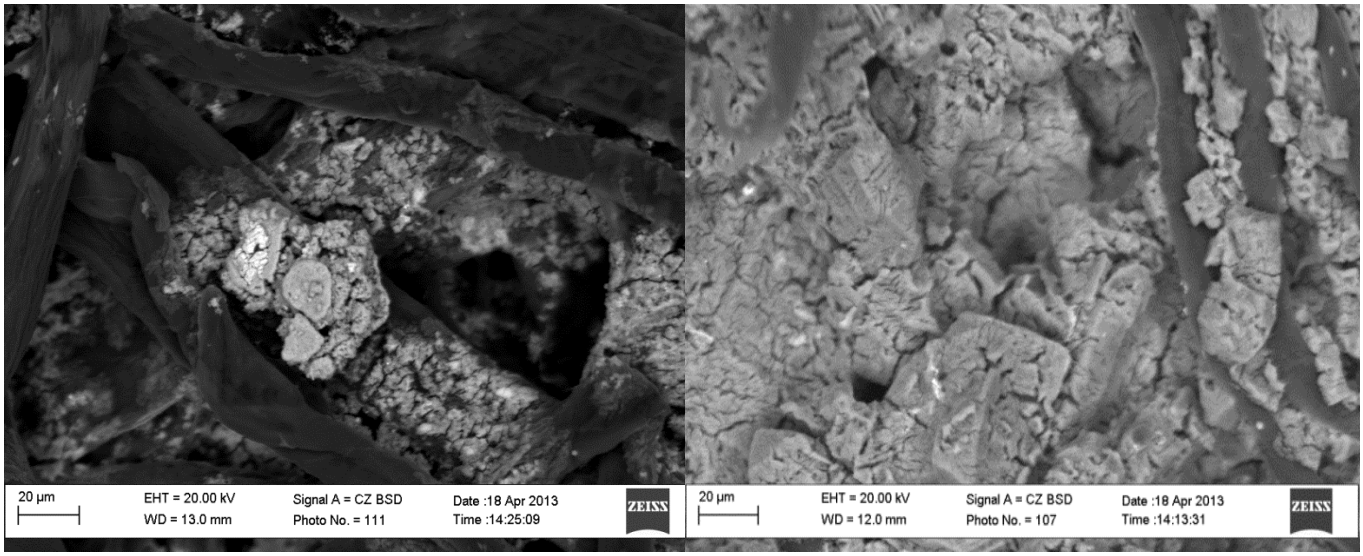

a) b)

Figure 4.12: SEM images of the precipitates obtained after the completion of the SO_2-based experiments performed: a. at normal condition b. with improved agitation condition.

.

Table 4.5: Quantitative EDX analyses (wt%) of solid sample obtained after the completion of the SO_2-based experiment performed at normal condition

Analysis	Rh*	Ru*	Ir*	Ni*	Fe*	Pb*	Cu*	Se*	Te*	S*	Total
1	0	1.08	0	0.57	0	0	85.09	1.42	0.79	11.06	100.01
2	0	0.83	0	0	0	1.25	84.00	0	0	13.92	100.00
3	0	0	0	1.58	0	0	74.79	4.10	1.27	18.25	99.99
Average (wt%)	0	0.64	0	0.72	0	0.42	81.29	1.84	0.69	14.41	100.01
*Elements combined with oxygen											
Entire sample analysed thrice											

Table 4.6: Quantitative EDX analyses (wt%) of solid sample obtained after the completion of the SO_2-based experiment performed with improved agitation condition

Analysis	Rh*	Ru*	Ir*	Ni*	Fe*	Pb*	Cu*	Se*	Te*	S*	Total
1	0	1.57	0	7.94	0	3.39	44.59	0	0	42.51	100.00
2	0	1.41	0	14.28	0.25	2.87	38.03	2.17	0.48	40.52	100.01
3	0	1.75	0.63	27.90	0.39	6.05	15.46	4.86	0	42.95	99.99
Average (wt%)	0	1.58	0.21	16.71	0.21	4.10	32.69	2.34	0.16	41.99	99.99
*Elements combined with oxygen											
Entire sample analysed thrice											

4.3.2. Effect of SO_2 addition

Figure 4.13 b shows the SEM image of the solid sample formed during the test performed using a higher SO_2 flow rate. As illustrated in this figure, tiny evenly distributed crystal structures suggestive of cuprous selenide particles were observed, when this solid sample was analysed.

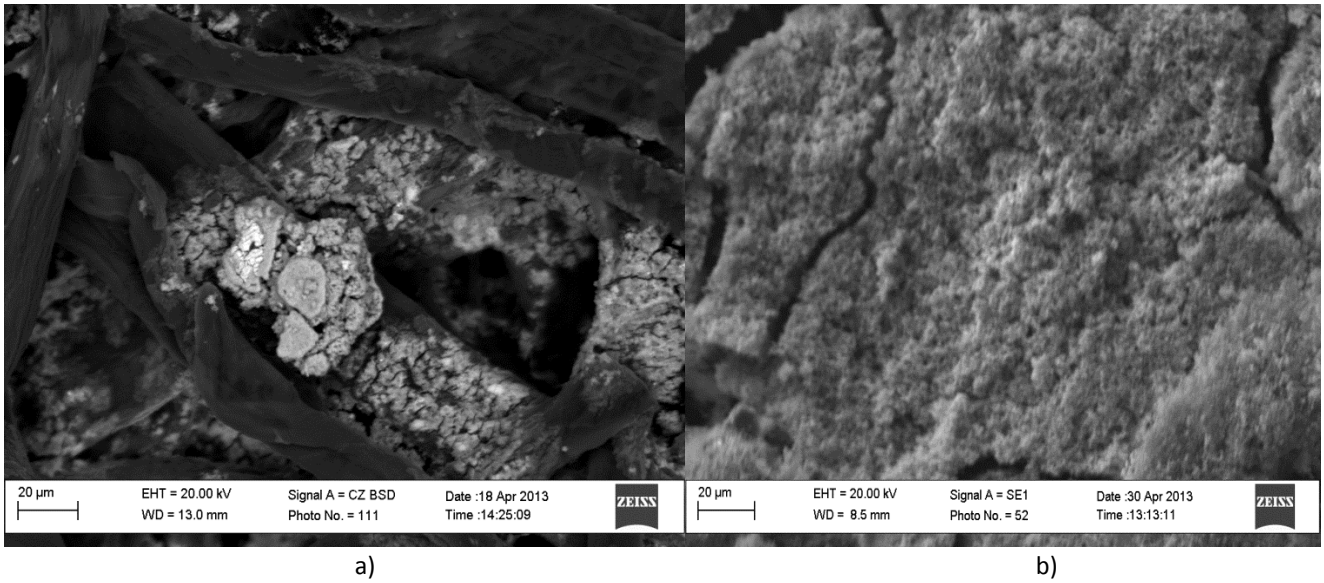

a) b)

Figure 4.13: SEM image of precipitate obtained after the completion of the SO_2-based experiment performed : a. at normal condition b. with higher SO_2 addition rate

The outcome of the quantitative EDX analyses of this sample is summarised in table 4.7. As shown in this table, there is a relatively high Se and Te content in this sample. The high Se and Te concentrations seen in the solid sample is also in agreement with the observation made in sections 4.1.1 and 4.1.2, where it was shown that high SO_2 flow rate resulted in better selenium and tellurium precipitation. One can also observe that there is a significant improvement in the concentrations of the PGMs present in the sample when compared with what was achieved for the test performed at normal condition.

When a mineralogical study of the sample was done, Cu_2Se and CuS were found to be the major phases present. The occurrence of Cu_2Se as a major phase in the solid sample is in agreement with the observation made in section 4.1.1 where it was stated that the high Se precipitation achieved with increase in SO_2 flow rate could be attributed to the reductive precipitation of selenium as cuprous selenide. The minor phases detected in the sample are the Fe-Pb-Ni-Cu oxide and Cu_2Te phases and minute inclusion of PGMs.

Table 4.7: Quantitative EDX analyses (wt%) of solid sample obtained after the completion of the SO_2-based experiment performed using higher SO_2 addition rate

Analysis	**Rh***	**Ru***	**Ir***	**Ni***	**Fe***	**Pb***	**Cu***	**Se***	**Te***	**S***	**Total**
1	1.54	5.80	1.19	2.95	0.65	3.61	29.40	20.15	9.05	25.68	100.02
2	1.11	5.54	1.43	3.96	0.67	3.84	29.33	16.04	9.07	29.01	100.00
3	1.24	6.18	1.26	2.78	0.68	4.33	28.10	21.11	8.92	25.38	99.99
Average (wt%)	1.30	5.84	1.29	3.23	0.67	3.93	28.94	19.10	9.01	26.69	100.00
*Elements combined with oxygen											
Entire sample analysed thrice											

4.3.3. Effect of temperature

Fig 4.14 b shows the SEM image of the solid sample formed during the experiment performed at high temperature condition, while table 4.8 shows the relative concentrations of elements found in the solid sample after quantitative SEM-EDX analysis was performed. As seen in this figure, the sample analysed consists of cubical-shaped and needle-shaped crystal structures typical of precipitation processes involving high temperature condition (Demopoulos, 2009).

In addition, a mineralogical examination of the solid sample revealed copper crystals and Cu-oxide phases as the predominant components present in the precipitate with tiny inclusions of Cu_2Se and CuS phases present on the surfaces of the crystals. By comparing table 4.5 with table 4.8, one can also observe that the Se and Te contents of the precipitate obtained for the test performed at high temperature are very low, while the Cu concentration is very large. This observation could be

attributed to the fact that larger amount of metallic Cu was precipitated out of the solution for the test performed at that operating condition. The presence of large copper crystals in this sample is in agreement with the earlier discussion (in sections 4.1.1 and 4.1.2) where it was argued that the high Te and Se precipitation achieved at high temperature condition was as a result of the cementation reactions between these impurities, and the metallic copper deposits produced during the disproportionation of cuprous.

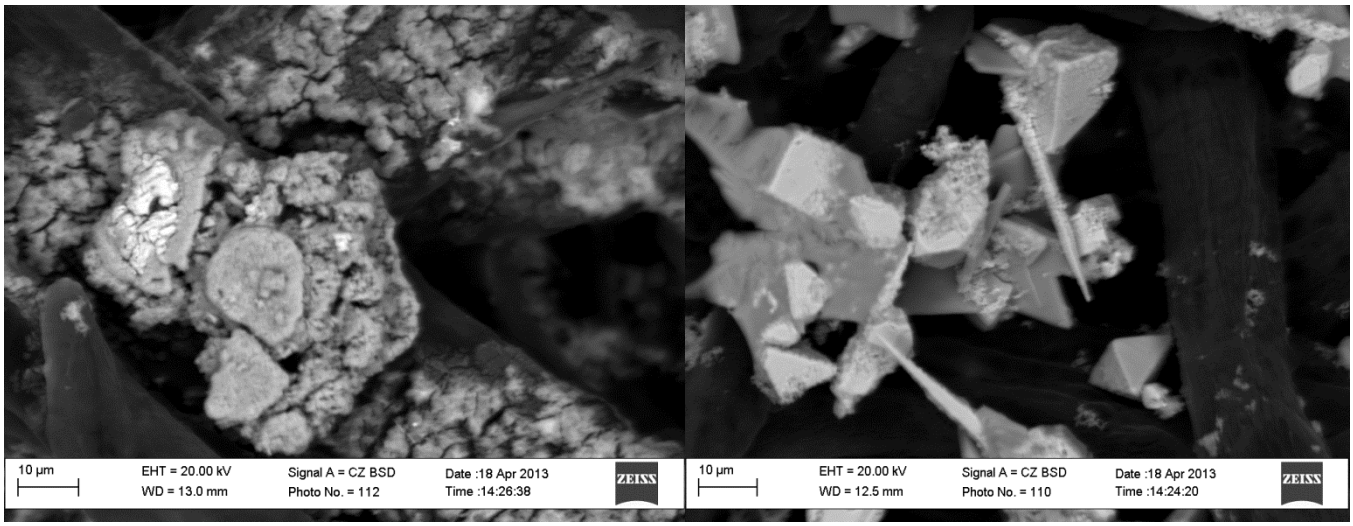

a) b)

Figure 4.14: SEM image of precipitate obtained after the completion of the SO_2-based experiment performed at: a. normal condition b. higher temperature condition

Table 4.8: Quantitative EDX analyses (wt%) of solid sample obtained after the completion of the SO_2-based experiment performed at high temperature condition.

Spectrum	Rh*	Ru*	Ir*	Ni*	Fe*	Pb*	Cu*	Se*	Te*	S*	Total
1	0	0	0	0.17	0	0	99.36	0	0	0.47	100.00
2	0	0.42	0	0	0	0.68	97.40	0.52	0	0.97	99.99
3	0	0	0	0	0	0	100.00	0	0	0	100.00
4	0	0	0	0	0	0	99.30	0	0	0.70	100.00
Average (wt%)	0	0.11	0	0.04	0	0.17	99.00	0.13	0	0.54	99.99
*Elements combined with oxygen											
Sites of interest analysed											

4.4. Effects of factors on precipitation with SO_2 and Cu plate

4.4.1. Se precipitation

Agitation has similar effects on Se precipitation for the tests performed with copper plate addition and the tests performed without any copper addition. Figure 4.15 shows the effect of increasing the

agition rate on selenium precipitation for the tests performed at 65˚C with the use of SO_2 (4.4 cm³/min SO_2 flow rate) as a precipitation agent and copper plate (202.5 mm²/L surface area) as a precipitation enhancing agent. As shown in this figure, increasing the agitation rate from 250 to 500 rpm resulted in a noticeable improvement in Se precipitation rate during the first 60 minutes, while the percentages Se precipitation achieved after eight hours are comparable (93% and 94%, respectively) for the two agitation conditions.

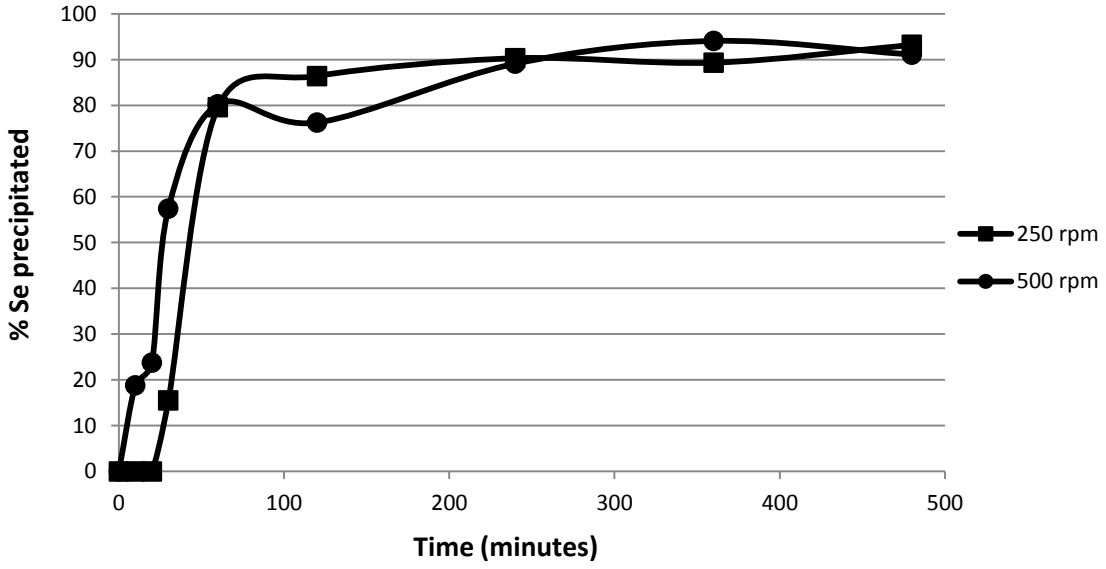

Figure 4.15: Effect of agitation on Se precipitation via SO_2 and Cu plate-based experimental method.

The extents of Se precipitation are also comparable for the tests performed at other process conditions, though increasing the agitation speed from 250 to 500 rpm did not result in significantly faster Se removal rate at early period (0-60 minutes) for all the tests performed at 95˚C using this experimental method. This observation is illustrated in figures 4.19 a through 4.20 b. The slight improvement noticed for the tests performed at 65˚C with increase in agitation rate could also be attributed to high nucleation rate brought about by high rate of stirring (Sohnel and Garside, 1992).

As was the case for the effect of SO_2 flow rate on Se precipitation behaviour for the first experimental method, the effect of SO_2 flow rate was also pronounced on selenium precipitation rate for this processing technique. Figure 4.16 shows the result of the test performed at 65˚C and 250 rpm agitation rate with a copper plate of 202.5 mm²/L surface area, as an illustration of a typical Se precipitation behaviour observed when the SO_2 flow rate was increased. As shown in this figure, higher SO_2 flow rate allowed the Se precipitation to proceed at an earlier point in time; 65% Se precipitation was achieved in 20 minutes when the SO_2 flow rate was increased from 4.4 to

5.8 cm³/min. By comparing figure 4.19 a with figure 4.19 b and figure 4.20 a with figure 4.20 b, one can see the effects of increasing the SO_2 flow rate on Se precipitation for all the tests performed using this experimental method.

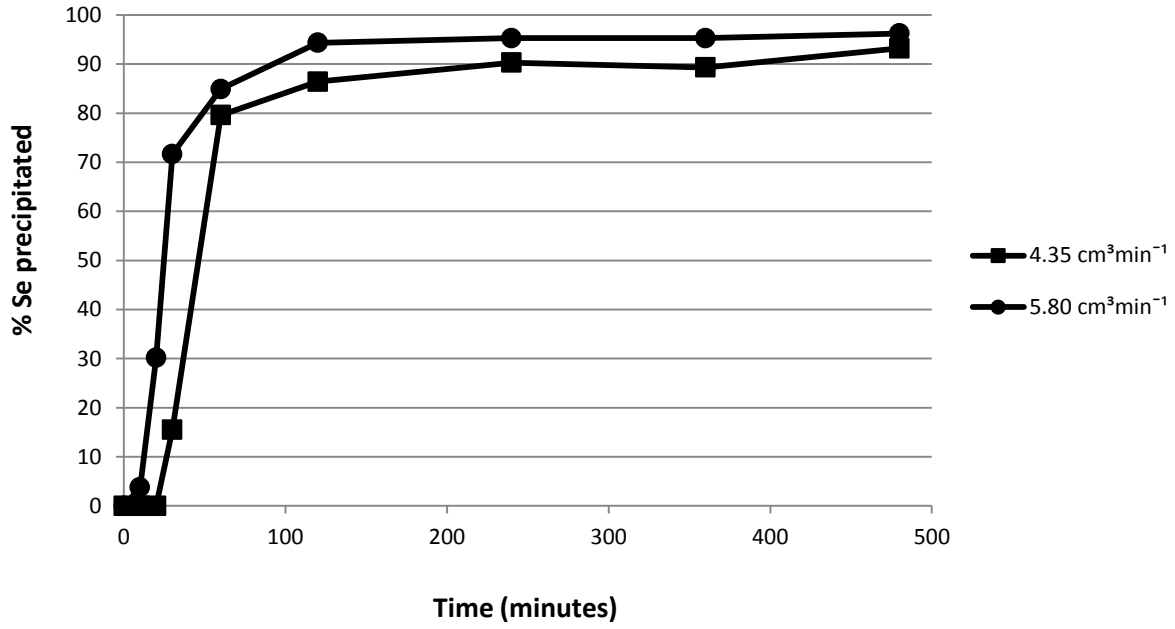

Figure 4.16: Effect of SO_2 flow rate on Se precipitation via SO_2 and Cu plate-based experimental method.

As discussed in section 4.1.1, increasing the SO_2 flow rate could accelerate both the reductive precipitation of selenium ions as elemental Se (equation 2.30) and the formation of cuprous ions (equation 2.22) which could potentially precipitate selenium from the copper sulphate solution as Cu_2Se according to equations 2.23 and 2.24.

The use of copper plate(s) of larger surface areas also resulted in significantly faster Se precipitation rate. An example of the faster selenium precipitation kinetics observed with increase in the surface area of copper plate used for this processing technique is illustrated in figure 4.17. Figure 4.17 shows the result of the test performed at 65˚C and 250 rpm agitation rate using a SO_2 flow rate of 4.4 cm³/min. As shown in this figure, increasing the surface area of the copper plate used from 202.5 to 405.0 mm²/L, resulted in a faster Se removal rate; 65% percentage Se precipitation was achieved in 20 minutes. The introduction of a copper plate of a larger surface area enhanced the selenium precipitation according to reaction 2.29. By comparing fig. 4.19 a with fig. 4.20 a and fig. 4.19 b with fig. 4.20 b, one can also see that increasing the surface area of copper plate did not have a significant effect on Se precipition.

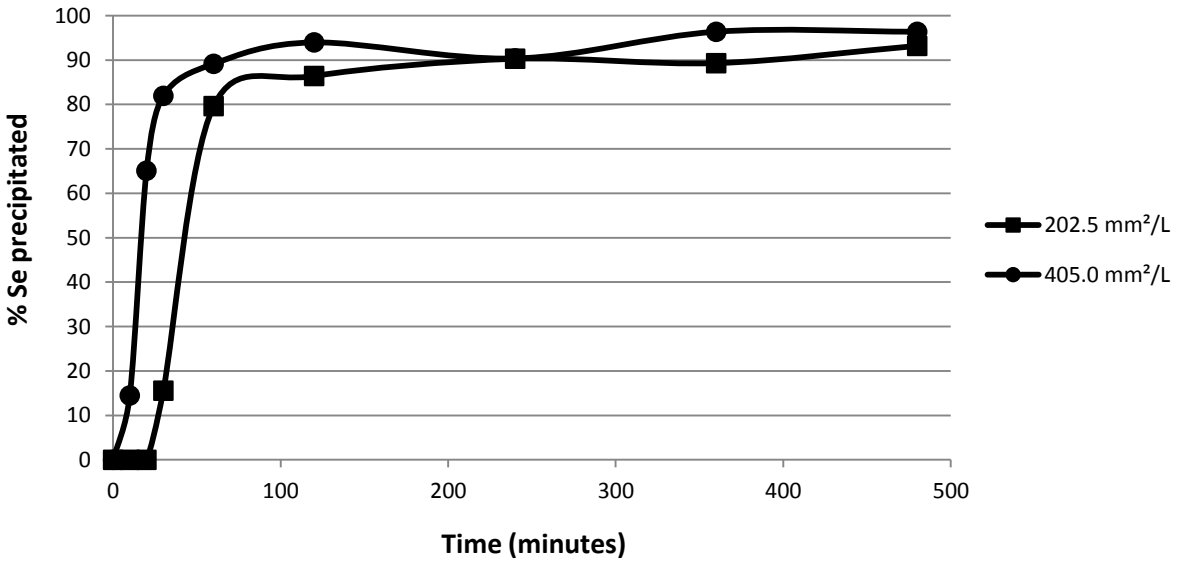

Figure 4.17: Effect of increasing surface area of Cu plate on Se precipitation via SO_2 and Cu plate-based experimental method.

As discussed before, temperature also has a pronounced effect on the selenium precipitation behaviour observed for this experimental method. Figure 4.18 shows the result of the test performed at an agitation rate of 250 rpm using SO_2 (4.4 cm^3/min flow rate) and copper plate (202.5 mm^2 surface area) as precipitation reagents. As shown in this figure, increasing the temperature from 65 to 95˚C resulted in a faster rate of Se precipitation achieved; higher temperature achieved not less than 80% Se precipitation at initial period (0-30 minutes).

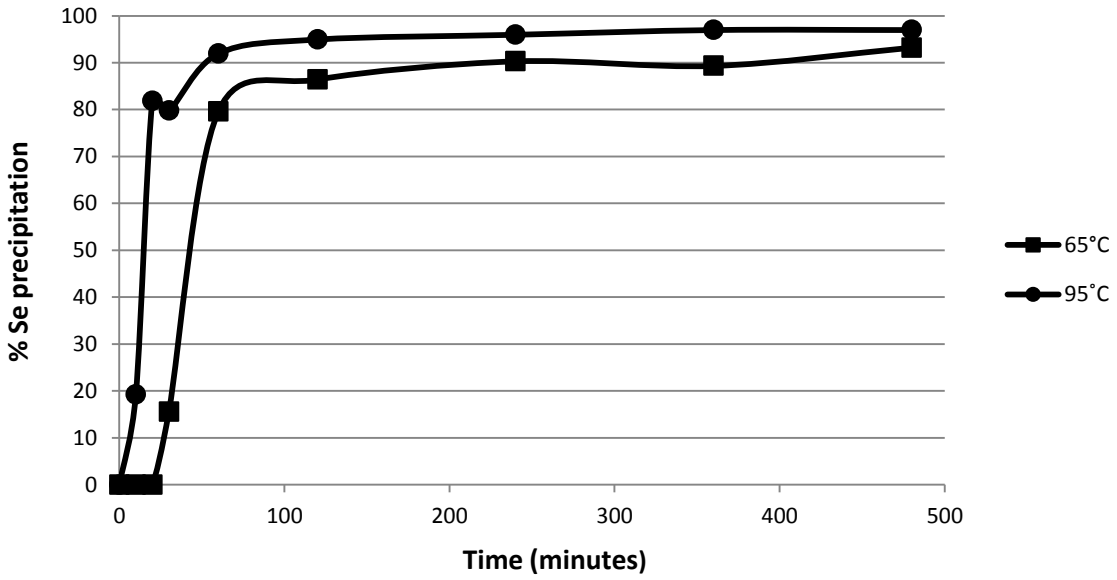

Figure 4.18: Effect of temperature on Se precipitation via SO_2 and Cu plate-based experimental method

Similar results were also obtained for the tests performed at other operating conditions (figures 4.19 and 4.20). One can observe from figures 4.19 and 4.20 that faster Se removal was achieved for all the tests performed at higher temperature condition. As discussed previously, it seems increasing the temperature also accelerated the reductive precipitation of selenium by metallic copper (via cementation reaction according to reaction 2.29) and the formation of cuprous ions which also enhances Se precipitation as Cu_2Se (equations 2.23-2.24)

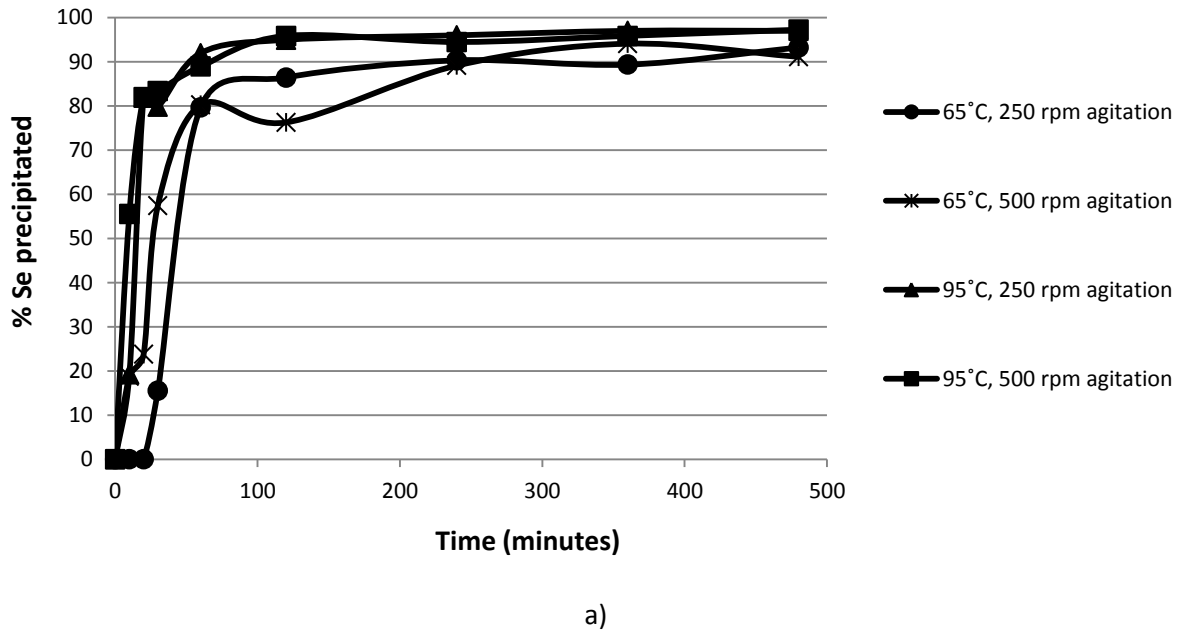

a)

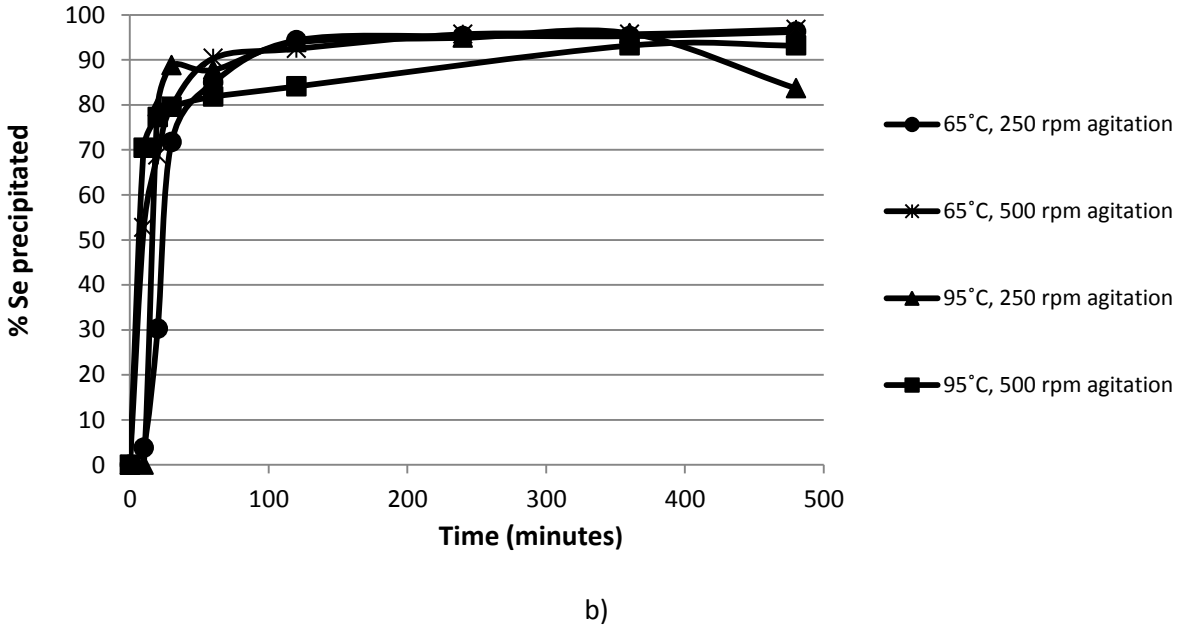

b)

Figure 4.19: Percentage Se precipitation achieved with: a. 4.4 cm^3/min SO_2 flow rate and 202.5 mm^2/L Cu plate b. 5.8 cm^3/min SO_2 flow area and 202.5 mm^2/L Cu plate at typical operating conditions

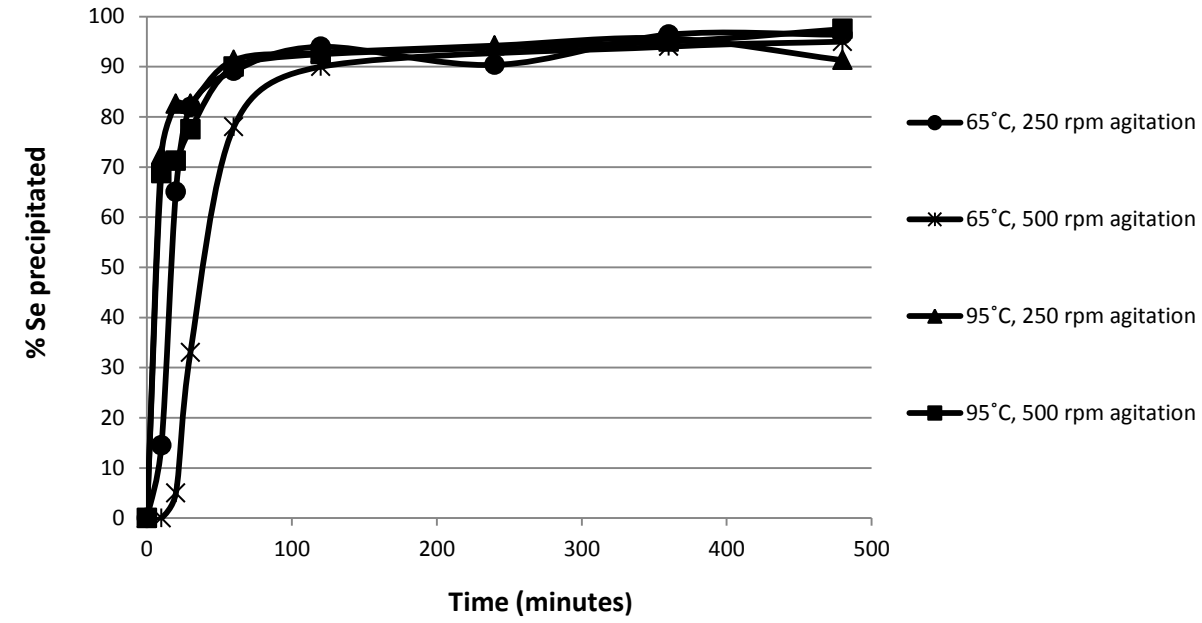

a)

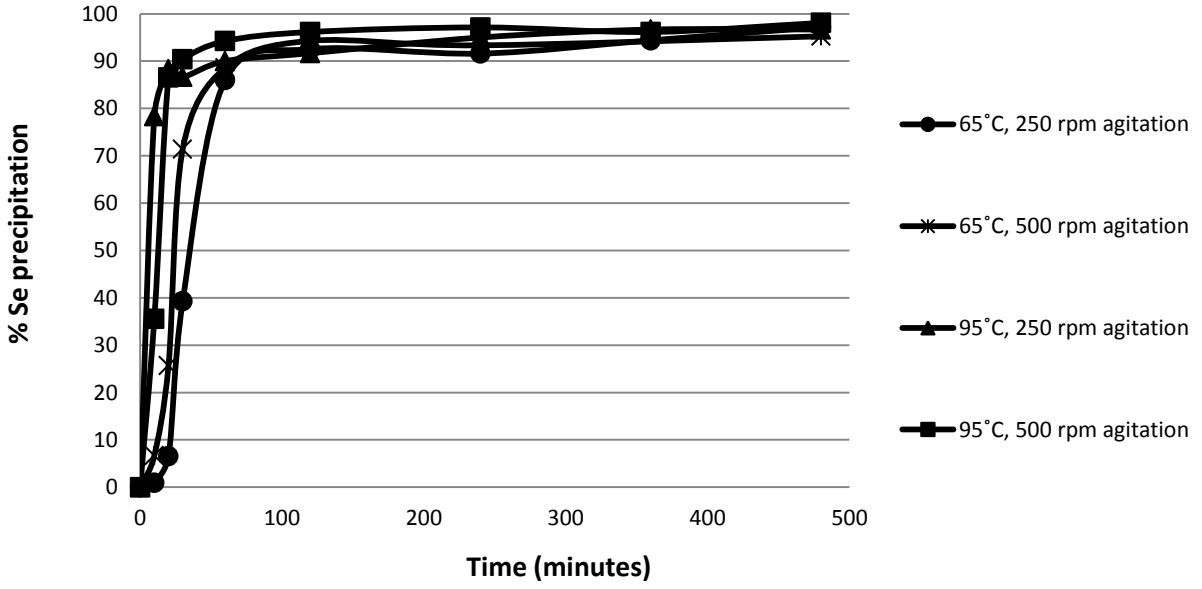

b)

Figure 4.20: Percentage Se precipitation achieved with: a. 4.4 cm^3/min SO_2 flow rate and 405.0 mm^2/L Cu plate b. 5.8 cm^3/min SO_2 flow rate and 405.0 mm^2/L Cu plate at typical operating conditions

4.4.2. Te precipitation

As was the case for the tests performed at 65˚C with SO_2 only, the tests performed at lower agitation rates with Cu plate addition also achieved higher percentages Te precipitation after eight hours (88 % Te precipitation on average) than the tests performed at higher agitation rates (77 %

Te precipitation on average). The results for the test performed at 65˚C with a SO_2 flow rate of 4.4 cm^3/min and a copper plate with surface area of 202.5 mm^2 are shown in figure 4.21 as an example of the typical Te precipitation behaviour observed using this processing technique. At 95˚C, the agitation rate did not significantly influence percentage Te precipitation achieved after eight hours for either the tests utilizing SO_2 only or the tests utilizing Cu plates as precipitation enhancing reagent (figures 4.25 and 4.26). However, it is not clear why increased agitation resulted in poor Te precipitation achieved for this processing technique too.

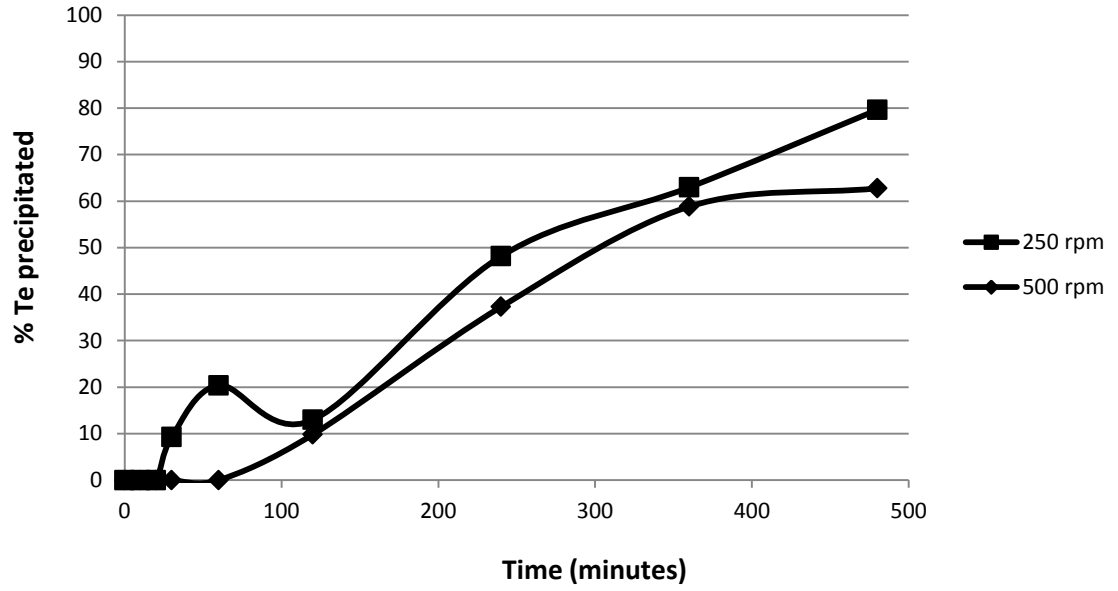

Figure 4.21: Effect of agitation on Te precipitation via SO_2 and Cu plate-based experimental method

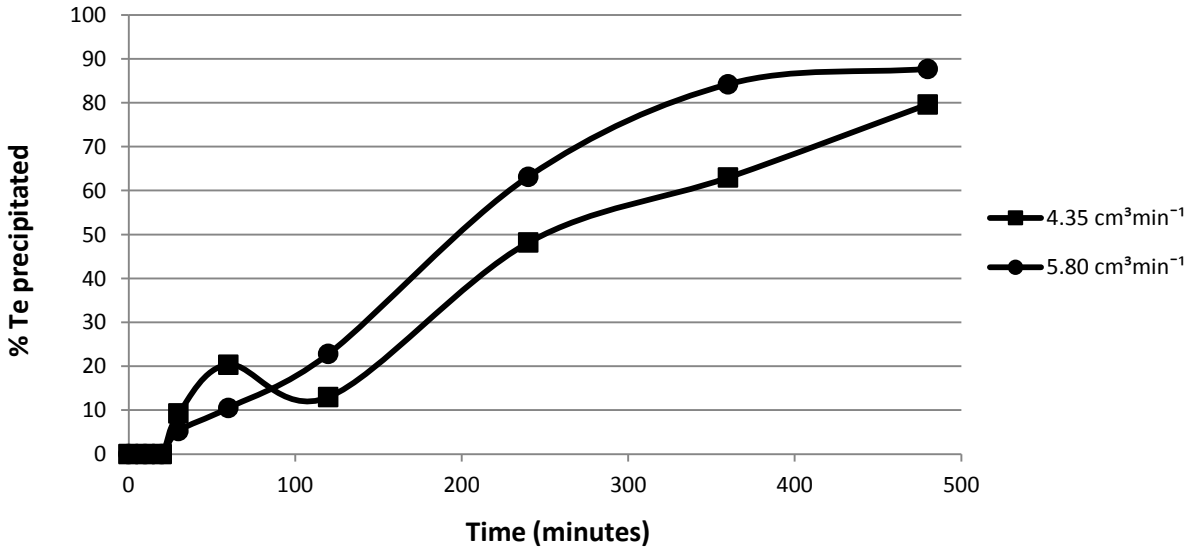

Figure 4.22: Effect of SO_2 flow rate on Te precipitation via SO_2 and Cu plate-based experimental method

Both the effects of agitation and SO_2 addition are only significant at a temperature of 65˚C for the tests performed with SO_2 only and with Cu plate as a precipitation enhancing reagent. The result achieved for the test performed at 65˚C and 250 rpm agitation rate with a copper plate of 202.5 mm² surface area is shown in figure 4.22 for illustrative purpose. For clarity, the outcomes of the tests performed at other process conditions are also shown in figures 4.25 and 4.26.

From figure 4.22, it can be seen that Te precipitation started at an earlier point in time, and that the effect of the SO_2 flow rate on the precipitation kinetics was less profound than for the test performed with SO_2 only (shown in figure 4.6); increasing the SO_2 flow rate did, however, result in an increase from 80 to 88 % Te precipitation achieved after 8 hours. It can thus be concluded that, although metallic copper was added, the specific surface area of the copper plate was not sufficiently large to eliminate the dependence of tellurium precipitation on the reduction of cupric ions and the formation of elemental copper from the process solution. The SO_2 flow rate did not affect the Te precipitation achieved using this processing technique at a temperature of 95˚C (fig. 4.25 and 4.26). At this temperature, the rate of cupric reduction was sufficiently fast with both SO_2 flow rates that the tellurium precipitation occurred at similar rates.

Additionally, enlarging the surface area of the copper plate used also resulted in improved Te precipitation for the tests performed at 65˚C. Figure 4.23 shows the effect of increasing the surface area of Cu plate on Te precipitation achieved for the test performed at 65˚C and 250 rpm agitation rate using a SO_2 flow rate of 4.4 cm³/min.

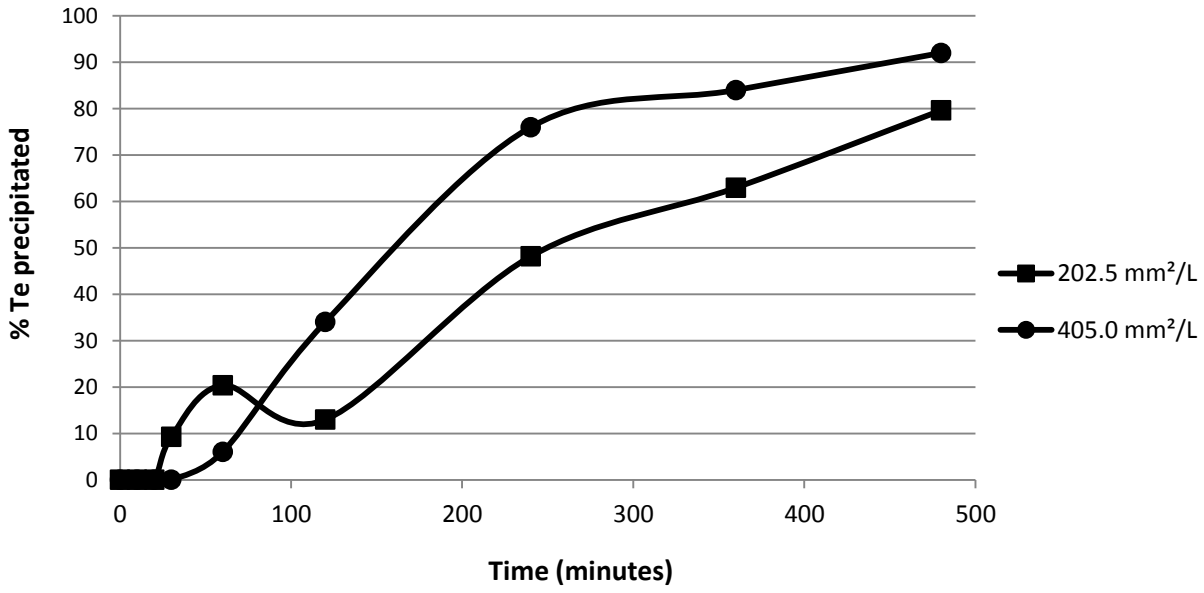

Figure 4.23: Effect of increasing surface area of Cu plate on Te precipitation via SO_2 and Cu plate-based experimental method

By comparing figure 4.25 a with figure 4.26 a and figure 4.25 b with figure 4.26 b, one can see the effects of surface area of metallic copper on Te precipitation for all the tests performed using this experimental method. As shown in these figures, increasing the surface area of copper plate from 202.5 to 405.0 mm² resulted in a faster Te precipitation rate but did not result in a larger extent of Te precipitation observed. From these figures, one can also observe that faster Te removal rate was achieved for all the tests performed at 95°C especially during the initial period (0-30 minutes).

The faster tellurium precipitation kinetics noticed with increase in the surface area of the copper plates used (especially at high temperature) is in agreement with the observations of Shibasaki *et al*. (1992) and Sugawara *et al*. (1992) who showed that enlarging the surface areas of metallic copper could potentially enhance the rate of Te precipitation via secondary cementation reaction according to equations 2.27 and 2.28.

Although larger amounts of tellurium and selenium were precipitated from the solution by the effect of cupric reduction with SO_2 at different process conditions, it can nevertheless be argued that the introduction of copper plates enhanced the Te removal rate observed for this experimental method. A proof of this fact is the presence of Cu_2 (Te, Se) phase as significant inclusions in the precipitates stripped from the copper plates, after the completion of the tests performed using this processing technique. This observation is however illustrated in tables 5.122 through 5.130 (Appendix F) and further discussed in section 4.6.4.

As discussed in section 4.1.2, the formation of cuprous ions and the subsequent production of metallic copper (according to reactions 2.22 and 2.25) were enhanced as the temperature was increased from 65 to 95˚C. This explains why the rate of tellurium precipitation was noticeably faster at 95˚C than at 65˚C for the tests performed using this processing technique too. A typical example of the faster Te precipitation kinetics noticed for the test performed at an agitation rate of 250 rpm using SO_2 (4.4 cm³ SO_2 flow rate) and copper plate (202.5 mm² surface area) is shown in figure 4.24. As seen in this figure, the percentage Te precipitation increased from about 80 to 92 % after eight hours, when the temperature was increased from 65 to 95˚C for this test.

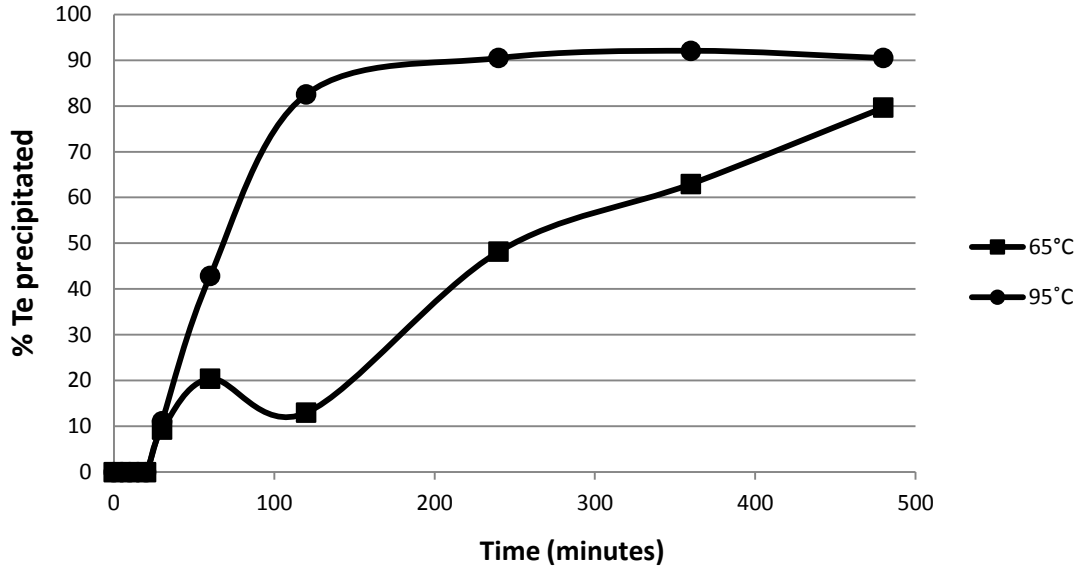

Figure 4.24: Effect of temperature on Te precipitation via SO_2 and Cu plate-based experimental method

The tellurium precipitation behaviour with increase in temperature is further illustrated in figures 4.25 and 4.26 which show the results of the tests performed at different process conditions using this processing technique. It can be seen in these figures that the Te removal rate becomes faster as the temperature was increased, and that the percentage Te precipitation achieved after eight hours was higher at 95°C; on average the percentage tellurium precipitation increased from 83 to 92 % when the the temperature was increased from 65 to 95°C.

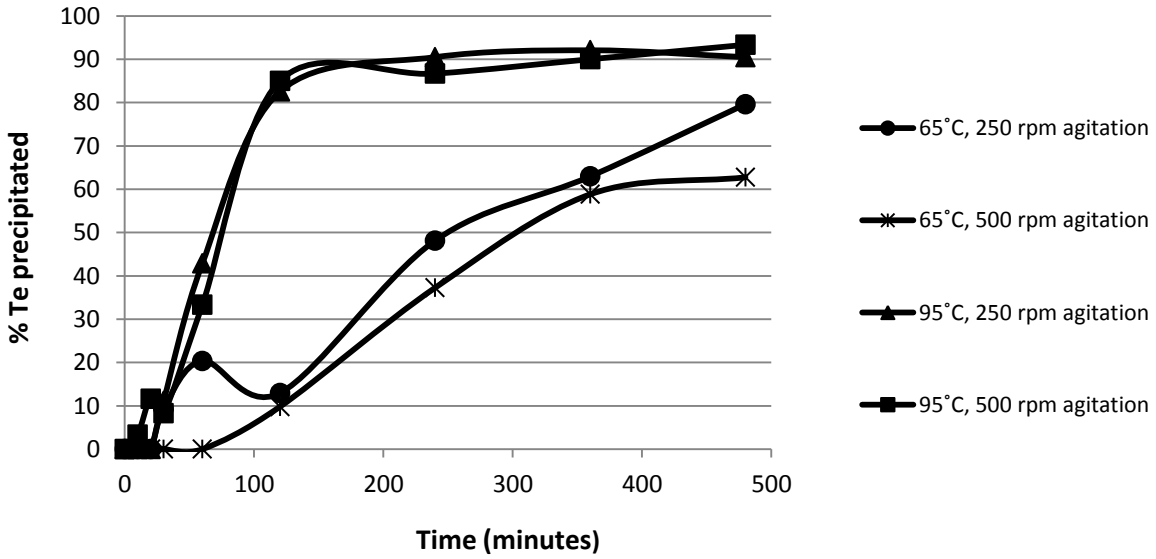

a)

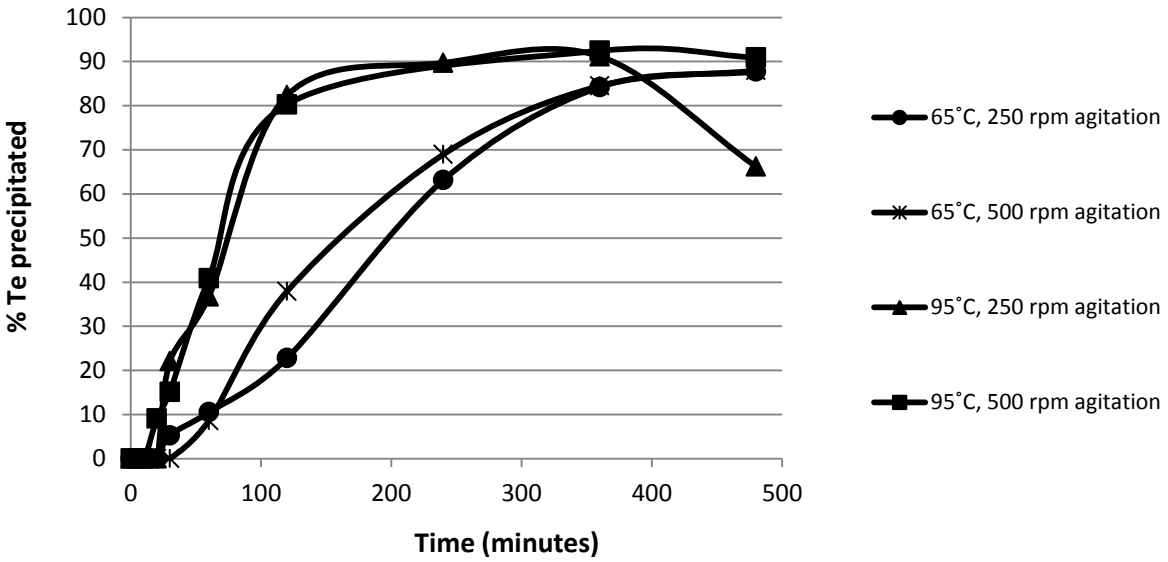

b)

Figure 4.25: Percentage Te precipitation achieved with: a. 4.4 cm^3/min SO_2 flow rate and 202.5 mm^2/L Cu plate b. 5.8 cm^3/min SO_2 flow rate and 202.5 mm^2/L Cu plate at typical operating conditions

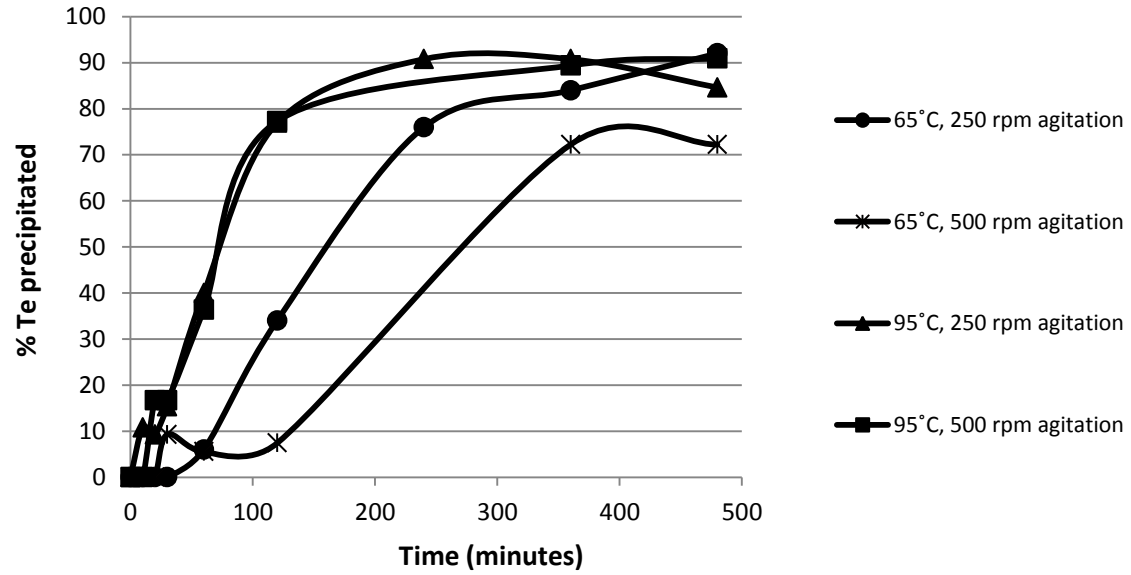

a)

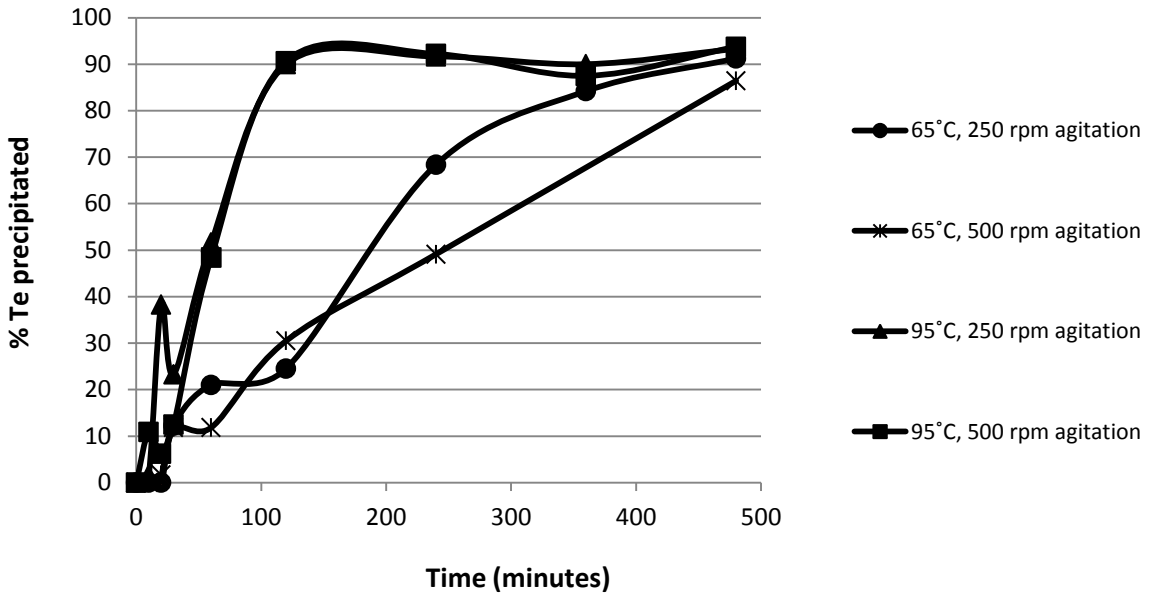

b)

Figure 4.26: Percentage Te precipitation achieved with: a. 4.4 cm^3/min SO_2 flow rate and 405.0 mm^2/L Cu plate b. 5.8 cm^3/min SO_2 flow rate and 405.0 mm^2/L Cu plate at typical operating conditions

4.4.3. Base metal precipitation

The co-precipitation of the base metals noticed during the Te and Se precipitation was also poor for all the tests performed using this processing technique. Tables 5.20 through 5.35 (Appendix D.2) show the base metals concentrations observed for the tests performed at different operating conditions using this experimental method. When the percentages base metals precipitation were computed, approximately 8 % co-precipitation of Cu was observed after eight hours on average.

As discussed in section 4.1.3, the tellurium and selenium concentrations present in the copper sulphate solution used for this study were approximately 3 order of magnitude lower than the copper concentration. This is not the case for the study performed by Wang *et al.* (2003) where selenium and tellurium concentrations were about one order of magnitude lower than the copper concentration found in the solution used. Thus, it is very likely that relatively smaller stoichiometric amount of dissolved copper (less than 1g/L) would be required in order to achieve significant selenium and tellurium precipitation as Cu_2Te and Cu_2Se (according to reactions 2.27, 2.28 and 2.29). This explains why large copper precipitation was not observed for all the tests performed using these different processing techniques unlike the outcomes of the experiments performed by Wang *et al*. (2003).

Additionaly, the introduction of Cu plates into the copper sulphate solution did not result in a significant increase in copper concentrations as a result of cuprous formation as expected. This observation could be attributed to the fact that the secondary cementation reaction between Te (or Se) and the metallic copper (reported in sections 4.4.1 and 4.4.2) only occurred on the surface(s) of the copper plate(s) used for this experimental method.

It seems cupric reduction by SO_2 and the subsequent elemental copper formation which precipitates tellurium proceeded in the solution used as an independent precipitation process. Evidence of this fact was the formation of dark precipitates indicative of copper selenide and telluride particles on the Cu plate(s) removed from the said solution, after the completion of the tests performed using this experimental method, especially those performed at high temperature condition.

4.4.4. OPMs precipitation

Tables 5.20 through 5.35 also show the changes observed in OPMs concentrations at different process conditions during Te and Se precipitation via the second experimental method.

As was the case for the first experimental method discussed in section 4.1.4, the co-precipitation of OPMs was also poor at all the process conditions for the tests performed using this processing technique; a maximum of 17 % Ru and approximately 10% Rh and Ir precipitation was achieved for all the tests (table 5.35). From these results, one can conclude that the introduction of copper plates into the leach solution did not result in a significant improvement in the precipitation of precious metals.

4.5. SO_2 and Cu plate: Statistical analysis

As discussed in section 4.2, the maximum Te and Se yield were also chosen as the responses for this processing technique in order to achieve the main objective of this study, which is to maximize the recovery of Te and Se from the copper sulphate solution. Figure 4.27 shows the maximum Te and Se yield achieved for the various tests performed with copper plate addition as a precipitation enhancing agent, while the experimental runs for these tests and their responses are provided in table 4.9. The values of the responses for these experimental runs were also used to determine the process variables that have the main effects on Te and Se yield.

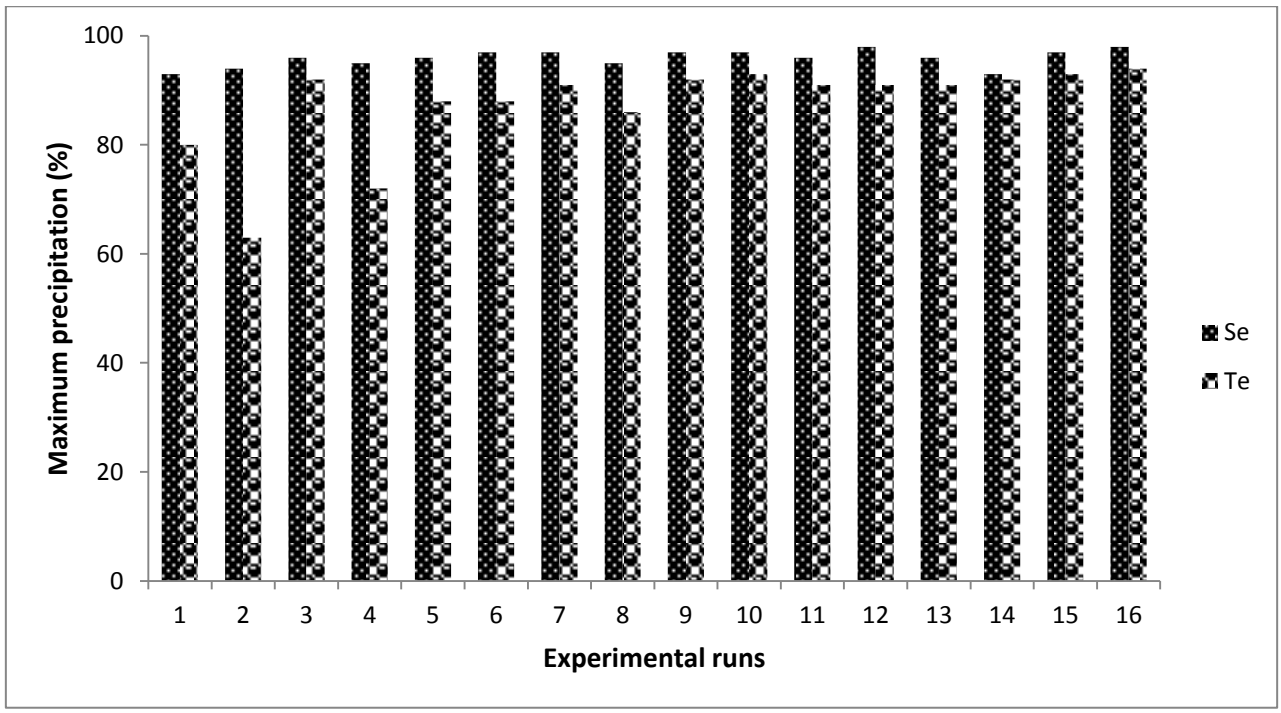

Figure 4.27: Observed maximum Se and Te precipitation for the sixteen runs of the SO_2 and Cu plate-based experimental method

Table 4.9: Summary of treatment combinations and their observed responses for SO_2 and Cu plate-based experimental method

Runs	Factors and Levels				Responses	
	A	B	C	D	x	y
#1	65	4.4	250	202.5	80	93
#2	65	4.4	500	202.5	63	94
#3	65	4.4	250	405	92	96
#4	65	4.4	500	405	72	95
#5	65	5.8	250	202.5	88	96
#6	65	5.8	500	202.5	88	97
#7	65	5.8	250	405	91	97
#8	65	5.8	500	405	86	95
#9	95	4.4	250	202.5	92	97
#10	95	4.4	500	202.5	93	97
#11	95	4.4	250	405	91	96
#12	95	4.4	500	405	91	98
#13	95	5.8	250	202.5	91	96
#14	95	5.8	500	202.5	92	93
#15	95	5.8	250	405	93	97
#16	95	5.8	500	405	94	98

Where:

A represents the temperature (^oC)

B represents the SO_2 flow rate (cm^3/min)

C represents the agitation speed (rpm)

D represents the surface area of the copper plate used in mm^2/L

x represents the maximum tellurium precipitation achieved via the SO_2 and Cu plate-based experimental method

y represents the maximum selenium precipitation achieved via the SO_2 and Cu plate-based experimental method

4.5.1. Analysis of variance

ANOVA was used to investigate the process variables and the interactions that influence the Te and Se precipitation. The model terms, their p-values and the R^2 for the responses are provided in tables 4.10 and 4.11. As shown in table 4.10, the p-values of less than 0.05 for temperature, SO_2 flow rate, agitation rate and surface area of copper plate indicate that all these process variables have significant effects on the maximum Te yield achieved via this method. The small p-values of temperature and surface area of copper plate as shown in table 4.11 also indicate that these variables have significant effects on the maximum Se yield realized using this method.

The insignificant model terms and interactions are removed from the models, but are shown in these tables for clarity. Though higher-order interactions are not often used for process optimization in the industry, their effects are nevertheless analysed in this study for illustrative purpose.

The temperature-SO_2 flow rate interaction, temperature-agitation interaction, temperature-Cu surface area interaction and SO_2 flow rate-agitation interaction were found to have major effects on maximum Te precipitation; the temperature-SO_2 flow rate interaction is the only second order interaction that has a pronounced effect on maximum Se precipitation.

Figures 4.28 a through f show the effects of second order interactions on maximum tellurium yield, while the effects of second order interactions on maximum Se yield are illustrated in figures 4.29 a through f. The temperature-SO_2 addition interaction indicates that SO_2 flow rate has a major positive effect on Te yield at a low level of temperature but has no significant effect at high temperature (figure 4.28 a). The temperature-agitation interaction indicates that agitation has a major positive effect on Te yield at a low temperature but has a mild effect at high temperature (figure 4.28 b).

Table 4.10: ANOVA table (Derived from Design Expert) showing the effects of significant model terms on the maximum Te precipitation achieved via the SO_2 and Cu plate-based experimental method.

Model Terms	Coefficient Estimate	p-value
Intercept	87.31	
A - Temperature	4.81	**0.0002**
B – SO_2 flow rate	3.06	**0.0016**
C - Agitation	-2.44	**0.0042**
D – Surface area of Cu plate	1.44	**0.0328**
AB	-2.69	**0.0028**
AC	2.81	**0.0023**
AD	-1.31	**0.0443**
BC	2.06	**0.0085**
BD	-	0.1444
CD	-	02048
ABC	-1.94	**0.0109**
ABD	1.69	**0.0185**
ACD	-	0.2578
BCD	-	0.7952
		R-squared = 0.9826
		Adj. R-squared = 0.9479

Table 4.11: ANOVA table (Derived from Design Expert) showing the effects of significant model terms on the maximum Se precipitation achieved via the SO_2 and Cu plate-based experimental method

Model Terms	Coefficient Estimate	p-value
Intercept	95.94	
A - Temperature	0.56	**0.0023**
B – SO_2 flow rate	-	0.2152
C - Agitation	-	0.6376
D – Surface area of Cu plate	0.56	**0.0023**
AB	-0.69	**0.0006**
AC	-	0.6376
AD	-	0.2152
BC	-0.31	**0.0438**
CD	-	0.6376
ABC	-	0.2152
ABD	0.69	**0.0006**
ACD	0.69	**0.0006**
BCD	-	0.6376
		R-squared = 0.9306
		Adj. R-squared = 0.8844

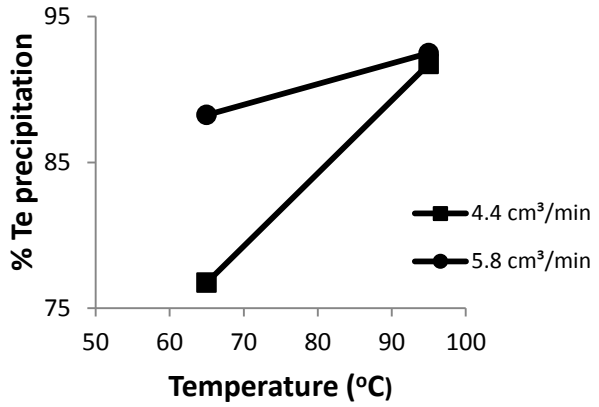

a. Effect of temperature – SO_2 flow rate interaction on Te yield

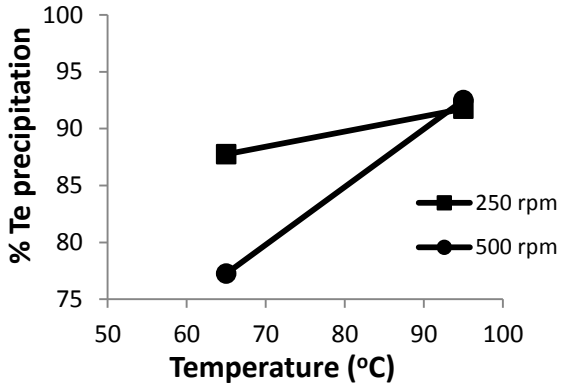

b. Effect of temperature – agitation interaction on Te yield

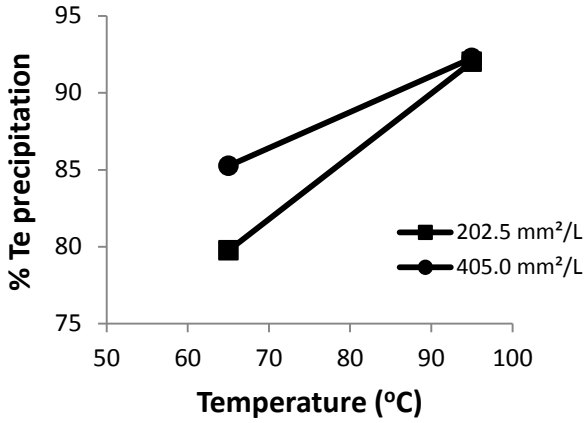

c. Effect of temperature – surface area of Cu plate interaction on Te yield

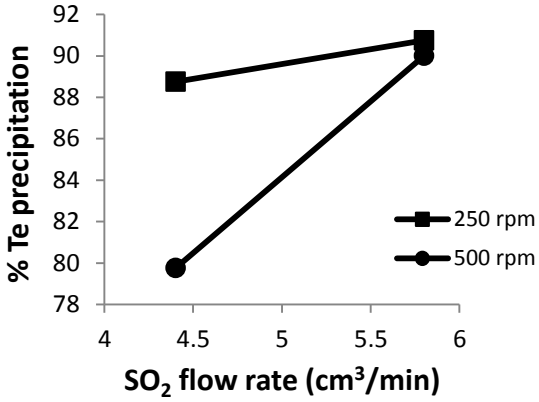

d. Effect of SO_2 flow rate – agitation interaction on Te yield

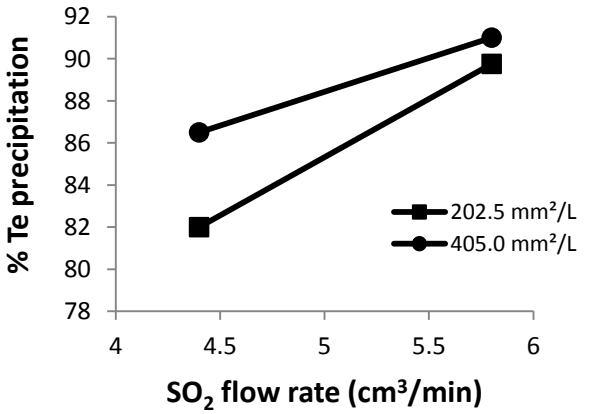

e. Effect of SO_2 flow rate – Surface area of Cu plate on Te yield

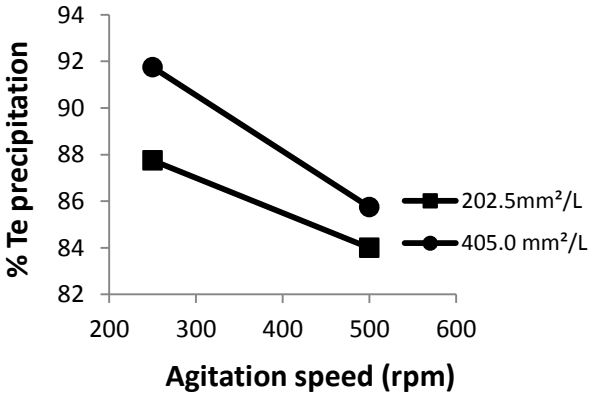

f. Effect of surface area of Cu plate – agitation interaction on Te yield

Figure 4.28: Effects of 2-order factor interactions on maximum Te yield via the SO_2 and Cu plate-based experimental method.

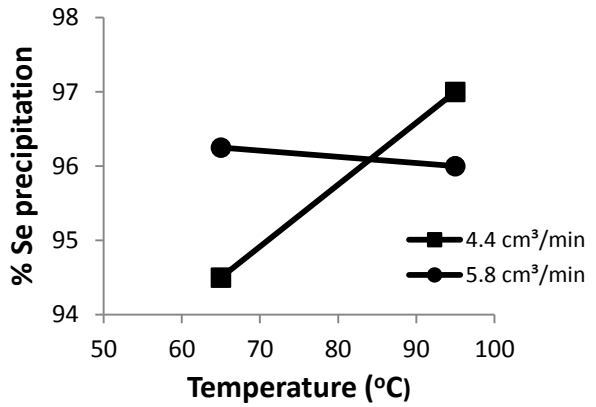

a. Effect of temperature – SO_2 flow rate interaction on Se yield

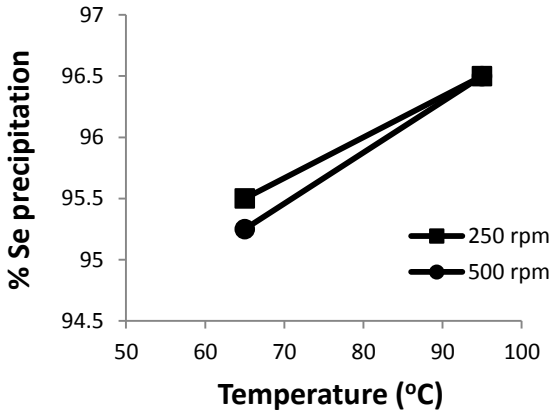

b. Effect of temperature – agitation interaction on Se yield

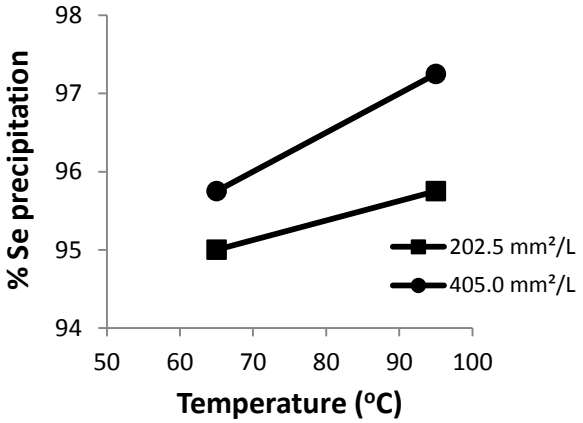

c. Effect of temperature – surface area of Cu plate interaction on Se yield

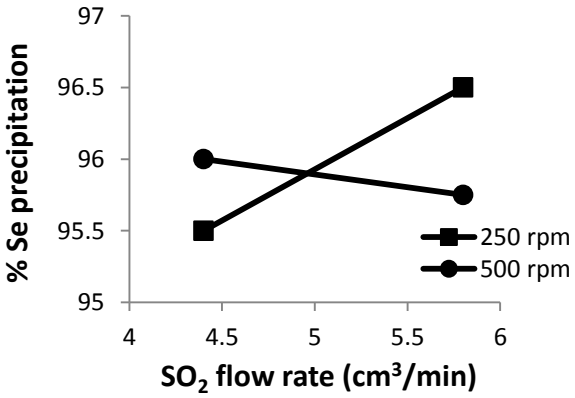

d. Effect of SO_2 flow rate – agitation interaction on Se yield

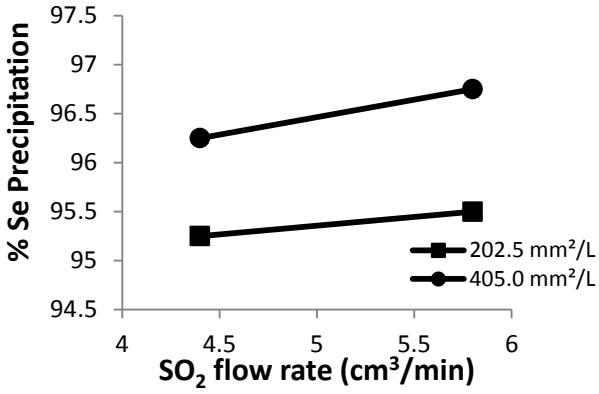

e. Effect of surface area of Cu plate – SO_2 flow rate interaction on Se yield

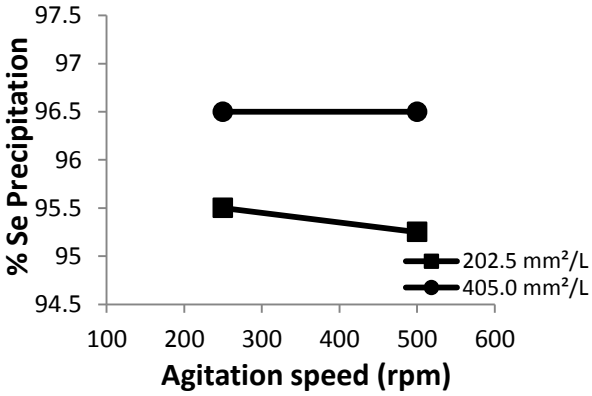

f. Effect of Surface area of Cu plate – agitation interaction on Se yield

Figure 4.29: Effects of 2-order factor interactions on maximum Se yield via the SO_2 and Cu plate-based experimental method

The interaction between the temperature and the surface area of Cu plate indicates that enlarging the surface area of the Cu plate used has a significant effect on Te yield at a low temperature, but has a slight effect at a high temperature, with the maximum tellurium recovery realised at a high temperature, and when a larger surface area of Cu plate was used (figure 4.28 c). The SO_2 flow rate-agitation interaction indicates that agitation has a large positive effect on Te yield at a low SO_2 flow rate but a mild effect at a high SO_2 addition rate, with the maximum Te recovery achieved at a low agitation condition (figure 4.28 d). These observations are, however, in agreement with the qualitative analysis of the experimental data presented in section 4.4.2, where it was shown that all the process variables discussed in this section have pronounced effects on Te yield achieved via the second experimental method.

In addition, the temperature-SO_2 flow rate interaction also indicates that the SO_2 flow rate has a major positive effect on Se yield at a low level of temperature but has a little effect on Se yield at a high temperature (fig. 4.29 b). This observation and that discussed previously, are also in line with the qualitative analysis of the experimental data presented in sections 4.4.1, where it was shown that temperature, SO_2 flow rate and Cu plate addition are the three most significant factors that influence the Se yield.

Based on the statistical analysis performed in this section , the regression models (given in terms of actual factors) that determine the maximum Te and Se yield achieved for this method are thus given as follows:

$$\textbf{Maximum Te yield} = 232.84 - 1.63 \times \text{Temperature } (^{\circ}C) - 28.27 \times SO_2 \text{ flow rate } (cm^3/min) - 0.86 \times \text{Agitation (rpm)} + 0.08 \times \text{Cu surface area } (mm^2) + 0.32 \times \text{Temperature } (^{\circ}C) \times SO_2 \text{ flow rate } (cm^3/min) + (9.00 \times 10^{-3}) \times \text{Temperature } (^{\circ}C) \times \text{Agitation (rpm)} - (4.33 \times 10^{-4}) \times \text{Temperature } (^{\circ}C) \times \text{Cu surface area } (mm^2) + 0.14 \times SO_2 \text{ flow rate } (cm^3/min) \times \text{Agitation (rpm)} - (1.48 \times 10^{-3}) \times \text{Temperature } (^{\circ}C) \times SO_2 \text{ flow rate } (cm^3/min) \times \text{Agitation (rpm)} - (8.45 \times 10^{-5}) \times \text{Temperature } (^{\circ}C) \times SO_2 \text{ flow rate } (cm^3/min) \times \text{Cu surface area } (mm^2) \quad (4.3)$$

$$\textbf{Maximum Se yield} = 96.03 + (7.53 \times 10^{-3}) \times \text{Temperature } (^{\circ}C) - (6.66 \times 10^{-3}) \times \text{Cu surface area } (mm^2) - (3.22 \times 10^{-3}) \times \text{Temperature } (^{\circ}C) \times SO_2 \text{ flow } (cm^3/min) - (5.62 \times 10^{-4}) \times SO_2 \text{ flow rate } (cm^3/min) \times \text{Agitation (rpm)} + (2.23 \times 10^{-5}) \times \text{Temperature } (^{\circ}C) \times SO_2 \text{ flow rate } (cm^3/min) \times \text{Cu surface area } (mm^2) + (1.4 \times 10^{-7}) \times \text{Temperature } (^{\circ}C) \times \text{Agitation (rpm)} \times \text{Cu surface area } (mm^2) \quad (4.4)$$

4.5.2. Optimizing Te yield

Since the selenium recovery realized using this experimental method was satisfactory, the focus of this study was therefore shifted to maximising the tellurium yield. In order to maximise the tellurium recovery achieved via this method, however, the effects of the model terms and the significant interactions on Te yield (discussed in section 4.5.1) were examined.

The Design Expert software was also employed to find the optimum solutions for the optimum criteria specified in table 4.12 using the desirability method (Derringer and Suich, 1980). Potential optimum conditions obtained for this experimental method are summarized in table 4.13, with the proposed optimum operating condition and its corresponding responses highlighted.

Table 4.12: Selection of optimum criteria for Te yield via SO_2 and Cu plate-based experimental method (derived from Design Expert)

Name	Goal	Lower value	Upper values	Importance
A: Temperature (°C): factor	In range	65	95	3
B: SO_2 flow rate (cm^3/min): factor	In range	4.4	5.8	3
C: Agitation (rpm): factor	In range	250	500	3
D: Cu surface area (mm^2): factor	In range	202.5	405	3
Maximum Te yield, x (%): Response	Maximise	63	94	3
Maximum Se yield, y (%): Response	Maximise	93	98	3

Table 4.13: Numerical optimization solution showing the possible optimum operating conditions for the $SO_2$and Cu plate-based experimental method and their responses

S/N	Process Variables				Responses		Desirability
	Temperature (°C)	SO_2 flow rate (cm^3)	Agitation (rpm)	Cu surface area (mm^2)	x (%)	y (%)	
1	95	4.4	250	202.5	93	98	0.953
2	95	5.8	500	405.0	95	97	0.943
3	**80**	**5.8**	**250**	**405.0**	**92**	**97**	**0.848**
4	65	5.8	250	405.0	91	97	0.835
5	65	5.8	500	202.5	86	97	0.726

4.6. SO_2 and Cu plate: Precipitate analysis

This section of the study was devoted to investigating the effects of the different process variables on the characteristics of the precipitates obtained from the solution, and those stripped from the copper plates. The first experimental run in table 4.9 was considered the normal experimental condition, while the second, third, fifth and the ninth experimental runs were regarded as the

experimental conditions involving improved agitation condition, the use of additional Cu plate, higher SO_2 addition rate and high temperature condition respectively.

The quantitative EDX analyses of the precipitates filtered from the solutions after the completion of the tests performed at other process conditions are summarized in tables 5.100 through 5.110 (Appendix F), while the SEM images that show the particle morphologies and crystallinities are provided in figures 5.8 (a-d), 5.9 (a-d) and 5.10 a (Appendix F)

4.6.1. Effect of agitation

Tables 4.14 and 4.15 show the quantitative analyses of the precipitates formed during the tests performed at normal condition and with improved agitation condition. By comparing table 4.14 with table 4.15, one can see that there is no significant improvement in the average Se and Te concentrations found in the precipitates as the agitation rate was increased from 250 to 500 rpm. This observation is in agreement with the discussion in sections 4.4.1 and 4.4.2, where it was shown that increasing the stirring speed did not result in larger extents of selenium and tellurium precipitation achieved for this processing technique. One can also observe that higher agitation did not result in significant increase in the sulphur and nickel contents of the solid samples, unlike what was observed for the test utilizing only SO_2 as a reducing agent. It is however not clear why this is the case for this precipitation method. A mineralogical study of both samples, however, revealed the presence of CuS and Ni-Fe-Pb oxide phases as the dominant phases in all the spots analysed. Traces of PGMs and minute amounts of Cu_2Se-Cu_2Te were also found in the precipitates as significant inclusions.

Table 4.14: Quantitative electron microprobe (wt. %) of solid sample obtained after the completion of the SO_2 and Cu plate-based experiment performed at normal condition.

Analysis	Rh*	Ru*	Ir*	Ni*	Fe*	Pb*	Cu*	Se*	Te*	S*	Total
1	0.00	1.81	0.00	10.25	0.33	3.20	41.47	0.92	0.73	41.29	100.00
2	0.00	1.78	0.00	6.88	0.29	3.12	41.08	0.00	0.61	46.25	100.00
3	0.62	4.14	1.37	4.61	0.22	2.56	27.24	31.30	3.12	24.82	100.00
4	0.00	3.61	0.80	9.51	0.27	3.71	23.98	8.95	1.67	47.50	100.00
Avg. (wt %)	0.16	2.84	0.54	7.81	0.28	3.15	33.43	10.29	1.53	39.97	100.00
*Elements combined with oxygen											
Site of interest analysed											

Table 4.15: Quantitative electron microprobe (wt. %) of solid sample obtained after the completion of the SO_2 and Cu plate-based experiment performed with improved agitation condition.

Analysis	Rh*	Ru*	Ir*	Ni*	Fe*	Pb*	Cu*	Se*	Te*	S*	Total
1	0.00	2.72	0.78	6.54	0.35	2.67	36.15	13.58	1.81	35.39	100.00
2	0.53	2.58	0.72	3.20	0.40	2.83	42.60	7.06	2.95	37.12	100.00
3	0.73	4.33	1.35	10.09	0.00	1.98	26.70	19.96	4.20	30.66	100.00
Avg. (wt %)	0.42	3.21	0.95	6.61	0.25	2.49	35.15	13.53	2.99	34.39	99.99
*Elements combined with oxygen											
Sites of interest analysed											

4.6.2. Effect of enlarging Cu surface area

Figure 4.30 shows the SEM image of the precipitate formed during the experiment performed with the use of additional copper plate, while the result of the quantitative EDX analysis of the solid sample is summarised in table 4.16. By comparing table 4.14 with table 4.16, one can see that enlarging the surface area of copper plate did not result in a significant increase in the Se and Te contents of the solid sample obtained, despite better Te and Se precipitation achieved for the test performed with additional copper plate.

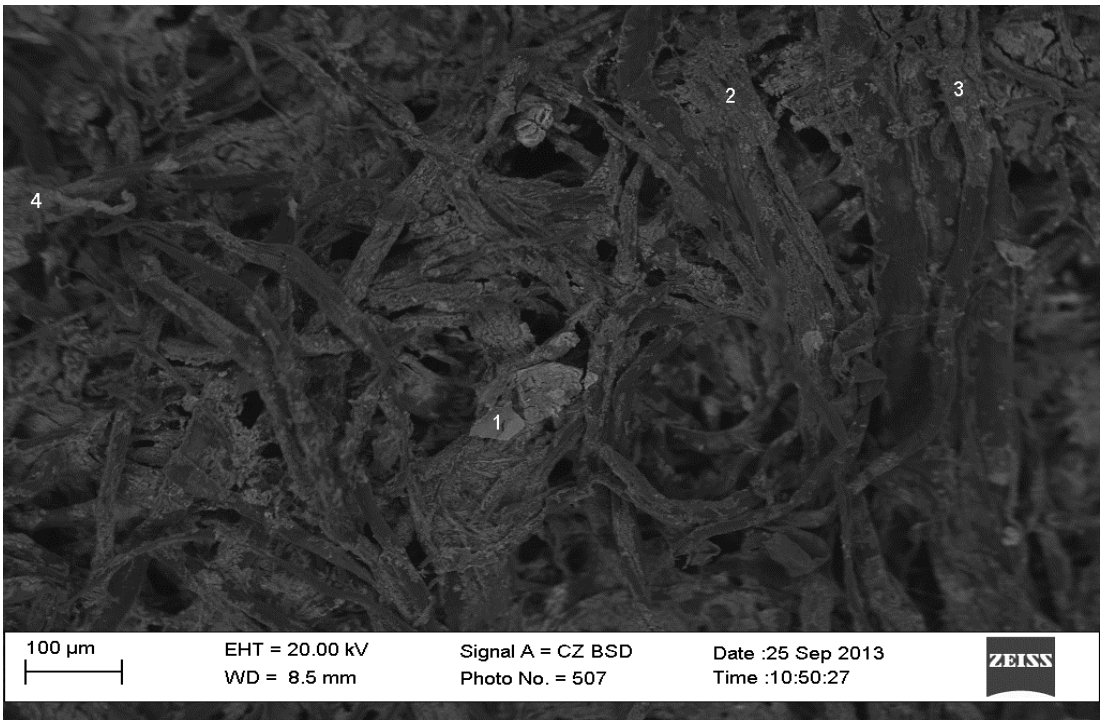

Figure 4.30: SEM image of the precipitate obtained after the completion of the SO_2 and Cu plate-based experiment performed using additional copper plate.

Table 4.16: Quantitative electron microprobe (wt. %) of the precipitate obtained after the completion of the SO_2 and Cu plate-based experiment performed using additional copper plate.

Analysis	Rh*	Ru*	Ir*	Ni*	Fe*	Pb*	Cu*	Se*	Te*	S*	Total
1	0.00	0.00	0.00	17.28	0.44	0.00	66.84	0.71	4.47	10.26	100.00
2	0.00	1.05	0.00	12.00	0.00	2.23	55.52	2.03	3.58	23.60	100.00
3	0.00	0.00	0.00	22.29	0.53	1.31	52.74	0.42	1.77	20.94	100.00
4	0.00	1.10	0.00	18.77	0.00	2.24	41.20	0.79	1.74	34.17	100.00
*Elements combined with oxygen											
Sites of interest analysed											

As discussed in section 4.4.3, tellurium and selenium precipitation also occurred on the surfaces of the metallic copper plate for the tests performed using this experimental method. This is in addition to the precipitation reactions that occurred in the process solution. For clarity, the elemental compositions of the precipitates stripped from the copper plates, after the completion of these tests are provided in tables 5.122 to 5.130.

Additionally, a mineralogical examination of the solid sample revealed the presence of CuS, Cu_2O, Ni-oxide and minute inclusion of Cu_2(Se, Te) phases in spot 1. The dominant phases observed in spots 2 and 3 are: CuS, Cu_2O and Pb-Ni oxide phases. CuS and Ni-oxide phases are the major phases detected in spot 4, with small traces of Cu_2(Se, Te) phase also found as inclusion.

4.6.3. Effect of SO_2 addition

Figure 4.31 shows the SEM image of the precipitate formed during the experiment performed with a high SO_2 addition rate, while the outcome of the quantitative EDX analysis of the solid sample is provided in table 4.17.

By comparing table 4.14 with table 4.17, one can observe that increasing the SO_2 flow rate resulted in significant improvement in the concentration of selenium found in the precipitate analysed for this test. This observation is also in agreement with the results presented in section 4.4.1, where it was shown that higher SO_2 flow rate resulted in larger extent of selenium precipitation achieved for this experimental method.

When a mineralogical examination of the solid sample was performed, spheroidal-shaped particles of Cu_2Se intergrown with Cu_2Te were detected, with traces of CuS, Ni-Fe-Pb oxide and minute PGMs species also present in the precipitate as inclusions.

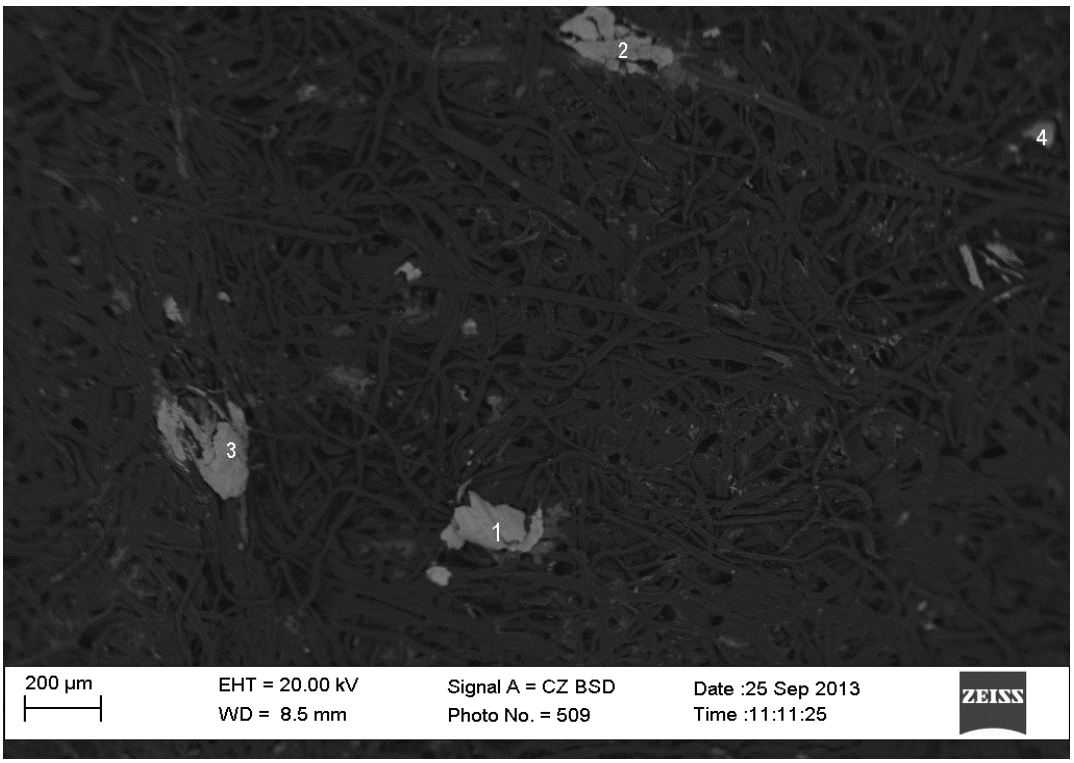

Figure 4.31: SEM image of precipitate obtained after the completion of the SO_2 and Cu plate-based experiment performed using high SO_2 addition rate.

Table 4.17: Quantitative electron microprobe (wt. %) of the precipitate obtained after the completion of the SO_2 and Cu plate-based experiment performed using high SO_2 addition rate.

Analysis	Rh*	Ru*	Ir*	Ni*	Fe*	Pb*	Cu*	Se*	Te*	S*	Total
1	1.60	4.78	0.81	0.76	0.19	1.02	27.80	52.53	4.01	6.50	100.00
2	1.41	4.81	0.00	2.54	0.73	1.18	48.62	25.81	7.81	7.10	100.00
3	1.74	7.28	1.42	2.49	0.57	1.15	32.56	42.77	6.11	3.92	100.00
4	2.73	10.82	2.25	1.83	0.57	1.67	13.60	57.13	5.81	3.58	100.00
Avg. (wt %)	1.87	6.92	1.12	1.91	0.52	1.26	30.65	44.56	5.94	5.28	100.00
*Elements combined with oxygen											
Sites of interest analysed											

4.6.4. Effect of temperature

Figure 4.32 shows the SEM image of the precipitate formed during the experiment performed at a high temperature condition, while table 4.18 shows the relative concentrations of elements found in the solid sample after quantitative SEM-EDX analysis was performed. As illustrated in figure 4.32, the sample analysed consists of a needle-shaped crystal structure typical of precipitation processes involving high temperature condition (Demopoulos, 2009).

By comparing table 4.14 with table 4.18, one can observe a larger Cu content in the solid sample obtained for the test performed at a high temperature. One can also observe small concentrations of

Se and Te in the solid sample analysed for the test performed at that process condition. A possible explanation for this observation, however, is that larger amount of metallic copper was precipitated from the solution for the test performed at a high temperature using this processing technique. This metallic copper was produced in the solution as a result of the disproportionation reaction. However, a mineralogical examination of this sample revealed the presence of Cu crystals with minute inclusions of Cu_2O, CuS and Ni-oxide (found in spots 2 and 3). The major phases detected in spots 1 and 4 are CuS and dark Cu_2O, while Ni-Pb oxide and minute inclusions of PGMs and Cu_2Se-Cu_2Te are the minor phases also noticed in these spots.

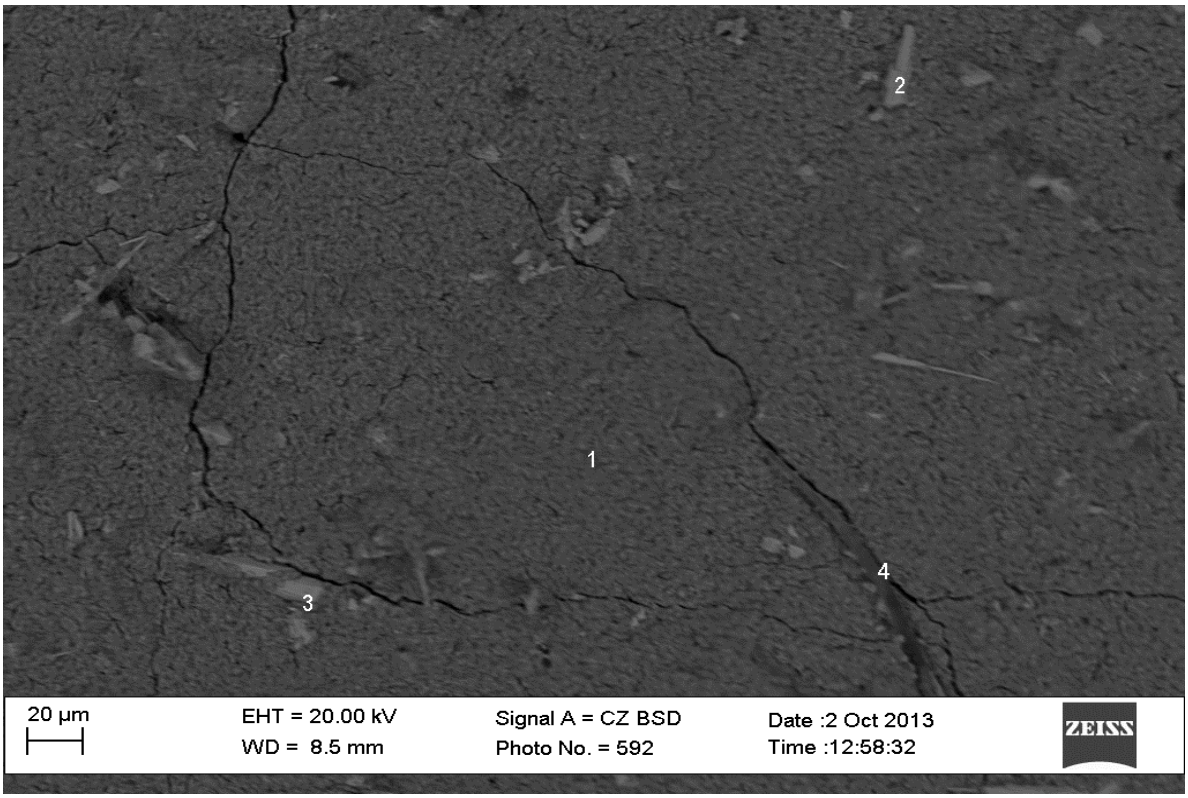

Figure 4.32: SEM image of the precipitate obtained after the completion of the SO_2 and Cu plate-based experiment performed at high temperature condition.

Table 4.18: Quantitative electron microprobe (wt. %) of the precipitate obtained after the completion of the SO_2 and Cu plate-based experiment performed at high temperature condition.

Analysis	Rh*	Ru*	Ir*	Ni*	Fe*	Pb*	Cu*	Se*	Te*	S*	Total
1	0.00	2.40	0.00	8.92	0.00	2.19	51.41	2.98	1.48	30.62	100.00
2	0.00	0.00	0.00	0.43	0.00	0.00	98.56	0.00	0.00	1.01	100.00
3	0.00	0.00	0.00	0.44	0.00	0.00	98.90	0.00	0.00	0.66	100.00
4	0.00	3.07	0.00	7.57	0.17	2.54	51.87	3.44	2.30	29.05	100.00
Avg. (wt %)	0.00	1.37	0.00	4.34	0.04	1.18	75.19	1.61	0.95	15.34	100.00
*Elements combined with oxygen											
Sites of interest analysed											

In addition, the chemical compositions of the precipitates stripped from the copper plates after the completion of one of the tests performed at low and high temperature conditions are provided in tables 4.19 and 4.20, respectively. The results of the quantitative EDX analyses of the precipitates stripped from the copper plates, for the tests performed at other operating conditions, are summarized in tables 5.122 through 5.130 (Appendix F). Figure 4.33 a and b show the SEM images of the precipitates stripped from the copper plates for the tests performed at these two conditions. The SEM images of the precipitates stripped from the copper plates at other process conditions are also shown in figures 5.17 (a and b), 5.18 and 5.19 (Appendix F). By comparing figure 4.33 a with figure 4.33 b, one can observe that the morphologies of the particles seen during the precipitate analysis are somewhat identical. This suggests that similar phases are present in the samples analysed for the two experimental conditions. Similar observations were also made for the SEM images shown in figures 5.17 through 5.19.

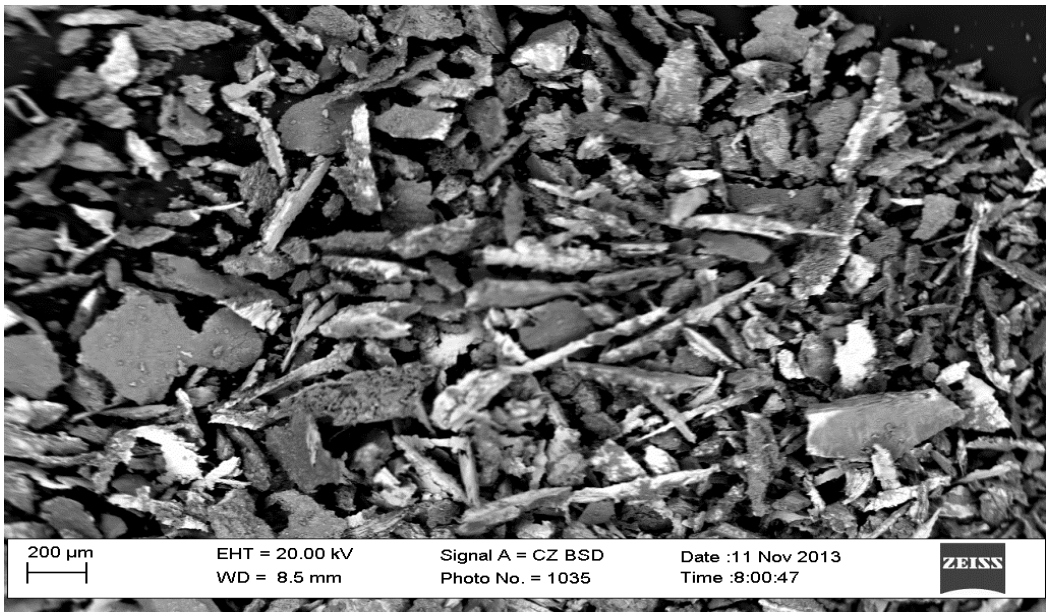

a)

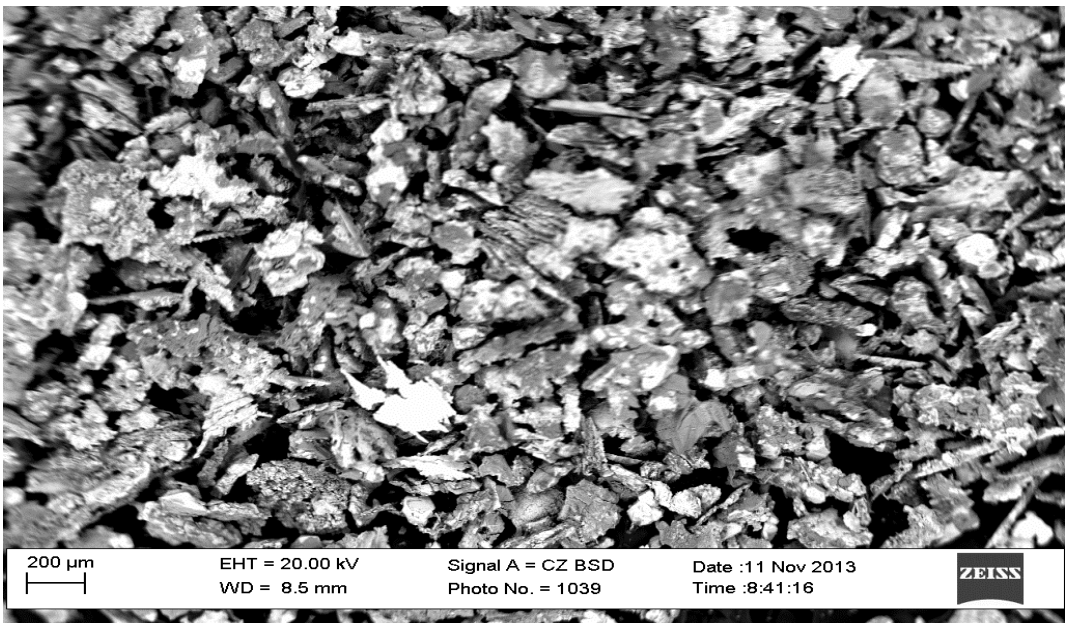

b)

Figure 4.33: SEM images of the precipitates stripped from copper plate(s) after the completion of the test performed at: a. 65˚C and 250 rpm (4.4 cm³/min SO_2 flow rate and 202.5 mm²/L Cu plate) b. 95˚C and 250 rpm (4.4 cm³/min SO_2 flow rate and 405.0 mm²/L Cu plate), showing particle morphologies

Table 4.19: Quantitative electon microprobe (wt. %) analysis of precipitate stripped from copper plate after the completion of the test performed at 65˚C and 250 rpm (4.4 cm³/min SO_2 flow rate and 202.5 mm²/L Cu plate)

Analysis	**Rh***	**Ru***	**Ir***	**Ni***	**Fe***	**Pb***	**Cu***	**Se***	**Te***	**S***	**Total**
1	0.00	0.99	0.00	7.38	0.00	1.85	67.29	3.14	0.00	19.36	100
2	0.00	0.88	0.00	7.47	0.00	1.96	67.33	2.95	0.38	19.03	100
Average (wt. %)	0.00	0.94	0.00	7.43	0.00	1.91	67.31	3.05	0.19	19.20	100
*Elements combined with oxygen											
Entire sample analysed											

Table 4.20: Quantitative electon microprobe (wt. %) analysis of precipitate stripped from copper plate after the completion of the test performed at 95˚Cand 250 rpm (4.4 cm³/min SO_2 flow rate and 405.0 mm²/L Cu plate)

Analysis	**Rh***	**Ru***	**Ir***	**Ni***	**Fe***	**Pb***	**Cu***	**Se***	**Te***	**S***	**Total**
1	0.00	0.59	0.00	5.14	0.19	1.06	74.68	1.42	0.74	16.19	100.00
2	0.00	1.06	0.00	5.25	0.00	1.91	74.26	1.35	0.47	15.71	100.00
Average (wt. %)	0.00	0.82	0.00	5.19	0.09	1.48	74.47	1.38	0.60	15.95	100.00
*Elements combined with oxygen											
Entire sample analysed											

When a mineralogical study of the precipitates retrieved from the copper plates was performed, Cu crystals, CuS and Cu_2O were the dominant phases which were found in the solid samples. Minute traces of Cu_2Se-Cu_2Te phase, Ni-Pb oxide phase and small inclusion of PGMs (notably ruthenium oxide) were also detected in the solid samples analysed.

4.7. Effects of factors on precipitation with SO_2 and Cu powder

4.7.1. Selenium precipitation

Figure 4.34 shows the effect of agitation on Se precipitation achieved with the addition of 1g of copper power as a precipitation enhancing reagent, for the test performed at 65˚C and at a SO_2 flow rate of 4.4 cm^3/min. As shown in this figure, increasing the agitation rate did not significantly influence the extents of selenium precipitation observed; 93 % Se precipitation was achieved after eight hours for the experiments performed at both agitation conditions. This observation is also illustrated in figures 4.38 a through 4.39 b. One can see in these figures that the extents of Se precipitation achieved are comparable for all the tests performed at 65˚C using different agitation rates.

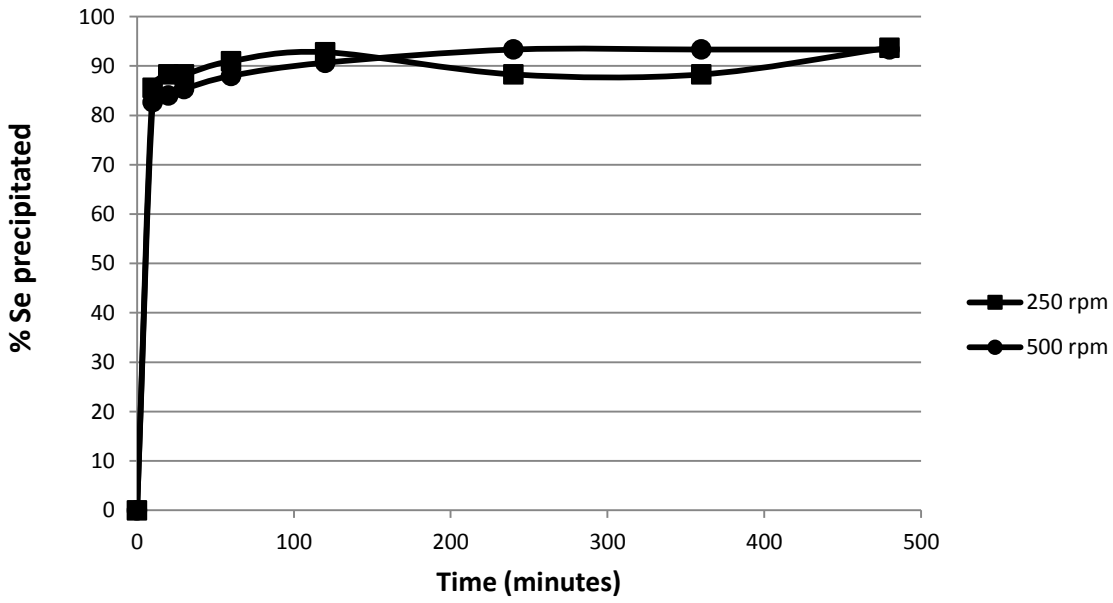

Figure 4.34: Effect of agitation on Se precipitation via SO_2 and Cu powder-based experimental method

As was the case for the effect of the agitation rate on selenium precipitation behaviour, the effect of SO_2 flow rate and copper addition were also less profound on Se precipitation for the tests conducted with SO_2 as a precipitation reagent and with copper powder as a precipitation enhancing reagent. Figure 4.35 shows the effect of SO_2 flow rate on selenium precipitation for the test

performed at 65˚C and 250 rpm agitation speed with the addition of 1g of copper powder as an additional precipitation reagent. One can observe in this figure that there is no significant improvement in the extents of Se precipitation achieved for the different SO_2 flow rates used. By comparing figure 4.38 a with figure 4.38 b and figure 4.39 a with 4.39 b, one can also see that similar results were obtained for the tests performed at other process conditions using this processing technique.

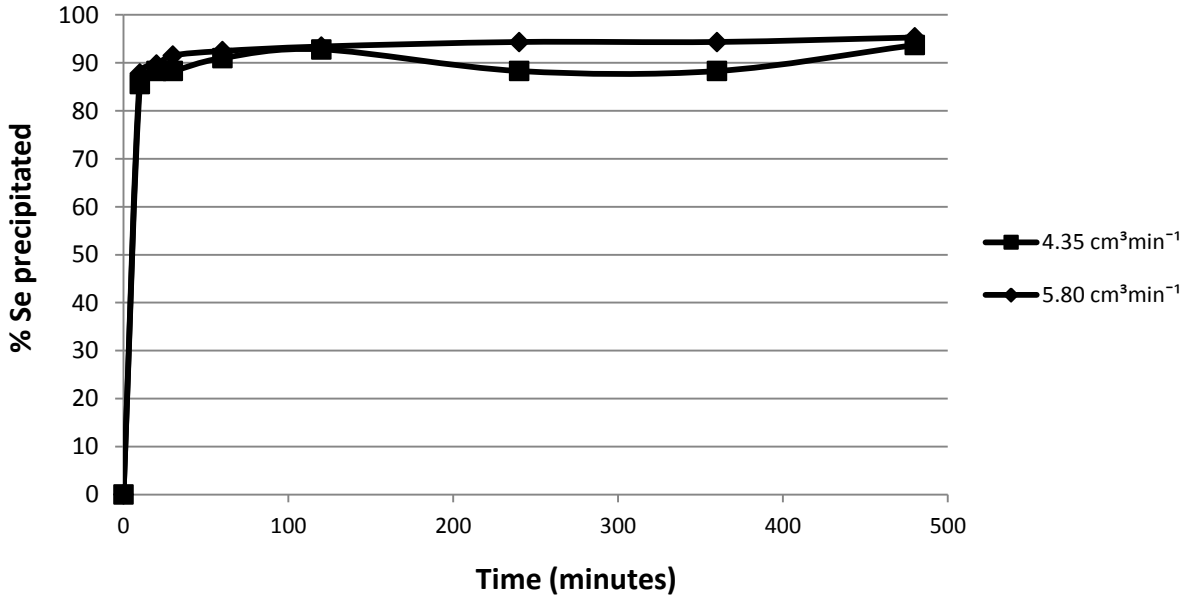

Figure 4.35: Effect of SO_2 flow rate on Se precipitation via SO_2 and Cu powder-based experimental method

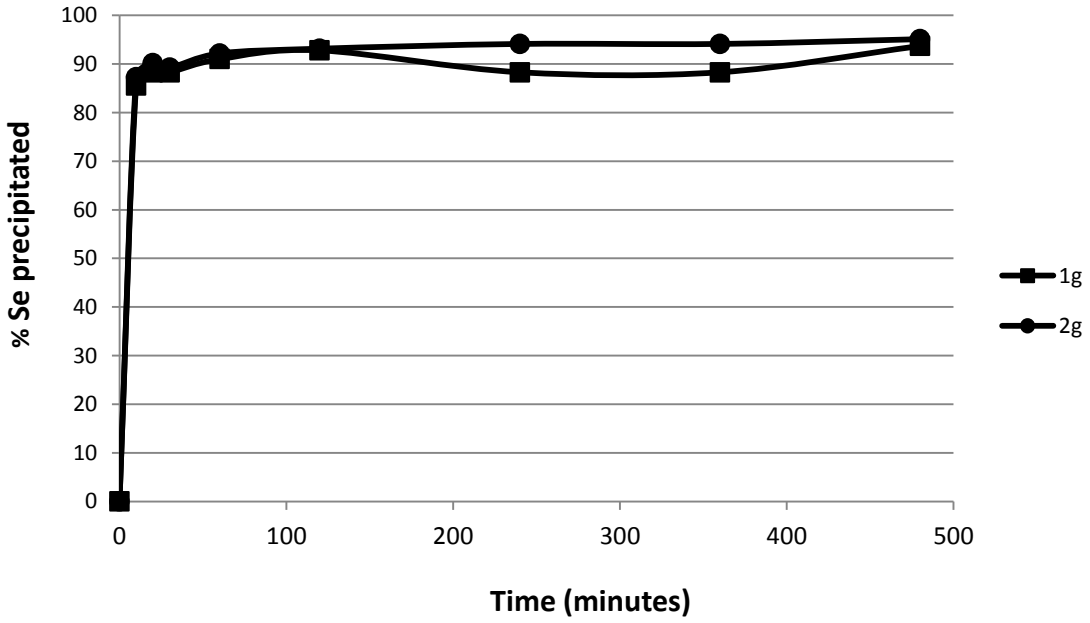

Figure 4.36: Effect of Cu powder addition on Se precipitation via SO_2 and Cu powder-based experimental method

As discussed previously, increasing the amount of copper powder added into the copper sulphate leach solution also did not result in a larger extent of selenium precipitation achieved. A typical example of the selenium precipitation behaviour with an increase in copper powder addition is illustrated in figure 4.36, for the test performed at 65˚C and 250 rpm agitation rate with a SO_2 flow rate of 4.4 cm³/min. As shown in this figure, the addition of more copper powder did not result in better Se yield after eight hours; 95 % Se precipitation was achieved regardless of the quantities of copper powder added. By comparing figure 4.38 a with figure 4.39 a and figure 4.38 b with figure 4.39 b, one can also observe that similar results were obtained for the test performed at other operating conditions using this experimental method.

A possible explanation for these observations is that the addition of one gram of copper powder offered a sufficiently large surface area of metallic copper for the production of cuprous ions, and guaranteed the attainment of equilibrium between the cuprous copper and the cupric copper present in the said solution (equation 2.25). This could potentially enhance the reductive precipitation of selenium ions by SO_2 significantly according to reaction 2.30.

Temperature had a noticeable effect on selenium precipitation achieved using this processing technique. Figure 4.37 shows the effect of increasing the temperature from 65 to 95˚C on selenium precipitation for the test performed with SO_2 (4.4 cm³/min SO_2 flow rate) and Cu powder (1g/L Cu addition) at an agitation rate of 250 rpm, as an illustration of the Se precipitation behaviour observed with increase in temperature.

As seen in this figure, a higher temperature resulted in a larger extent of Se precipitation after eight hours; 94 and 100 % percentages Se precipitation were achieved for the tests performed at 65 and 95˚C, respectively. This observation is further illustrated in figures 4.38 and 4.39, although the effect of temperature was less profound for the tests conducted using a high SO_2 flow rate.

As discussed in section 2.4.2, temperature has a profound effect on cuprous formation especially with the use of metallic copper. This is because the reaction of cupric copper with metallic copper to produce cuprous ions (equation 2.25) is endothermic (Ladriere, 1973). Therefore, increasing the temperature from 65 to 95˚C, would speed up the rate of cuprous formation (equation 2.25), and the subsequent reductive precipitation of selenious acid as Cu_2Se according to reactions 2.23 and 2.24.

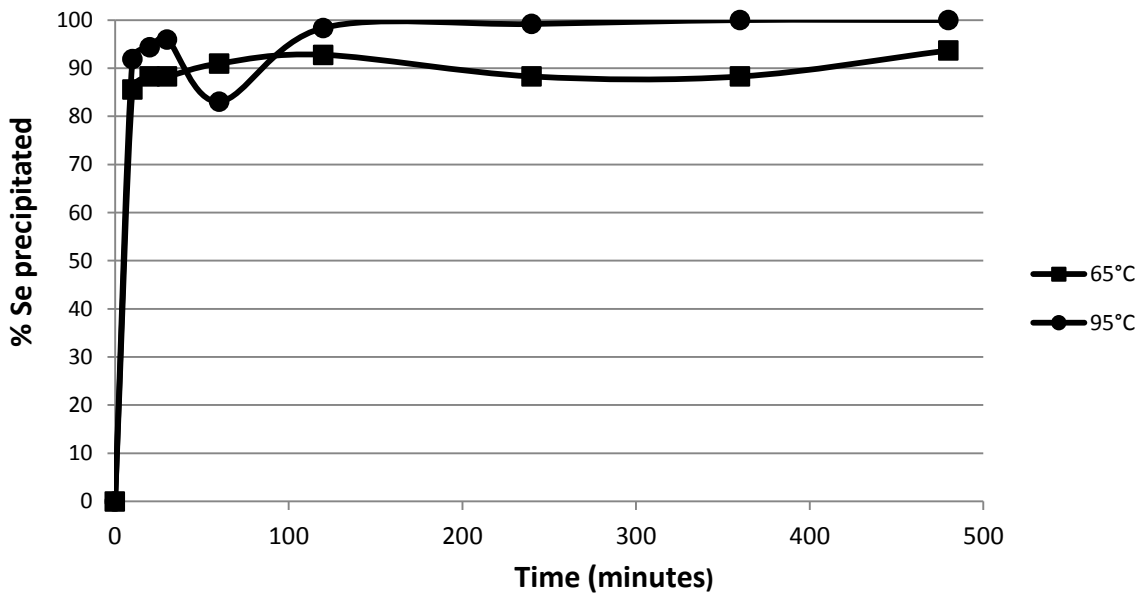

Figure 4.37: Effect of temperature on Se precipitation via SO_2 and Cu powder-based experimental method

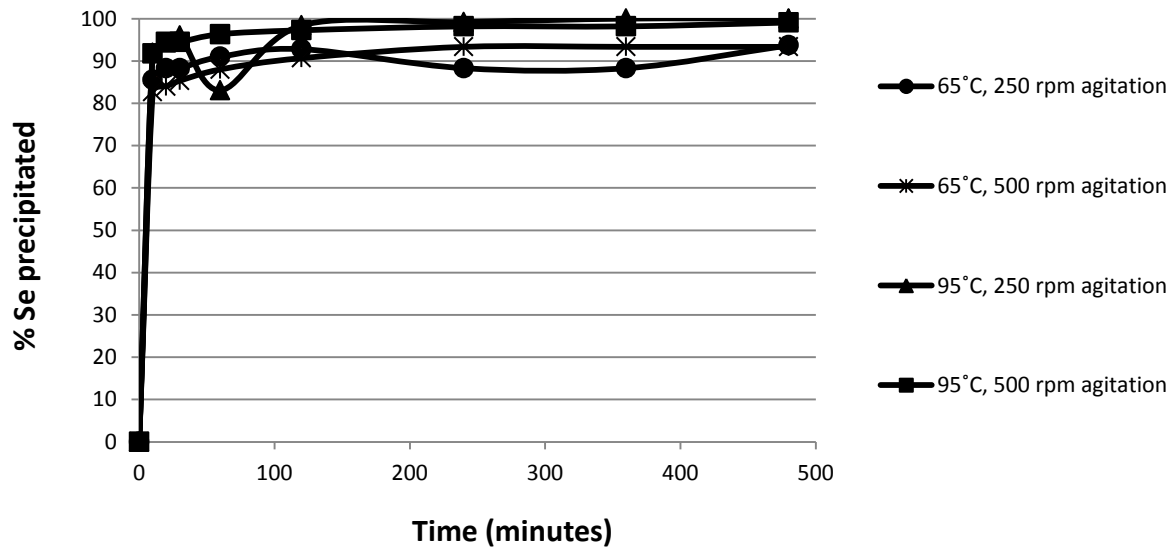

a)

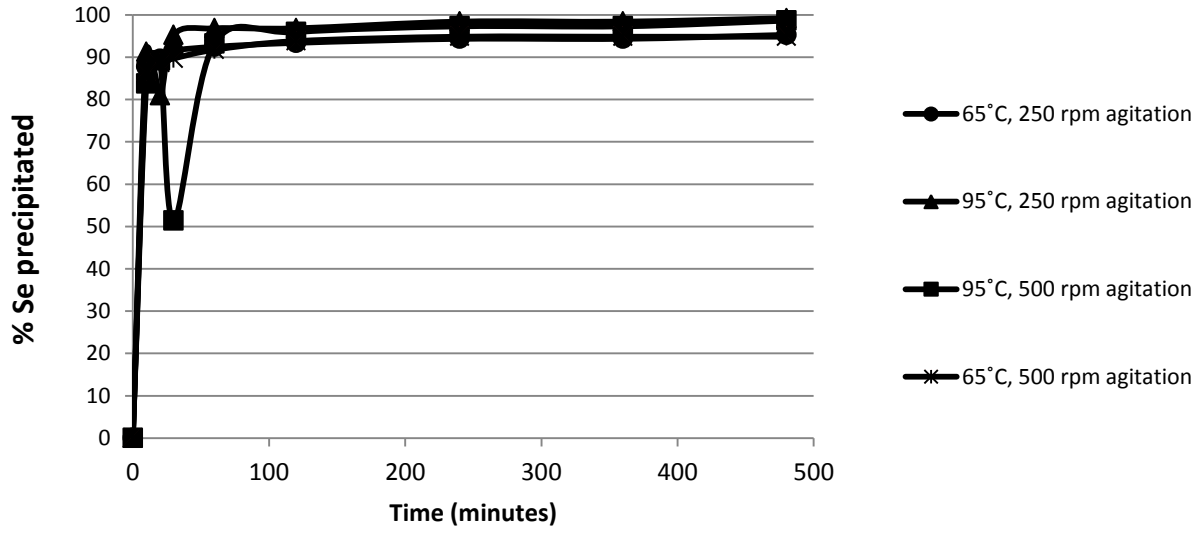

b)

Figure 4.38: Percentage Se precipitation achieved with: a. 4.4 cm^3/min SO_2 flow rate and 1 g/L Cu powder addition b. 5.8 cm^3/min SO_2flow rate and 1 g/L Cu powder addition at typical operating conditions

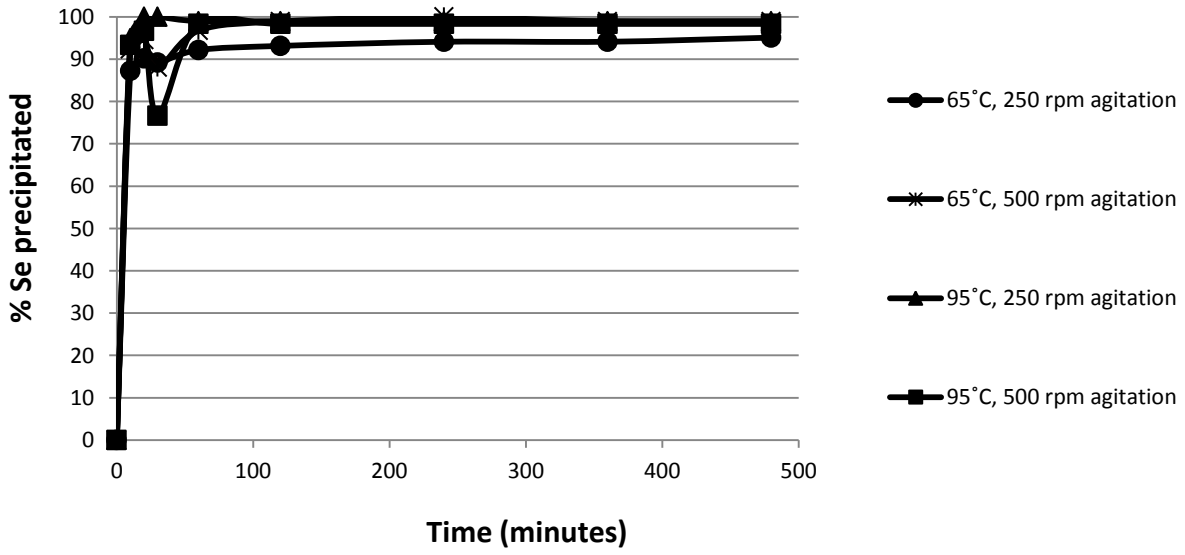

a)

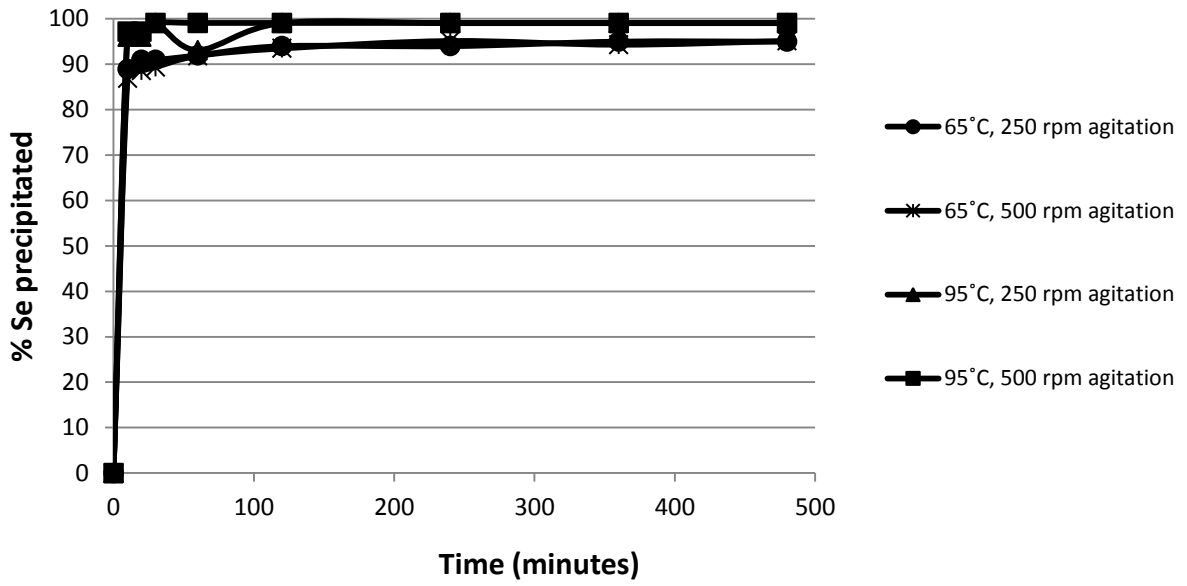

b)

Figure 4.39: Percentage Se precipitation achieved with: a. 4.4 cm³/min SO_2 flow rate and 2 g/L Cu powder addition b. 5.8 cm³/min SO_2 flow rate and 2 g/L Cu powder addition at typical operating conditions

4.7.2. Tellurium precipitation

Figure 4.40 shows the effect of agitation on tellurium precipitation achieved with the addition of 1g of copper powder for the test performed at 65˚C and at a SO_2 flow rate of 4.4 cm³/min. As shown in this figure, the agitation speed did not significantly influence the percentage tellurium precipitation achieved; 91 % Te precipitation was achieved after 8 hours for the tests performed at both agitation conditions. This observation is furthermore illustrated in figures 4.44 through 4.45. One can observe in these figures that there are no significant differences in the extents of Te precipitation achieved for all the tests performed at different agitation rates regardless of the effects of the other process variables.

There was also no pronounced effect of SO_2 flow rate on Te precipitation achieved after eight hours when using copper powder as the precipitation enhancing reagent, compared to what was noticed for the tests performed either with only SO_2 or with SO_2 and copper plate (discussed in sections 4.1.2 and 4.4.2, respectively). With copper powder as a precipitation enhancing reagent, tellurium precipitation proceeded mainly by reaction with the added metallic copper (according to equations 2.27 and 2.28), and any metallic copper formation as a result of cupric reduction by SO_2 did not significantly influence the tellurium precipitation.

A typical example of the tellurium precipitation behaviour observed with a higher SO_2 addition rate for this experimental method is illustrated in figure 4.41 for the test performed with 1g of copper

powder at 65˚C and at an an agitation rate of 250 rpm. As shown in this figure, the extents of Te precipitation achieved are comparable for the two SO_2 flow rates (92 % Te precipitation on average), although higher SO_2 flow rate resulted in slightly faster Te precipitation kinetics at initial period (0-120 minutes). By comparing figure 4.44 a with figure 4.44 b and figure 4.45 a with figure 4.45 b, one can also observe that similar results were achieved for the tests performed at other operating conditions.

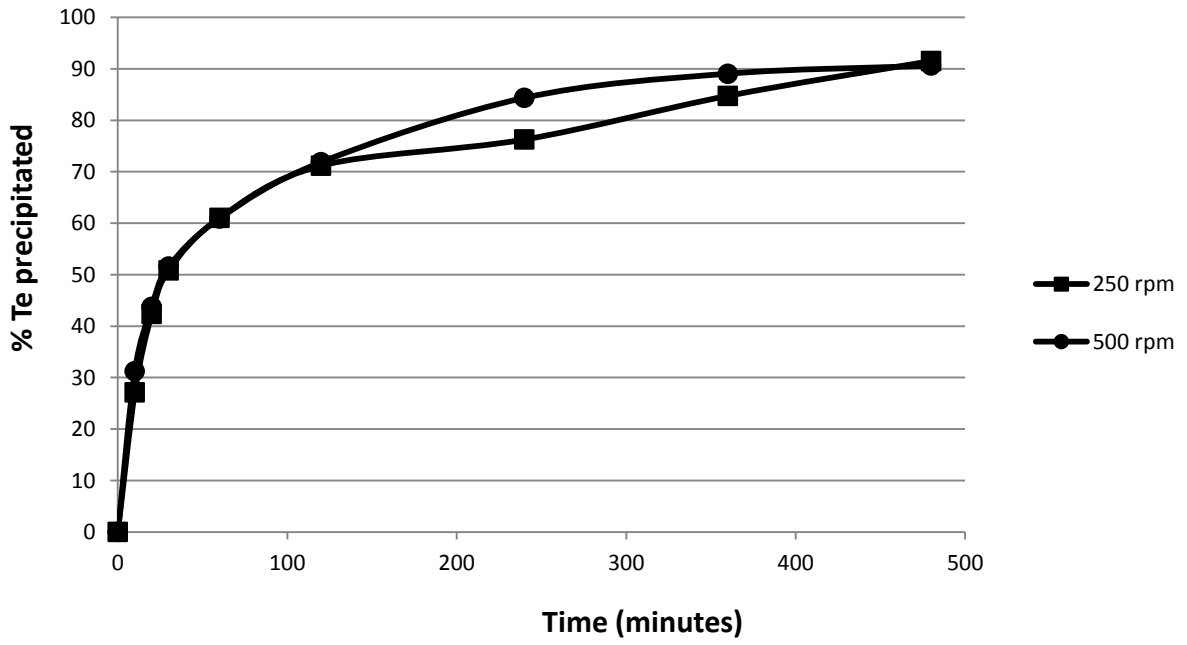

Figure 4.40: Effect of agitation on Te precipitation via SO_2 and Cu powder-based experimental method

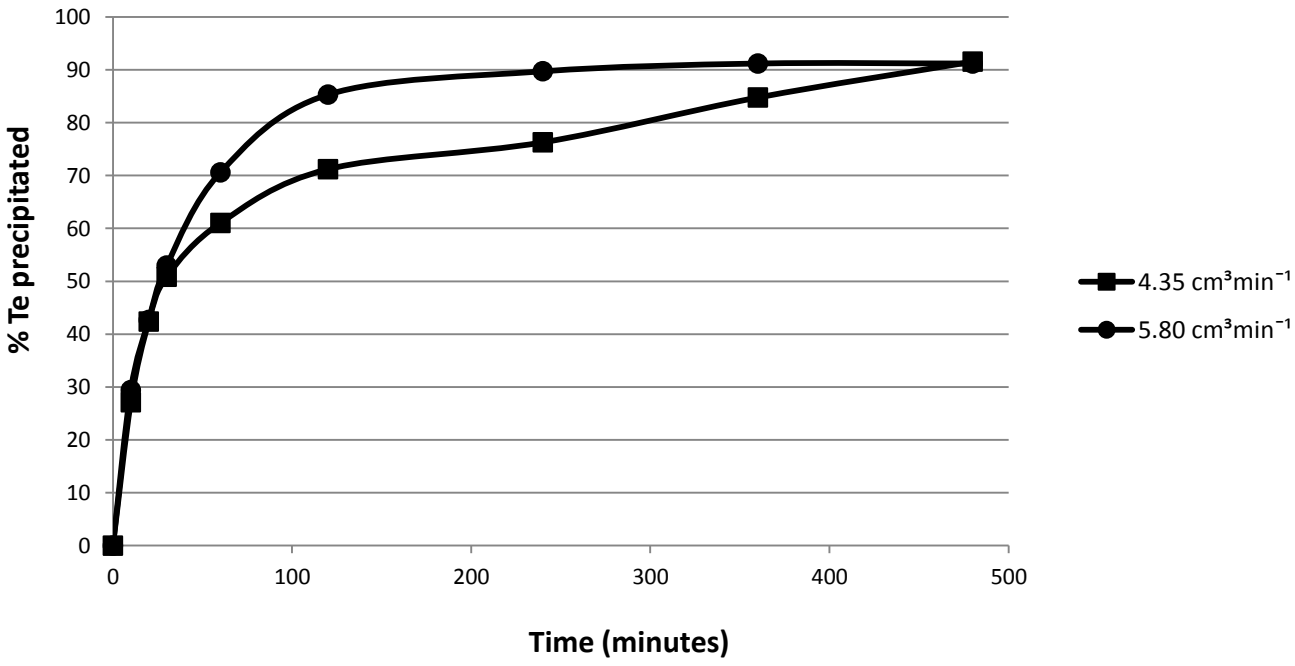

Figure 4.41: Effect of SO_2flow rate on Te precipitation via SO_2 and Cu powder-based experimental method

The amount of copper powder did not affect the percentage tellurium precipitation achieved after 8 hours; the precipitation kinetics did, however, appear to be slightly faster for the tests conducted with 2 g/L Cu powder than for the tests conducted with 1 g/L Cu powder due to the larger solid surface area. Figure 4.42 shows the effect of increasing the copper addition on tellurium precipitation kinetics for the test performed at 65˚C and 250 rpm agitation rate using a SO_2 flow rate of 4.4 cm³/min. As shown in this figure, the extents of Te precipitation achieved (91 % Te precipitation on average) are comparable for the two different masses of Cu powder used, though the addition of more copper powder resulted in a slightly faster Te precipitation kinetics.

Similar observations were made for the tests conducted at other process conditions. By comparing figure 4.44 a with figure 4.45 a and figure 4.44 b with figure 4.45 b, one can observe the effects of increasing the amount of Cu powder for the tests performed at other experimental conditions using this processing technique.

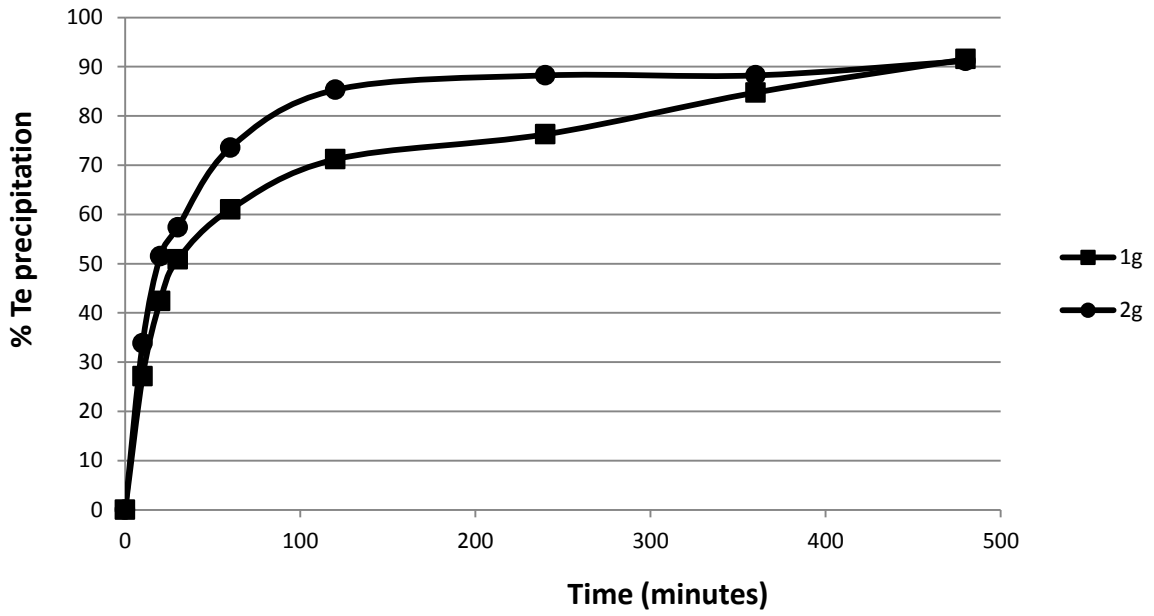

Figure 4.42: Effect of Cu powder addition on Te precipitation via SO_2 and Cu powder-based experimental method

The precipitation tests utilizing copper powder, where the tellurium precipitation is not dependent on the reduction of cupric and the formation of elemental copper, also show dependence on temperature. On average, the percentage tellurium precipitation achieved after eight hours were 94 % at high temperature conditions and 92 % at low temperature conditions. The slightly faster precipitation observed for the higher temperature tests (shown in figure 4.43 and figures 4.44 a through 4.5 b) could be an indication that the rate of tellurium precipitation between dissolved

tellurium ions and metallic copper (equations 2.27 and 2.28) was chemical reaction controlled. This is in agreement with the findings of Jennings *et al*. (1969) and Shibasaki *et al.*(1992) which were discussed in section 2.4.2.

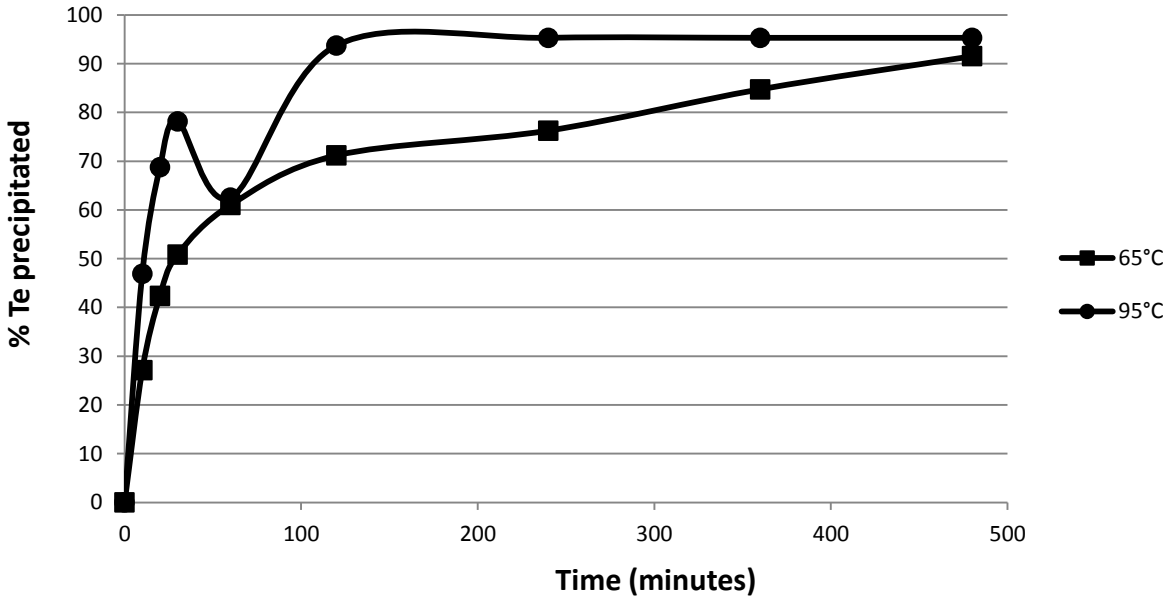

Figure 4.43: Effect of temperature on Te precipitation via SO_2 and Cu powder-based experimental method

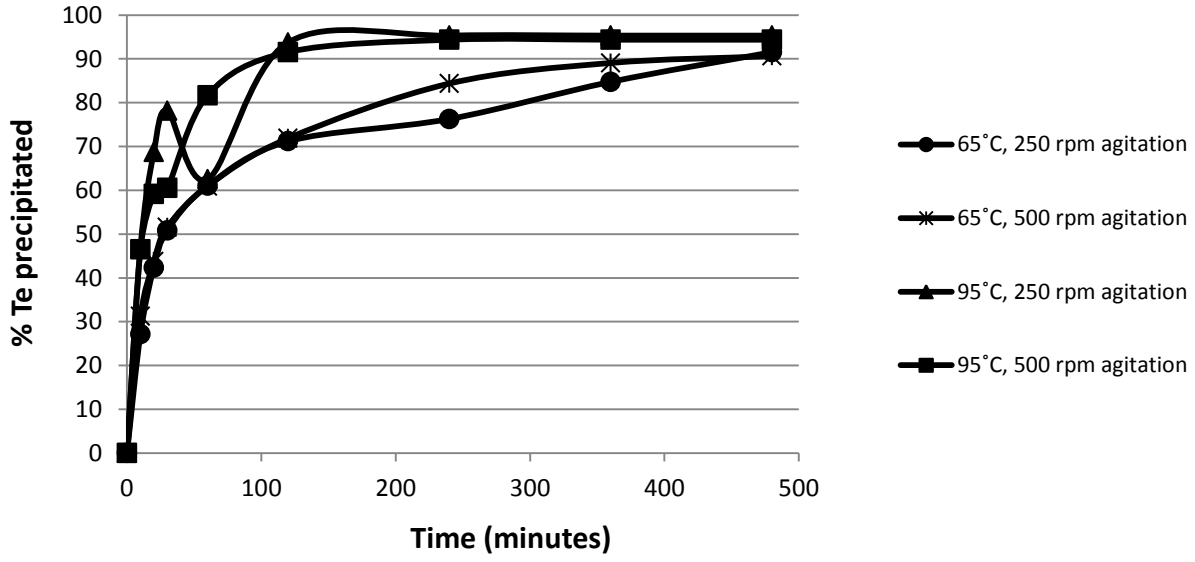

a)

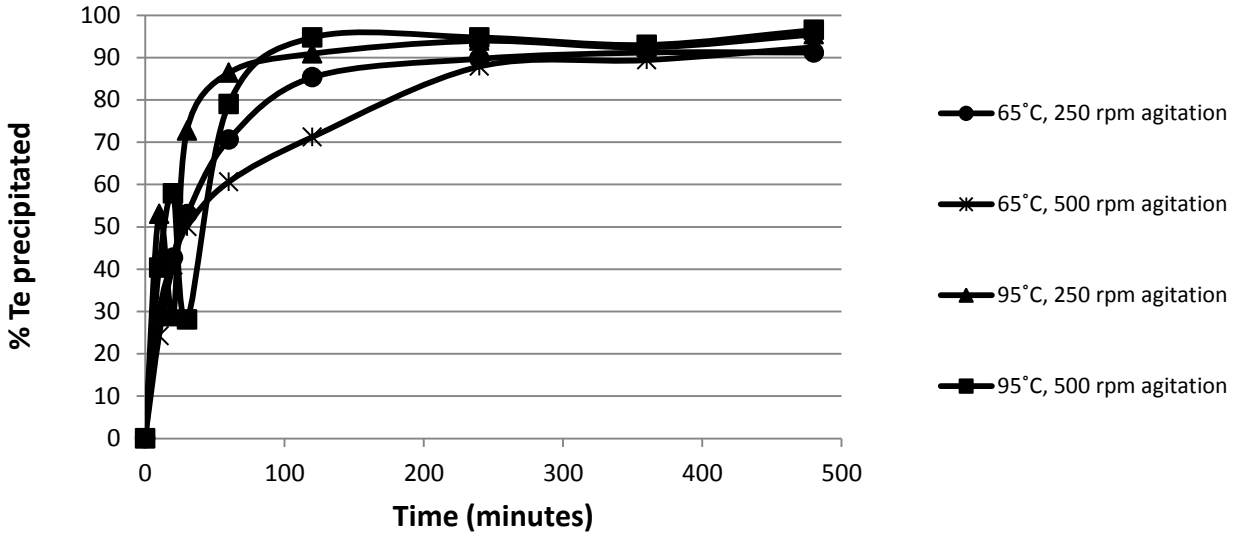

b)

Figure 4.44: Percentage Te precipitation achieved with: a. 4.4 cm³/min SO_2 flow rate and 1 g/L Cu powder addition b. 5.8 cm³/min SO_2 flow rate and 1 g/L Cu powder addition at typical operating conditions

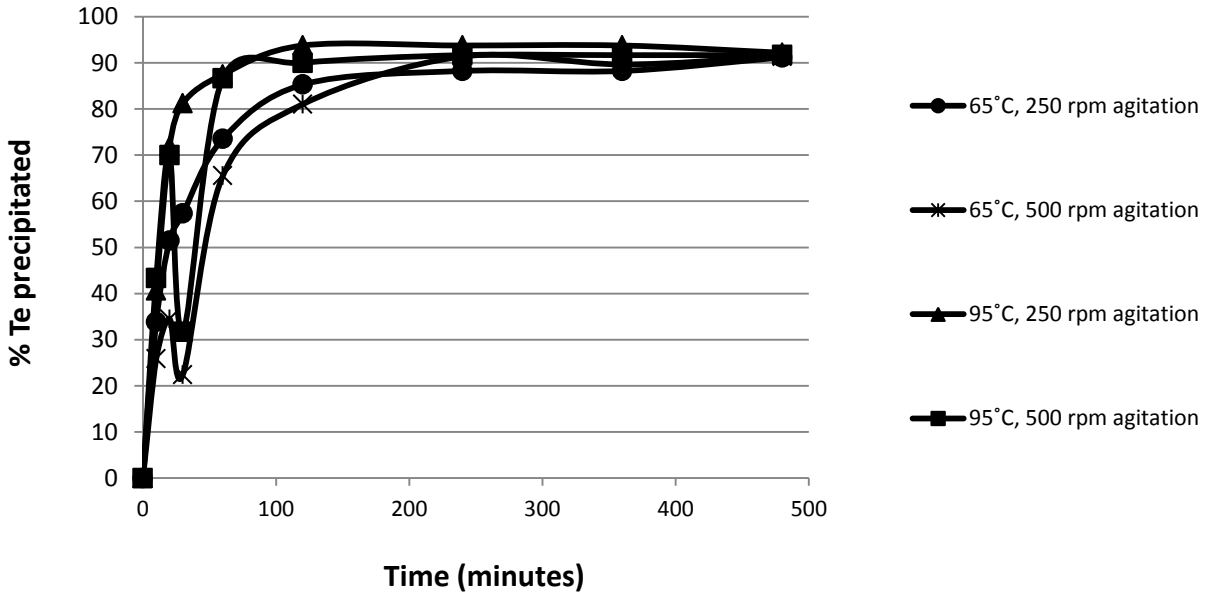

a)

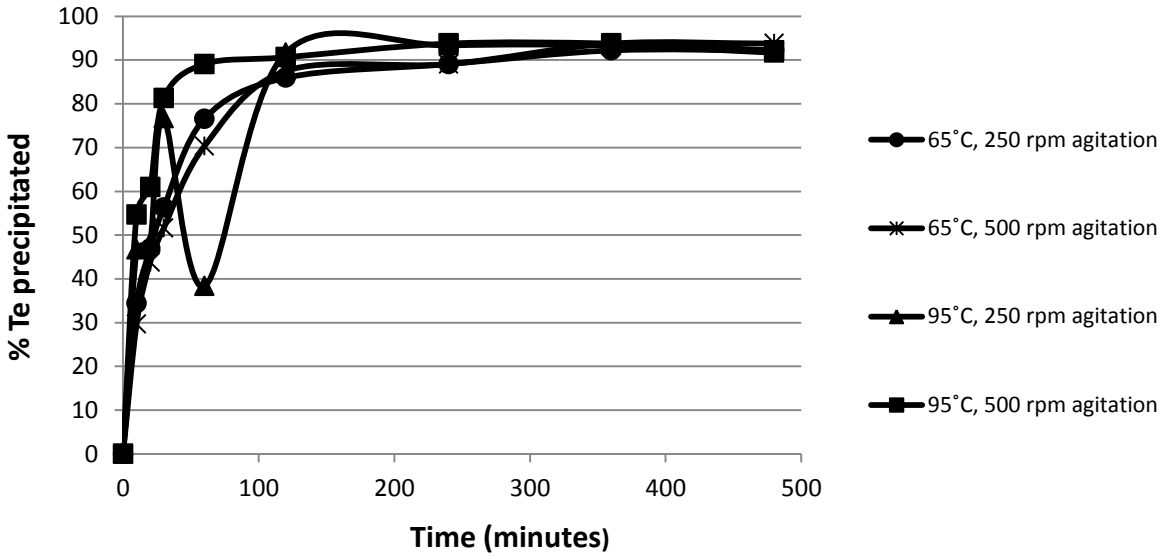

b)

Figure 4.45: Percentage Te precipitation achieved with: a. 4.4 cm³/min SO_2 flow rate and 2 g/L Cu powder addition b. 5.8 cm³/min SO_2 flow rate and 2 g/L Cu powder addition at typical operating conditions

4.7.3. Base metals precipitation

Tables 5.52 through 5.67 show the changes observed in Cu, Ni and Fe concentrations at different operating conditions during Te and Se precipitation via the third experimental method. As illustrated in these tables, no marked reductions were observed in the concentrations of Cu, Ni and Fe for any of the tests performed using this method; a maximum of 8 % percentage precipitation was noticed for these base metals.

A similar explanation to the one provided in sections 4.1.3 and 4.4.3 for the poor co-precipitation of copper with the use of SO_2 alone and with the use of SO_2 and Cu plate also holds for the low extraction of base metals noticed for this experimental method.

4.7.4. OPMs precipitation

Tables 5.52 through 5.67 show the changes noticed in OPMs concentrations at different operating conditions during Te and Se precipitation via this processing technique. As discussed in sections 4.1.4 and 4.4.4, the OPMs precipitation was poor for the test performed using this experimental method. A maximum of 16 % OPMs precipitation (13 % Ru, 16 % Rh and 5 % Ir) was achieved.

The outcome of this study clearly revealed that SO_2 is not ideal for the precipitation of OPMs. It also revealed that the addition of metallic copper as a precipitation enhancing reagent would not result in a significant improvement in the precipitation of other precious metals.

4.8. SO_2 and Cu powder: Statistical analysis

As was the case for the other experimental methods, the maximum Te and Se yield were also considered as the two responses for this experimental method. Figure 4.46 graphically illustrates the maximum Te and Se precipitation achieved for the experiments conducted using this precipitation method, while the experimental runs and responses are summarized in table 4.21.

4.8.1. Analysis of variance

Analysis of variance was also used to quantify the effects of the process variables and the interactions on the Te and Se yield. The model terms, their p-values and the R^2 for the responses are provided in tables 4.22 and 4.23.

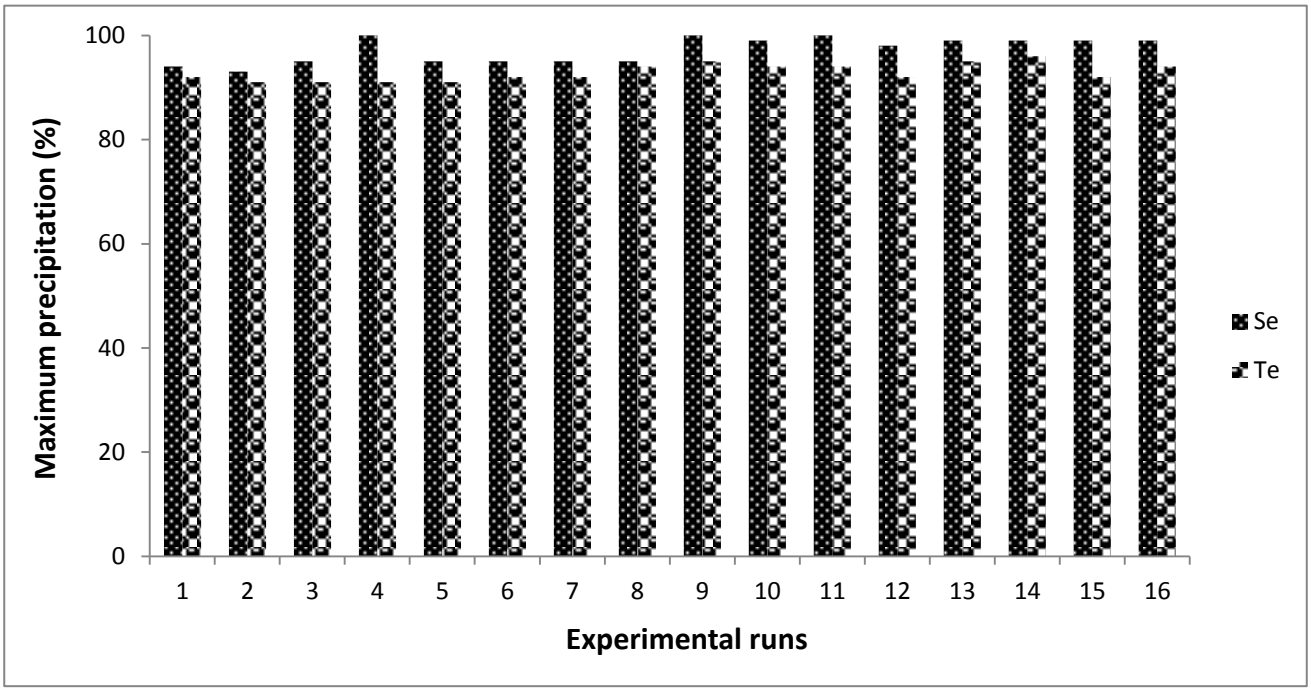

Figure 4.46: Observed maximum Se and Te precipitation for the sixteen runs of the SO_2 and Cu powder-based experimental method

As shown in table 4.22, the p-value of less than 0.0001 for temperature indicates that this process variable has the most significant effect on the Te yield. The p-value of 0.015 for SO_2 flow rate and copper powder addition indicate that these process variables also have significant effects on the maximum Te yield, but not as significant as the effect of temperature. In contrast, the qualitative analyses of the results presented in section 4.7.2 indicate that increasing the SO_2 flow rate and the quantity of the copper powder used did not result in increased Te precipitation. It is not clear, however, why the statistical analysis performed contradicts the qualitative observations discussed in section 4.7.2.

The p-value of 0.0002 for temperature as shown in table 4.23 also indicates that this process variable is the only variable that has a significant effect on Se yield. The insignificant model terms are only shown in these tables for illustrative purpose; they were not included in the models used for the process optimization.

With the exception of temperature-copper powder addition interaction and SO_2 flow rate-agitation interaction, which have major effects on maximum Te yield, no other second order interaction has a statistically significant effect on the two responses. Figures 4.47 a through f show the effects of the second order interactions on maximum Te yield, while figures 4.48 a through f graphically illustrate the effects of the second order interactions on the maximum Se yield. The temperature-copper powder addition interaction shows that high Te yield could be achieved at high temperature with little quantity of copper powder (figure 4.47c). The SO_2 addition-agitation interaction shows no significant increase in Te precipitation when increasing SO_2 flow rate and agitation condition (figure 4.47 d). From this analysis it is clear that high tellurium yield could be realized at a high temperature with small quantities of SO_2 and copper powder used.

Table 4.21: Summary of treatment combinations and their responses for the SO_2 and Cu powder-based experimental method

Runs	Factors and Levels				Responses	
	A	B	C	D	x	y
#1	65	4.4	250	1	92	94
#2	65	4.4	500	1	91	93
#3	65	4.4	250	2	91	95
#4	65	4.4	500	2	91	100
#5	65	5.8	250	1	91	95
#6	65	5.8	500	1	92	95
#7	65	5.8	250	2	92	95
#8	65	5.8	500	2	94	95
#9	95	4.4	250	1	95	100
#10	95	4.4	500	1	94	99
#11	95	4.4	250	2	94	100
#12	95	4.4	500	2	92	98
#13	95	5.8	250	1	95	99
#14	95	5.8	500	1	96	99
#15	95	5.8	250	2	92	99
#16	95	5.8	500	2	94	99

Where:

A represents the temperature (^{o}C)

B represents the SO_2 flow rate (cm^3/min)

C represents the agitation speed (rpm)

D represents the mass of copper powder measured in grammes

x represents the maximum tellurium precipitation achieved via the SO_2 and Cu powder-based experimental method

y represents the maximum selenium precipitation achieved via the SO_2 and Cu powder-based experimental method

Table 4.22: ANOVA table (Derived from Design Expert) showing the effects of significant model terms on the maximum Te precipitation achieved via the SO_2 and Cu powder-based experimental method

Model Terms	**Coefficient Estimate**	**p-value**
Intercept	92.88	
A - Temperature	1.12	< **0.0001**
B – SO_2 addition	0.37	**0.0150**
C – Agitation	-	0.3739
D – Cu powder addition	-0.38	**0.0150**
AB	-	0.3739
AC	-	0.3739
AD	-0.62	**0.0070**
BC	0.63	**0.0070**
BD	-	0.3739
CD	-	0.3739
ABC	-	0.4854
ABD	-0.38	**0.0150**
ACD	-	0.4854
BCD	-	0.4854
		R-squared = **0.9461**
		Adj. R-squared = **0.9102**

Table 4.23: ANOVA table (Derived from Design Expert) showing the effects of significant model terms on the maximum Se precipitation achieved via the SO_2 and Cu powder -based experimental method.

Model Terms	Coefficient Estimate	p-value
Intercept	97.19	
A - Temperature	1.94	**0.0002**
B – SO_2 addition	-	0.7422
C - Agitation	-	0.9097
D – Cu powder addition	-	0.5000
AB	-	0.9097
AC	-	0.5000
AD	-	0.4208
BC	-	0.9097
BD	-	0.5000
CD	-	0.6051
ABC	-	0.5000
ABD	-	0.4208
ACD	-	0.5000
BCD	-	0.6051
		R-squared = **0.6498**
		Adj. R-squared = **0.6247**

Based on the statistical analysis performed in this section , the regression models (given in terms of actual factors) that determine the maximum Te and Se yield achieved using this processing technique are thus given as follows:

Maximum Te yield = $75.02 + 0.20 \times$ *Temperature* (˚C) $+ 0.46 \times$ SO_2 *flow rate* (cm^3/min) $+ 5.92 \times$ *Cu powder addition* (g) $- 0.081 \times$ *Temperature* (˚C) $\times$ *Cu powder addition* (g) $+ (3.25 \times 10^{-4}) \times$ SO_2 *flow rate* (cm^3/min) $\times$ *Agitation rate* (rpm) $- (4.13 \times 10^{-4}) \times$ *Temperature* (˚C) $\times$ SO_2 *flow rate* (cm^3/min) $\times$ *Cu powder addition* (g) (4.5)

Maximum Se yield = $86.85 + 0.13 \times$ *Temperature* (˚C) (4.6)

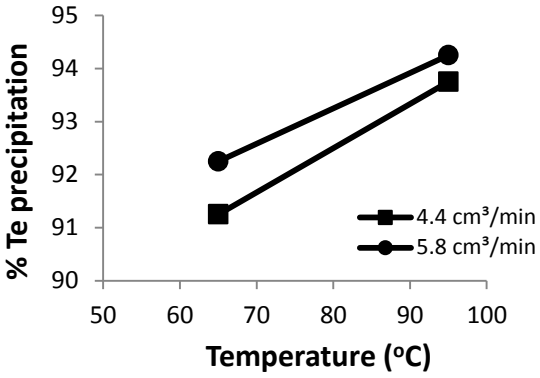

a. Effect of Temperature – SO_2 flow rate interaction on Te yield

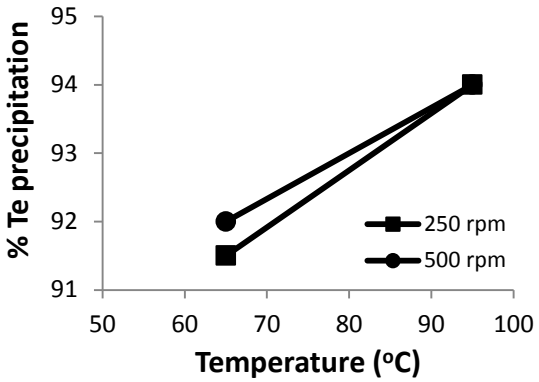

b. Effect of Temperature – agitation interaction on Te yield

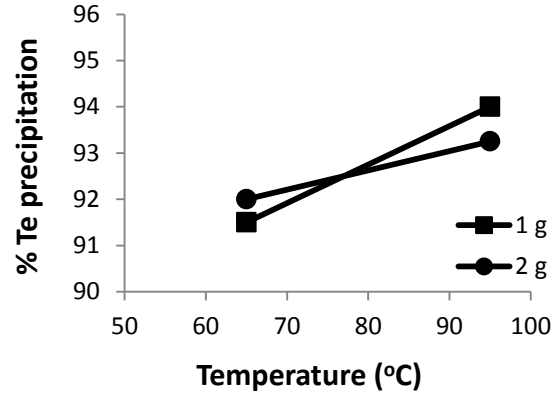

c. Effect of Temperature – Cu addition interaction on Te yield

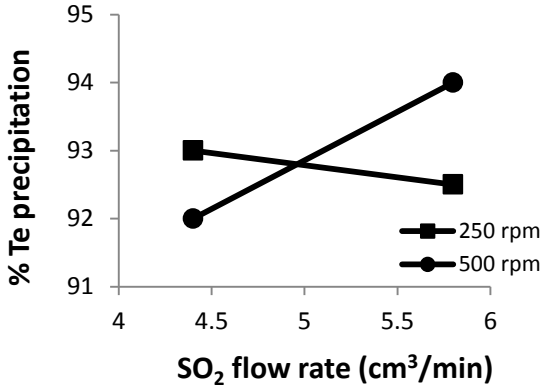

d. Effect of SO_2 flow rate – agitation interaction on Te yield

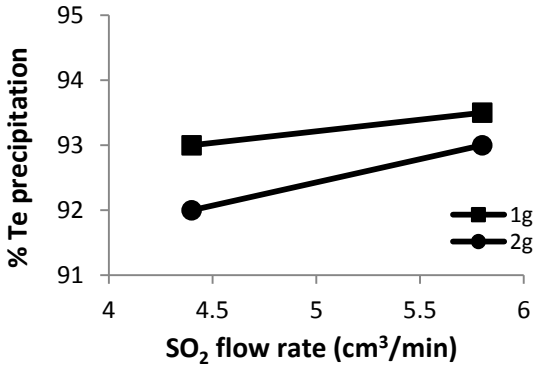

e. Effect of SO_2 flow rate – Cu addition interraction on Te yield

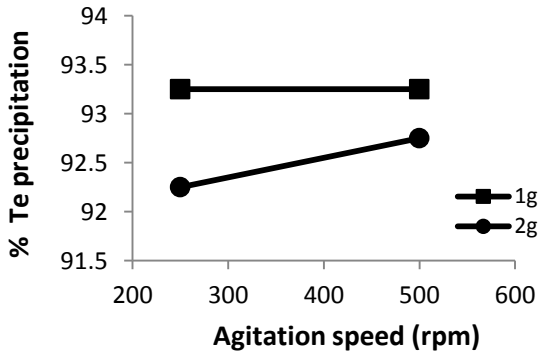

f. Effect of Cu addition –agitation interaction on Te yield

Figure 4.47: Effects of 2-order factor interactions on maximum Te yield achieved via the SO_2 and Cu powder-based experimental method.

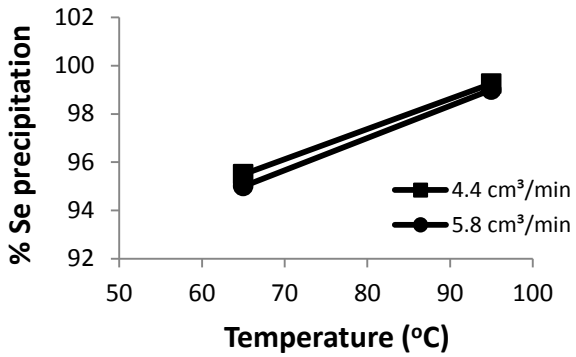

a. Effect of Temperature – SO_2 flow rate interaction on Se yield

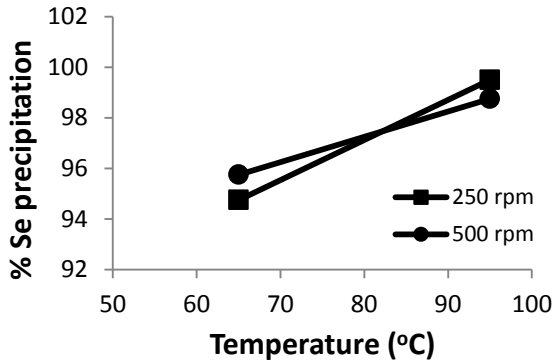

b. Effect of Temperature – agitation interaction on Se yield

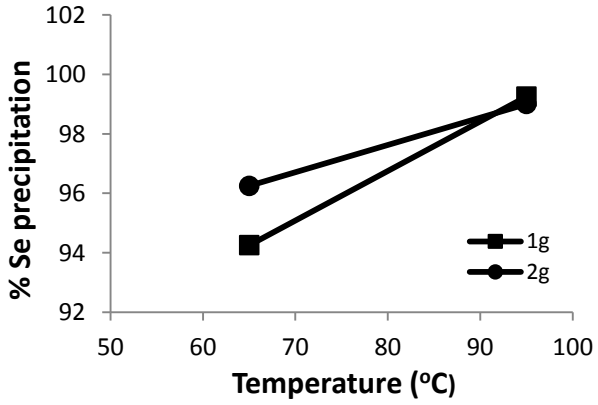

c. Effect of Temperature – Cu addition interaction on Se yield

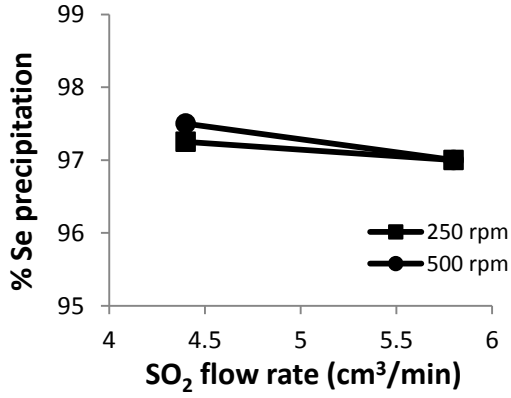

d. Effect of SO_2 flow rate – agitation interaction on Se yield

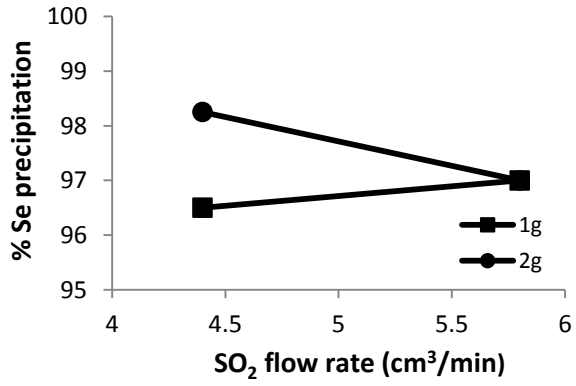

e. Effect of SO_2 flow rate – Cu addition interraction on Se yield

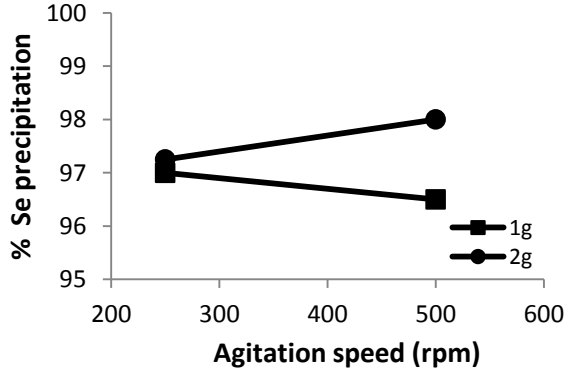

f. Effect of Cu addition –agitation interaction on Se yield

Figure 4.48: Effects of 2-order factor interactions on maximum Se yield achieved via the SO_2 and Cu powder-based experimental method.

4.8.2. Optimizing Te yield

As was the case for the other experimental methods discussed in sections 4.2.2 and 4.5.2, the third experimental method also precipitates selenium satisfactorily (97 % Se precipitation on) for all the investigated conditions. Therefore, the focus of the study was shifted to optimizing tellurium recovery.

The Design Expert software was also used to investigate the optimum solutions for the optimum criteria specified in table 4.24 using the desirability method suggested by Derringer and Suich (1980). The potential optimum conditions obtained for this processing technique are provided in table 4.25.

Table 4.24: Selection of optimum criteria for Te yield via the SO_2 and Cu powder-based experimental method (Derived from Design Expert)

Name	Goal	Lower value	Upper values	Importance
Temperature (˚C): factor	In range	65	95	3
SO_2 flow rate (cm^3/min): factor	In range	4.4	5.8	3
Agitation (rpm): factor	In range	250	500	3
Cu powder addition (g): factor	In range	1	2	3
Maximum Te yield (%): Response	Maximise	91	96	3
Maximum Se yield (%): Response	Maximise	93	100	3

Table 4.25: Numerical optimization solution (Derived from Design Expert) showing the possible optimum operating conditions (for the SO_2 and Cu powder-based experimental method) and their responses

S/N	Process Variables				Responses		
	Temperature (˚C)	SO_2 (cm^3/min)	Agitation (rpm)	Cu addition (g)	x (%)	y (%)	Desirability
1	75	4.4	250	1	93	97	0.454
2	85	4.4	250	1	94	98	0.638
3	90	4.4	250	1	94	98	0.730
4	90	4.4	250	2	94	98	0.649
5	95	4.4	250	1	95	99	0.825

4.9. SO_2 and Cu powder: Precipitate analysis

This section of the study was devoted to investigating the effects of different factors, including the addition of Cu powder into the leach solution, on the characteristics of the precipitates formed at the different experimental conditions. The first experimental run in table 4.21 was considered the normal experimental condition, while the second, third, fifth and ninth experimental runs were regarded as experimental conditions involving improved agitation condition, the use of additional

Cu powder, higher SO_2 addition rate and high agitation condition, respectively. The quantitative EDX analysis of the solid samples obtained during the different experiments are provided in tables 5.111 through 5.121 (Appendix F). The SEM images that show the particle morphologies and crystallinities of these precipitates are also provided in figures 5.10 b through 5.16.

4.9.1. Effect of agitation

Figures 4.49 a and b show the SEM images of the precipitates formed during the experiments performed at the normal condition and with improved agitation condition. As shown in figure 4.49 a, the sample consists of amorphous structures that are typically found in solid samples produced from precipitation reactions carried out at a low temperature (Demopoulos, 2009).

The results for the quantitative EDX analyses are summarised in tables 4.26 and 4.27. By comparing table 4.26 with table 4.27, one can observe that increasing the agitation rate resulted in a decrease in the Se and Te concentrations, and an increase in the nickel and sulphur concentrations found in the solid sample. The relatively high sulphur content seen in table 4.27 compared to table 4.26 could be ascribed to the fact that higher agitation resulted in the formation of additional metal sulphide phases (notably Ni_3S_2) for the test performed at 65˚C and at a SO_2 flow rate of 4.4 cm^3/min. It is however not clear why improved agitation resulted in a decrease in selenium and tellurium concentrations.

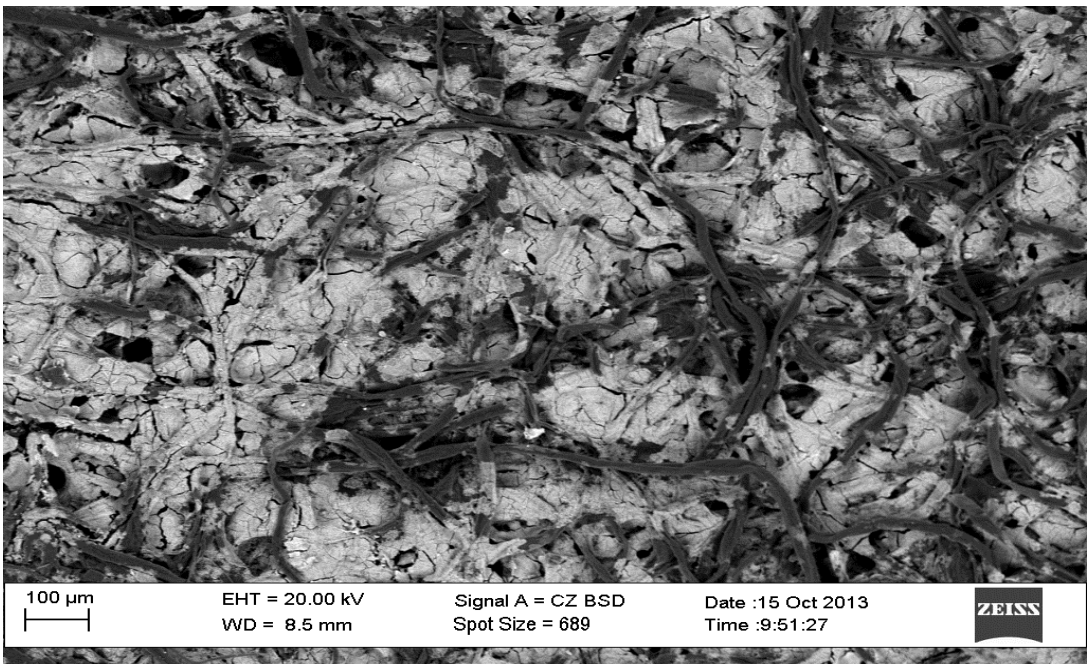

a)

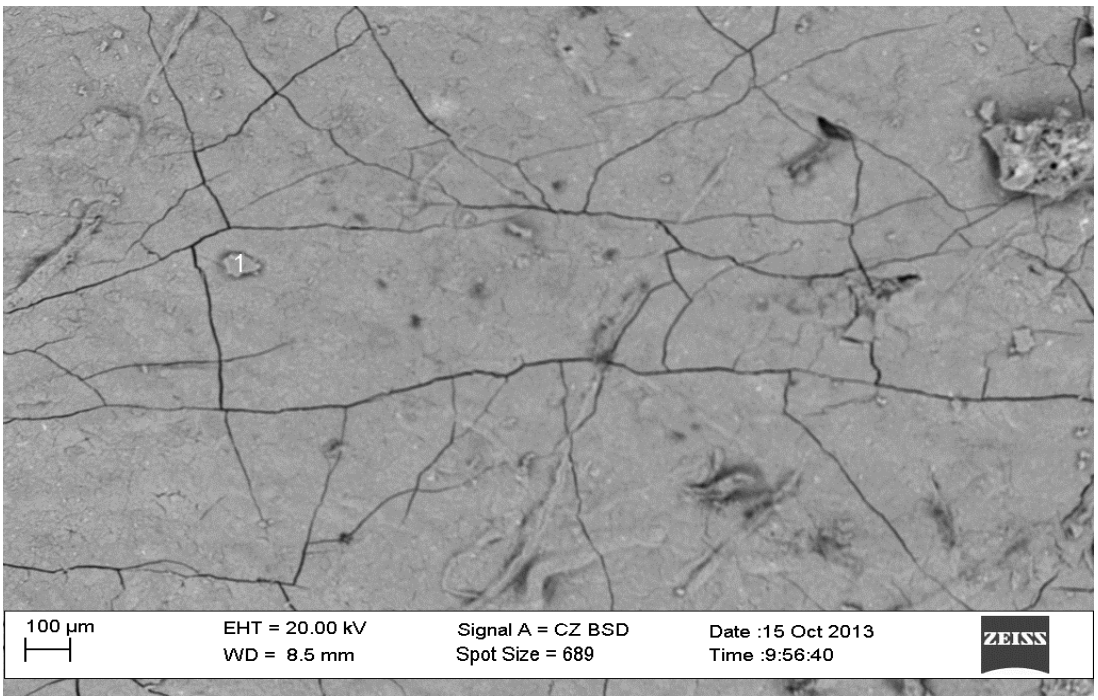

b)

Figure 4.49: SEM images of the precipitates obtained after the completion of the SO_2 and Cu powder-based experiment performed: a. at normal condition b. with improved agitation condition, showing the formation of different metal sulphide (CuS, Ni_3S_2 and PbS) phases

Table 4.26: Quantitative electron microprobe (wt. %) of solid sample obtained after the completion of the SO_2 and Cu powder-based experiment performed at normal condition.

Analysis	**Rh***	**Ru***	**Ir***	**Ni***	**Fe***	**Pb***	**Cu***	**Se***	**Te***	**S***	**Total**
1	0.00	3.02	0.00	6.05	0.00	0.00	42.31	15.40	4.52	28.69	100
2	0.00	3.19	0.00	6.08	0.00	3.21	40.46	14.55	5.03	27.47	100
Average (wt. %)	0.00	3.11	0.00	6.07	0.00	1.61	41.38	14.98	4.78	28.08	100
*Elements combined with oxygen											
Entire sample analysed twice											

Table 4.27: Quantitative electron microprobe (wt. %) of solid sample obtained after the completion of the SO_2 and Cu powder-based experiment performed with improved agitation.

Analysis	**Rh***	**Ru***	**Ir***	**Ni***	**Fe***	**Pb***	**Cu***	**Se***	**Te***	**S***	**Total**
1	0.00	2.31	0.00	15.93	0.54	4.27	24.82	3.05	1.96	47.11	100
2	0.00	3.82	0.00	14.10	0.00	6.92	21.71	3.20	0.00	50.25	100
3	0.00	3.95	0.00	13.37	0.00	5.88	21.12	4.11	1.17	50.39	100
Average (wt. %)											
*Elements combined with oxygen											
Entire sample analysed twice											

A mineralogical study of both samples revealed the presence of CuS as the major phase present in the samples, with small traces of Cu_2Se–Cu_2Te phase, Ni_3S_2 and PbS phase also present in the samples as minute inclusions.

4.9.2. Effect of Cu powder addition

Figure 4.50 shows the SEM image of the precipitate formed during the experiment performed with the use of additional copper powder, while the outcome of the quantitative EDX analysis is provided in table 4.28. By comparing table 4.26 with table 4.28, one can also observe a decrease in the Se and Te contents of the solid samples with the addition of more copper powder. This could be due to the fact that larger amount of copper powder than necessary was added into the solution for this test. As a result, the ratios of Cu to Te and Cu to Se found in the precipitate increased. When a mineralogical examination of the solid sample was done, CuS was also found as a major phase. Ni_3S_2, PbS and traces of Cu_2Te-Cu_2Se were detected as minute inclusions.

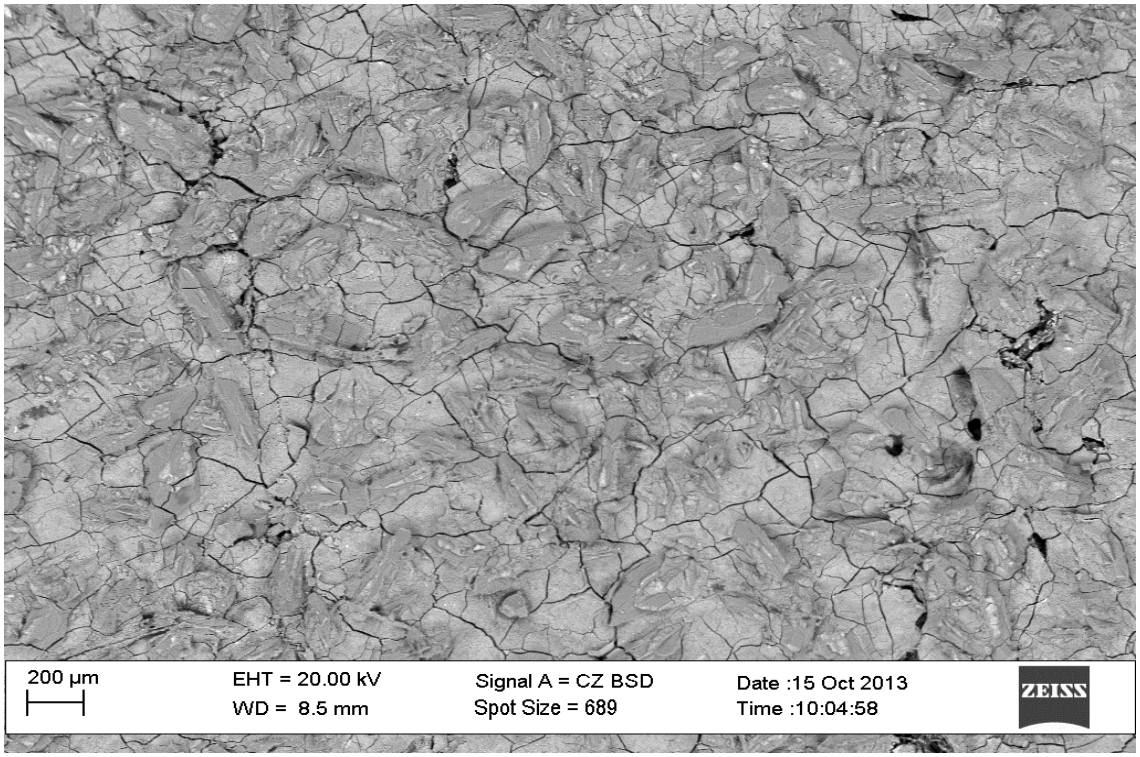

Figure 4.50: SEM images of the precipitate obtained after the completion of the SO_2 and Cu powder-based experiment performed using additional Cu powder

Table 4.28: Quantitative electron microprobe (wt. %) of solid sample obtained after the completion of the SO_2 and Cu powder-based experiment performed using additional copper powder

Analysis	Rh*	Ru*	Ir*	Ni*	Fe*	Pb*	Cu*	Se*	Te*	S*	Total
1	0.00	3.68	0.00	14.85	0.00	4.17	30.78	4.35	2.17	40.00	100
2	0.00	3.52	0.00	14.95	0.00	3.61	30.87	5.20	2.24	39.61	100
3	0.00	3.65	0.00	14.75	0.00	4.54	29.89	5.15	2.80	39.23	100
Average (wt. %)	0.00	3.61	0.00	14.85	0.00	4.11	30.51	4.90	2.40	39.61	100
*Elements combined with oxygen											
Entire sample analysed twice											

4.9.3. Effect of SO_2 addition

Figure 4.51 shows the SEM image of the precipitate formed during the experiment performed using a high SO_2 addition rate, while the outcome of the quantitative EDX analysis is summarized in table 4.29. By comparing table 4.26 with 4.29, one can observe that increasing the SO_2 flow rate from 4.4 to 5.8 cm^3/min did not result in a significant increase in the concentrations of Se and Te in the precipitate. A mineralogical study of the solid sample indicated that CuS was the dominant phase with Cu_2Te-Cu_2Se phase, PGMs, PbS and Ni_3S_2 phases also present as significant inclusions.

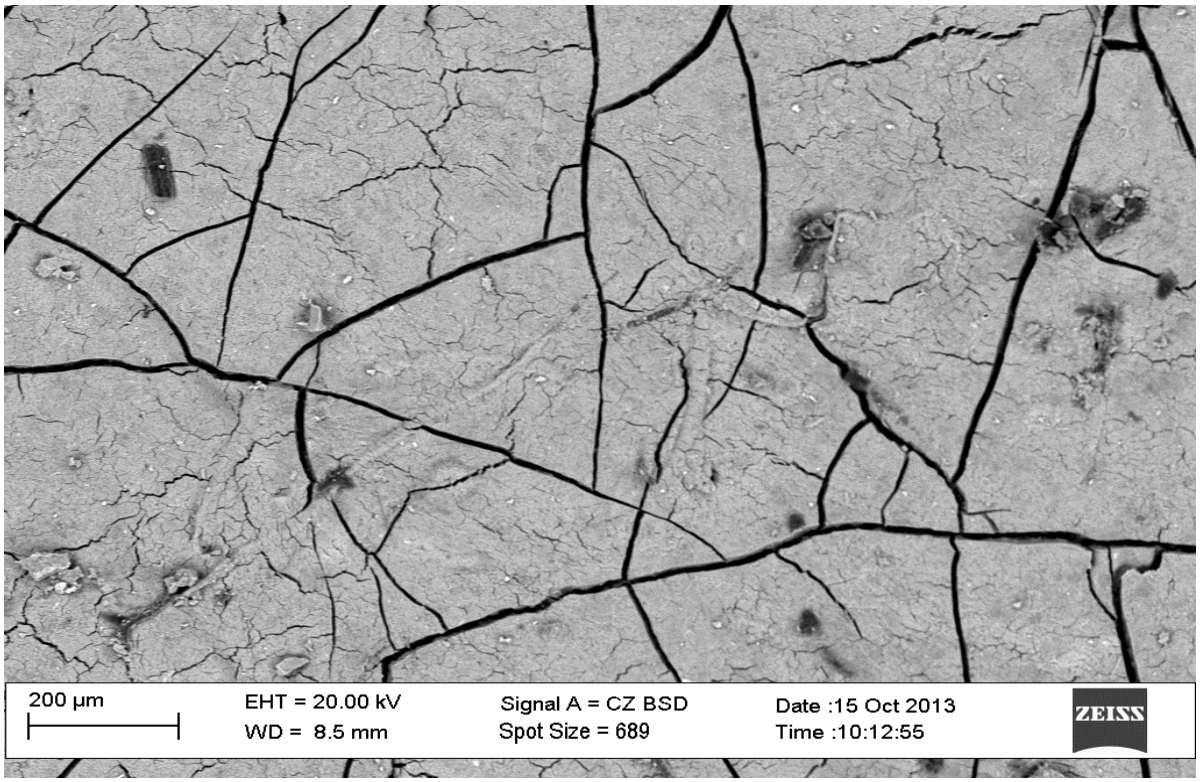

Figure 4.51: SEM image of the precipitate obtained after the completion of the SO_2 and Cu powder-based experiment performed using high SO_2 addition rate.

Table 4.29: Quantitative electron microprobe (wt. %) of solid sample obtained after the completion of the SO_2 and Cu powder-based experiment performed using high SO_2 addition rate.

Analysis	Rh*	Ru*	Ir*	Ni*	Fe*	Pb*	Cu*	Se*	Te*	S*	Total
1	0.00	5.61	1.25	8.10	0.00	4.55	32.74	9.58	3.91	34.28	100
2	1.14	5.20	0.00	8.16	0.00	3.50	33.30	10.60	3.32	34.78	100
3	0.98	5.32	0.00	8.32	0.00	3.88	33.31	10.23	3.02	34.93	100
Average (wt. %)	0.71	5.37	0.42	8.19	0.00	3.98	33.12	10.13	3.42	34.66	100
*Elements combined with oxygen											
Entire sample analysed thrice											

4.9.4. Effect of temperature

Fig 4.52 shows the SEM image of the solid sample formed during the experiment performed at a high temperature, while table 4.32 shows the relative concentrations of elements in the precipitate determined by quantitative SEM-EDX analysis. As shown in this figure, the sample analysed consists of needle-shaped crystal structures typical of precipitation processes carried out at a high temperature (Demopoulos, 2009).

Figure 4.52: SEM image of the precipitate obtained after the completion of the SO_2 and Cu powder-based experiment performed at high temperature condition.

By comparing table 4.26 with table 4.30, one can observe a large copper content in the solid sample obtained for the test performed at a high temperature using this processing technique. The poor Te

and Se contents of the solid sample for this test could be ascribed to the fact that large amount of metallic copper was precipitated from the solution along with the Te and Se impurities.

However, when a mineralogical examination of the sample was performed, Cu crystals and CuS were detected in the sample as the dominant phases. Small traces of Cu_2Te-Cu_2Se phase were also found in the precipitate as minute inclusions.

Table 4.30: Quantitative electron microprobe (wt. %) of solid sample obtained after the completion of the SO_2 and Cu powder-based experiment performed at high temperature condition.

Analysis	Rh*	Ru*	Ir*	Ni*	Fe*	Pb*	Cu*	Se*	Te*	S*	Total
1	0.00	0.00	0.00	0.51	0.00	0.70	98.22	0.00	0.00	0.57	100
2	0.00	0.00	0.00	0.87	0.00	0.00	97.14	0.00	0.00	1.99	100
3	0.00	0.00	0.00	0.74	0.00	0.00	99.26	0.00	0.00	0.00	100
3 different spots analysed											
4	0.00	3.90	0.00	10.05	0.00	3.35	38.19	8.20	2.72	33.60	100
5	0.52	3.41	0.00	9.89	0.00	3.78	38.91	7.05	2.23	34.20	100
Average (wt. %)											
*Elements combined with oxygen											
Entire sample analysed twice											

4.10. Comparing the three precipitation methods

Considering the tests performed at 65˚C, as illustrated in figures 4.53 a and 4.54 a, the Te and Se precipitation kinetics achieved when using copper powder as an additional reducing agent is noticeably faster than when using copper plate as an additional reducing agent. The addition of copper plate does, however, improve the Te precipitation kinetics compared to the utilization of SO_2 only. This is in agreement with the discussion regarding the dependence of tellurium precipitation on the reduction of cupric and the formation of elemental copper.

At 95˚C, the extents of tellurium and selenium precipitation achieved after eight hours were comparable for all the tests, regardless of whether copper was added as precipitation enhancing reagent or not (figures 4.5.3 b and 4.5.4 b). Although the tests conducted with copper powder continued to exhibit the fastest precipitation kinetics, the differences in the Te precipitation rates obtained with the different processing techniques were significantly smaller than at 65˚C. The effect of the amount of copper available for cementation reactions was also less noticeable for the tests performed at a higher temperature.

From this analysis, one can conclude that the precipitation method involving the utilization of Cu powder is the best of the three processing techniques, because it offers the advantage of faster Te precipitation kinetics than any other processing technique, for all the experimental conditions which were investigated.

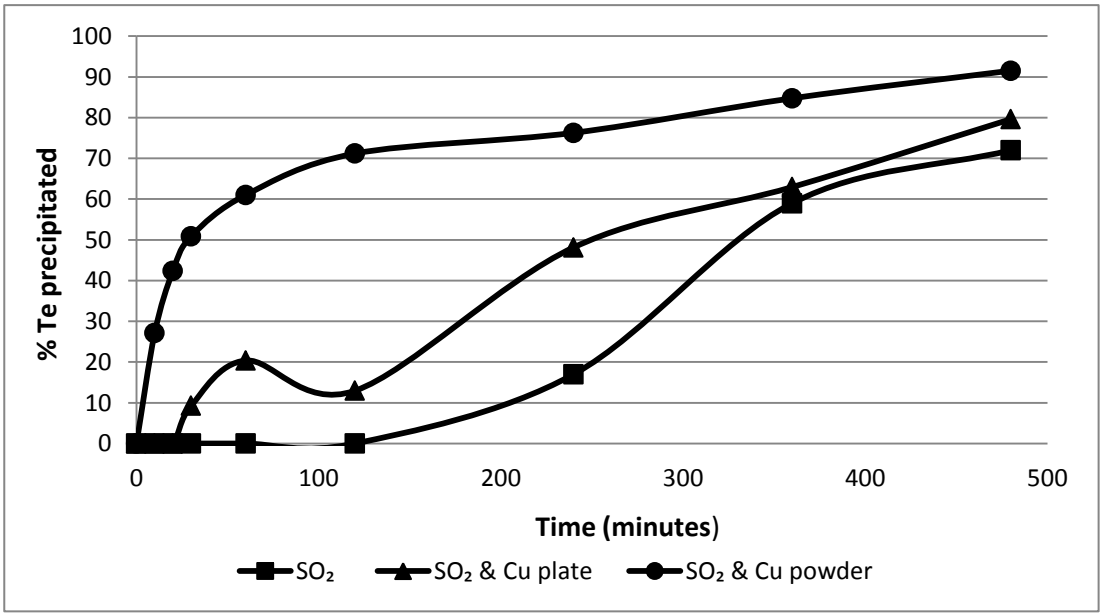

a)

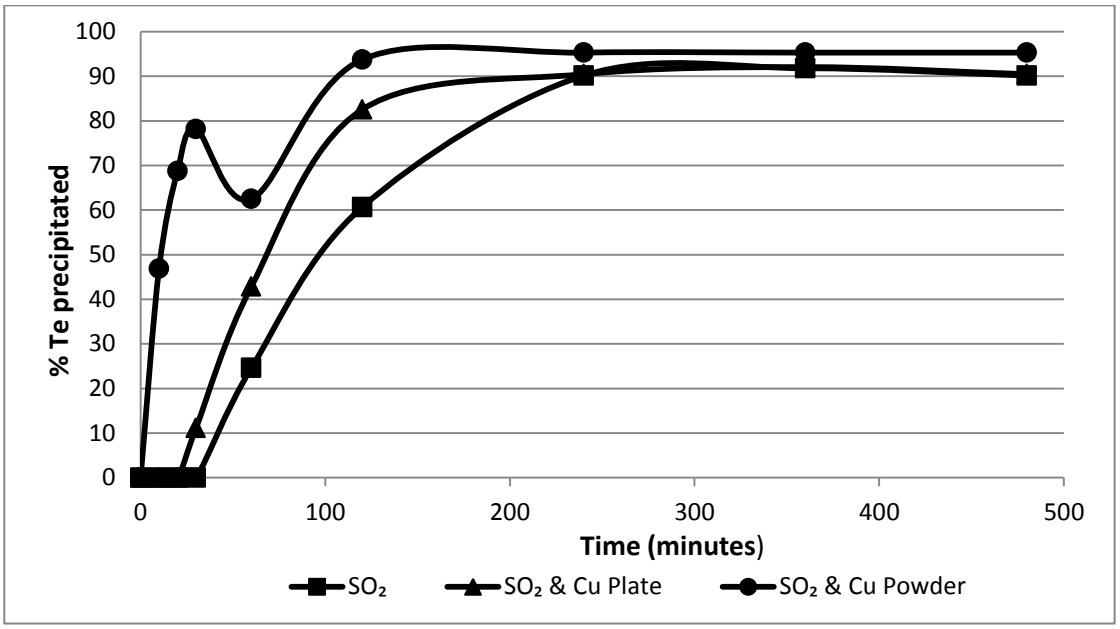

b)

Figure 4.53: A comparison of the effects of the different reagents used on Te precipitation at: a. low temperature (65°C) and b. high temperature (95°C). other parameters (4.4 cm^3/min SO_2 addition rate, 202.5 mm^2/L Cu plate (or 1g/L Cu powder addition) and 250 rpm agitation speed)

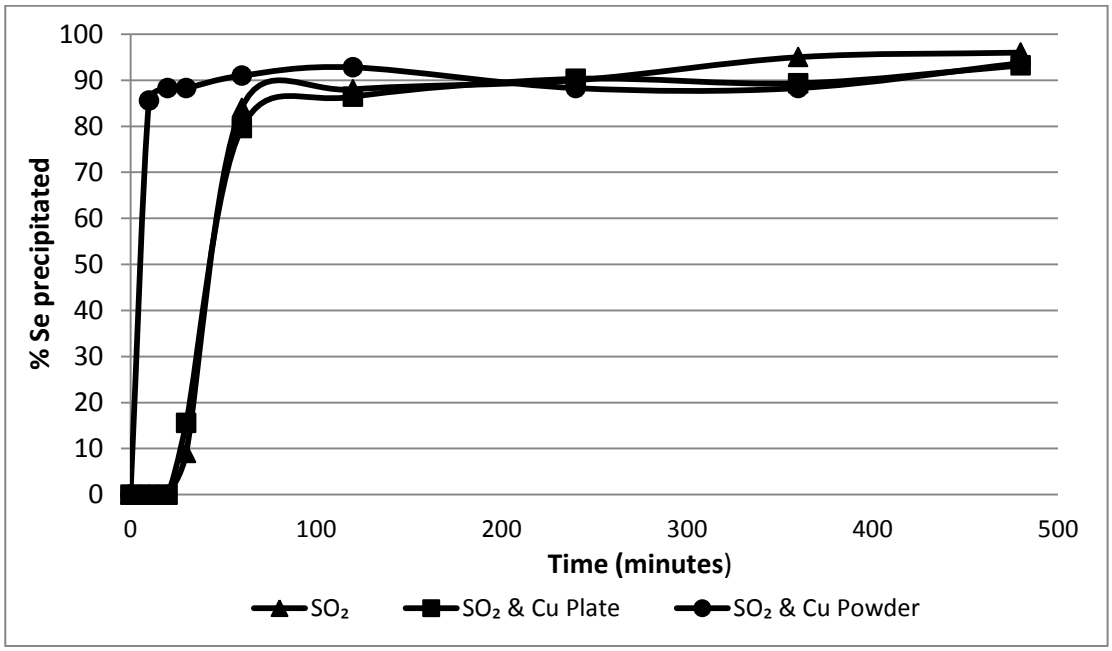

a)

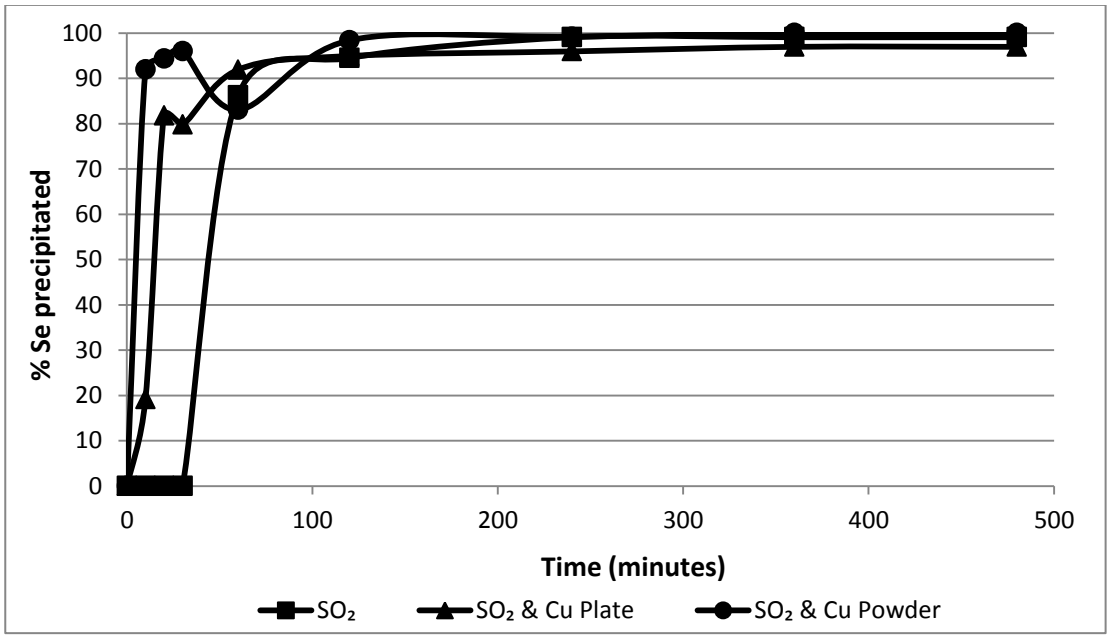

b)

Figure 4.54: A comparison of the effects of the different reagents used on Se precipitation at: a. low temperature (65°C) and b. high temperature (95°C). other parameters (4.4 cm^3/min SO_2 addition rate, 202.5 mm^2/L Cu plate (or 1g/L Cu powder addition) and 250 rpm agitation speed).

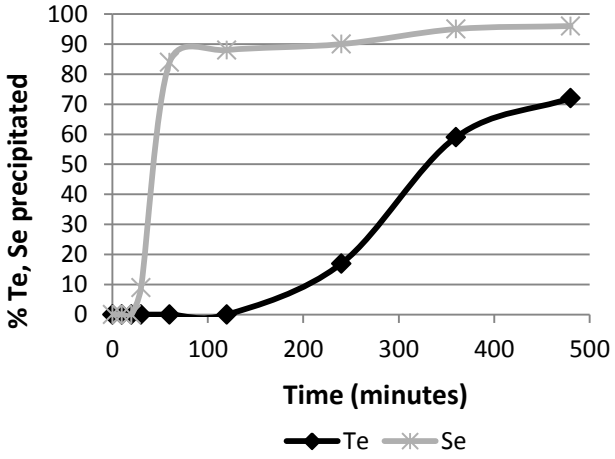

a) % Te and Se precipitated at 65°C, 4.4 cm^3/min SO_2 flow rate and 250 rpm agitation speed

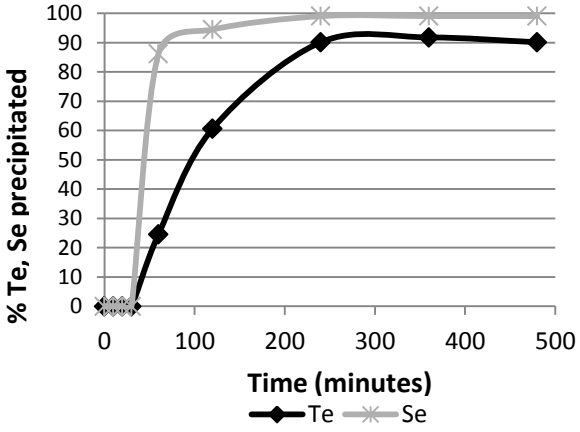

b) % Te and Se precipitated at 95°C, 4.4 cm^3/min SO_2 flow rate and 250 rpm agitation speed

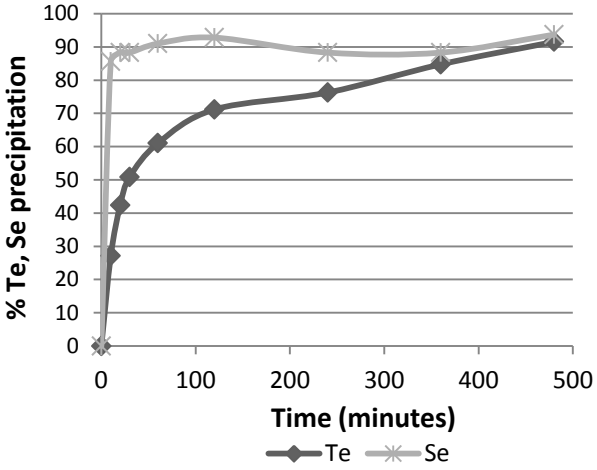

c) % Te and Se precipitated at 65°C, 4.4 cm^3/min SO_2 flow rate rate , 250 rpm agitation speed and 1 g/L Cu powder addition

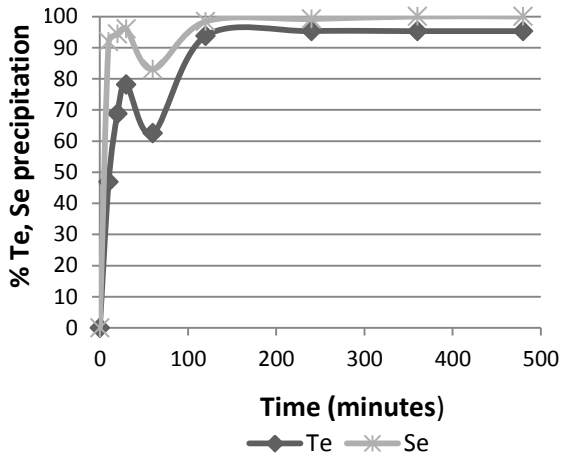

d) % Te and Se precipitated at 95°C, 4.4 cm^3/min SO_2 flow rate, 250 agitation speed and 1 g/L Cu powder addition

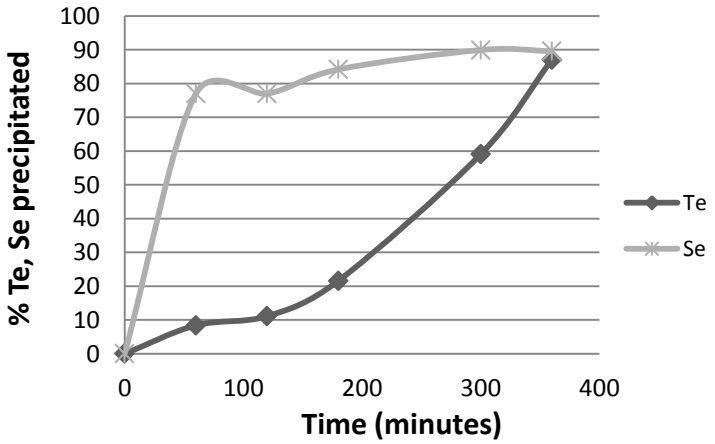

e) % Te and Se precipitated at 65-95°C (Adapted from (Wang *et al*., 2003))

Figure 4.55: A comparison of Te and Se precipitation achieved at typical operating condition, with the outcome of the test performed by Wang *et al*. (2003)

When the percentages tellurium and selenium precipitation achieved at typical operating conditions were compared (figures 4.55 a through d), it was found that selenium exhibited faster precipitation kinetics than tellurium for all the conditions investigated, including when the temperature was increased. The relatively faster Se precipitation rate, however, is in agreement with findings reported by Wang *et al*. (2003) which is illustrated in figure 4.55 e.

Chapter 5 : Conclusions

Different methods of precipitating tellurium and selenium from copper sulphate solutions were investigated in this study. The outcome of the study revealed that both Te and Se can be precipitated from the $CuSO_4$ medium with SO_2 alone or with the addition of metallic copper as a precipitation enhancing reagent. Thus, two process routes were identified for the removal of these impurities from the solution. The first process route involves the use of only SO_2, while the second process route requires the introduction of metallic copper as an additional precipitation reagent, in order to enhance the tellurium precipitation kinetics. Copper was added in the form of powder and rectangular plates for the tests involving the utilization of metallic copper.

The effects of agitation rate (250 rpm and 500 rpm), SO_2 flow rate (4.4 cm^3/min and 5.8 cm^3/min), temperature (65°C and 95°C), and copper addition on tellurium and selenium precipitation behaviour in the $CuSO_4$-H_2SO_4 medium were investigated. It was found that the agitation rate and the SO_2 flow rate only affected tellurium precipitation for the tests performed at 65°C utilizing only SO_2 or SO_2 with copper plates as precipitation reagents. At 95°C, the reduction of cupric ions by SO_2 and the subsequent metallic copper formation and tellurium precipitation were noticeably faster than at 65°C. It was concluded that the specific surface area of the copper plate was too small to allow the precipitation reaction between the dissolved tellurium and metallic copper to proceed at a sufficiently fast rate. As a result, the tellurium precipitation in this process was still dependent on the cupric reduction and elemental copper formation to proceed.

With the copper powder as a precipitation enhancing reagent, the large specific surface area of the metallic copper allowed tellurium precipitation to proceed mainly by reaction with the added metallic copper; any metallic copper formation as a result of SO_2 addition did not significantly influence the tellurium precipitation. The tellurium precipitation kinetics achieved when using copper powder as a precipitation enhancing reagent were consequently noticeably faster than for the other precipitation processes. On an industrial scale, however, challenges associated with the prevention of copper surface passivation as well as materials handling and solid-liquid separation might render the use of copper plates more feasible than copper powder.

Selenium precipitation was satisfactory for all the tests performed. Co-precipitation of other precious metals and the base metals of interest observed were low for all the tests. Optimum operating conditions for Te and Se recovery were proposed based on numerical optimization techniques; these conditions include a temperature of 85-95^oC, a SO_2 flow rate of 4.4 cm^3/min SO_2,

and 1g/L copper powder addition. Operating at these conditions would guarantee 94 % Te and 98 % Se precipitation, and would reduce the concentrations of these impurities to acceptable levels for the solution to be fed to copper electrowinning (Weir *et al*., 1982).

A mineralogical examination of the precipitates was also conducted with scanning electron microscopy. For the tests performed with only SO_2, the effects of SO_2 flow rate and agitation rate on the precipitate characteristics were pronounced, especially at 65˚C. The major phases detected in the precipitates produced from the tests performed at agitation rates of 250 rpm and 500 rpm are Cu_2S and CuS, respectively. In the case of the test performed at SO_2 flow rates of 4.4 and 5.8 cm^3/min, the dorminant phases seen in the precipitates are elemental selenium and copper selenide particles, respectively. Similar observations were made for the tests performed with copper plate addition, except that Cu_2S was not found in the precipitates produced from the tests performed at an agitation rate of 250 rpm.

The addition of copper powder as a precipitation enhancing reagent resulted in the formation of different metal sulphide phases (notably CuS, Ni_3S_2 and PbS), for the tests conducted at 65˚C regardless of the values of the other process variables. At 95˚C, Cu crystals, Cu_2O and minute inclusion of Cu_2 (Se, Te) were the prominent phases present in the precipitate.

References

Birchumshaw, L. (2008). Base metal refinery process overview, *Lonmin Internal Communication*, 16 April 2008.

Crundwell, F., Moats, M., Ramachandran, V., Robinson, T. and Davenport, W. (2011). *Extractive metallurgy of nickel, cobalt and platinum group metals*. Elsevier Science Limited, Oxford, United Kingdom, pp 457-488.

Demopoulos, G.P. (2009). Aqueous precipitation and crystallization for the production of particulate solids with desired properties. *Hydrometallurgy*, 96(3): 199-214.

Design Expert version 8.0.4, Stat-Ease,Inc. *Minneapolis*, MN 55413.

Derringer, G. and Suich, R. (1980). Simultaneous optimization of several response variables. *Journal of Quality Technology*, 12: 214-219.

Dirksen, J.A. and Ring, T.A. (1991). Fundamentals of crystallization: Kinetic effects on particle size distributions and morphology. *Chemical Engineering Science*, 46(10): 2389-2427.

Habashi, F. (1999). *Textbook of Hydrometallurgy*. Sainte-Foy, Quebec: Metallurgie Extractive.

Harañczyk, I., Szafirska, B. and Fitzner, K. (2002). The influence of the rate of selenium crystallization from aqueous solutions on its morphology. *Journal of Mining and Metallurgy: Section B: Metallurgy*, 38(1-2): 33-48.

Hoffmann, J.E., King, M.G., Carapella, S., Oldfield, J. and Putnam, R. (2001). Tellurium and tellurium compounds. *Kirk-Othmer Encyclopedia of Chemical Technology*, Wiley Online Library.

Hofirek, Z. (1983). Process for removing dissolved selenium values from an acidic aqueous copper sulphate solution. *United States Patent*, Patent number: 4 377 556.

Jackson, E. (1986). *Hydrometallurgical extraction and reclamation*. Ellis Horwood Limited, Chichester, West Sussex, England.

Jennings, P.H., Themelis, N.J. and Stratigakos, E.S. (1969). A continous-flow reactor for the precipitation of tellurium. *Canadian Metallurgical Quarterly*, 8(3): 281-286.

Ladriere, J. (1973). Reduction of selenic acid by copper in the presence of cupric ions. *Bulletin Des Sociétés Chimiques Belges*, 82(1-2): 99-122.

Lamya, R.M.(2007). A fundamental evaluation of the atmospheric pre-leaching section of the nickel-copper matte treatment process. *PhD Dissertation*, Department of Process Engineering, Stellenbosch University, South Africa.

Lewis, A. E. (2010). Review of metal sulphide precipitation. *Hydrometallurgy*, 104(2): 222-234.

Lottering, C. (2011). Rhodium precipitation from copper sulphate solutions in the selenium/tellurium removal section. *Final year research project*, Department of Process Engineering, Stellenbosch University, South Africa.

Lottering, C., Eksteen, J.J. and Steenekamp, N. (2012). Precipitation of rhodium from a copper sulphate leach solution in the selenium/tellurium removal section of a base metal refinery. *Journal of the Southern African Institute of Mining and Metallurgy*, 112(4): 287-294.

Mangere, M., Nathoo, J., and Lewis, A.E. (2010). Nucleation kinetics of selenium (+4) precipitation from acidic copper sulphate solution. *Journal of Crystal Growth*, 312(21): 3178-3182.

Mokmeli, M., Wassink, B. and Dreisinger, D. (2012). Equilibrium cuprous concentrations in copper sulphate-sulphuric acid solutions containing 50-110 g/L Cu^{2+} and 10-200 g/L H_2SO_4 at 50-95^{o}C. *Hydrometallurgy*, 121-124: 100-106.

Mokmeli, M., Wassink, B., and Dreisinger, D. (2013). Kinetics study of selenium removal from copper sulphate-sulfuric acid solution. *Hydrometallurgy*, 139: 13-25.

Mohan, R. and Myerson, A.S. (2002). Growth kinetics: A thermodynamic approach. *Chemical Engineering Science*, 57(20): 4277-4285.

Montgomery, D.C. (2013). *Design and analysis of experiment*. John Wiley and Sons, Singapore.

Mullin, J.W. (1993). *Crystallization*. Butterworth-Heinemann, United Kingdom.

OLI systems Inc. Stream Analyser, Version 9.0.7, OLI Systems Inc. Morris Plains, New Jersey, (2013).

Seby, F., Potin-Gautier, M., Giffaut, E., Borge, G. and Donard, O. (2001). A critical review of thermodynamic data for selenium species at 25˚C. *Chemical Geology*, 171(3): 173-194.

Schlesinger, M.E., King, M.J., Sole, K.C. and Davenport, W.G.I. (2011). *Extractive metallurgy of copper*. 5th Edition, Elsevier, Oxford, United Kingdom.

Sherritt Gordon Mines Limited. (1983). Selenium removal and residue treatment operating manual. *Western Platinum Limited*, Base Metal Refinery, pp. 1-8.

Shibasaki, T., Abe, K. and Takeuchi, H. (1992). Recovery of tellurium from decopperizing leach solution of copper refinery slimes by a fixed bed reactor. *Hydrometallurgy*, 29(1-3): 399-412.

Sohnel, O. and Garside, J. (1992). *Precipitation: Basic principles and industrial applications*. Butterworth-Heinemann, Oxford, United Kingdom.

Sugawara, Y., Hayashi, M., Konishi, J. and Hayashi, S. (1992). Process for recovering tellurium from copper electrolysis slime. *United States Patent*, Patent number5 160 588.

Wang, S., Wesstrom, B. and Fernandez, J. (2003). A novel process for recovery of Te and Se from copper slimes autoclave leach solution. *Journal of Minerals and Materials Characterization and Engineering*, 2(1): 53-64.

Weir, D.R., Kerfoot, D.G.E. and Scheie, H.C. (1982). Removal of selenium (IV) and (VI) from acidic copper sulphate solutions. *United States Patent*, Patent number 4 330 508.

Appendix A: Sample calculations

A.1 Reaction Stoichiometry

$Fe_2(SO_4)_3(aq)+H_2SO_3(aq)+H_2O(l)\rightarrow 2FeSO_4(aq)+2H_2SO_4(aq)$ from reaction 2.31

$X_{Fe} = 0.598$ g/L

$V_{soln} = 1L$

$m_{Fe} = X_{Fe} \times V_{soln}$ (5.1)

$m_{Fe} = (0.598g/L)x(1L)$ from equation 5.1

$m_{Fe} = 0.598$ g

$Mw_{Fe} = 55.845$ g/mol

$n_{Fe} = m_{Fe} / Mw_{Fe}$ (5.2)

$n_{Fe}= (0.598g) / (55.845g/mol)$ from equation 5.2

$n_{Fe} = 0.010708$ mol

$Fe_2(SO_4)_3$ and H_2SO_3 dissociate in the aqueous solution according to the following equations:

$Fe_2(SO_4)_3 = 2Fe^{3+} + 3(SO_4)^{2-}$ (5.3)

$H_2SO_3 = SO_2 + H_2O$ (5.4)

Where n_{Fe} refers to the total concentration of Fe^{3+} in the solution, prior to reagent addition.

From the LHS of the reaction 2.31, 1 mol $Fe_2(SO_4)_3$ requires 1 mol H_2SO_3, but 0.010708 mol of Fe^{3+} can be found in $Fe_2(SO_4)_3$ when it dissociates according to equation 5.3.

Therefore, 0.005354 mol H_2SO_3 will be required for the reaction to proceed.

1 mol SO_2 gas dissolves in 1 mol H_2O to produce 1 mol H_2SO_3

Then, 0.005354 mol SO_2 gas will dissolve in 0.005354 mol of H_2O to produce 0.005354 mol of H_2SO_3 according to equation 5.4.

A.2 Estimating SO_2 flow rate and percentage excess of SO_2

Conditions for the estimation of SO_2 flow rates into the pressure vessel from the reagent cylinder for the two process routes are given as follows:

- Equation of state for an ideal gas was used to estimate the volume of SO_2 gas required for the experiments irrespective of routes.
- An ambient temperature of 20^{o}C and an atmospheric pressure were used in the estimation of SO_2 volumetric flow rates, from the reagent cylinder for the two process routes.
- Sulphur dioxide gas was sparged into 1 litre of the process solution for 3 hours.
- SO_2 flow rates remained unchanged for the 2 routes.
- The duration of each experiment was 8 hours irrespective of process routes.

A.2.1 Estimating Percentage excess of SO_2

X_{Se} = 0.427 g/L

Mw_{Se} = 78.96 g/mol

$m_{Se} = X_{Se} \times V_{soln}$

m_{Se} = (0.427 g/L) × (1 L)

m_{Se} = 0.427 g

$n_{Se} = m_{Se} / Mw_{Se}$ (5.5)

n_{Se}=0.427g/78.96 g/mol from equation 5.5

n_{Se} = 0.005408 mol

For 500% excess, nSO_2 = 6 x 0.005408 mol

n_{SO2} = 0.0321 mol

n_{SO2} / n_{Se} = 0.032125 mol SO_2 per 0.005408 mol dissolved selenium ions

n_{SO2} / n_{Se} = 5.940 mol SO_2 per 1 mol dissolved selenium ions

For 700% excess, n_{SO2} = 8 x 0.005354 mol

n_{SO2} = 0.0428 mol

n_{SO2} / n_{Se} = 7.921 mol SO_2 per 1 mol dissolved selenium ions.

These values are in agreement with the recommendation of Hofirek (1983).

A.2.2 Estimating SO_2 flow rates

n_{SO2} = 0.005354 mol (without excess)

V = nRT / P (from equation of state for ideal gases) (5.6)

R = 0.08206 (atm)(L)(mol^{-1})(K^{-1})

Temperature = 293.15 K

Pressure = 0.9869 atm

For 500% excess of SO_2

n_{SO2} = 0.032125 mol

V = (0.005354 mol)(0.08206)(293.15 K) / (0.9869 atm)

V = 0.7830291 L

V = 783.029 cm^3

F = V/T (5.7)

F = (783.028 cm^3) / (180 min) = 4.35 cm^3/min

Using similar analyses for 700% excess of SO_2 gas, a flow rate of 5.80 cm^3/min was obtained. These flow rates were used for the two process routes.

A.3 Estimating specific surface area of copper plates

Surface area of cuboidal plate = 2(LW + WH + HL) (5.8)

H = 1.5 mm

W = 7.5 mm

L = 10 mm

Surface area of copper plate = 2((10x7.5) + (7.5x1.5) + (10x1.5)) from equation 5.6

Surface area of copper plate = 202.5 mm^2

The surface area of the large plate is 405 mm^2 per litre, which is twice that of the small copper plate.

Appendix B: Experimental design

Table 5.1: Experimental runs of the 1st method of Te recovery with the use of SO_2 only

Runs	Temperature (^oC)	SO_2 flow rate (cm^3/min)	Agitation speed (rpm)
#1	65	4.4	250
#2	65	4.4	500
#3	65	5.8	250
#4	65	5.8	500
#5	95	4.4	250
#6	95	4.4	500
#7	95	5.8	250
#8	95	5.8	500

Table 5.2: Experimental runs of the 3rd method of Te recovery with the use of SO_2 and Cu powder

Runs	Temperature (^oC)	SO_2 flow rate ($cm^{3/}min$)	Copper addition (g/L)	Agitation (rpm)
#1	65	4.4	1	250
#2	65	4.4	1	500
#3	65	4.4	2	250
#4	65	4.4	2	500
#5	65	5.8	1	250
#6	65	5.8	1	500
#7	65	5.8	2	250
#8	65	5.8	2	500
#9	95	4.4	1	250
#10	95	4.4	1	500
#11	95	4.4	2	250
#12	95	4.4	2	500
#13	95	5.8	1	250
#14	95	5.8	1	500
#15	95	5.8	2	250
#16	95	5.8	2	500

Table 5.3: Experimental runs of the 2nd method of Te recovery with the use of SO_2 and Cu plate

Runs	**Temperature (^oC)**	**SO_2 flow rate (cm^3/min)**	**Surface area of Cu plate per solution volume (mm^2/L)**	**Agitation (rpm)**
#1	65	4.4	202.5	250
#2	65	4.4	202.5	500
#3	65	4.4	405.0	250
#4	65	4.4	405.0	500
#5	65	5.8	202.5	250
#6	65	5.8	202.5	500
#7	65	5.8	405.0	250
#8	65	5.8	405.0	500
#9	95	4.4	202.5	250
#10	95	4.4	202.5	500
#11	95	4.4	405.0	250
#12	95	4.4	405.0	500
#13	95	5.8	202.5	250
#14	95	5.8	202.5	500
#15	95	5.8	405.0	250
#16	95	5.8	405.0	500

Appendix C: Operating procedures

C.1: Operating procedure of the 1st experimental method

- Switch on the SO_2 extractor fan in the fume cupboard
- Ensure that the valve that controls the flow of SO_2 gas from the reagent cylinder into the flow meter next to the pressure vessel is firmly closed.
- Ensure that the valve of the variable area flow meter is closed.
- Close the sampling valve.
- Ensure that the bleed valve is opened.
- Ensure that the safety latch and safety ring are both opened.
- Lower pressure vessel by rotating the lever.
- Pour 1 litre of the process solution into the vessel.
- Raise the pressure vessel to stop.
- Close both the safety ring and safety latch.
- Close the bleed/relief valve.
- Ensure that the tap that supplies cooling water to the vessel's jacket is opened.
- Turn on the autoclave temperature controller. Set the temperature (T_R) to the desired value.
- Turn on the agitator and set its speed to 250 rpm. This will ensure the thorough mixing of the solution for uniform distribution of heat.
- Switch off agitator when the temperature of the solution attains the desired value.
- Open the valve of the tap that supplies cooling water to the condenser that condenses the vapour emanating from the process solution upon heating.
- Open the bleed valve
- Open the valves of the reagent (SO_2) cylinder.
- Gently open the valve of the variable area flow meter. Set the flow rate of SO_2 according to the experimental run.
- Ensure that the non-return return valve is opened (while the 2 valves of the SO_2 gas sparger are closed)
- Take the first (initial sample) after the desired temperature is attained.
- Close the non-return and open the 2 valves of the SO_2 gas sparger; when the desired flow rate is measured.

- Set the agitator's speed to the required value (250 rpm or 500 rpm) depending on the experimental unit when the temperature of the solution attains the desired value.
- Begin collecting samples. Samples were taken at the following intervals (in minutes): 10, 20, 30, 60, 120, 240, 360 and 480.
- Open the non-return valve and close the 2 valves of the SO_2 gas sparger; after sparging SO_2 for 3 hours.
- Close the valve of the flow meter by turning it clockwise
- Close the valve of the reagent (SO_2) cylinder.
- Reduce the value of T_R to 20^oC. This will guarantee cooling prior to shut down.
- Turn off the heater when T_R attains a value of 20^o Celsius.
- Close the valve of the tap that supplies cooling water to the condenser.
- Open the bleed/relief valve.
- Open the safety ring and safety latch.
- Gently lower the pressure vessel to a desired position.
- Open the drain valve to empty the vessel after it is cool.
- Wash the vessel with concentrated sulphuric acid.
- Wash the process vessel with distilled water.

C.2: Operating procedure of 2nd and 3rd experimental method

- Switch on the SO_2 extractor fan in the fume cupboard.
- Ensure all valves and fittings are leak tight. Presumably, a leak test must have been performed prior to the first experiment in accordance to the guidelines found in the operating manual. If not, conduct a leak test.
- Ensure that the (3) valves that control the flow of SO_2 gas from the reagent cylinder into the flow meter next to the pressure vessel is firmly closed. Close the valves by turning them in this order: clockwise, anticlockwise and clockwise.
- Ensure that the valve of the variable area flow meter is closed (by turning it clockwise).
- Close the sampling valve (by turning it anticlockwise).
- Ensure that the bleed valve is closed (by turning it clockwise).
- Ensure that the relief valve is opened (by pulling it up).
- Ensure that the safety latch and safety ring are both opened.
- Open the non-return valve (but close the 2 valves of the SO_2 gas sparger)
- Lower pressure vessel by rotating the lever.
- Pour 1 litre of the process solution into the vessel.
- Raise the pressure vessel to stop.
- Close both the safety ring and safety latch.
- Close the relief valve (by pulling it down)
- Open the valve of the tap that supplies cooling water to the condenser by turning it anticlockwise.
- Ensure that the valve of the tap that supplies cooling water to the vessel's jacket is opened. If not, open it by turning it anticlockwise.
- Turn on the autoclave temperature controller. Set the temperature (T_R) to the desired value (65 or 95^oC) depending on the experimental unit.
- Turn on the agitator and set its speed to 250 rpm. This will ensure a thorough mixing of the solution for uniform distribution of heat.
- Open the valves of the reagent (SO_2) cylinder by turning them in this order: anticlockwise, clockwise and anticlockwise.
- Gently open the valve of the variable area flow meter (by turning it anticlockwise). Set the flow rate of SO_2 according to the experimental run.
- Turn off the agitator when the temperature of the reactor (T_R) has attained its set value.

- Turn off the autoclave temperature controller.
- Open the bleed valve, relief valve, and safety ring and safety latch.
- Gently lower the pressure vessel to a desired position
- Take the first (initial) sample.
- Sprinkle 1g or 2g of copper powder (or hang 10x7.5x1.5mm copper plate(s) on the agitator's blade) into the solution depending on the experimental unit or method.
- Repeat steps 12, 13 and 14.
- Turn on the temperature controller. The value of T_R has been recorded in the memory of the programmable heater. You do not need to reset it.
- Turn on the agitator. Set its value to 250 rpm or 500 rpm depending on the experimental unit.
- Open the 2 valves of the SO_2 gas sparger by turning them anticlockwise, but close the non-return valve
- Begin collecting samples. Samples were take at the following intervals (in minutes): 10, 20, 30, 60, 120, 240, 360 and 480.
- Close the valves of the reagent after sparging SO_2 for 3 hours by turning them in this order: clockwise, anticlockwise and clockwise.
- Repeat step 9.
- Close the valve of the flow meter cylinder by turning it clockwise.
- The bleed valve should be left opened throughout the experiment, to purge the vessel of impurities, and to prevent the build up of pressure in the reactor.
- Reduce the value of T_R to 20^o Celsius. This will guarantee cooling prior to shut down.
- Turn off the heater when T_R attains a value of 20^o Celsius.
- Close the valve of the tap that supplies cooling water to the condenser.
- Open the relief valve.
- Close the bleed valve.
- Switch off the extractor fan for SO_2
- Open the safety ring and safety latch.
- Gently lower the pressure vessel to a desired position.
- Open the drain valve to empty the vessel after it is cool.
- Remove the unreacted copper from the empty vessel or copper plate(s) from the agitator's blade for the 'Te precipitation withplates' experiments.
- Wash the vessel with concentrated sulphuric acid.
- Wash the process vessel with distilled water

Appendix D: Experimental data

D.1 Experimental Data – Te recovery with SO_2 only

Table 5.4: ICP result for #1 of 1st experimental method

Time (minutes)	Cu (g/L)	Fe (g/L)	Ni (g/L)	Ir (mg/L)	Rh (mg/L)	Ru (mg/L)	Se (mg/L)	Te (mg/L)
0	94.00	0.57	47.27	37.40	29.43	184.00	50.55	27.10
10	106.15	0.73	52.05	39.57	31.54	196.60	53.65	29.09
20	110.85	0.87	53.35	41.89	32.67	207.55	55.25	30.72
30	111.35	0.90	53.35	41.73	32.05	207.20	45.76	30.91
60	107.10	0.90	52.20	40.01	31.87	201.85	8.02	28.92
120	109.80	0.96	53.55	40.44	32.13	209.90	6.05	29.00
240	109.80	0.95	55.10	41.86	30.54	199.65	5.00	22.55
360	104.40	0.91	51.25	40.71	30.62	204.00	2.57	11.00
480	106.50	0.94	51.90	40.08	30.46	206.95	1.76	7.27

Table 5.5: ICP results for #2 of 1st experimental method

Time (minutes)	Cu (g/L)	Fe (g/L)	Ni (g/L)	Ir (mg/L)	Rh (mg/L)	Ru (mg/L)	Se (mg/L)	Te (mg/L)
0	104.80	0.76	50.10	39.35	29.82	192.05	51.35	28.99
10	109.85	0.86	53.10	41.82	31.70	202.55	54.05	31.06
20	110.20	0.90	53.05	41.16	30.01	203.15	44.85	30.87
30	109.95	0.91	53.05	40.85	31.11	199.40	13.21	30.15
60	106.70	0.91	51.50	41.97	30.45	200.00	6.46	27.51
120	107.30	0.91	53.40	39.86	30.46	185.05	4.03	26.43
240	109.70	0.88	53.60	40.36	29.41	186.20	2.45	20.34
360	107.65	0.89	52.90	40.49	29.48	185.60	2.16	13.74
480	108.75	0.89	54.00	39.62	29.55	191.30	3.19	9.85

Table 5.6: ICP results for #3 of 1st experimental method

Time (minutes)	Cu (g/L)	Fe (g/L)	Ni (g/L)	Ir (mg/L)	Rh (mg/L)	Ru (mg/L)	Se (mg/L)	Te (mg/L)
0	97.55	0.68	48.05	38.52	29.67	193.95	50.95	28.25
10	110.50	0.88	54.25	41.60	32.05	203.55	17.55	31.54
20	114.25	0.94	55.20	42.16	31.35	204.25	8.93	28.62
30	109.40	0.92	53.25	41.29	30.98	202.00	5.79	28.94
60	109.00	0.90	52.45	39.21	30.44	184.65	3.60	26.09
120	108.50	0.80	53.55	40.14	30.13	188.60	2.45	7.73
240	115.30	0.91	57.05	38.95	29.66	197.60	2.11	6.98
360	108.85	0.84	53.75	39.52	29.68	193.45	1.19	3.37
480	127.80	1.02	62.65	37.08	28.76	187.70	3.30	3.37

Table 5.7: ICP results for #4 of 1st experimental method

Time (minutes)	Cu (g/L)	Fe (g/L)	Ni (g/L)	Ir (mg/L)	Rh (mg/L)	Ru (mg/L)	Se (mg/L)	Te (mg/L)
0	101.80	0.71	50.50	40.51	30.51	189.70	51.15	29.31
10	107.50	0.82	53.90	41.51	32.89	195.55	53.80	31.31
20	109.70	0.89	54.35	41.13	32.95	203.35	49.49	31.85
30	108.30	0.90	54.35	41.62	32.10	195.55	22.08	31.91
60	109.90	0.94	55.45	40.37	32.10	201.50	8.95	29.68
120	110.40	0.85	55.30	40.86	31.66	185.40	4.46	26.32
240	109.50	0.83	53.65	39.83	30.39	186.80	1.45	12.13
360	109.30	0.84	54.75	40.02	30.18	198.10	2.06	7.09
480	104.05	0.87	52.95	38.86	29.52	188.25	2.47	5.87

Table 5.8: ICP results for #5 of 1st experimental method

Time (minutes)	Cu (g/L)	Fe (g/L)	Ni (g/L)	Ir (mg/L)	Rh (mg/L)	Ru (mg/L)	Se (mg/L)	Te (mg/L)
0	106.25	0.76	53.55	42.14	30.65	201.35	54.55	30.68
10	105.45	0.81	53.85	42.01	31.01	206.80	54.40	30.67
20	104.05	0.81	53.05	41.46	31.16	201.60	54.50	31.10
30	107.00	0.86	55.55	39.72	32.03	205.45	55.85	31.30
60	107.45	0.88	55.40	40.25	30.36	196.90	7.67	23.18
120	104.00	0.88	54.10	40.37	29.89	191.30	2.95	11.87
240	101.55	0.89	53.10	39.91	28.54	189.40	0.47	3.22
360	103.75	0.89	53.05	41.39	28.33	189.45	0.44	2.65
480	105.90	0.91	53.75	38.93	28.49	190.50	0.33	2.83

Table 5.9: ICP results for #6 of 1st experimental method

Time (minutes)	Cu (g/L)	Fe (g/L)	Ni (g/L)	Ir (mg/L)	Rh (mg/L)	Ru (mg/L)	Se (mg/L)	Te (mg/L)
0	102.30	0.82	51.45	41.63	31.80	201.05	45.88	29.57
10	109.55	0.89	55.50	42.28	31.89	204.75	46.85	29.76
20	108.25	0.86	54.45	41.19	31.01	208.75	49.17	30.12
30	110.45	0.90	55.20	42.30	31.60	207.95	46.70	28.82
60	105.75	0.87	53.00	38.59	30.48	194.60	5.54	25.33
120	101.55	0.86	51.60	36.80	28.91	187.15	1.28	10.55
240	98.55	0.87	51.05	37.74	27.26	180.15	0.50	1.47
360	105.80	0.92	55.15	38.52	28.71	191.20	0.50	2.43
480	102.25	0.96	53.50	37.90	28.17	188.60	0.50	2.46

Table 5.10: ICP results for #7 of 1st experimental method

Time (minutes)	Cu (g/L)	Fe (g/L)	Ni (g/L)	Ir (mg/L)	Rh (mg/L)	Ru (mg/L)	Se (mg/L)	Te (mg/L)
0	96.20	0.77	49.02	37.76	29.16	187.45	51.40	26.64
10	110.00	0.88	54.85	40.68	31.93	206.60	55.80	29.17
20	104.35	0.84	52.45	39.40	30.78	196.30	24.74	27.07
30	102.70	0.86	52.60	39.33	30.62	195.80	6.62	24.23
60	102.45	0.87	51.65	39.46	30.09	193.30	12.30	24.00
120	105.75	0.91	54.60	37.63	28.24	189.15	1.48	6.18
240	102.85	0.92	54.20	40.05	28.12	192.75	0.73	1.65
360	101.90	0.90	53.95	37.34	28.13	183.75	0.77	2.24
480	94.90	0.85	53.20	38.35	27.30	182.90	0.50	1.80

Table 5.11: ICP results for #8 of 1st experimental method

Time (minutes)	Cu (g/L)	Fe (g/L)	Ni (g/L)	Ir (mg/L)	Rh (mg/L)	Ru (mg/L)	Se (mg/L)	Te (mg/L)
0	96.80	0.74	52.90	31.50	31.50	201.60	56.35	27.30
10	99.05	0.85	53.85	31.69	31.69	203.80	50.55	29.79
20	99.50	0.87	54.05	30.36	30.36	194.50	7.33	24.95
30	103.00	0.92	55.95	31.52	31.52	200.70	5.73	24.19
60	102.50	0.92	55.90	29.09	29.09	186.50	2.81	12.93
120	98.20	0.90	54.95	28.70	28.70	186.30	1.72	5.29
240	92.75	0.87	51.85	27.77	27.77	183.80	1.76	2.32
360	96.75	0.90	55.00	28.45	28.45	187.05	0.50	1.16
480	97.35	0.91	55.95	29.44	29.44	190.45	0.50	1.06

Table 5.12: Percentages of species precipitated at different sampling periods of #1 of 1st experimental method

Time (minutes)	Ir (%)	Rh (%)	Ru (%)	Se (%)	Te (%)
0	0	0	0	0	0
10	0	0	0	0	0
20	0	0	0	0	0
30	1	0	0	9	0
60	5	0	3	84	0
120	4	0	0	88	0
240	0	5	4	90	17
360	4	4	2	95	59
480	5	5	0	96	72

Table 5.13: Percentages of species precipitated at different sampling periods of #2 of 1st experimental method

Time (minutes)	Ir (%)	Rh (%)	Ru (%)	Se (%)	Te (%)
0	0	0	0	0	0
10	0	1	0	0	0
20	2	5	0	13	0
30	2	1	2	75	0
60	2	3	1	87	5
120	5	3	9	92	9
240	4	7	8	95	29
360	4	6	9	96	53
480	6	6	6	94	66

Table 5.14: Percentages of species precipitated at different sampling periods of #3 of 1st experimental method

Time (minutes)	Ir (%)	Rh (%)	Ru (%)	Se (%)	Te (%)
0	0	0	0	0	0
10	0	0	0	66	0
20	0	2	0	82	0
30	2	3	1	88	0
60	7	5	10	93	7
120	4	6	8	95	73
240	7	7	3	96	75
360	6	7	5	98	88
480	12	10	8	93	88

Table 5.15: Percentages of species precipitated at different sampling periods of #4 of 1st experimental method

Time (minutes)	Ir (%)	Rh (%)	Ru (%)	Se (%)	Te (%)
0	0	0	0	0	0
10	0	0	0	0	0
20	0	0	0	3	0
30	0	0	0	57	0
60	0	0	0	82	0
120	0	0	2	91	10
240	1	0	1	97	59
360	1	2	0	96	76
480	4	3	1	95	80

Table 5.16: Percentages of species precipitated at different sampling periods of #5 of 1st experimental method

Time (minutes)	Ir (%)	Rh (%)	Ru (%)	Se (%)	Te (%)
0	0	0	0	0	0
10	0	0	0	0	0
20	1	0	3	0	0
30	5	0	1	0	0
60	3	5	5	86	25
120	3	7	8	94	61
240	4	11	9	99	90
360	0	11	8	99	92
480	5	11	8	99	90

Table 5.17: Percentages of species precipitated at different sampling periods of #6 of 1st experimental method

Time (minutes)	Ir (%)	Rh (%)	Ru (%)	Se (%)	Te (%)
0	0	0	0	0	0
10	0	0	0	0	0
20	1	3	0	0	0
30	0	2	0	0	2
60	7	5	3	88	14
120	11	9	7	97	64
240	10	14	10	99	95
360	7	11	5	99	92
480	8	13	6	100	92

Table 5.18: Percentages of species precipitated at different sampling periods of #7 of 1st experimental method

Time (minutes)	Ir (%)	Rh (%)	Ru (%)	Se (%)	Te (%)
0	0	0	0	0	0
10	0	0	0	0	0
20	0	0	0	52	0
30	0	0	0	87	9
60	0	0	0	76	9
120	1	3	0	97	77
240	0	3	0	99	94
360	1	3	2	98	92
480	0	5	2	99	92

Table 5.19: Percentages of species precipitated at different sampling periods of #8 of 1st experimental method

Time (minutes)	Ir (%)	Rh (%)	Ru (%)	Se (%)	Te (%)
0	0	0	0	0	0
10	0	0	0	11	0
20	1	3	3	87	9
30	0	0	0	90	13
60	2	8	7	95	53
120	2	10	7	97	80
240	4	11	9	96	91
360	1	10	7	99	96
480	2	6	5	99	96

D.2 Experimental Data – Te recovery with SO_2 and Cu plate

Table 5.20: ICP result fo r #1 of 2nd experimental method

Time (minutes)	Cu (g/L)	Fe (g/L)	Ni (g/L)	Ir (mg/L)	Rh (mg/L)	Ru (mg/L)	Se (mg/L)	Te (mg/L)
0	97.25	0.69	53.20	41.24	34.30	177.05	51.25	26.87
10	98.60	0.76	55.25	41.51	34.68	183.80	52.10	26.93
20	96.40	0.78	54.20	40.97	35.37	179.30	51.45	27.21
30	87.45	0.73	48.30	37.10	31.38	163.05	43.45	24.41
60	81.25	0.70	45.13	34.10	28.43	149.45	10.32	21.43
120	95.75	0.82	53.65	39.91	33.44	173.60	6.81	23.69
240	85.25	0.71	46.98	35.46	28.45	151.60	5.16	13.96
360	95.20	0.79	52.85	38.12	31.30	167.50	5.61	10.21
480	94.20	0.79	52.30	38.71	30.97	168.75	3.65	5.72

Table 5.21: ICP result fo r #2 of 2nd experimental method

Time (minutes)	Cu (g/L)	Fe (g/L)	Ni (g/L)	Ir (mg/L)	Rh (mg/L)	Ru (mg/L)	Se (mg/L)	Te (mg/L)
0	94.35	0.63	52.15	38.99	32.54	168.40	50.25	25.37
10	88.25	0.62	49.42	38.53	30.96	161.90	41.13	25.47
20	96.95	0.74	54.10	41.99	34.74	179.95	38.36	27.45
30	96.05	0.76	53.55	35.88	33.70	168.45	21.50	27.89
60	93.25	0.78	51.90	35.51	33.11	168.75	9.90	25.93
120	96.40	0.82	53.25	34.34	31.61	155.65	12.23	23.07
240	107.55	0.89	59.45	34.94	32.53	164.00	5.50	15.86
360	98.30	0.84	54.45	35.14	31.38	162.10	3.18	10.72
480	100.00	0.84	55.50	33.97	31.12	159.85	4.50	9.31

Table 5.22: ICP result fo r #3 of 2nd experimental method

Time (minutes)	Cu (g/L)	Fe (g/L)	Ni (g/L)	Ir (mg/L)	Rh (mg/L)	Ru (mg/L)	Se (mg/L)	Te (mg/L)
0	78.85	0.47	43.58	30.59	28.06	141.00	41.44	24.81
10	97.85	0.75	54.20	36.61	34.10	172.95	35.54	29.81
20	90.30	0.71	50.05	33.28	32.26	160.45	14.36	26.83
30	99.65	0.82	55.25	36.46	34.59	175.35	7.74	27.90
60	86.55	0.72	48.01	33.26	30.35	154.75	4.71	23.71
120	89.10	0.72	49.78	31.58	29.46	146.45	2.64	16.70
240	97.80	0.77	53.85	35.13	31.66	166.35	3.96	6.07
360	91.80	0.72	50.05	32.81	29.79	158.00	1.74	4.19
480	95.65	0.76	52.70	33.69	31.60	165.40	1.65	2.19

Table 5.23: ICP result for #4 of 2nd experimental method

Time (minutes)	Cu (g/L)	Fe (g/L)	Ni (g/L)	Ir (mg/L)	Rh (mg/L)	Ru (mg/L)	Se (mg/L)	Te (mg/L)
0	93.15	0.66	51.60	35.43	33.29	168.20	50.15	27.04
10	95.45	0.72	52.35	35.56	34.26	172.75	50.50	27.52
20	94.80	0.73	51.65	36.36	34.26	173.75	47.63	26.91
30	81.80	0.63	44.70	30.86	29.29	153.10	33.42	24.54
60	95.95	0.78	53.40	35.13	33.36	170.35	11.01	25.71
120	102.90	0.84	56.50	37.59	34.58	174.45	5.25	24.82
240	100.45	0.83	55.25	35.53	33.01	165.00	11.10	21.16
360	78.05	0.62	41.98	27.36	25.27	128.60	2.81	7.40
480	98.00	0.79	53.15	36.41	31.79	168.65	2.59	7.72

Table 5.24: ICP result for #5 of 2nd experimental method

Time (minutes)	Cu (g/L)	Fe (g/L)	Ni (g/L)	Ir (mg/L)	Rh (mg/L)	Ru (mg/L)	Se (mg/L)	Te (mg/L)
0	101.55	0.78	55.85	36.64	34.71	176.60	52.80	28.44
10	101.30	0.80	55.80	36.71	35.11	177.70	51.15	27.82
20	101.90	0.82	55.85	36.82	34.54	180.85	36.90	28.92
30	99.00	0.80	53.90	36.07	33.75	176.45	14.77	27.21
60	99.85	0.82	55.30	36.70	32.55	170.80	7.92	25.55
120	102.65	0.84	56.15	36.52	32.30	163.45	2.90	21.94
240	102.90	0.79	56.60	36.53	30.51	168.50	2.27	10.47
360	100.65	0.79	55.75	36.55	31.47	174.05	2.39	4.46
480	100.20	0.80	54.85	35.26	29.52	168.50	2.01	3.33

Table 5.25: ICP result fo r #6 of 2nd experimental method

Time (minutes)	Cu (g/L)	Fe (g/L)	Ni (g/L)	Ir (mg/L)	Rh (mg/L)	Ru (mg/L)	Se (mg/L)	Te (mg/L)
0	91.10	0.72	49.93	33.63	30.18	165.45	46.54	27.04
10	97.40	0.78	54.10	36.70	32.73	178.70	21.86	28.98
20	96.55	0.79	53.75	36.98	32.97	179.00	14.25	29.44
30	103.25	0.86	57.15	38.11	35.71	182.35	9.68	29.03
60	100.15	0.82	55.45	37.34	31.90	174.95	4.41	26.37
120	98.30	0.74	54.40	36.64	31.50	172.25	3.63	17.90
240	97.00	0.76	53.35	34.38	29.83	169.00	2.10	9.18
360	98.15	0.78	53.90	34.02	29.13	168.25	2.02	4.43
480	101.55	0.79	55.80	35.37	30.46	175.75	1.63	3.67

Table 5.26: ICP result fo r #7 of 2nd experimental method

Time (minutes)	Cu (g/L)	Fe (g/L)	Ni (g/L)	Ir (mg/L)	Rh (mg/L)	Ru (mg/L)	Se (mg/L)	Te (mg/L)
0	101.00	0.75	55.60	39.16	33.56	186.15	53.70	28.52
10	99.40	0.75	54.90	39.24	33.74	188.65	53.00	28.25
20	101.55	0.80	56.00	38.51	33.24	189.25	50.20	28.70
30	86.55	0.71	47.48	33.84	28.46	163.05	32.50	24.81
60	81.00	0.67	45.21	33.27	28.42	160.40	7.57	22.71
120	101.90	0.79	55.95	37.65	32.45	178.95	3.89	21.58
240	100.40	0.78	54.85	36.69	30.74	174.25	4.62	9.02
360	99.80	0.77	54.75	35.18	30.50	178.55	2.76	4.62
480	92.40	0.72	51.00	33.40	28.59	166.15	1.40	2.71

Table 5.27: ICP result for #8 of 2nd experimental method

Time (minutes)	Cu (g/L)	Fe (g/L)	Ni (g/L)	Ir (mg/L)	Rh (mg/L)	Ru (mg/L)	Se (mg/L)	Te (mg/L)
0	101.55	0.75	56.10	37.92	33.62	188.05	52.35	29.39
10	102.65	0.82	56.85	38.54	33.79	191.10	48.90	29.74
20	101.25	0.90	56.20	37.21	33.72	187.55	38.95	29.09
30	92.20	0.74	51.30	35.22	30.15	174.10	15.13	26.08
60	98.65	0.78	54.05	37.00	30.91	177.00	5.76	25.77
120	86.35	0.64	47.59	31.72	27.42	149.30	3.13	20.54
240	100.20	0.78	55.95	36.01	30.72	173.00	3.57	15.17
360	100.10	0.77	54.70	36.20	30.90	170.60	10.81	13.15
480	99.95	0.78	55.60	35.54	30.93	178.40	2.34	4.21

Table 5.28: ICP result fo r #9 of 2nd experimental method

Time (minutes)	Cu (g/L)	Fe (g/L)	Ni (g/L)	Ir (mg/L)	Rh (mg/L)	Ru (mg/L)	Se (mg/L)	Te (mg/L)
0	88.85	0.77	53.00	37.75	30.99	170.90	49.48	31.47
10	96.40	0.89	57.05	39.19	33.89	180.25	40.09	34.16
20	93.90	0.85	56.15	39.55	34.09	180.05	8.85	32.69
30	88.95	0.81	52.95	37.78	31.93	168.65	9.97	27.91
60	95.00	0.88	58.90	39.58	31.06	165.75	3.98	18.17
120	88.90	0.83	55.15	36.80	29.70	157.00	2.32	5.65
240	92.20	0.87	58.80	38.31	31.04	169.95	2.09	3.22
360	84.55	0.84	56.10	37.00	29.22	161.45	1.33	2.65
480	84.15	0.84	59.05	37.93	30.83	166.65	1.49	3.06

Table 5.29: ICP result fo r #10 of 2nd experimental method

Time (minutes)	Cu (g/L)	Fe (g/L)	Ni (g/L)	Ir (mg/L)	Rh (mg/L)	Ru (mg/L)	Se (mg/L)	Te (mg/L)
0	83.55	0.80	56.15	37.55	32.73	174.55	35.94	29.91
10	87.00	0.82	58.35	36.68	31.75	165.40	16.02	28.80
20	82.05	0.78	55.45	35.48	30.29	160.75	6.42	26.26
30	93.70	0.89	59.45	39.13	33.05	178.05	5.79	27.27
60	92.85	0.87	57.55	38.95	32.55	170.40	4.19	19.89
120	67.10	0.63	43.41	27.64	22.66	125.25	1.67	4.39
240	92.25	0.88	61.60	37.78	31.15	170.70	2.13	3.91
360	88.00	0.86	60.25	38.17	31.01	168.25	1.60	3.17
480	80.95	0.78	54.70	35.09	28.49	155.15	1.12	2.24

Table 5.30: ICP result fo r #11 of 2nd experimental method

Time (minutes)	Cu (g/L)	Fe (g/L)	Ni (g/L)	Ir (mg/L)	Rh (mg/L)	Ru (mg/L)	Se (mg/L)	Te (mg/L)
0	88.55	0.83	59.60	38.82	33.77	177.10	34.59	32.64
10	81.05	0.78	56.95	36.83	31.85	167.75	9.35	29.03
20	85.45	0.81	59.40	38.78	32.49	173.15	5.99	29.43
30	90.25	0.86	61.95	39.16	32.60	175.65	5.88	27.58
60	90.65	0.85	61.40	37.87	30.58	159.05	3.17	19.44
120	89.00	0.86	60.70	37.60	29.89	162.00	2.61	7.38
240	93.10	1.76	58.55	38.81	31.00	173.40	1.85	2.80
360	92.05	0.90	61.15	39.41	31.76	174.45	1.58	2.80
480	94.25	0.91	60.15	40.04	32.29	176.25	3.09	4.85

Table 5.31: ICP result fo r #12 of 2nd experimental method

Time (minutes)	Cu (g/L)	Fe (g/L)	Ni (g/L)	Ir (mg/L)	Rh (mg/L)	Ru (mg/L)	Se (mg/L)	Te (mg/L)
0	92.95	0.86	56.60	38.89	33.66	179.00	39.93	32.88
10	102.25	0.95	60.45	42.08	36.61	190.30	12.42	33.12
20	86.50	0.82	52.80	36.34	31.94	166.15	11.56	27.47
30	90.25	0.86	57.85	38.71	33.30	173.65	9.07	27.58
60	99.05	0.94	62.25	40.35	34.68	172.90	4.02	20.85
120	99.15	0.96	61.15	40.39	34.13	180.10	3.11	7.26
240	94.25	0.91	57.85	41.08	34.70	179.65	8.03	25.65
360	101.85	0.98	59.60	40.75	34.11	182.95	1.89	3.52
480	96.10	0.94	57.25	39.37	32.74	174.20	1.07	3.13

Table 5.32: ICP result fo r #13 of 2nd experimental method

Time (minutes)	Cu (g/L)	Fe (g/L)	Ni (g/L)	Ir (mg/L)	Rh (mg/L)	Ru (mg/L)	Se (mg/L)	Te (mg/L)
0	95.05	0.83	52.90	40.74	36.55	189.05	49.20	33.88
10	98.15	0.86	54.75	41.66	37.22	192.10	51.10	34.03
20	101.45	0.91	54.60	41.51	36.78	186.65	10.15	32.42
30	100.15	0.92	55.40	40.63	35.30	179.10	5.61	26.57
60	105.35	0.98	58.35	41.60	35.12	176.00	5.89	21.54
120	97.80	0.94	58.70	40.52	35.18	178.55	2.95	6.15
240	97.55	0.95	58.00	41.15	34.57	179.90	2.64	3.70
360	99.15	0.96	57.20	41.21	35.39	180.20	1.82	2.95
480	92.55	0.92	57.40	41.19	34.89	181.05	8.05	11.36

Table 5.33: ICP result fo r #14 of 2nd experimental method

Time (minutes)	Cu (g/L)	Fe (g/L)	Ni (g/L)	Ir (mg/L)	Rh (mg/L)	Ru (mg/L)	Se (mg/L)	Te (mg/L)
0	89.85	0.80	53.40	39.82	36.25	180.75	22.11	33.10
10	92.75	0.86	57.40	43.00	38.27	195.75	6.61	34.09
20	94.65	0.87	55.80	40.42	35.57	181.45	4.96	30.24
30	96.50	0.89	53.95	40.08	35.52	175.60	4.29	27.99
60	96.50	0.92	57.35	40.05	34.89	174.55	3.81	19.29
120	97.70	0.99	59.40	40.48	35.51	182.05	3.44	6.42
240	96.05	0.93	59.45	43.92	39.18	198.85	6.84	13.96
360	96.50	0.93	56.15	40.98	34.46	179.00	1.54	2.48
480	96.50	0.95	55.55	39.90	34.33	175.20	1.28	2.91

Table 5.34: ICP result fo r #15 of 2nd experimental method

Time (minutes)	Cu (g/L)	Fe (g/L)	Ni (g/L)	Ir (mg/L)	Rh (mg/L)	Ru (mg/L)	Se (mg/L)	Te (mg/L)
0	95.00	0.80	52.40	38.72	34.57	179.75	30.17	29.94
10	100.25	0.94	57.95	41.54	35.19	184.05	6.71	29.73
20	68.35	0.62	39.29	29.30	24.16	126.80	3.31	18.58
30	97.65	0.92	53.35	39.19	33.66	167.20	3.98	22.94
60	102.85	1.00	57.85	37.64	31.60	156.70	2.77	14.30
120	97.15	0.94	55.60	39.21	33.37	176.10	2.27	2.99
240	104.65	1.03	57.20	39.27	33.37	177.20	1.74	2.66
360	103.10	1.00	52.10	38.68	33.08	174.70	1.14	2.85
480	101.80	0.99	51.75	38.65	32.30	171.65	0.81	2.17

Table 5.35: ICP result fo r #16 of 2nd experimental method

Time (minutes)	Cu (g/L)	Fe (g/L)	Ni (g/L)	Ir (mg/L)	Rh (mg/L)	Ru (mg/L)	Se (mg/L)	Te (mg/L)
0	98.40	0.86	49.83	39.79	35.05	182.40	51.80	31.91
10	89.70	0.78	46.05	34.74	30.22	158.20	33.69	28.59
20	103.80	0.95	54.05	40.30	34.27	177.50	7.11	29.94
30	102.10	0.93	53.20	40.05	33.43	173.50	5.15	27.94
60	101.20	0.93	53.10	38.51	33.69	167.45	3.22	16.60
120	81.10	0.76	43.98	31.95	26.96	143.95	2.00	3.11
240	94.35	0.90	51.10	37.27	30.73	167.40	1.64	2.48
360	94.40	0.90	50.75	36.22	30.53	162.80	2.16	4.12
480	90.10	0.86	47.73	34.68	29.30	154.00	0.93	2.18

Table 5.36: Percentages of species precipitated at different sampling periods of #1 of 2nd experimental method

Time (minutes)	Ir (%)	Rh (%)	Ru (%)	Se (%)	Te (%)
0	0	0	0	0	0
10	0	2	0	0	0
20	1	0	3	0	0
30	11	12	11	16	9
60	18	20	19	80	20
120	4	6	6	86	13
240	15	20	18	90	48
360	8	12	9	89	63
480	7	13	8	93	80

Table 5.37: Percentages of species precipitated at different sampling periods of #2 of 2nd experimental method

Time (minutes)	Ir (%)	Rh (%)	Ru (%)	Se (%)	Te (%)
0	7	6	6	0	0
10	8	10	10	19	0
20	0	0	0	24	0
30	15	2	6	57	0
60	15	4	6	80	0
120	18	8	14	76	10
240	17	6	9	89	37
360	16	9	10	94	59
480	19	10	11	91	63

Table 5.38: Percentages of species precipitated at different sampling periods of #3 of 2nd experimental method

Time (minutes)	Ir (%)	Rh (%)	Ru (%)	Se (%)	Te (%)
0	0	0	0	0	0
10	0	0	1	14	0
20	9	5	9	65	0
30	0	0	0	82	0
60	9	11	12	89	6
120	13	13	17	94	34
240	4	7	5	90	76
360	10	12	10	96	84
480	8	7	6	96	92

Table 5.39: Percentages of species precipitated at different sampling periods of #4 of 2nd experimental method

Time (minutes)	Ir (%)	Rh (%)	Ru (%)	Se (%)	Te (%)
0	3	0	0	0	0
10	3	0	0	0	0
20	3	0	0	5	0
30	18	15	12	33	9
60	6	3	2	78	6
120	0	0	0	90	7
240	5	4	5	78	22
360	-	-	-	94	72
480	3	8	3	95	72

Table 5.40: Percentages of species precipitated at different sampling periods of #5 of 2nd experimental method

Time (minutes)	Ir (%)	Rh (%)	Ru (%)	Se (%)	Te (%)
0	1	1	0	0	0
10	1	0	0	4	0
20	0	1	0	30	0
30	3	4	3	72	5
60	1	7	6	85	11
120	1	8	10	94	23
240	1	13	7	95	63
360	1	10	4	95	84
480	5	16	7	96	88

Table 5.41: Percentages of species precipitated at different sampling periods of #6 of 2nd experimental method

Time (minutes)	Ir (%)	Rh (%)	Ru (%)	Se (%)	Te (%)
0	0	0	0	0	0
10	0	0	2	53	0
20	0	0	2	69	0
30	0	0	0	80	0
60	2	10	4	90	9
120	4	11	6	92	38
240	10	16	7	96	69
360	10	17	8	96	84
480	7	14	4	97	88

Table 5.42: Percentages of species precipitated at different sampling periods of #7 of 2nd experimental method

Time (minutes)	Ir (%)	Rh (%)	Ru (%)	Se (%)	Te (%)
0	0	0	0	0	0
10	0	0	0	1	0
20	1	0	0	7	0
30	13	15	14	39	12
60	15	15	15	86	21
120	3	3	6	93	25
240	6	8	8	92	68
360	10	9	6	94	84
480	14	15	12	97	91

Table 5.43: Percentages of species precipitated at different sampling periods of #8 of 2nd experimental method

Time (minutes)	Ir (%)	Rh (%)	Ru (%)	Se (%)	Te (%)
0	0	0	0	0	0
10	0	0	0	7	0
20	3	1	2	26	2
30	9	11	9	71	12
60	4	9	7	89	12
120	18	19	22	94	31
240	6	10	9	93	49
360	6	9	11		
480	8	9	7	95	86

Table 5.44: Percentages of species precipitated at different sampling periods of #9 of 2nd experimental method

Time (minutes)	Ir (%)	Rh (%)	Ru (%)	Se (%)	Te (%)
0	0	0	0	0	0
10	0	0	0	19	0
20	0	0	0	82	0
30	4	6	7	80	11
60	0	9	8	92	43
120	7	13	13	95	83
240	3	9	6	96	90
360	6	14	11	97	92
480	4	9	8	97	90

Table 5.45: Percentages of species precipitated at different sampling periods of #10 of 2nd experimental method

Time (minutes)	Ir (%)	Rh (%)	Ru (%)	Se (%)	Te (%)
0	0	0	0	0	0
10	0	0	0	56	3
20	0	0	0	82	12
30	0	0	0	83	8
60	0	1	4	89	33
120	-	-	-	96	85
240	3	6	4	94	87
360	2	6	5	96	90
480	10	14	13	97	93

Table 5.46: Percentages of species precipitated at different sampling periods of #11 of 2nd experimental method

Time (minutes)	Ir (%)	Rh (%)	Ru (%)	Se (%)	Te (%)
0	0	1	0	0	0
10	8	6	1	72	11
20	3	4	2	83	9
30	2	4	3	83	15
60	5	10	4	91	40
120	6	12	5	93	77
240	3	9	6	94	91
360	1	7	7	96	91
480	0	5	8	91	85

Table 5.47: Percentages of species precipitated at different sampling periods of #12 of 2nd experimental method

Time (minutes)	Ir (%)	Rh (%)	Ru (%)	Se (%)	Te (%)
0	0	0	0	0	0
10	0	0	0	69	0
20	13	13	13	71	17
30	8	9	9	78	17
60	4	5	9	90	36
120	4	7	5	93	77
240	2	5	6	95	89
360	3	7	4	-	-
480	6	10	9	98	91

Table 5.48: Percentages of species precipitated at different sampling periods of #13 of 2nd experimental method

Time (minutes)	Ir (%)	Rh (%)	Ru (%)	Se (%)	Te (%)
0	0	0	0	0	0
10	0	0	0	0	0
20	0	1	3	80	0
30	2	5	7	89	22
60	0	5	8	88	37
120	2	5	7	94	82
240	1	7	6	95	90
360	1	4	6	96	91
480	1	6	6	84	66

Table 5.49: Percentages of species precipitated at different sampling periods of #14 of 2nd experimental method

Time (minutes)	Ir (%)	Rh (%)	Ru (%)	Se (%)	Te (%)
0	0	1	0	0	0
10	2	1	2	70	0
20	8	9	9	77	9
30	9	9	12	80	15
60	9	11	12	82	41
120	8	9	9	84	80
240	-	-	-	-	-
360	7	12	10	93	92
480	9	12	0	93	91

Table 5.50: Percentages of species precipitated at different sampling periods of #15 of 2nd experimental method

Time (minutes)	Ir (%)	Rh (%)	Ru (%)	Se (%)	Te (%)
0	0	0	0	0	0
10	0	0	0	78	2
20	-	-	-	88	38
30	6	4	9	87	23
60	9	10	15	90	52
120	6	5	4	92	90
240	5	5	4	95	92
360	7	5	5	97	90
480	7	8	7	97	93

Table 5.51: Percentages of species precipitated at different sampling periods of #16 of 2nd experimental method

Time (minutes)	Ir (%)	Rh (%)	Ru (%)	Se (%)	Te (%)
0	2	0	0	0	0
10	14	14	13	36	11
20	0	2	3	87	6
30	1	4	5	90	13
60	5	4	8	94	48
120	-	-	-	96	91
240	8	12	8	97	92
360	11	13	11	96	88
480	14	16	16	98	94

D.3 Experimental Data – Te recovery with SO_2 and Cu powder

Table 5.52: ICP result for #1 of 3rd experimental method

Time (minutes)	Cu (g/L)	Fe (g/L)	Ni (g/L)	Ir (mg/L)	Rh (mg/L)	Ru (mg/L)	Se (mg/L)	Te (mg/L)
0	93.50	0.69	53.45	39.34	30.87	196.70	55.70	29.28
10	98.25	0.82	56.00	41.13	31.61	207.35	8.01	21.33
20	97.60	0.83	55.25	40.33	30.09	202.05	6.62	17.01
30	97.00	0.82	55.15	40.45	30.09	202.60	6.66	14.59
60	96.90	0.82	54.60	39.38	28.91	190.90	5.08	11.26
120	96.70	0.76	54.65	40.05	28.72	188.80	3.82	8.55
240	96.30	0.75	54.10	38.98	29.06	195.00	6.46	7.14
360	97.60	0.79	54.50	39.97	29.23	198.45	6.30	4.74
480	99.00	0.81	55.20	39.58	29.59	201.90	3.67	2.53

Table 5.53: ICP result for #2 of 3rd experimental method.

Time (minutes)	Cu (g/L)	Fe (g/L)	Ni (g/L)	Ir (mg/L)	Rh (mg/L)	Ru (mg/L)	Se (mg/L)	Te (mg/L)
0	91.55	0.82	50.75	38.56	33.44	181.35	37.62	31.77
10	97.65	0.87	52.95	38.85	32.77	178.15	6.63	22.19
20	104.60	0.95	53.00	40.27	33.94	184.95	6.02	18.23
30	101.95	0.94	53.00	40.32	34.06	184.25	5.48	15.63
60	102.20	0.93	53.60	39.95	32.53	179.10	4.45	12.27
120	103.75	0.94	54.80	39.01	31.39	172.40	3.66	9.04
240	96.85	0.86	54.75	36.71	31.01	168.75	2.67	5.23
360	100.75	0.91	52.90	38.24	30.90	175.05	2.58	3.43
480	105.65	0.95	54.05	38.21	31.21	175.55	2.45	3.02

Table 5.54: ICP result for #3 of 3rd experimental method

Time (minutes)	Cu (g/L)	Fe (g/L)	Ni (g/L)	Ir (mg/L)	Rh (mg/L)	Ru (mg/L)	Se (mg/L)	Te (mg/L)
0	98.90	0.91	52.05	39.09	34.07	181.00	50.95	33.84
10	102.10	0.94	54.20	39.06	33.23	178.05	6.41	22.59
20	95.40	0.89	51.45	36.62	31.24	167.65	4.93	16.55
30	108.40	0.99	56.90	39.39	34.03	179.85	5.29	14.42
60	101.95	0.95	51.75	38.80	32.20	169.90	4.19	8.85
120	103.95	0.91	52.60	37.53	32.11	170.65	3.34	5.14
240	104.40	0.95	53.10	38.64	33.43	176.45	2.91	3.84
360	110.70	0.99	55.45	40.06	34.88	183.15	2.81	4.11
480	106.50	0.96	52.45	38.32	33.63	172.15	2.73	2.90

Table 5.55: ICP result for #4 of 3rd experimental method

Time (minutes)	Cu (g/L)	Fe (g/L)	Ni (g/L)	Ir (mg/L)	Rh (mg/L)	Ru (mg/L)	Se (mg/L)	Te (mg/L)
0	98.50	0.76	50.40	38.95	31.65	190.65	46.12	28.94
10	104.90	0.87	52.40	40.55	32.05	195.85	3.65	21.63
20	108.15	0.90	53.50	39.62	31.74	198.40	2.50	18.81
30	102.30	0.84	50.65	39.64	30.48	188.60	5.71	22.42
60	106.00	0.83	53.00	37.51	29.76	178.80	1.26	9.97
120	105.65	0.77	52.30	38.11	29.29	178.45	0.50	5.58
240	107.15	0.75	53.20	37.44	30.66	180.25	0.50	2.46
360	101.85	0.71	50.55	36.42	29.85	180.45	0.50	2.91
480	104.00	0.75	51.60	38.72	31.06	182.90	0.50	2.74

Table 5.56: ICP result for #5 of 3rd experimental method

Time (minutes)	Cu (g/L)	Fe (g/L)	Ni (g/L)	Ir (mg/L)	Rh (mg/L)	Ru (mg/L)	Se (mg/L)	Te (mg/L)
0	96.00	0.84	48.46	39.37	36.83	180.05	52.95	34.05
10	99.35	0.89	49.48	38.19	34.58	174.45	6.34	23.90
20	97.05	0.88	49.73	38.23	34.64	169.90	5.43	19.69
30	99.20	0.90	49.95	37.69	34.08	168.50	4.74	15.83
60	97.30	0.94	49.28	36.11	33.15	152.10	4.17	9.88
120	102.25	0.92	51.80	37.68	34.36	163.95	3.42	4.90
240	104.90	0.94	52.85	38.41	34.06	166.80	3.00	3.73
360	98.50	0.88	48.97	37.80	32.87	167.65	2.82	3.22
480	102.00	0.92	51.00	37.87	32.63	167.85	2.52	3.08

Table 5.57: ICP result for #6 of 3rd experimental method

Time (minutes)	Cu (g/L)	Fe (g/L)	Ni (g/L)	Ir (mg/L)	Rh (mg/L)	Ru (mg/L)	Se (mg/L)	Te (mg/L)
0	88.55	0.78	46230	37.31	34.68	172.15	48.65	32.78
10	100.45	0.92	53500	38.70	33.78	173.40	6.34	24.81
20	91.75	0.83	48495	37.35	33.61	169.55	5.37	19.30
30	98.90	0.91	51800	37.47	32.71	166.55	4.81	16.56
60	96.80	0.89	51150	36.96	31.05	152.15	4.04	12.80
120	101.20	0.90	52200	36.80	31.92	161.70	3.21	9.73
240	109.85	1.01	58050	37.16	31.59	165.05	2.61	4.19
360	99.20	0.89	51950	38.08	30.57	171.30	2.36	3.53
480	98.15	0.89	51450	37.02	30.41	167.40	2.28	2.36

Table 5.58: ICP result for #7 of 3rd experimental method

Time (minutes)	Cu (g/L)	Fe (g/L)	Ni (g/L)	Ir (mg/L)	Rh (mg/L)	Ru (mg/L)	Se (mg/L)	Te (mg/L)
0	92.90	0.87	48.43	38.00	32.50	178.50	49.50	32.00
10	99.95	0.89	52.70	37.89	31.88	174.90	5.63	21.02
20	101.85	0.94	54.25	38.35	31.75	172.90	4.69	16.76
30	101.05	0.92	54.20	37.67	31.70	167.30	4.47	13.95
60	101.50	0.94	54.60	37.14	30.94	158.30	4.05	7.27
120	101.60	0.90	54.20	36.41	31.17	160.60	3.22	4.61
240	105.45	0.94	56.70	37.15	32.65	161.25	2.84	3.60
360	100.05	0.91	52.90	35.65	31.01	157.90	2.60	2.67
480	95.70	0.88	50.30	35.70	30.57	156.85	2.31	2.75

Table 5.59: ICP result for #8 of 3rd experimental method

Time (minutes)	Cu (g/L)	Fe (g/L)	Ni (g/L)	Ir (mg/L)	Rh (mg/L)	Ru (mg/L)	Se (mg/L)	Te (mg/L)
0	92.00	0.65	51.65	41.48	30.95	202.20	60.80	31.86
10	97.65	0.82	54.00	42.10	30.63	204.80	8.07	22.27
20	98.95	0.84	54.45	42.66	30.30	206.80	7.11	17.91
30	99.00	0.86	54.70	41.60	30.23	201.80	6.73	15.25
60	98.55	0.82	54.05	40.61	29.44	191.85	4.91	9.42
120	98.65	0.76	54.30	40.14	28.74	190.95	3.86	3.90
240	101.85	0.83	55.10	40.46	29.20	199.65	3.22	3.30
360	96.70	0.78	52.70	39.45	28.01	192.45	3.33	2.12
480	98.10	0.80	53.65	39.91	29.21	193.70	2.79	1.89

Table 5.60: ICP result for #9 of 3rd experimental method

Time (minutes)	Cu (g/L)	Fe (g/L)	Ni (g/L)	Ir (mg/L)	Rh (mg/L)	Ru (mg/L)	Se (mg/L)	Te (mg/L)
0	95.65	0.77	53.70	41.92	32.26	206.15	62.20	32.15
10	93.70	0.84	52.30	40.40	29.60	200.45	5.05	17.02
20	96.10	0.86	53.00	40.54	28.78	199.80	3.63	9.90
30	94.50	0.91	52.70	40.35	28.17	196.50	2.62	7.25
60	95.65	0.85	52.90	40.17	29.23	196.75	10.36	11.91
120	95.05	0.85	53.00	40.96	27.81	191.95	1.14	1.92
240	93.00	0.86	52.55	40.39	27.23	193.30	0.57	1.73
360	93.75	0.87	53.80	40.40	27.33	193.40	0.00	1.48
480	94.75	0.88	54.15	40.75	28.27	195.45	0.00	1.72

Table 5.61: ICP result for #10 of 3rd experimental method

Time (minutes)	Cu (g/L)	Fe (g/L)	Ni (g/L)	Ir (mg/L)	Rh (mg/L)	Ru (mg/L)	Se (mg/L)	Te (mg/L)
0	106.80	0.94	57.00	41.28	37.97	191.05	54.30	35.57
10	103.45	0.94	55.95	39.62	32.77	178.55	4.39	19.22
20	97.15	0.85	51.85	35.14	29.65	161.20	3.08	14.73
30	102.60	0.91	52.65	38.64	32.87	176.00	3.00	13.83
60	95.70	0.88	51.20	37.33	32.94	167.05	2.03	6.61
120	101.20	1.01	53.80	37.36	31.85	165.20	1.65	3.14
240	87.40	0.82	47.55	33.71	28.25	149.80	0.90	1.76
360	101.40	0.98	57.10	37.97	32.33	173.10	0.79	1.79
480	97.80	0.93	54.95	37.49	30.64	166.50	0.32	1.79

Table 5.62: ICP result for #11 of 3rd experimental method

Time (minutes)	Cu (g/L)	Fe (g/L)	Ni (g/L)	Ir (mg/L)	Rh (mg/L)	Ru (mg/L)	Se (mg/L)	Te (mg/L)
0	106.80	0.80	54.05	41.00	34.88	205.10	49.49	31.89
10	108.10	0.86	54.70	40.65	33.28	201.40	2.50	18.82
20	106.50	0.84	53.40	39.55	31.38	198.50	0.20	8.99
30	107.90	0.86	54.85	40.27	31.59	196.95	0.11	6.05
60	112.30	0.90	57.00	40.19	31.69	193.25	0.50	3.77
120	108.40	0.87	54.95	39.33	30.48	188.50	0.50	1.85
240	105.50	0.87	54.75	39.64	30.31	193.75	0.50	2.16
360	105.15	0.87	55.05	38.82	30.24	191.90	0.50	2.22
480	115.90	0.88	56.25	38.67	29.19	186.75	0.50	2.27

Table 5.63: ICP result for #12 of 3rd experimental method

Time (minutes)	Cu (g/L)	Fe (g/L)	Ni (g/L)	Ir (mg/L)	Rh (mg/L)	Ru (mg/L)	Se (mg/L)	Te (mg/L)
0	103.15	0.80	51.45	38.84	32.03	198.50	30.24	30.16
10	109.40	0.83	54.70	41.26	32.54	207.85	2.06	16.84
20	109.55	0.83	54.00	41.49	31.86	208.05	1.08	8.88
30	113.15	0.87	55.75	41.82	33.26	213.65	7.10	20.53
60	111.45	0.86	55.30	41.75	31.19	197.50	0.50	4.13
120	102.95	0.80	51.20	37.67	28.45	182.05	0.50	2.86
240	107.60	0.84	54.15	40.36	30.46	200.55	0.50	2.55
360	105.25	0.84	53.95	40.01	30.19	195.05	0.50	2.62
480	109.45	0.88	55.95	41.01	31.47	202.80	0.50	2.61

Table 5.64: ICP result for #13 of 3rd experimental method

Time (minutes)	Cu (g/L)	Fe (g/L)	Ni (g/L)	Ir (mg/L)	Rh (mg/L)	Ru (mg/L)	Se (mg/L)	Te (mg/L)
0	94.05	0.80	52.45	42.73	32.30	210.95	63.15	33.18
10	100.55	0.91	55.95	42.31	31.59	207.10	5.30	15.60
20	100.10	0.90	55.30	42.54	30.99	205.50	12.16	23.25
30	99.20	0.89	54.80	41.80	29.51	203.05	3.25	9.05
60	97.95	0.90	54.50	40.64	28.22	190.00	2.18	4.51
120	95.25	0.87	53.20	39.51	27.36	188.30	2.17	3.16
240	98.75	0.91	56.50	41.69	28.55	197.45	0.93	1.91
360	89.90	0.85	51.45	38.82	27.01	186.70	1.20	2.38
480	99.25	0.94	57.35	42.01	28.39	201.80	0.45	1.26

Table 5.65: ICP result for #14 of 3rd experimental method

Time (minutes)	Cu (g/L)	Fe (g/L)	Ni (g/L)	Ir (mg/L)	Rh (mg/L)	Ru (mg/L)	Se (mg/L)	Te (mg/L)
0	89.30	0.80	49.47	38.64	28.92	192.75	37.10	28.37
10	97.60	0.87	53.30	41.67	28.72	200.80	5.97	16.95
20	98.10	0.88	53.65	42.36	29.11	203.05	4.23	11.77
30	86.40	0.78	47.46	37.78	26.70	182.50	18.11	20.48
60	97.10	0.88	52.95	41.31	28.11	190.45	2.69	6.18
120	87.75	0.75	48.56	37.66	25.44	178.90	1.29	1.63
240	95.40	0.86	54.25	40.73	27.63	197.70	0.82	1.29
360	94.05	0.87	53.15	40.39	27.34	194.30	1.19	1.84
480	92.95	0.89	53.05	40.23	26.62	190.95	0.36	1.01

Table 5.66: ICP result for #15 of 3rd experimental method

Time (minutes)	Cu (g/L)	Fe (g/L)	Ni (g/L)	Ir (mg/L)	Rh (mg/L)	Ru (mg/L)	Se (mg/L)	Te (mg/L)
0	100.20	0.71	50.95	39.53	33.22	196.00	50.40	30.17
10	115.55	0.91	58.60	43.32	34.62	216.25	1.92	16.00
20	111.30	0.88	57.15	42.18	33.19	211.25	1.89	15.45
30	109.30	0.87	55.25	40.96	30.60	197.15	0.75	6.77
60	109.30	0.88	54.65	40.46	30.84	189.10	3.63	18.26
120	99.70	0.77	50.65	38.08	28.66	185.80	0.75	2.28
240	105.30	0.86	54.40	40.94	31.05	197.70	0.75	1.78
360	106.15	0.87	55.00	41.23	30.36	194.30	0.75	1.95
480	108.30	0.91	56.75	40.04	30.54	196.75	0.75	2.25

Table 5.67: ICP result for #16 of 3rd experimental method

Time (minutes)	Cu (g/L)	Fe (g/L)	Ni (g/L)	Ir (mg/L)	Rh (mg/L)	Ru (mg/L)	Se (mg/L)	Te (mg/L)
0	106.15	0.77	54.15	42.22	34.21	209.95	53.20	32.03
10	111.35	0.87	55.95	42.03	33.22	213.75	1.25	14.30
20	111.50	0.89	56.05	41.65	31.71	208.80	1.28	12.60
30	108.70	0.88	54.20	40.53	30.50	197.05	0.50	6.14
60	105.35	0.85	52.25	41.01	29.91	188.75	0.50	3.35
120	106.80	0.84	54.00	41.01	30.70	201.65	0.50	2.86
240	103.25	0.86	53.50	41.58	30.04	202.80	0.50	2.24
360	105.25	0.90	54.55	42.39	30.24	203.70	0.50	2.11
480	103.55	0.90	54.95	41.10	30.42	202.40	0.50	2.33

Table 5.68: Percentages of species precipitated at different sampling periods of #1 of 3rd experimental method

Time (minutes)	Ir (%)	Rh (%)	Ru (%)	Se (%)	Te (%)
0	0	0	0	0	0
10	0	0	0	86	27
20	2	4	3	88	42
30	1	4	2	88	51
60	4	8	8	91	61
120	2	9	9	93	71
240	5	8	6	88	76
360	3	7	4	88	85
480	3	6	3	94	92

Table 5.69: Percentages of species precipitated at different sampling periods of #2 of 3rd experimental method

Time (minutes)	Ir (%)	Rh (%)	Ru (%)	Se (%)	Te (%)
0	0	0	0	0	0
10	0	0	4	83	31
20	0	0	0	84	44
30	0	0	0	85	52
60	1	4	3	88	61
120	4	8	7	91	72
240	9	9	9	93	84
360	6	9	5	93	89
480	6	8	5	93	91

Table 5.70: Percentages of species precipitated at different sampling periods of #3 of 3rd experimental method

Time (minutes)	Ir (%)	Rh (%)	Ru (%)	Se (%)	Te (%)
0	0	0	0	0	0
10	2	5	3	87	34
20	8	11	8	90	51
30	2	3	2	89	57
60	3	8	7	92	74
120	6	8	7	93	85
240	3	5	4	94	88
360	0	0	0	94	88
480	4	4	6	95	91

Table 5.71: Percentages of species precipitated at different sampling periods of #4 of 3rd experimental method

Time (minutes)	Ir (%)	Rh (%)	Ru (%)	Se (%)	Te (%)
0	0	0	0	0	0
10	0	0	0	92	26
20	0	0	0	95	34
30	0	3	1	88	22
60	4	5	6	97	66
120	3	6	6	99	81
240	4	3	5	100	91
360	6	5	5	99	90
480	1	2	4	99	91

Table 5.72: Percentages of species precipitated at different sampling periods of #5 of 3rd experimental method

Time (minutes)	Ir (%)	Rh (%)	Ru (%)	Se (%)	Te (%)
0	0	0	0	0	0
10	3	7	3	88	29
20	3	6	6	90	43
30	5	8	6	92	53
60	9	10	16	92	71
120	5	7	9	93	85
240	3	8	7	94	90
360	4	11	7	94	91
480	4	12	7	95	91

Table 5.73: Percentages of species precipitated at different sampling periods of #6 of 3rd experimental method

Time (minutes)	Ir (%)	Rh (%)	Ru (%)	Se (%)	Te (%)
0	0	0	0	0	0
10	0	2	0	87	24
20	3	3	2	89	41
30	3	5	4	90	50
60	4	10	12	92	61
120	4	7	7	94	71
240	3	8	5	95	88
360	1	11	1	95	89
480	4	12	4	95	92

Table 5.74: Percentages of species precipitated at different sampling periods of #7 of 3rd experimental method

Time (minutes)	Ir (%)	Rh (%)	Ru (%)	Se (%)	Te (%)
0	0	0	0	0	0
10	0	2	2	89	34
20	0	2	3	91	47
30	1	2	6	91	56
60	2	5	11	92	77
120	4	4	10	94	86
240	2	0	10	94	89
360	6	5	11	95	92
480	6	6	12	95	92

Table 5.75: Percentages of species precipitated at different sampling periods of #8 of 3rd experimental method

Time (minutes)	Ir (%)	Rh (%)	Ru (%)	Se (%)	Te (%)
0	0	0	0	0	0
10	1	1	1	87	30
20	0	2	0	89	44
30	2	2	3	89	52
60	4	5	7	92	70
120	6	7	8	93	88
240	5	6	4	95	89
360	7	10	7	94	94
480	6	6	6	95	94

Table 5.76: Percentages of species precipitated at different sampling periods of #9 of 3rd experimental method

Time (minutes)	Ir (%)	Rh (%)	Ru (%)	Se (%)	Te (%)
0	0	0	0	0	0
10	4	9	3	92	47
20	3	11	3	94	69
30	4	13	5	96	78
60	4	10	4	83	63
120	2	14	7	98	94
240	4	16	6	99	95
360	4	16	6	100	95
480	3	13	5	100	95

Table 5.77: Percentages of species precipitated at different sampling periods of #10 of 3rd experimental method

Time (minutes)	Ir (%)	Rh (%)	Ru (%)	Se (%)	Te (%)
0	0	0	0	0	0
10	5	14	7	92	46
20	15	22	16	94	59
30	7	14	8	94	61
60	10	13	13	96	82
120	10	16	14	97	92
240	19	26	22	98	94
360	9	15	9	98	94
480	10	19	13	99	94

Table 5.78: Percentages of species precipitated at different sampling periods of #11 of 3rd experimental method

Time (minutes)	Ir (%)	Rh (%)	Ru (%)	Se (%)	Te (%)
0	0	0	0	0	0
10	1	4	2	95	41
20	4	10	3	100	72
30	1	10	4	100	81
60	2	10	6	99	88
120	4	13	8	99	94
240	4	13	5	99	94
360	5	14	6	99	94
480	6	17	9	99	92

Table 5.79: Percentages of species precipitated at different sampling periods of #12 of 3rd experimental method

Time (minutes)	Ir (%)	Rh (%)	Ru (%)	Se (%)	Te (%)
0	0	0	0	0	0
10	2	2	3	93	43
20	1	4	3	97	70
30	0	0	0	77	32
60	1	6	7	98	87
120	10	14	15	98	90
240	4	8	6	98	92
360	5	9	9	98	92
480	2	5	5	98	92

Table 5.80: Percentages of species precipitated at different sampling periods of #13 of 3rd experimental method

Time (minutes)	Ir (%)	Rh (%)	Ru (%)	Se (%)	Te (%)
0	0	0	0	0	0
10	0	3	2	91	53
20	0	5	3	81	29
30	2	9	4	95	73
60	4	13	10	97	86
120	7	16	11	97	91
240	2	12	6	98	94
360	9	17	12	98	92
480	1	13	4	99	95

Table 5.81: Percentages of species precipitated at different sampling periods of #14 of 3rd experimental method

Time (minutes)	Ir (%)	Rh (%)	Ru (%)	Se (%)	Te (%)
0	0	0	0	0	0
10	2	1	1	84	40
20	0	0	0	89	58
30	11	8	10	51	28
60	3	3	6	93	79
120	11	12	12	96	95
240	4	5	3	97	95
360	5	6	4	97	93
480	5	8	6	99	96

Table 5.82: Percentages of species precipitated at different sampling periods of #15 of 3rd experimental method

Time (minutes)	Ir (%)	Rh (%)	Ru (%)	Se (%)	Te (%)
0	0	0	0	0	0
10	0	0	0	96	47
20	0	0	0	96	48
30	0	8	0	99	77
60	0	6	4	93	38
120	4	14	5	99	92
240	0	6	0	99	93
360	0	8	1	99	93
480	0	8	0	99	92

Table 5.83: Percentages of species precipitated at different sampling periods of #16 of 3rd experimental method

Time (minutes)	Ir (%)	Rh (%)	Ru (%)	Se (%)	Te (%)
0	0	0	0	0	0
10	0	3	0	97	55
20	1	7	0	97	61
30	4	10	6	99	81
60	2	12	10	99	89
120	2	10	4	99	91
240	1	12	3	99	94
360	0	12	3	99	94
480	2	10	4	99	92

D.4 ICP results of replicates

Table 5.84: ICP result of the replicate of #4 of the 1st experimental method

Time (minutes)	Cu (g/L)	Fe (g/L)	Ni (g/L)	Ir (mg/L)	Rh (mg/L)	Ru (mg/L)	Se (mg/L)	Te (mg/L)
0	96.10	0.70	48.03	38.16	35.46	175.25	41.51	32.34
10	101.05	0.76	49.48	38.46	35.26	180.75	37.06	33.04
20	93.40	0.73	46.11	35.47	31.39	161.70	16.76	29.19
30	95.05	0.76	47.78	38.81	34.18	178.10	14.27	32.31
60	102.30	0.89	50.15	37.15	33.03	171.10	5.46	30.88
120	96.85	0.91	49.67	36.66	32.78	163.00	3.99	30.01
240	97.65	0.91	51.65	35.86	31.38	163.90	2.67	18.63
360	95.25	0.88	50.40	35.90	31.85	165.55	2.57	10.64
480	97.10	0.89	50.40	36.36	32.96	169.40	2.46	5.20

Table 5.85: ICP result of the replicate of #2 of the 3rd experimental method

Time (minutes)	Cu (g/L)	Fe (g/L)	Ni (g/L)	Ir (mg/L)	Rh (mg/L)	Ru (mg/L)	Se (mg/L)	Te (mg/L)
0	97.95	0.82	50.60	41.51	30.06	190.9	57.80	29.38
10	99.45	0.87	51.10	40.75	29.95	192.35	7.31	15.50
20	104.25	0.95	52.25	41.38	28.84	194.95	5.76	7.13
30	104.20	0.94	52.45	41.04	28.83	198.35	6.12	12.63
60	97.70	0.93	49.01	39.14	26.42	187.65	5.68	10.21
120	109.15	0.94	54.70	43.14	29.12	205.75	6.77	10.40
240	106.80	0.86	53.05	42.27	29.54	202.35	7.82	12.13
360	102.85	0.91	51.10	39.11	27.68	192.1	2.75	3.22
480	105.15	0.95	51.75	40.87	29.96	193.4	3.37	2.05

Table 5.86: ICP result of the replicate of #9 of the 3rd experimental method

Time (minutes)	Cu (g/L)	Fe (g/L)	Ni (g/L)	Ir (mg/L)	Rh (mg/L)	Ru (mg/L)	Se (mg/L)	Te (mg/L)
0	91.90	0.76	44.63	37.58	28.35	179.60	51.95	28.07
10	103.15	0.82	49.45	40.45	29.49	189.15	8.94	16.07
20	105.80	0.87	50.60	39.57	28.67	192.70	3.54	2.29
30	105.20	0.88	50.50	40.20	28.5	186.05	3.39	3.24
60	-		-	-	-	-		-
120	97.85	0.87	46.01	38.26	26.60	174.10	1.13	2.44
240	105.75	0.93	51.20	40.97	26.68	185.00	0.81	1.11
360	103.00	0.94	50.25	38.40	26.46	180.40	0.00	1.41
480	105.45	1.24	51.30	39.24	27.56	182.45	0.38	0.96

Table 5.87: Percentages of species precipitated at different sampling periods of the replicate of #4 of the SO_2 - based experimental method

Time (minutes)	Ir (%)	Rh (%)	Ru (%)	Se (%)	Te (%)
0	0	0	0	0	0
10	0	1	0	11	0
20	0	11	11	59	11
30	0	4	1	65	0
60	4	7	5	87	5
120	6	8	10	90	8
240	8	12	9	94	43
360	7	10	8	94	68
480	6	7	6	94	85

Table 5.88: Percentages of species precipitated at different sampling periods of the replicate of #2 of the SO_2 and Cu powder - based experimental method.

Time (minutes)	Ir (%)	Rh (%)	Ru (%)	Se (%)	Te (%)
0	0	0	0	0	0
10	2	0	3	87	47
20	0	4	2	90	76
30	1	4	2	90	58
60	6	12	5	91	66
120	6	3	5	88	64
240	6	2	3	86	59
360	6	8	3	96	90
480	2	0	2	94	93

Table 5.89: Percentages of species precipitated at different sampling periods of the replicate of #9 of the SO_2 and Cu powder - based experimental method.

Time (minutes)	Ir (%)	Rh (%)	Ru (%)	Se (%)	Te (%)
0	0	0	0	0	0
10	1	0	0	83	43
20	3	3	0	93	91
30	2	3	3	93	89
60	-	-	-	-	-
120	7	10	10	98	91
240	0	10	4	98	96
360	6	10	6	100	95
480	4	7	5	99	96

Appendix E: Statistical data

Table 5.90: Maximum Te yield, factorial ANOVA for SO_2-based method

ANOVA table [Partial sum of squares – Type III]						
Source	**Sum of squares**	**df**	**Mean Square**	**F value**	**p-value prob > F**	
Model	902.5	4	225.63	59.51	0.0034	
A – Temperature	630.13	1	630.13	166.19	0.0010	
B – SO_2 flow rate	136.13	1	136.13	35.9	0.0093	
AB	91.13	1	91.13	24.03	0.0162	
AC	45.12	1	45.12	11.9	0.0409	
Residual	11.37	3	3.79			
Cor Total	913.88	7				

Std. Dev.	1.95	**R-squared**	0.9876
Mean	85.38	**Adj R-squared**	0.9710
C.V. %	2.28	**Pred R-squared**	0.9115
PRESS	80.89	**Adeq Precision**	19.975

Table 5.91: Maximum Se yield, factorial ANOVA for SO_2-based method

ANOVA table [Partial sum of squares – Type III]						
Source	**Sum of squares**	**df**	**Mean Square**	**F value**	**p-value prob > F**	
Model	14.5	2	7.25	24.17	0.0027	
A – Temperature	12.5	1	12.5	41.67	0.0013	
AB	2	1	2	6.67	0.0493	
Residual	1.5	5	0.3			
Cor Total	16	7				

Std. Dev.	0.55	**R-squared**	0.9062
Mean	98	**Adj R-squared**	0.8687
C.V. %	0.56	**Pred R-squared**	0.76
PRESS	3.84	**Adeq Precision**	10.435

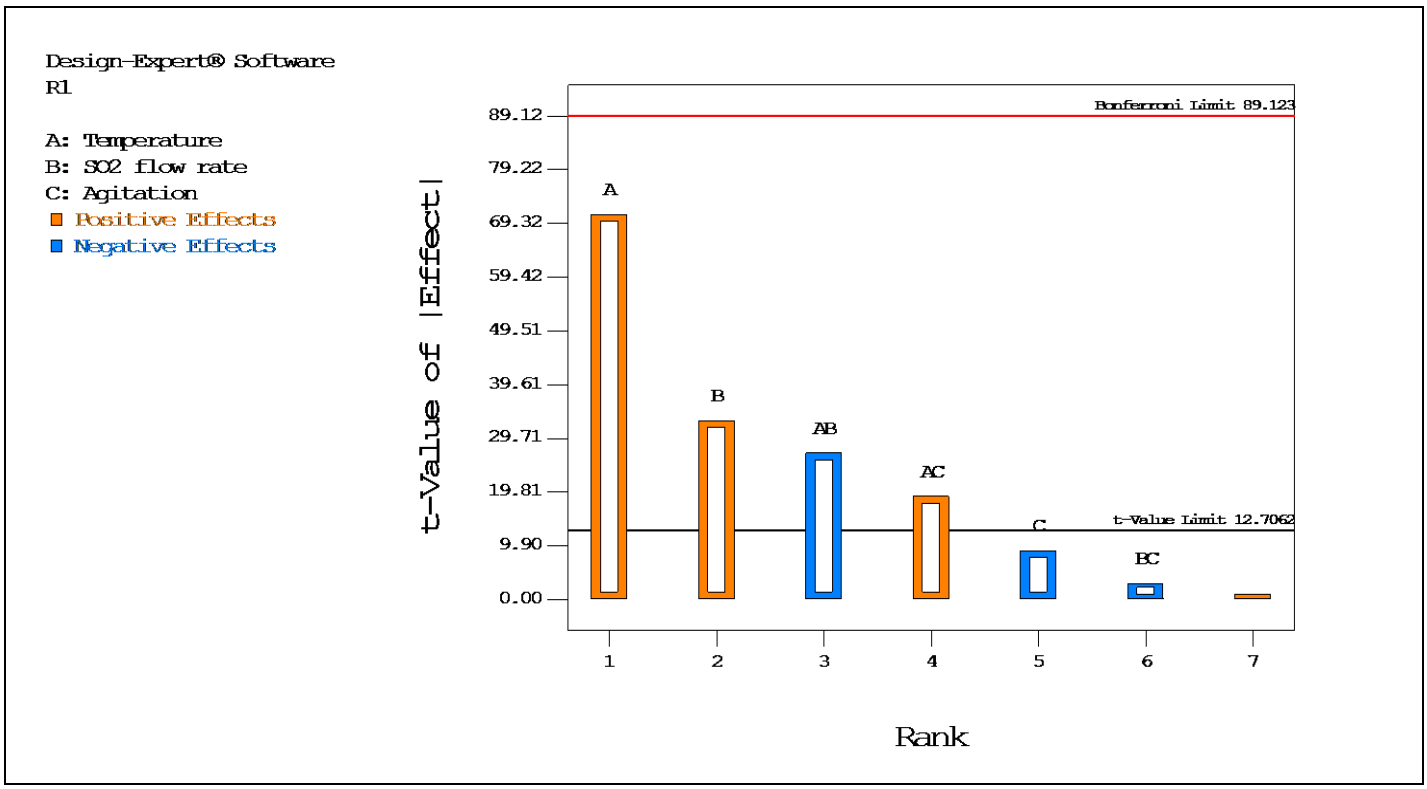

Figure 5.1: Pareto plot of standardardised effects on maximum Te recovery via the SO_2-based method (Derived from Design Expert).

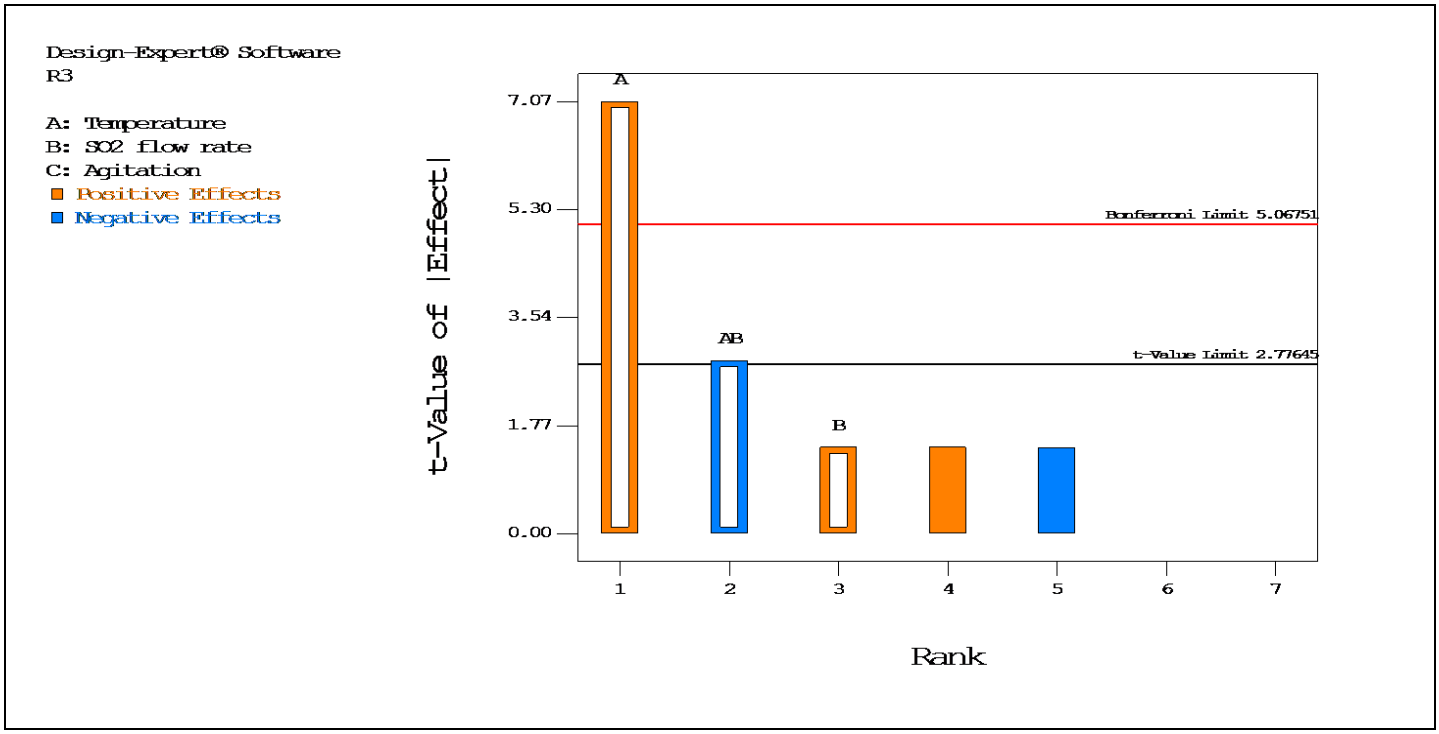

Figure 5.2: Pareto plot of standardardised effects on maximum Se recovery via the SO_2-based method (Derived from Design Expert).

Table 5.92: Maximum Te yield, factorial ANOVA table for SO_2 and Cu plate-based method .

ANOVA table [Partial sum of squares – Type III]						
Source	**Sum of squares**	**df**	**Mean Square**	**F value**	**p-value prob > F**	
Model	1092.13	10	109.21	28.28	0.0009	
A - Temperature	370.56	1	370.56	95.94	0.0002	
B – SO_2 flow rate	150.06	1	150.06	38.85	0.0016	
C - Agitation	95.06	1	95.06	24.61	0.0042	
D – Cu surf. area	33.06	1	33.06	8.56	0.0328	
AB	115.56	1	115.56	29.92	0.0028	
AC	126.56	1	126.56	32.77	0.0023	
AD	27.56	1	27.56	7.14	0.0443	
BC	68.06	1	68.06	17.62	0.0085	
ABC	60.06	1	60.06	15.55	0.0109	
ABD	45.56	1	45.56	11.8	0.0185	
Residual	19.31	5	3.86			
Cor. Total	1111.44	15				

Std. Dev.	1.97	**R-squared**	0.9826
Mean	87.31	**Adj. R-squared**	0.9479
C.V. %	2.25	**Pred. R-squared**	0.8221
PRESS	197.76	**Adeq. Precision**	19.484

Table 5.93: Maximum Se yield, factorial ANOVA table for SO_2 and Cu plate-based method.

ANOVA table [Partial sum of squares – Type III]						
Source	**Sum of squares**	**df**	**Mean Square**	**F value**	**p-value prob > F**	
Model	34.38	6	5.73	20.12	< 0.0001	
A - Temperature	5.06	1	5.06	17.78	0.0023	
D – Cu surf. area	5.06	1	5.06	17.78	0.0023	
AB	7.56	1	7.56	26.56	0.0006	
BC	1.56	1	1.56	5.49	0.0438	
ABD	7.56	1	7.56	26.56	0.0006	
ACD	7.56	1	7.56	26.56	0.0006	
Residual	2.56	9	0.28			
Cor. Total	36.94	15				

Std. Dev.	0.53	**R-squared**	0.9306
Mean	95.94	**Adj. R-squared**	0.8844
C.V. %	0.56	**Pred. R-squared**	0.7807
PRESS	8.1	**Adeq. Precision**	15.938

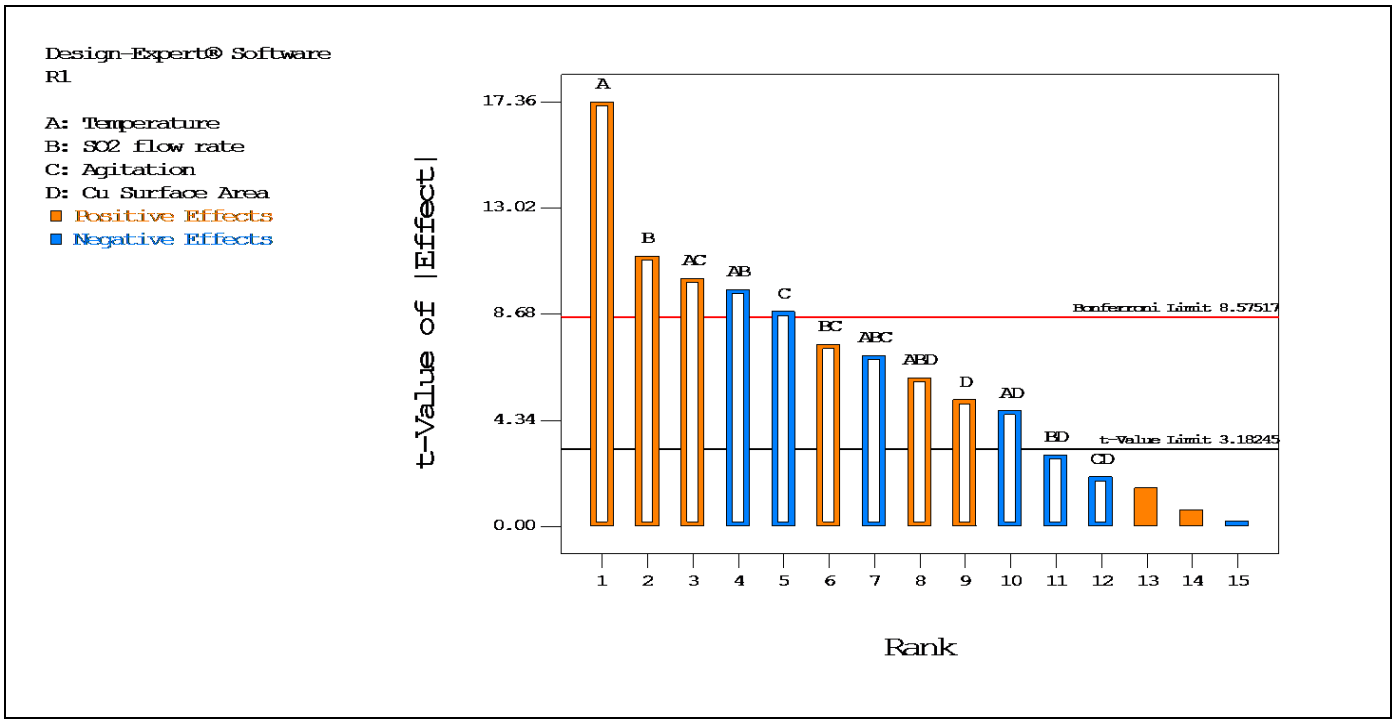

Figure 5.3: Pareto plot of standardised effects on maximum Te recovery via SO_2 and Cu plate- based method (Derived from Design Expert)

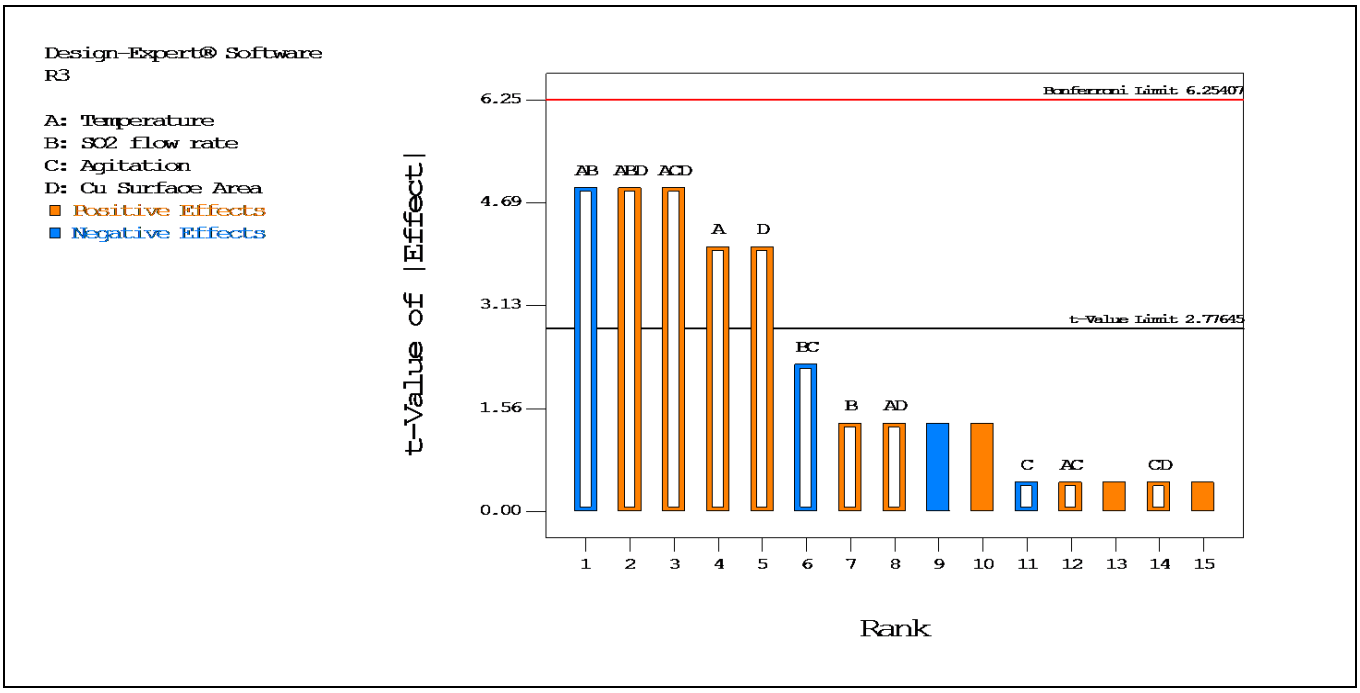

Figure 5.4: Pareto plot of standardised effects on maximum Se recovery via SO_2 and Cu plate-based method (Derived from Design Expert)

Table 5.94: Maximum Te yield, factorial ANOVA table for SO_2 and Cu powder-based experimental method

ANOVA table [Partial sum of squares – Type III]						
Source	**Sum of squares**	**df**	**Mean Square**	**F value**	**p-value prob > F**	
Model	39.5	6	6.58	26.33	< 0.0001	
A - Temperature	20.25	1	20.25	81	< 0.0001	
B – SO_2 addition	2.25	1	2.25	9	0.015	
D – Cu powder addition	2.25	1	2.25	9	0.015	
AD	6.25	1	6.25	25	0.0007	
BC	6.25	1	6.25	25	0.0007	
ABD	2.25	1	2.25	9	0.015	
Residual	2.25	9	0.25			
Cor Total	41.75	15				

Std. Dev.	0.50	**R-squared**	0.9461
Mean	92.88	**Adj. R-squared**	0.9102
C.V. %	0.54	**Pred. R-squared**	0.8297
PRESS	7.11	**Adeq. Precision**	17.386

Table 5.95: Maximum Se yield, factorial ANOVA table for SO_2 and Cu powder -based experimental method.

ANOVA table [Partial sum of squares – Type III]						
Source	**Sum of squares**	**df**	**Mean Square**	**F value**	**p-value prob > F**	
Model	60.06	1	60.06	25.97	0.0002	
A - Temperature	60.06	1	60.06	25.97	0.0002	
Residual	32.38	14	2.31			
Cor Total	92.44	15				

Std. Dev.	1.52	**R-squared**	0.6498
Mean	97.19	**Adj. R-squared**	0.6247
C.V. %	1.56	**Pred. R-squared**	0.5425
PRESS	42.29	**Adeq. Precision**	7.207

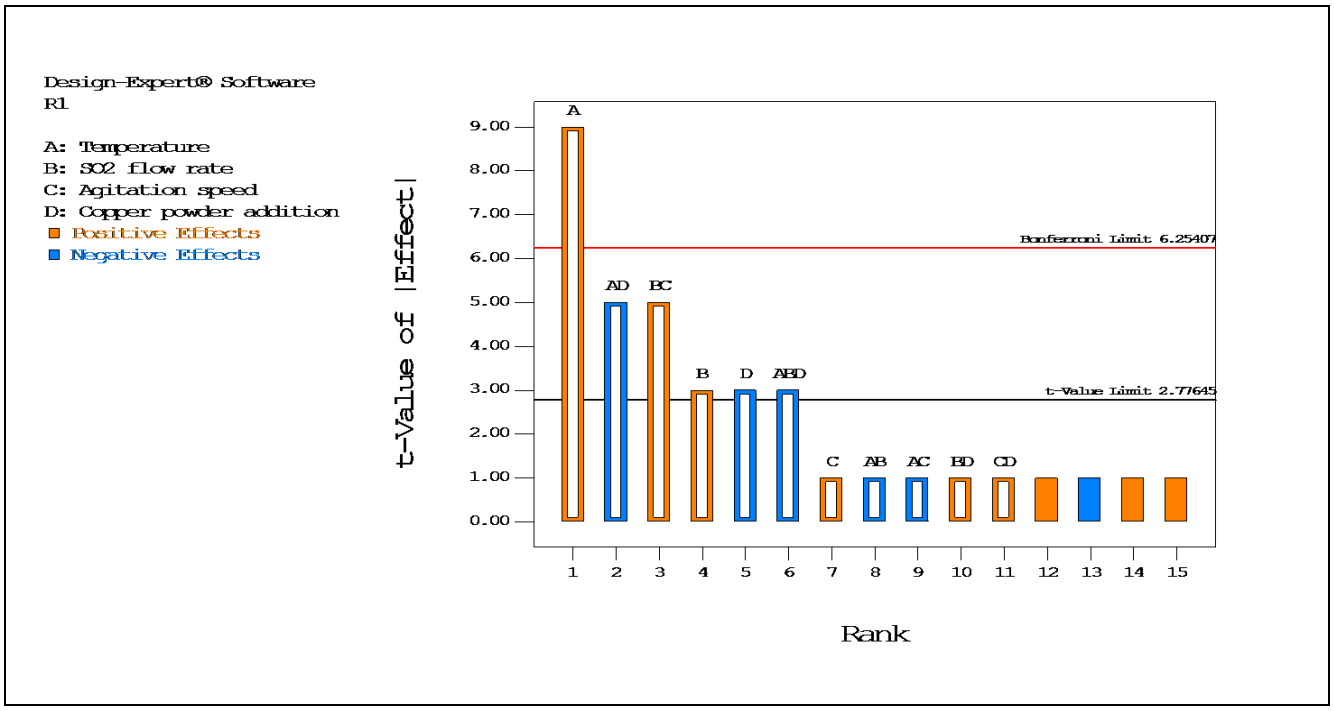

Figure 5.5: Pareto plot of standardised effects on maximum Te recovery via SO_2 and Cu powder-based method (Derived from Design Expert)

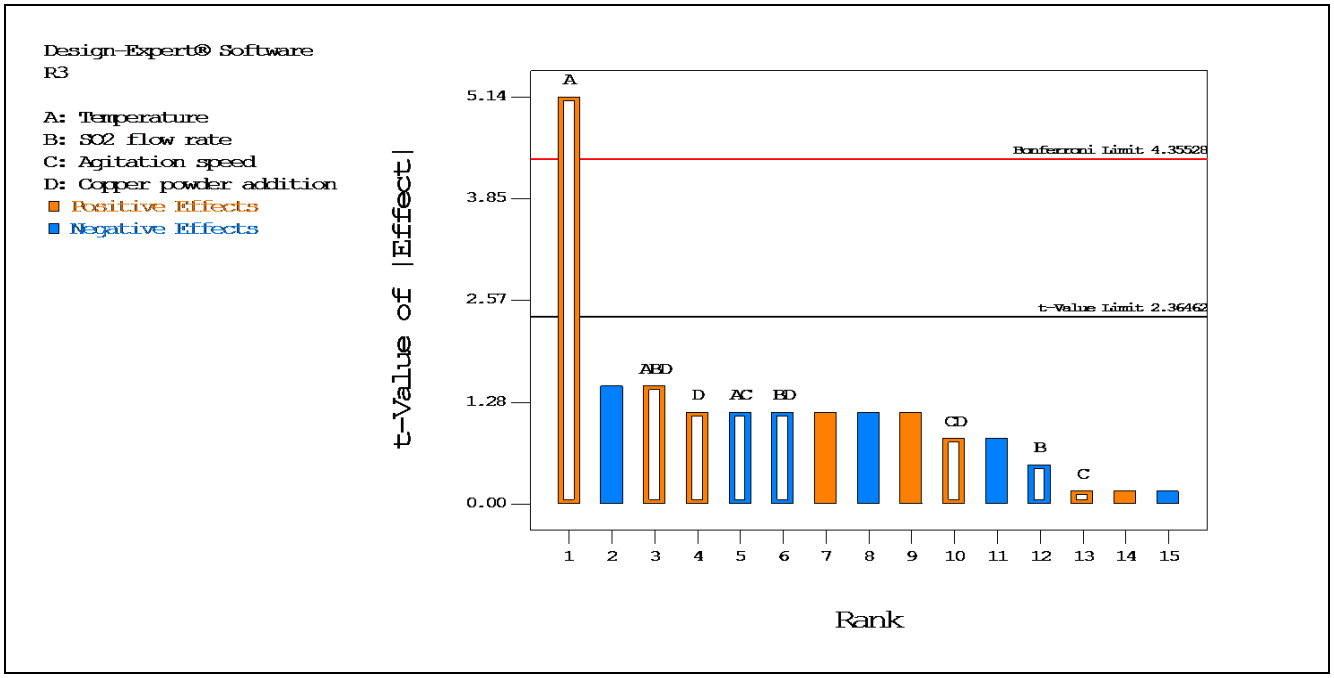

Figure 5.6: Pareto plot of standardised effects on maximum Se recovery via SO_2 and Cu powder- based experimental method (Derived from Design Expert).

Appendix F: Supplementary experimental data

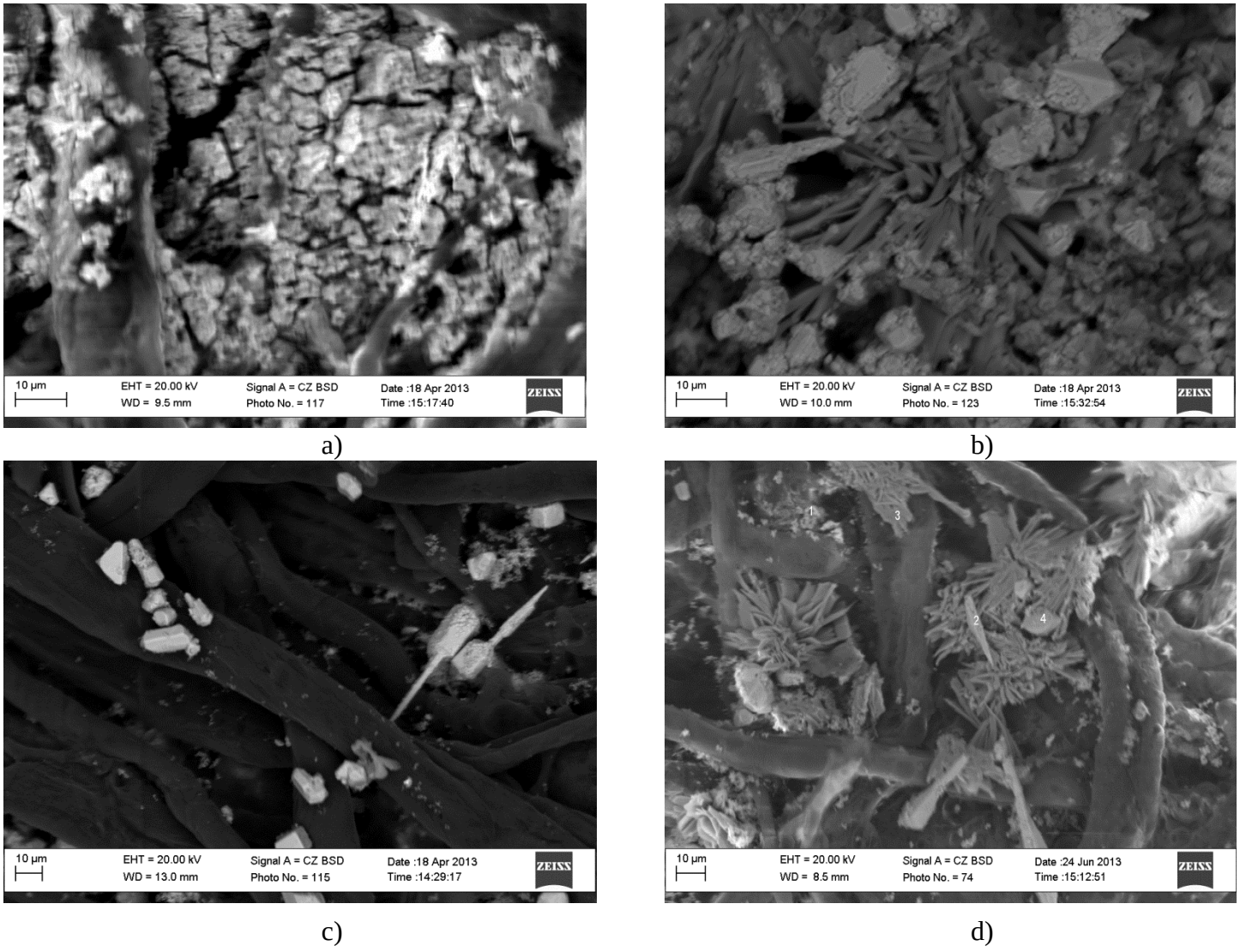

Figure 5.7: SEM image of the precipitate obtained after the completion of the test performed at: a. 65˚C and 500 rpm agitation speed (5.8 cm^3/min SO_2 flow rate) b. 95˚C and 500 rpm agitation speed (4.4 cm^3/min SO_2 flow rate) c. 95˚C and 250 rpm agitation speed (5.8 cm^3/min SO_2 flow rate) d. 95˚C and 500 rpm agitation speed (5.8 cm^3/min SO_2 flow rate).

Table 5.96: Quantitative EDX (wt. %) of the precipitate obtained after the completion of the test performed at 65˚C and 500 rpm agitation speed (5.8 cm³/min SO_2 flow rate)

Analysis	S*	Fe*	Ni*	Cu*	Se*	Ru*	Rh*	Te*	Ir*	Pb*	Total
1	30.42	0.48	4.26	37.61	12.95	4.86	1.13	3.89	1.00	3.39	100.00
2	28.41	0.87	4.18	31.74	11.32	6.60	2.02	5.76	1.52	7.58	100.00
3	33.22	0.65	2.40	17.57	23.67	8.86	2.42	5.21	1.83	4.16	100.00
Avg. (wt %)	30.68	0.67	3.61	28.97	15.98	6.77	1.86	4.95	1.45	5.04	100.00
*Elements combined with oxygen											

Table 5.97: Quantitative EDX (wt. %) of the precipitate obtained after the completion of the test performed at 95˚C and 500 rpm agitation speed (4.4 cm³/min SO_2 flow rate)

Analysis	S*	Fe*	Ni*	Cu*	Se*	Ru*	Rh*	Te*	Ir*	Pb*	Total
1	9.09	0.00	3.08	84.43	1.22	0.74	0.00	0.54	0.00	0.90	100.00
2	4.72	0.00	1.68	91.72	0.90	0.55	0.00	0.43	0.00	0.00	100.00
3	11.59	0.00	3.30	81.61	0.71	0.95	0.00	0.32	0.00	1.51	100.00
Avg. (wt %)	8.47	0.00	2.69	85.92	0.94	0.75	0.00	0.43	0.00	0.80	100.00
*Elements combined with oxygen											

Table 5.98: Quantitative EDX (wt. %) of the precipitate obtained after the completion of the test performed at 95˚C and 250 rpm agitation speed (5.8 cm³/min SO_2 flow rate)

Analysis	S*	Fe*	Ni*	Cu*	Se*	Ru*	Rh*	Te*	Ir*	Pb*	Total
1	21.94	0.42	3.99	35.91	19.64	4.73	0.90	5.07	0.77	6.64	100.00
2	29.46	0.62	3.72	23.76	17.98	5.89	1.26	4.98	2.58	9.75	100.00
3	30.17	0.61	4.30	26.40	15.60	6.71	1.44	9.28	1.92	3.58	100.00
Avg. (wt %)	27.19	0.55	4.00	28.69	17.74	5.77	1.20	6.44	1.75	6.66	100.00
*Elements combined with oxygen											

Table 5.99: Quantitative EDX (wt. %) of the precipitate obtained after the completion of the test performed at 95˚C and 500 rpm agitation speed (5.8 cm³/min SO_2 flow rate)

Analysis	S*	Fe*	Ni*	Cu*	Se*	Ru*	Rh*	Te*	Ir*	Pb*	Total
1	44.41	0.00	5.00	28.86	9.98	7.84	0.00	3.90	0.00	0.00	100.00
2	42.63	0.53	5.84	22.77	12.84	7.54	0.00	3.56	0.00	4.29	100.00
3	42.35	0.44	6.65	18.18	15.39	8.23	1.39	3.77	0.00	3.61	100.00
Avg. (wt %)	43.13	0.32	5.83	23.27	12.73	7.87	0.46	3.74	0.00	2.63	100.00
*Elements combined with oxygen											

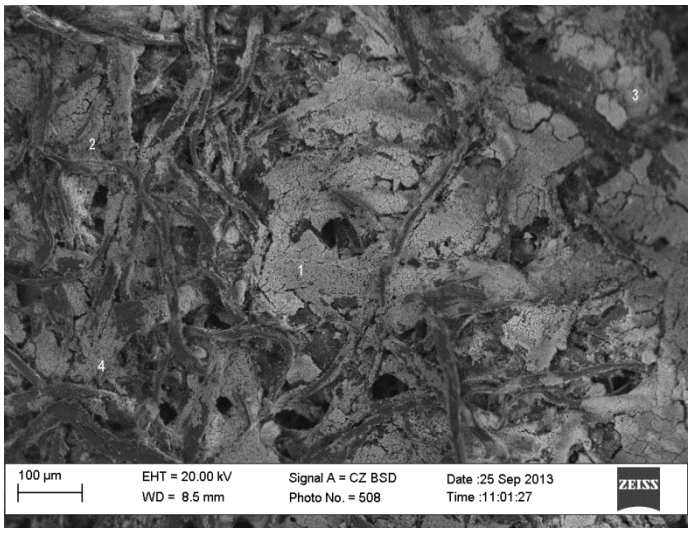

a)

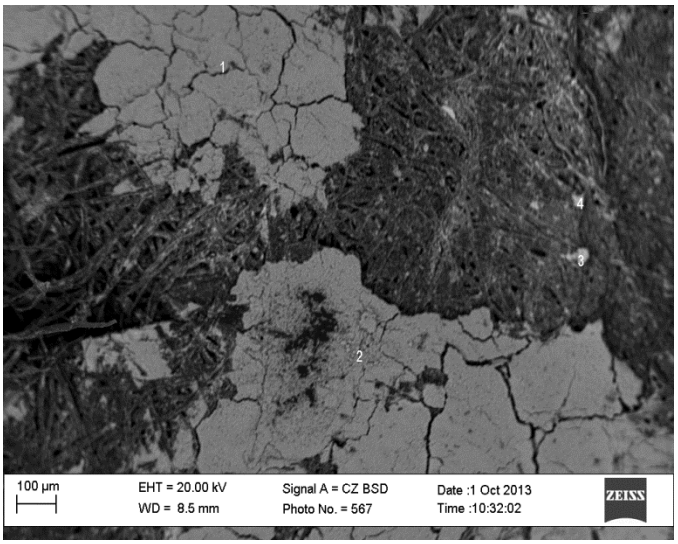

b)

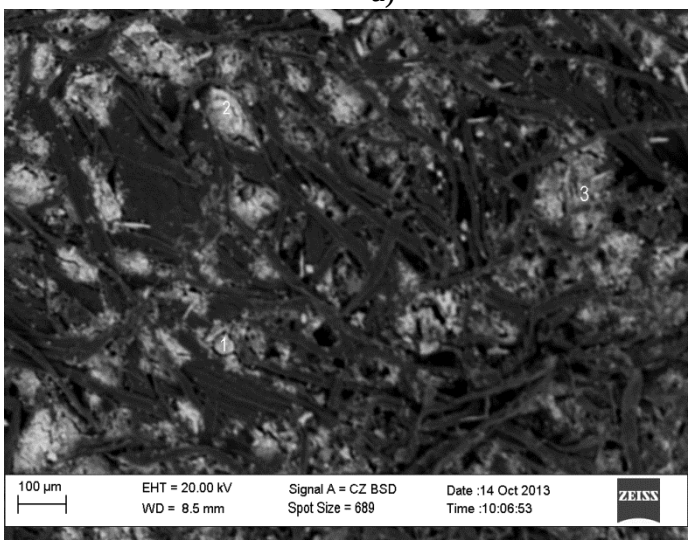

c)

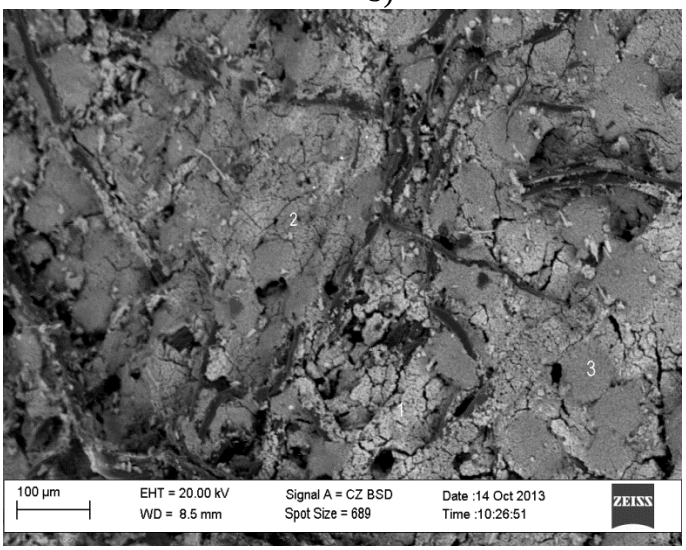

d)

Figure 5.8: SEM image of the precipitate obtained after the completion of the test performed at: a. 65˚C and 500 rpm agitation speed (4.4 cm³/min SO_2 flow rate and 405.0 mm²/L Cu plate) b. 65˚C and 500 rpm agitation speed (5.8 cm³/min SO_2 flow rate and 405.0 mm²/L Cu plate) c. 95˚C and 500 rpm agitation speed (4.4 cm³/min SO_2 flow rate and 405.0 mm²/L Cu plate) d. 95˚C and 250 rpm agitation speed (5.8 cm³/min SO_2 flow rate and 202.5 mm²/L Cu plate)

Table 5.100: Quantitative EDX (wt. %) of the precipitate obtained after the completion of the test performed at 65˚C and 500 rpm agitation speed (4.4 cm^3/min SO_2 flow rate and 405.0 mm^2/L Cu plate)

Analysis	S*	Fe*	Ni*	Cu*	Se*	Ru*	Rh*	Te*	Ir*	Pb*	Total
1	25.66	0.40	2.16	27.70	23.26	6.02	1.28	9.01	1.31	3.19	100.00
2	29.06	0.28	3.30	31.89	16.51	5.02	1.21	8.01	1.22	3.50	100.00
3	17.66	0.37	2.12	37.03	21.71	5.79	1.38	10.74	1.08	2.12	100.00
4	23.84	0.39	2.38	34.61	20.01	5.21	1.55	9.01	0.96	2.03	100.00
Avg. (wt %)	24.05	0.36	2.49	32.81	20.37	5.51	1.35	9.19	1.14	2.71	100.00
*Elements combined with oxygen											

Table 5.101: Quantitative EDX (wt. %) of the precipitate obtained after the completion of the test performed at 65˚C and 500 rpm agitation speed (5.8 cm^3/min SO_2 flow rate and 405.0 mm^2/L Cu plate)

Analysis	S*	Fe*	Ni*	Cu*	Se*	Ru*	Rh*	Te*	Ir*	Pb*	Total
1	8.03	0.00	0.56	28.03	35.25	8.32	2.05	13.91	1.73	2.12	100.00
2	4.23	0.00	0.60	21.81	35.08	11.34	2.85	20.43	2.12	1.53	100.00
3	10.31	0.00	0.53	36.85	31.75	6.07	1.24	10.91	0.97	1.37	100.00
4	25.49	0.00	2.60	28.63	24.12	5.55	0.00	8.23	2.03	3.35	100.00
Avg. (wt %)	12.02	0.00	1.07	28.83	31.55	7.82	1.54	13.37	1.71	2.09	100.00
*Elements combined with oxygen											

Table 5.102: Quantitative EDX (wt. %) of the precipitate obtained after the completion of the test performed at 95˚C and 500 rpm agitation speed (4.4 cm^3/min SO_2 flow rate and 405.0 mm^2/L Cu plate)

Analysis	S*	Fe*	Ni*	Cu*	Se*	Ru*	Rh*	Te*	Ir*	Pb*	Total
1	11.50	0.00	3.07	58.76	17.64	4.38	0.00	4.64	0.00	0.00	100.00
2	21.96	0.47	0.71	41.34	20.24	6.94	0.00	5.97	0.00	2.37	100.00
3	24.82	3.66	1.30	48.59	9.85	3.94	0.00	4.65	3.19	0.00	100.00
Avg. (wt %)	19.43	1.38	1.69	49.57	15.91	5.09	0.00	5.09	1.06	0.79	100.00
*Elements combined with oxygen											

Table 5.103: Quantitative EDX (wt. %) of the precipitate obtained after the completion of the test performed at 95˚C and 250 rpm agitation speed (5.8 cm^3/min SO_2 flow rate and 202.5 mm^2/L Cu plate)

Analysis	S*	Fe*	Ni*	Cu*	Se*	Ru*	Rh*	Te*	Ir*	Pb*	Total
1	35.20	0.00	5.49	38.49	8.79	5.42	0.00	3.43	0.00	3.18	100.00
2	41.21	0.00	2.81	37.74	5.41	5.32	0.00	2.19	1.31	4.02	100.00
3	38.74	0.00	6.83	49.08	0.00	2.30	0.00	0.00	0.00	3.05	100.00
Avg. (wt %)	38.38	0.00	5.04	41.77	4.73	4.35	0.00	1.87	0.44	3.42	100.00
*Elements combined with oxygen											

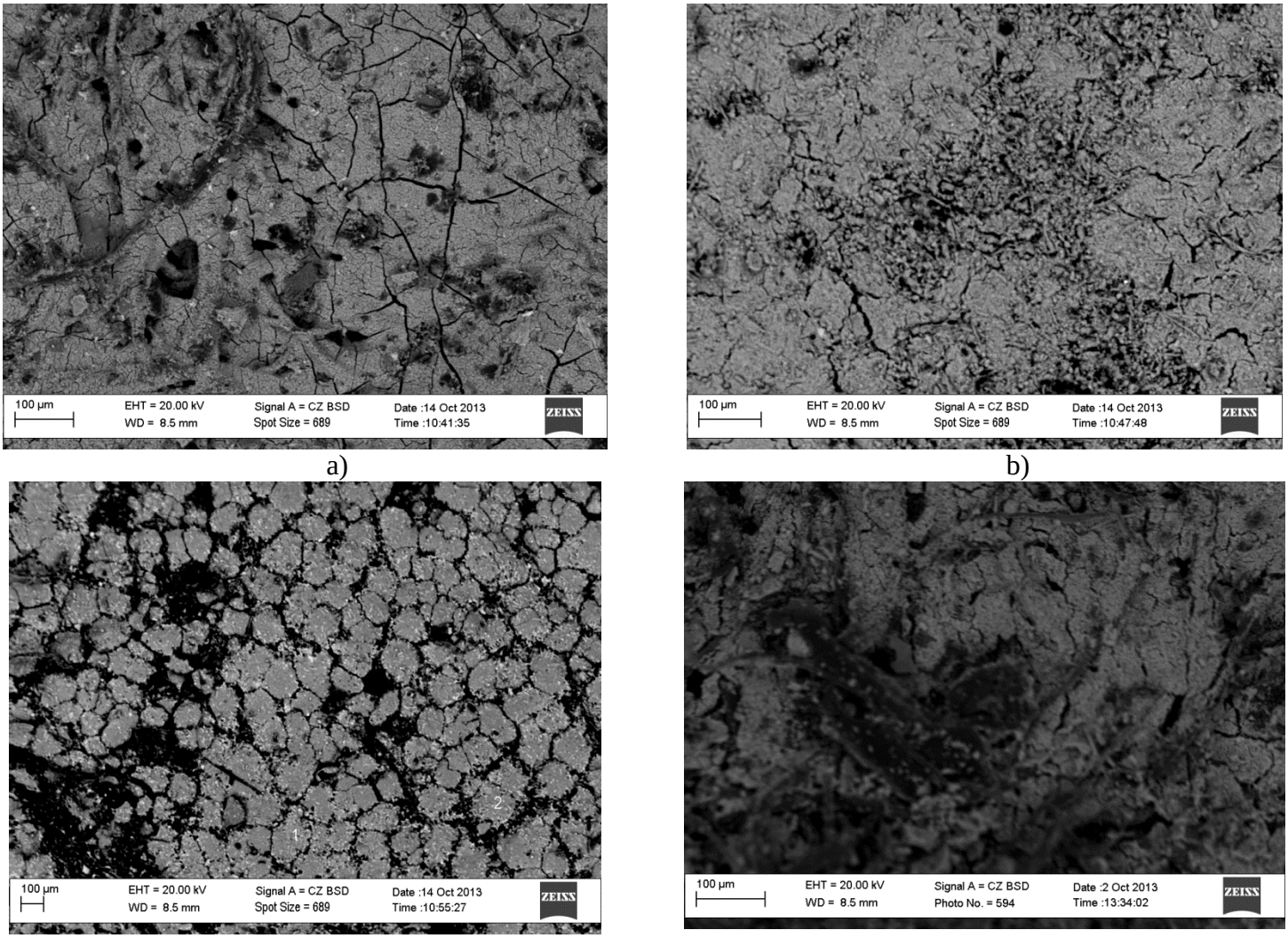

Figure 5.9: SEM image of the precipitate obtained after the completion of the test performed at: a. 95˚C and 500 rpm agitation speed (5.8 cm³/min SO_2 flow rate and 202.5 mm²/L Cu plate) b. 95˚C and 250 rpm agitation speed (5.8 cm³/min SO_2 flow rate and 405 mm²/L Cu plate) c. 95˚C and 500 rpm agitation speed (5.8 cm³/min SO_2 flow rate and 405 mm²/L Cu plate) d. 95˚C and 250 rpm agitation speed (4.4 cm³/min SO_2 flow rate and 405.0 mm²/L Cu plate)

Table 5.104: Quantitative EDX (wt. %) of the precipitate obtained after the completion of the test performed at 95˚C and 500 rpm agitation speed (5.8 cm^3/min SO_2 flow rate and 202.5 mm^2/L Cu plate)

Analysis	S*	Fe*	Ni*	Cu*	Se*	Ru*	Rh*	Te*	Ir*	Pb*	Total
1	42.39	0.00	15.26	26.05	3.53	3.97	1.13	2.66	1.70	3.32	100.00
2	44.14	0.61	15.46	28.38	3.50	4.57	0.00	3.34	0.00	0.00	100.00
Avg. (wt %)	43.26	0.31	15.36	27.21	3.52	4.27	0.56	3.00	0.85	1.66	100.00
*Elements combined with oxygen											

Table 5.105: Quantitative EDX (wt. %) of the precipitate obtained after the completion of the test performed at 95˚C and 250 rpm agitation speed (5.8 cm^3/min SO_2 flow rate and 405.0 mm^2/L Cu plate)

Analysis	S*	Fe*	Ni*	Cu*	Se*	Ru*	Rh*	Te*	Ir*	Pb*	Total
1	17.55	0.00	0.45	60.96	8.78	5.01	0.80	4.22	0.00	2.24	100.00
2	18.59	0.00	0.00	63.55	9.11	4.27	1.09	3.39	0.00	0.00	100.00
Avg. (wt %)	18.07	0.00	0.22	62.25	8.95	4.64	0.94	3.81	0.00	1.12	100.00
*Elements combined with oxygen											

Table 5.106: Quantitative EDX (wt. %) of the precipitate obtained after the completion of the test performed at 95˚C and 500 rpm agitation speed (5.8 cm^3/min SO_2 flow rate and 405.0 mm^2/L Cu plate)

Analysis	S*	Fe*	Ni*	Cu*	Se*	Ru*	Rh*	Te*	Ir*	Pb*	Total
1	32.22	0.00	4.94	52.02	2.52	3.19	0.00	1.47	0.00	3.64	100.00
2	30.12	0.00	5.97	53.42	2.92	3.03	0.00	0.88	0.00	3.65	100.00
3	22.04	0.00	3.86	67.14	3.61	1.52	0.00	1.83	0.00	0.00	100.00
4	20.65	0.00	4.50	67.28	3.80	2.00	0.00	1.78	0.00	0.00	100.00
Avg. (wt %)	26.26	0.00	4.82	59.96	3.21	2.44	0.00	1.49	0.00	1.82	100.00
*Elements combined with oxygen											

Table 5.107: Quantitative EDX (wt. %) of the precipitate obtained after the completion of the test performed at 95˚C and 250 rpm agitation speed (4.4 cm^3/min SO_2 flow rate and 405.0 mm^2/L Cu plate)

Analysis	S*	Fe*	Ni*	Cu*	Se*	Ru*	Rh*	Te*	Ir*	Pb*	Total
1	14.56	0.00	0.66	51.51	12.89	8.84	0.00	8.76	0.00	2.77	100.00
2	24.22	0.00	0.00	50.40	12.67	6.35	0.00	6.37	0.00	0.00	100.00
3	8.10	1.63	0.83	74.17	4.29	3.72	0.00	7.26	0.00	0.00	100.00
Avg. (wt %)	15.63	0.54	0.50	58.69	9.95	6.30	0.00	7.46	0.00	0.92	100.00
*Elements combined with oxygen											

Table 5.108: Quantitative EDX (wt. %) of the precipitate obtained after the completion of the test performed at 65˚C and 500 rpm agitation speed (5.8 cm³/min SO_2 flow rate and 202.5 mm²/L Cu plate)

Analysis	S*	Fe*	Ni*	Cu*	Se*	Ru*	Rh*	Te*	Ir*	Pb*	Total
1	7.77	0.68	2.66	34.05	27.89	10.47	3.03	7.86	3.12	2.47	100.00
2	13.45	0.24	0.96	28.59	47.61	3.48	0.70	2.69	0.60	1.68	100.00
3	9.10	0.20	0.81	28.06	52.98	3.49	0.91	1.99	0.89	1.58	100.00
4	16.39	0.58	2.06	22.59	38.05	8.42	1.60	5.66	2.18	2.48	100.00
Avg. (wt %)	11.68	0.43	1.62	28.32	41.63	6.46	1.56	4.55	1.70	2.05	100.00
*Elements combined with oxygen											

Table 5.109: Quantitative EDX (wt. %) of the precipitate obtained after the completion of the test performed at 65˚C and 250 rpm agitation speed (5.8 cm³/min SO_2 flow rate and 405.0 mm²/L Cu plate)

Analysis	S*	Fe*	Ni*	Cu*	Se*	Ru*	Rh*	Te*	Ir*	Pb*	Total
1	57.89	0.00	0.00	0.00	20.48	9.37	0.00	5.12	0.00	7.14	100.00
2	58.95	0.00	5.98	10.20	6.17	7.03	0.00	4.63	0.00	7.03	100.00
Avg. (wt %)	58.42	0.00	2.99	5.10	13.33	8.20	0.00	4.88	0.00	7.09	100.00
*Elements combined with oxygen											

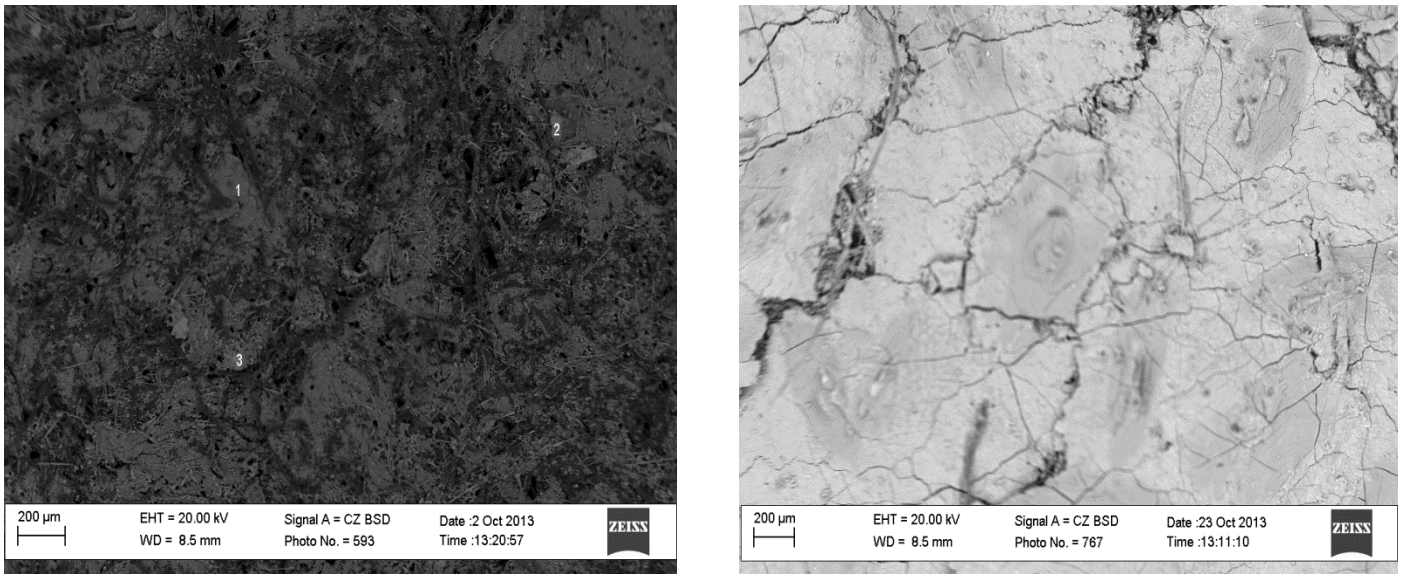

a) b)

Figure 5.10: SEM image of the precipitate obtained after the completion of the test performed at: a. 95˚C and 500 rpm (4.4 cm³/min SO_2 flow rate and 202.5 mm²/L Cu plate) b. 95˚C and 500 rpm (4.4 cm³/min SO_2 flow rate and 1 g/L Cu powder)

Table 5.110: Quantitative EDX (wt. %) of the precipitate obtained after the completion of the test performed at 95˚C and 500 rpm agitation speed (4.4 cm³/min SO_2 flow rate and 202.5 mm²/L Cu plate)

Analysis	S*	Fe*	Ni*	Cu*	Se*	Ru*	Rh*	Te*	Ir*	Pb*	Total
1	23.71	0.29	8.03	53.67	4.68	3.51	0.44	3.37	0.00	2.30	100.00
2	4.38	0.00	0.55	94.10	0.00	0.00	0.00	0.00	0.00	0.97	100.00
3	7.20	0.00	1.00	90.47	0.47	0.00	0.00	0.00	0.00	0.86	100.00
Avg. (wt %)	11.76	0.10	3.19	79.41	1.72	1.17	0.15	1.12	0.00	1.38	100.00
*Elements combined with oxygen											

Table 5.111: Quantitative EDX (wt. %) of the precipitate obtained after the completion of the test performed at 95˚C and 500 rpm agitation speed (4.4 cm³/min SO_2 flow rate and 1g/L Cu powder)

Analysis	S*	Fe*	Ni*	Cu*	Se*	Ru*	Rh*	Te*	Ir*	Pb*	Total
1	33.51	0.00	11.53	43.48	3.03	2.63	0.66	1.94	0.00	3.22	100.00
2	33.83	0.00	12.21	42.22	3.63	2.93	0.53	1.87	0.00	2.78	100.00
3	35.45	0.00	11.90	41.08	3.14	3.01	0.00	2.05	0.00	3.37	100.00
Avg. (wt %)	34.26	0.00	11.88	42.26	3.26	2.86	0.40	1.95	0.00	3.12	100.00
*Elements combined with oxygen											

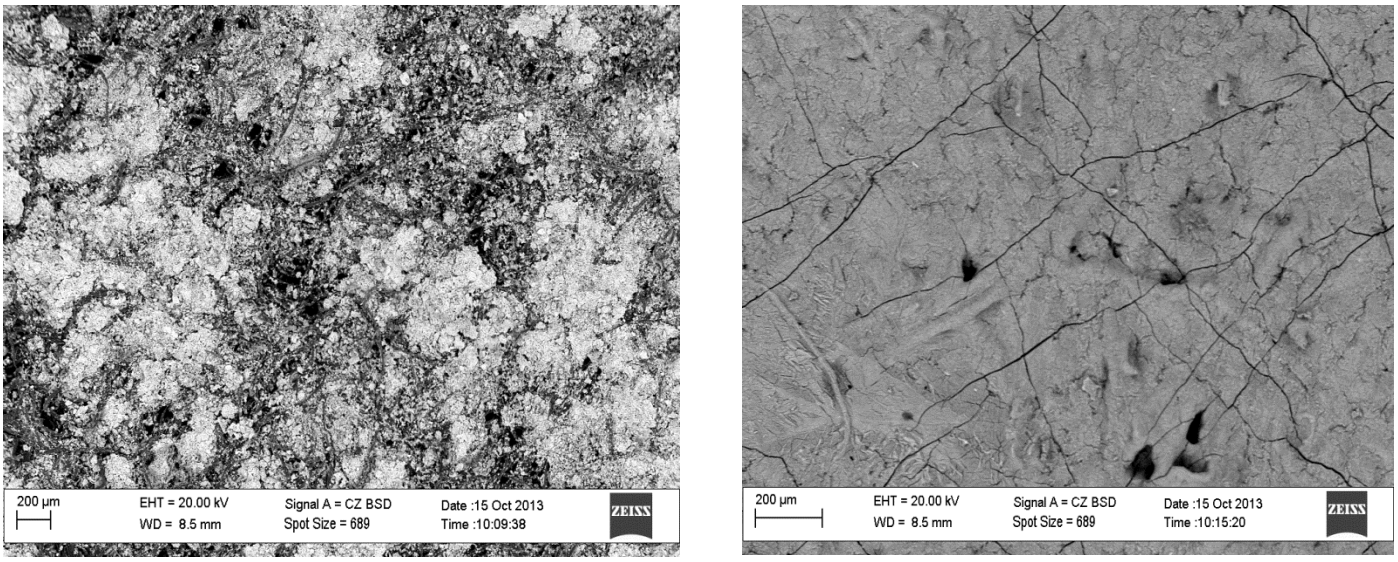

a) b)

Figure 5.11: SEM image of the precipitate obtained after the completion of the test performed at: a. 65˚C and 500 rpm (4.4 cm³/min SO_2 flow rate and 2g/L Cu powder) b. 65˚C and 500 rpm (5.8 cm³/min SO_2 flow rate and 1g/L Cu powder)

Table 5.112: Quantitative EDX (wt. %) of the precipitate obtained after the completion of the test performed at 65˚C and 500 rpm (4.4 cm³/min SO_2 flow rate and 2g/L Cu powder)

Analysis	S*	Fe*	Ni*	Cu*	Se*	Ru*	Rh*	Te*	Ir*	Pb*	Total
1	6.00	0.00	0.00	82.98	6.68	2.18	0.00	2.16	0.00	0.00	100.00
2	5.25	0.00	0.55	82.14	7.82	2.01	0.00	2.24	0.00	0.00	100.00
3	5.44	0.00	0.70	82.24	7.17	2.09	0.00	2.37	0.00	0.00	100.00
Avg. (wt %)	5.56	0.00	0.42	82.45	7.22	2.09	0.00	2.26	0.00	0.00	100.00
*Elements combined with oxygen											

Table 5.113: Quantitative EDX (wt. %) of the precipitate obtained after the completion of the test performed at 65˚C and 500 rpm (5.8 cm³/min SO_2 flow rate and 1g/L Cu powder)

Analysis	S*	Fe*	Ni*	Cu*	Se*	Ru*	Rh*	Te*	Ir*	Pb*	Total
1	48.10	0.00	20.19	24.18	2.05	1.58	0.00	0.67	0.00	3.23	100.00
2	44.83	0.00	20.49	24.76	1.89	2.73	0.00	0.97	0.00	4.32	100.00
3	45.62	0.00	20.59	23.29	1.79	2.53	0.00	0.97	1.15	4.07	100.00
Avg. (wt %)	46.18	0.00	20.42	24.08	1.91	2.28	0.00	0.87	0.38	3.87	100.00
*Elements combined with oxygen											

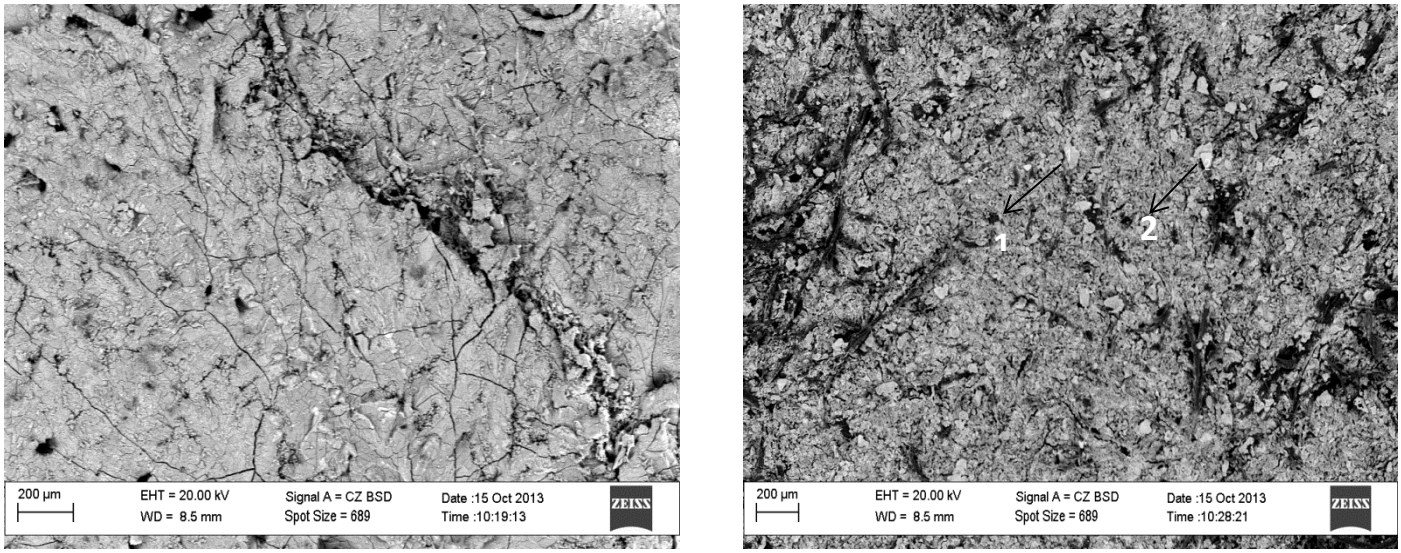

a) b)

Figure 5.12: SEM image of the precipitate obtained after the completion of the test performed at: a. 65˚C and 250 rpm (5.8 cm³/min SO_2 flow rate and 2g/L Cu powder) b. 65˚C and 500 rpm (5.8 cm³/min SO_2 flow rate and 2g/L Cu powder)

Table 5.114: Quantitative EDX (wt. %) of the precipitate obtained after the completion of the test performed at 65˚C and 250 rpm (5.8 cm³/min SO_2 flow rate and 2g/L Cu powder)

Analysis	S*	Fe*	Ni*	Cu*	Se*	Ru*	Rh*	Te*	Ir*	Pb*	Total
1	49.70	0.00	17.71	20.95	2.39	2.96	0.00	1.33	0.00	4.96	100.00
2	51.23	0.00	18.26	20.61	1.79	2.92	0.00	1.11	0.00	4.07	100.00
3	52.02	0.00	23.88	15.46	1.48	2.40	0.00	0.82	0.00	3.94	100.00
Avg. (wt %)	50.98	0.00	19.95	19.01	1.89	2.76	0.00	1.09	0.00	4.32	100.00
*Elements combined with oxygen											

Table 5.115: Quantitative EDX (wt. %) of the precipitate obtained after the completion of the test performed at 65˚C and 500 rpm (5.8 cm³/min SO_2 flow rate and 2g/L Cu powder)

Analysis	S*	Fe*	Ni*	Cu*	Se*	Ru*	Rh*	Te*	Ir*	Pb*	Total
1	2.15	0.00	0.32	95.47	0.58	0.44	0.00	0.36	0.00	0.69	100.00
2	2.41	0.00	0.71	96.21	0.00	0.00	0.00	0.00	0.67	0.00	100.00
2 spots analysed											
3	9.39	0.00	1.60	75.16	7.34	2.19	0.54	2.34	0.00	1.44	100.00
4	9.76	0.00	1.56	75.32	6.95	2.02	0.00	2.19	0.86	1.34	100.00
5	9.34	0.00	1.61	75.28	7.35	2.08	0.00	2.67	0.00	1.66	100.00
Avg. (wt %)	9.49	0.00	1.59	75.25	7.21	2.10	0.18	2.40	0.29	1.48	100.00
Entire sample analysed thrice											
*Elements combined with oxygen											

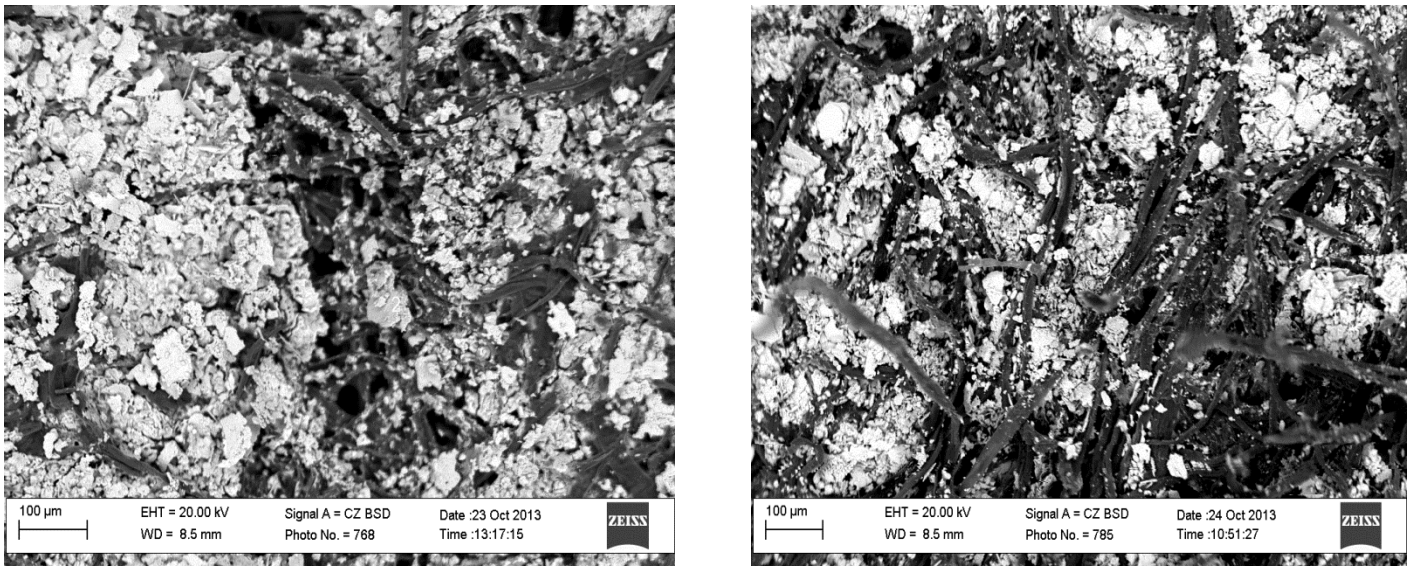

a) b)

Figure 5.13: SEM image of the precipitate obtained after the completion of the test performed at: a. 95˚C and 250 rpm (4.4 cm³/min SO_2 flow rate and 2g/L Cu powder) b. 95˚C and 250 rpm (5.8 cm³/min SO_2 flow rate and 2g/L Cu powder)

Table 5.116: Quantitative EDX (wt. %) of the precipitate obtained after the completion of the test performed at 95˚C and 250 rpm (4.4 cm³/min SO_2 flow rate and 2g/L Cu powder)

Analysis	S*	Fe*	Ni*	Cu*	Se*	Ru*	Rh*	Te*	Ir*	Pb*	Total
1	0.00	0.00	0.26	99.74	0.00	0.00	0.00	0.00	0.00	0.00	100.00
2	2.97	0.00	1.28	89.79	1.67	1.13	0.00	3.16	0.00	0.00	100.00
3	3.11	0.00	0.00	89.58	5.77	0.79	0.00	0.74	0.00	0.00	100.00
4	4.70	0.24	0.33	85.51	6.63	1.07	0.45	1.06	0.00	0.00	100.00
Avg. (wt %)	2.70	0.06	0.47	91.15	3.52	0.75	0.11	1.24	0.00	0.00	100.00
*Elements combined with oxygen											

Table 5.117: Quantitative EDX (wt. %) of the precipitate obtained after the completion of the test performed at 95˚C and 250 rpm (5.8 cm³/min SO_2 flow rate and 2g/L Cu powder)

Analysis	S*	Fe*	Ni*	Cu*	Se*	Ru*	Rh*	Te*	Ir*	Pb*	Total
1	0.65	0.00	0.00	98.48	0.56	0.00	0.00	0.31	0.00	0.00	100.00
2	2.22	0.00	0.00	92.72	3.00	0.92	0.00	1.13	0.00	0.00	100.00
3	3.00	0.00	0.00	91.68	3.44	0.68	0.00	1.22	0.00	0.00	100.00
4	3.45	0.00	0.00	91.11	3.44	0.87	0.00	1.12	0.00	0.00	100.00
Avg. (wt %)	2.33	0.00	0.00	93.50	2.61	0.62	0.00	0.95	0.00	0.00	100.00
*Elements combined with oxygen											

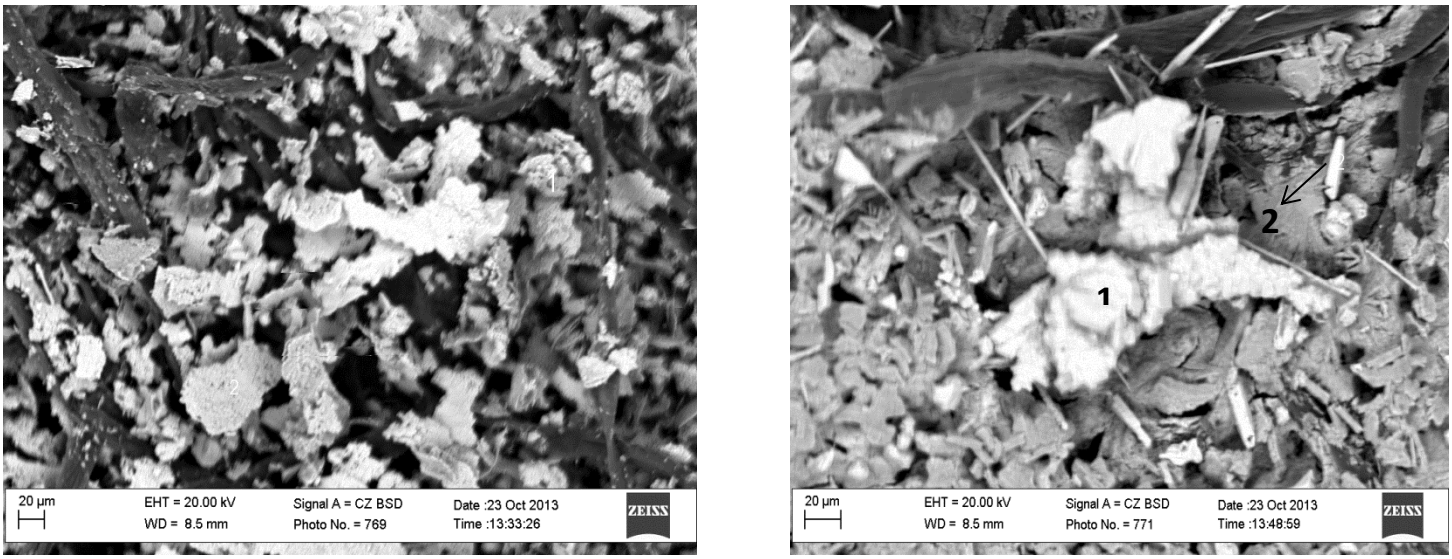

a) b)

Figure 5.14: SEM image of the precipitate obtained after the completion of the test performed at: a. 95˚C and 500 rpm (4.4 cm³/min SO_2 flow rate and 2g/L Cu powder) b. 95˚C and 250 rpm (5.8 cm³/min SO_2 flow rate and 1g/L Cu powder) showing copper crystals

Table 5.118: Quantitative EDX (wt. %) of the precipitate obtained after the completion of the test performed at 95˚C and 500 rpm (4.4 cm³/min SO_2 flow rate and 2g/L Cu powder)

Analysis	S*	Fe*	Ni*	Cu*	Se*	Ru*	Rh*	Te*	Ir*	Pb*	Total
1	0.11	0.00	0.00	99.89	0.00	0.00	0.00	0.00	0.00	0.00	100.00
2	0.47	0.00	0.00	98.43	0.53	0.00	0.00	0.57	0.00	0.00	100.00
3	3.04	0.00	0.00	90.62	3.59	0.92	0.41	1.42	0.00	0.00	100.00
4	3.14	0.00	0.00	90.55	3.70	1.19	0.00	1.43	0.00	0.00	100.00
Avg. (wt %)	1.69	0.00	0.00	94.87	1.96	0.53	0.10	0.86	0.00	0.00	100.00
*Elements combined with oxygen											

Table 5.119: Quantitative EDX (wt. %) of the precipitate obtained after the completion of the test performed at 95˚C and 250 rpm (5.8 cm³/min SO_2 flow rate and 1g/L Cu powder)

Analysis	S*	Fe*	Ni*	Cu*	Se*	Ru*	Rh*	Te*	Ir*	Pb*	Total
1	0.89	0.00	0.00	98.40	0.72	0.00	0.00	0.00	0.00	0.00	100.00
2	0.35	0.00	0.39	99.26	0.00	0.00	0.00	0.00	0.00	0.00	100.00
2 spots analysed											
3	17.03	0.00	4.04	69.71	4.28	1.81	0.00	1.67	0.00	1.47	100.00
4	16.50	0.00	4.11	69.05	4.32	1.75	0.45	1.80	0.00	2.02	100.00
Avg. (wt %)	16.77	0.00	4.08	69.38	4.30	1.78	0.22	1.73	0.00	1.75	100.00
*Elements combined with oxygen											

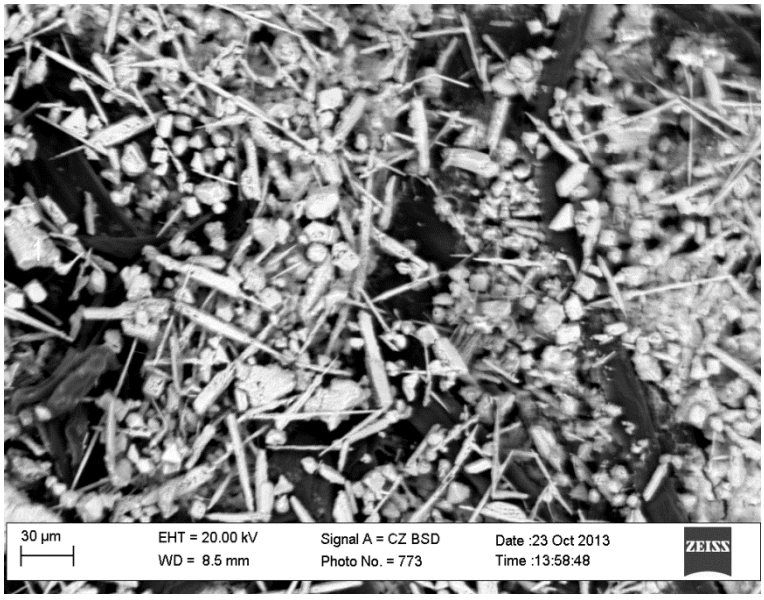

Figure 5.15: SEM image of the precipitate obtained after the completion of the test performed at 95˚C and 500 rpm (5.8 cm³/min SO_2 flow rate and 1g/L Cu powder)

Table 5.120: Quantitative EDX (wt. %) of the precipitate obtained after the completion of the test performed at 95˚C and 500 rpm (5.8 cm³/min SO_2 flow rate and 1g/L Cu powder)

Analysis	S*	Fe*	Ni*	Cu*	Se*	Ru*	Rh*	Te*	Ir*	Pb*	Total
1	4.61	0.00	0.25	87.64	4.73	1.30	0.00	1.47	0.00	0.00	100.00
2	2.82	0.00	0.00	91.98	3.53	0.56	0.00	1.10	0.00	0.00	100.00
3	3.37	0.00	0.00	91.06	3.31	0.95	0.31	1.00	0.00	0.00	100.00
Avg. (wt %)	3.60	0.00	0.08	90.23	3.86	0.94	0.10	1.19	0.00	0.00	100.00
*Elements combined with oxygen											

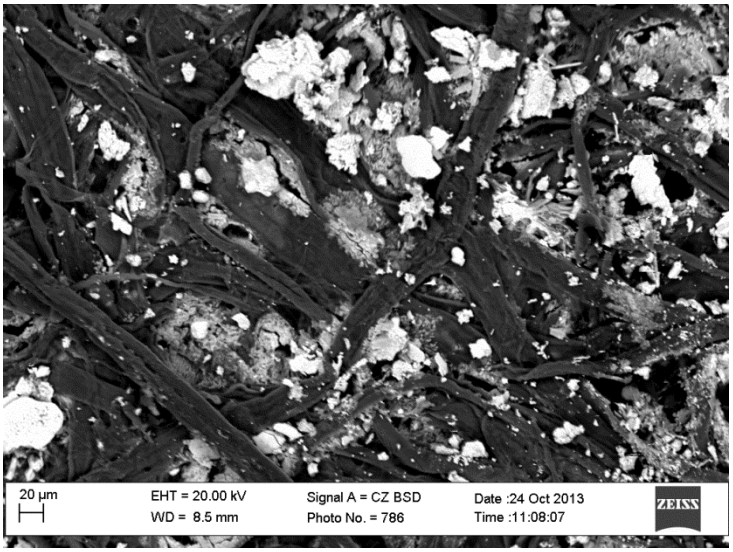

Figure 5.16: SEM image of the precipitate obtained after the completion of the test performed at 95˚C and 500 rpm (5.8 cm³/min SO_2 flow rate and 2g/L Cu powder)

Table 5.121: Quantitative EDX (wt. %) of the precipitate obtained after the completion of the test performed at 95˚C and 500 rpm (5.8 cm³/min SO_2 flow rate and 2g/L Cu powder)

Analysis	S*	Fe*	Ni*	Cu*	Se*	Ru*	Rh*	Te*	Ir*	Pb*	Total
1	17.45	0.00	3.66	69.20	4.69	1.80	0.44	1.15	0.00	1.62	100.00
2	5.28	0.00	0.73	90.39	2.21	0.61	0.00	0.78	0.00	0.00	100.00
3	11.02	0.00	3.33	80.54	1.97	1.36	0.00	0.68	0.00	1.10	100.00
Avg. (wt %)	11.25	0.00	2.57	80.04	2.96	1.26	0.15	0.87	0.00	0.91	100.00
*Elements combined with oxygen											

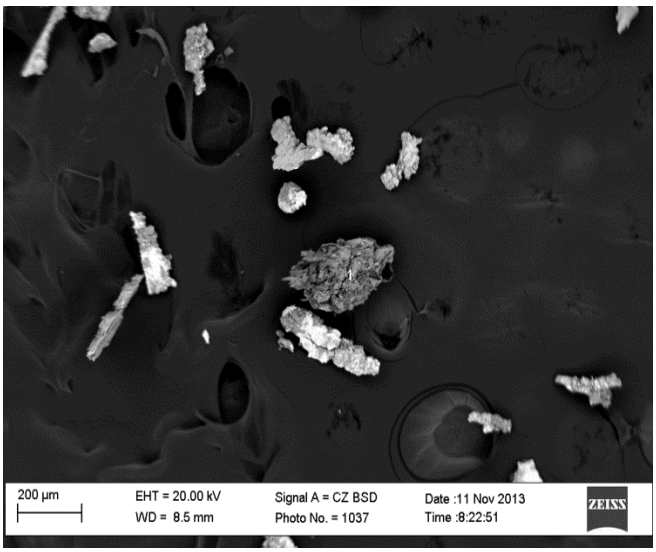

a)

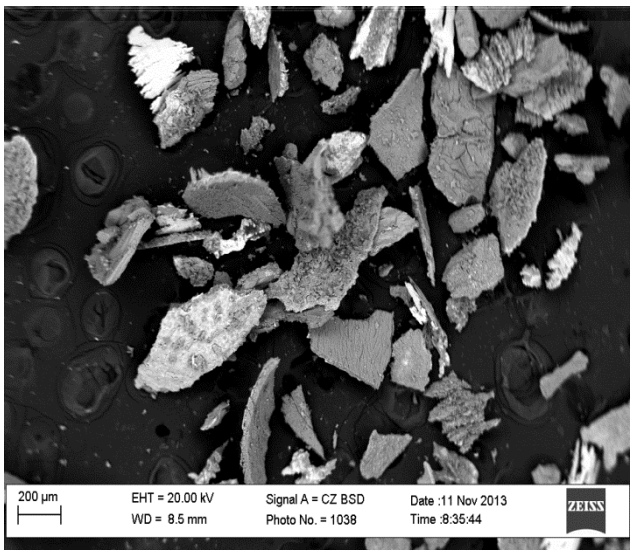

b)

Figure 5.17: SEM image of the precipitate stripped from Cu plate(s) after the completion of the test performed at: a. 65˚C and 500 rpm (4.4 cm³/min SO_2 flow rate and 202.5 mm²/L Cu plate) b. 65˚C and 250 rpm (4.4 cm³/min SO_2 flow rate and 405.0 mm²/L Cu plate)

Table 5.122: Quantitative EDX (wt. %) of the precipitate stripped from Cu plate after the completion of the test performed at 65˚C and 500 rpm (4.4 cm³/min SO_2 flow rate and 202.5 mm²/L Cu plate)

Analysis	S*	Fe*	Ni*	Cu*	Se*	Ru*	Rh*	Te*	Ir*	Pb*	Total
1	13.26	0.53	13.22	71.09	0.00	0.00	0.00	0.47	0.00	1.43	100.00
2	1.15	0.00	0.46	98.39	0.00	0.00	0.00	0.00	0.00	0.00	100.00
Avg. (wt %)	7.21	0.27	6.84	84.74	0.00	0.00	0.00	0.23	0.00	0.72	100.00
*Elements combined with oxygen											

Table 5.123: Quantitative EDX (wt. %) of the precipitate stripped from Cu plate after the completion of the test performed at 65˚C and 500 rpm (4.4 cm³/min SO_2 flow rate and 405.0 mm²/L Cu plate)

Analysis	S*	Fe*	Ni*	Cu*	Se*	Ru*	Rh*	Te*	Ir*	Pb*	Total
1	29.02	0.31	10.88	54.47	3.19	0.00	0.00	0.00	0.00	2.13	100.00
2	27.74	0.30	9.99	54.53	3.59	1.07	0.00	0.00	0.00	2.78	100.00
Avg. (wt %)	28.38	0.31	10.43	54.50	3.39	0.54	0.00	0.00	0.00	2.46	100.00
*Elements combined with oxygen											

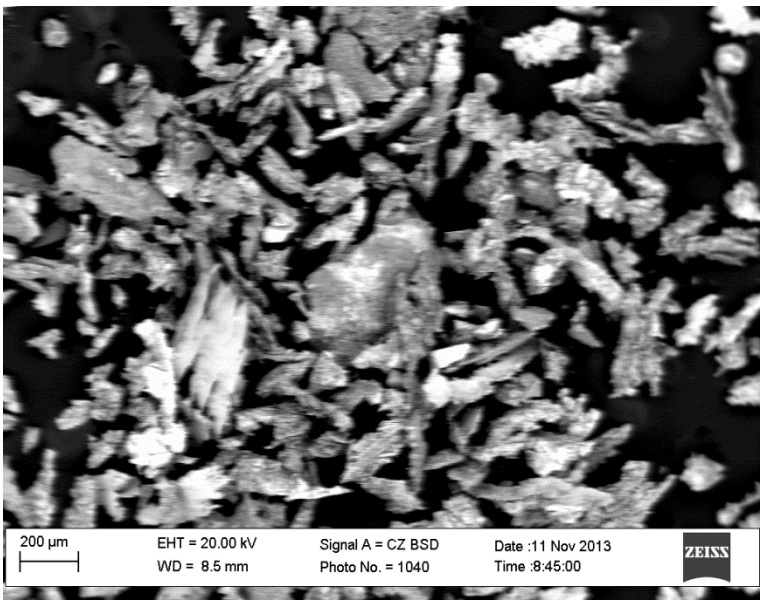

Figure 5.18: SEM image of the precipitate stripped from Cu plate(s) after the completion of the test performed at 95˚C and 250 rpm (5.8 cm³/min SO_2 flow rate and 202.5 mm²/L Cu plate)

Table 5.124: Quantitative EDX (wt. %) of the precipitate stripped from Cu plate after the completion of the test performed at 95˚C and 250 rpm (5.8 cm³/min SO_2 flow rate and 202.5 mm²/L Cu plate)

Analysis	**S***	**Fe***	**Ni***	**Cu***	**Se***	**Ru***	**Rh***	**Te***	**Ir***	**Pb***	**Total**
1	10.25	0.00	3.25	84.32	1.64	0.54	0.00	0.00	0.00	0.00	100.00
2	14.56	0.20	13.71	68.73	0.29	0.72	0.00	0.28	0.00	1.52	100.00
3	12.41	0.00	4.23	80.01	1.48	0.62	0.00	0.00	0.00	1.26	100.00
Avg. (wt %)	12.41	0.07	7.06	77.68	1.14	0.62	0.00	0.09	0.00	0.93	100.00
*Elements combined with oxygen											

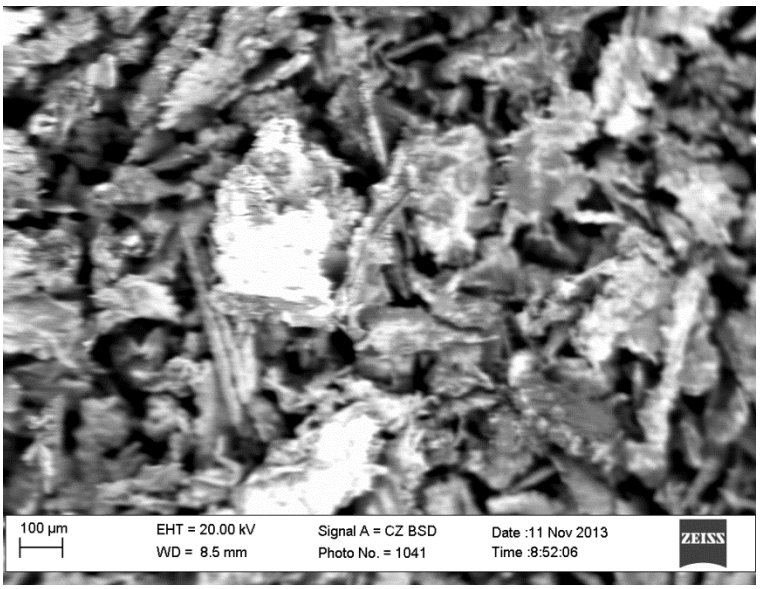

Figure 5.19: SEM image of the precipitate stripped from Cu plate(s) after the completion of the test performed at 95˚C and 500 rpm (5.8 cm³/min SO_2 flow rate and 202.5 mm²/L Cu plate)

Table 5.125: Quantitative EDX (wt. %) of the precipitate stripped from Cu plate after the completion of the test performed at 95˚C and 500 rpm (5.8 cm³/min SO_2 flow rate and 202.5 mm²/L Cu plate)

Analysis	S*	Fe*	Ni*	Cu*	Se*	Ru*	Rh*	Te*	Ir*	Pb*	Total
1	7.71	0.00	2.31	87.76	0.47	0.56	0.00	0.00	0.00	1.19	100.00
2	10.08	0.00	2.55	85.07	0.56	0.59	0.00	0.00	0.00	1.14	100.00
3	8.04	0.14	2.40	88.01	0.00	0.40	0.00	0.00	0.00	1.01	100.00
Avg. (wt %)	8.61	0.05	2.42	86.95	0.34	0.52	0.00	0.00	0.00	1.11	100.00
*Elements combined with oxygen											

Table 5.126: Quantitative EDX (wt. %) of the precipitate stripped from Cu plate after the completion of the test performed at 65˚C and 250 rpm (5.8 cm³/min SO_2 flow rate and 202.5 mm²/L Cu plate)

Analysis	S*	Fe*	Ni*	Cu*	Se*	Ru*	Rh*	Te*	Ir*	Pb*	Total
1	33.18	0.18	8.92	51.57	1.54	1.47	0.00	0.00	0.00	3.14	100.00
2	33.55	0.00	9.10	51.02	1.63	1.53	0.00	0.42	0.00	2.75	100.00
3	38.61	0.00	11.36	40.21	3.92	1.85	0.00	0.41	0.00	3.64	100.00
Avg. (wt %)	35.11	0.06	9.79	47.60	2.36	1.62	0.00	0.28	0.00	3.17	100.00
*Elements combined with oxygen											

Table 5.127: Quantitative EDX (wt. %) of the precipitate stripped from Cu plate after the completion of the test performed at 65˚C and 500 rpm (5.8 cm³/min SO_2 flow rate and 202.5 mm²/L Cu plate)

Analysis	S*	Fe*	Ni*	Cu*	Se*	Ru*	Rh*	Te*	Ir*	Pb*	Total
1	24.54	0.00	5.04	57.17	8.21	1.17	0.00	0.81	0.00	3.05	100.00
2	24.44	0.30	5.13	56.51	8.04	1.65	0.00	0.92	0.00	3.02	100.00
3	24.54	0.35	5.15	56.07	8.18	1.67	0.00	0.54	0.52	2.98	100.00
Avg. (wt %)	24.51	0.22	5.11	56.58	8.14	1.50	0.00	0.76	0.17	3.02	100.00
*Elements combined with oxygen											

Table 5.128: Quantitative EDX (wt. %) of the precipitate stripped from Cu plate after the completion of the test performed at 65˚C and 500 rpm (5.8 cm³/min SO_2 flow rate and 405.0 mm²/L Cu plate)

Analysis	S*	Fe*	Ni*	Cu*	Se*	Ru*	Rh*	Te*	Ir*	Pb*	Total
1	41.27	0.20	12.99	34.75	4.42	2.07	0.00	0.74	0.00	3.56	100.00
2	40.72	0.00	12.89	35.26	4.61	2.06	0.00	0.87	0.00	3.59	100.00
3	41.20	0.00	12.99	34.95	4.50	2.18	0.00	0.99	0.00	3.19	100.00
Avg. (wt %)	41.06	0.07	12.96	34.99	4.51	2.10	0.00	0.87	0.00	3.45	100.00
*Elements combined with oxygen											

Table 5.129: Quantitative EDX (wt. %) of the precipitate stripped from Cu plate after the completion of the test performed at 95˚C and 250 rpm (4.4 cm³/min SO_2 flow rate and 202.5 mm²/L Cu plate)

Analysis	S*	Fe*	Ni*	Cu*	Se*	Ru*	Rh*	Te*	Ir*	Pb*	Total
1	31.56	0.20	4.59	48.55	6.33	2.98	0.00	1.87	0.48	3.43	100.00
2	32.53	0.00	4.54	50.17	6.26	2.35	0.00	1.75	0.00	2.39	100.00
3	32.15	0.21	4.40	49.87	6.40	2.63	0.00	1.87	0.00	2.47	100.00
Avg. (wt %)	32.08	0.14	4.51	49.53	6.33	2.65	0.00	1.83	0.16	2.76	100.00
*Elements combined with oxygen											

Table 5.130: Quantitative EDX (wt. %) of the precipitate stripped from Cu plate after the completion of the test performed at 95˚C and 500 rpm (4.4 cm³/min SO_2 flow rate and 202.5 mm²/L Cu plate)

Analysis	S*	Fe*	Ni*	Cu*	Se*	Ru*	Rh*	Te*	Ir*	Pb*	Total
1	27.41	0.26	8.83	51.88	6.69	1.84	0.00	1.08	0.00	2.02	100.00
2	26.63	0.00	8.54	52.64	6.48	2.10	0.00	1.11	0.00	2.50	100.00
Avg. (wt %)	27.02	0.13	8.69	52.26	6.58	1.97	0.00	1.09	0.00	2.26	100.00
*Elements combined with oxygen											

Appendix G: Repeatability analysis

Except for the effects of metallic copper addition, the effects of other process variables on Te precipitation were similar for the tests involving Cu plate addition and those without any copper addition. For this reason, only one of the experimental runs (#4) of the 1st experimental method was repeated in order to prove the repeatability of the experimental data.

Figures 5.20 through 5.22 show a comparison of the percentages Te and Se precipitation achieved for #4 (of the 1st experimental method), #2 and #9 (of the 3rd experimental method) with those obtained for their respective replicates. Figures 5.23 through 5.25 show a comparison of the base metals concentrations noticed for #4 (of the 1st method), #2 and #9 (of the 3rd experimental method) with those of their replicates.

As shown in these figures, the extents of precipitation for Te and Se are almost the same, while the base concentrations observed for both the actual runs and the replicates are within the acceptable limits. Though there are slight variations between the precipitation curves depicting the outcomes of the actual runs and their replicates.

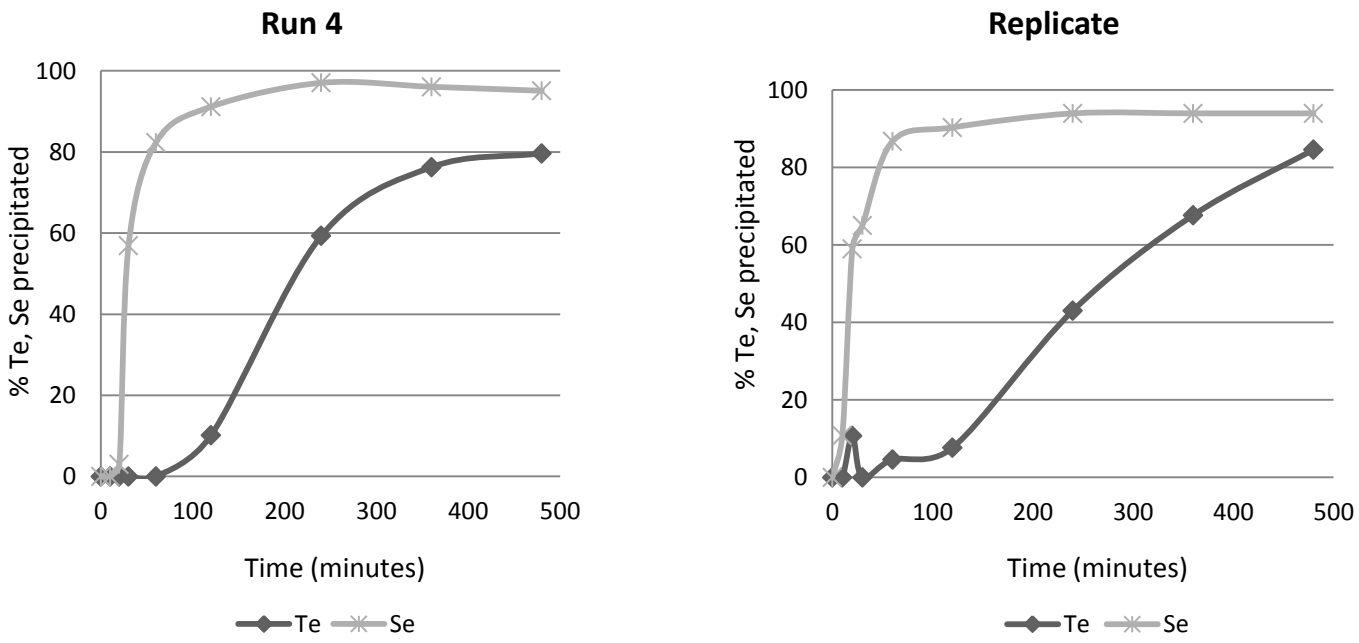

Figure 5.20: Comparing percentage Te and Se precipitation achieved for #4 of the 1st experimental method with that of its replicate.

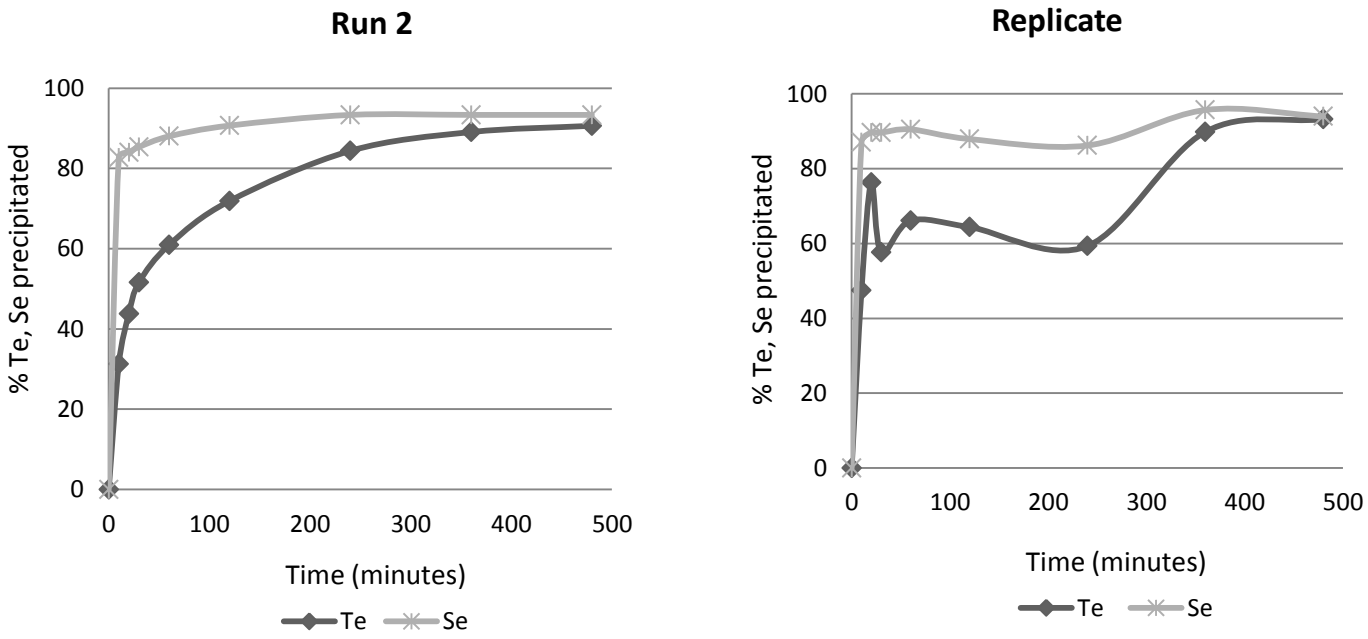

Figure 5.21: Comparing percentage Te and Se precipitation achieved for #2 of the 3rd experimental method with that of its replicate.

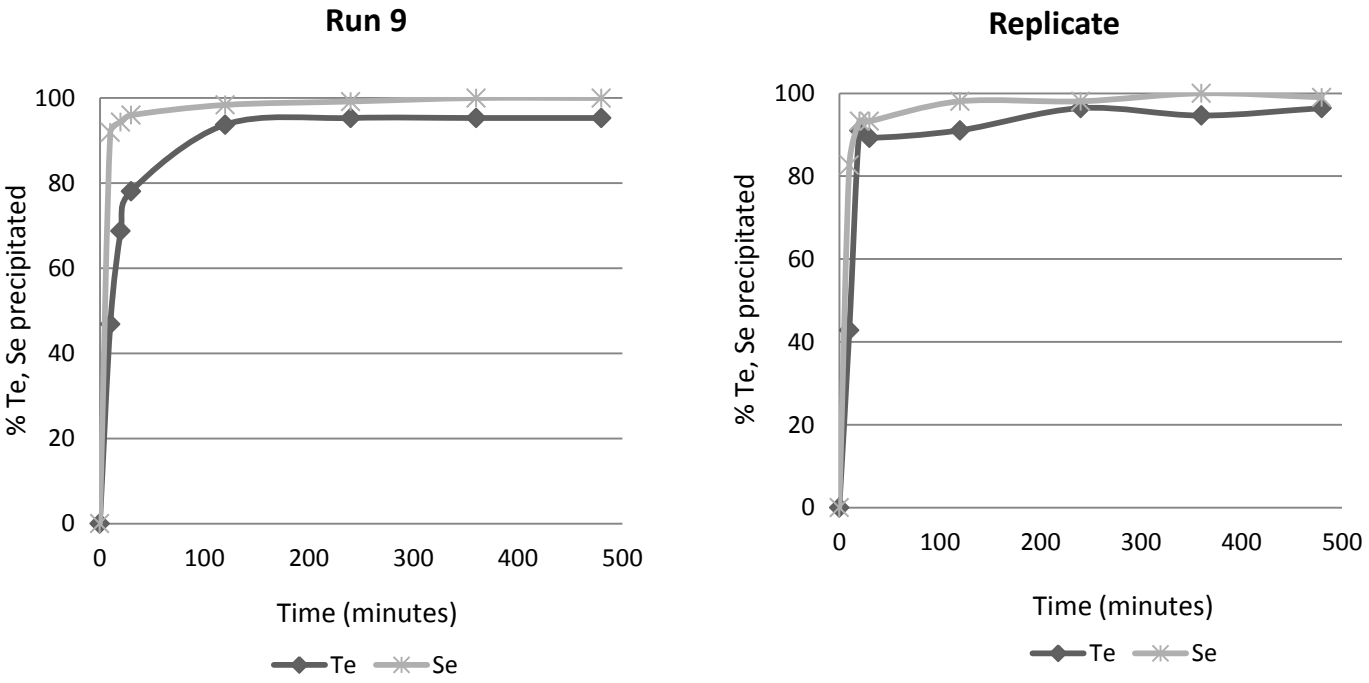

Figure 5.22: Comparing percentage Te and Se precipitation achieved for #9 of the 3rd experimental method with that of its replicate.

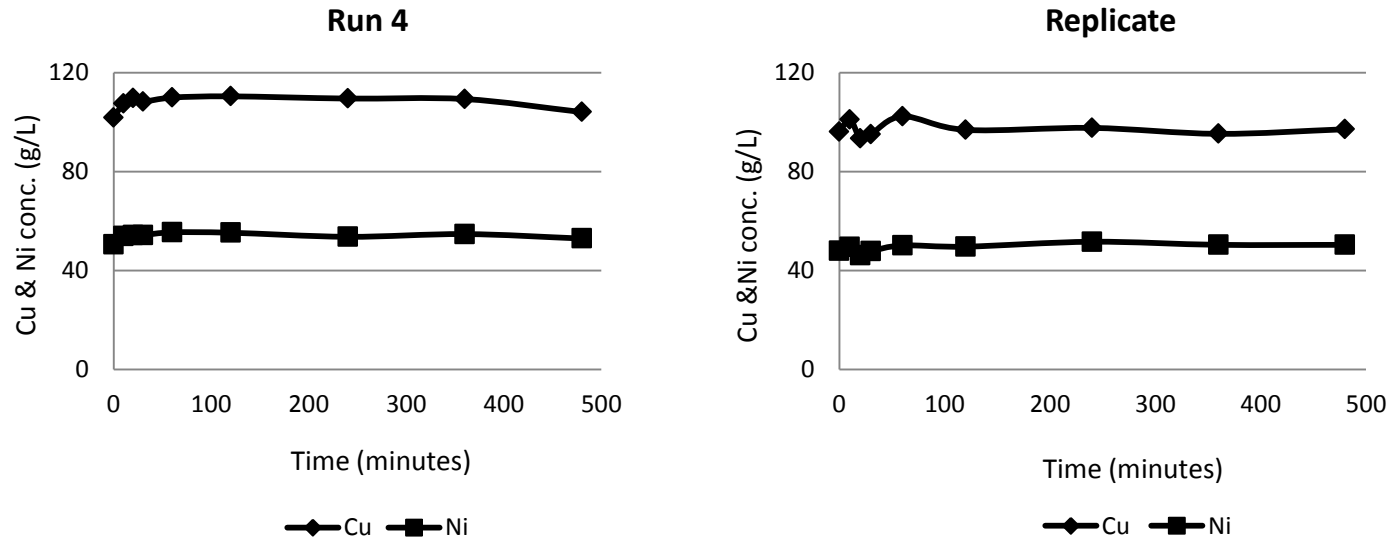

Figure 5.23: Comparing the base metals concentrations observed for #4 of the 1st experimental method with those of the replicate.

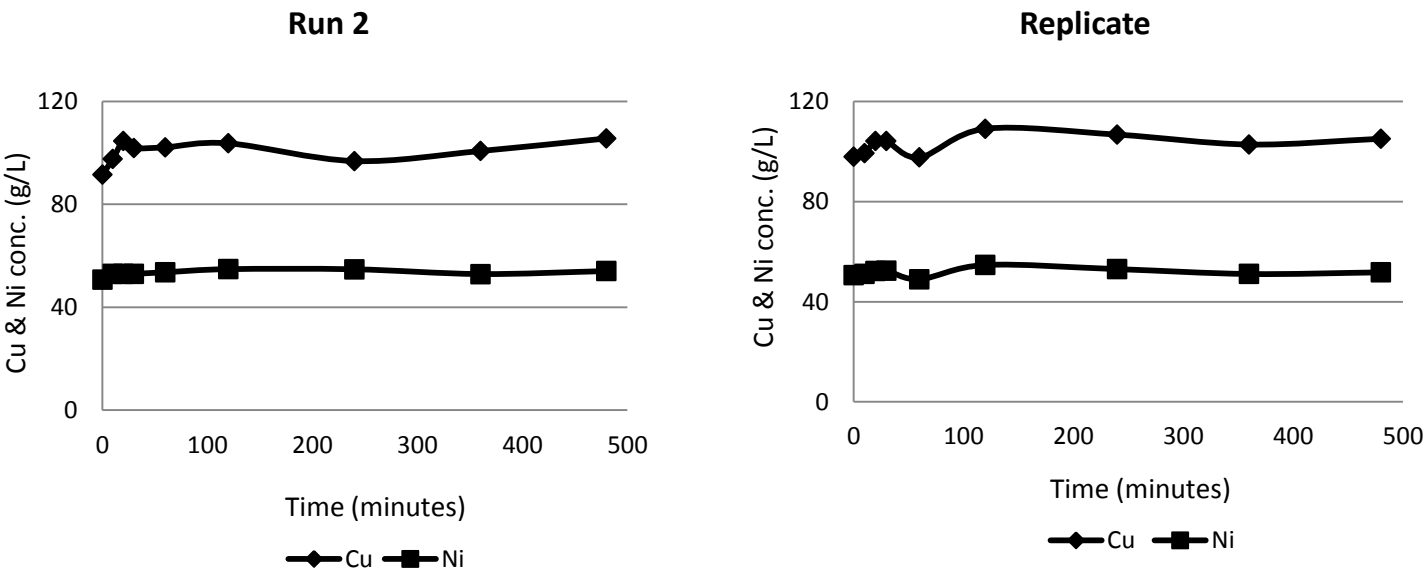

Figure 5.24: Comparing the base metals concentrations observed for #2 of the 3rd experimental method with those of the replicate.

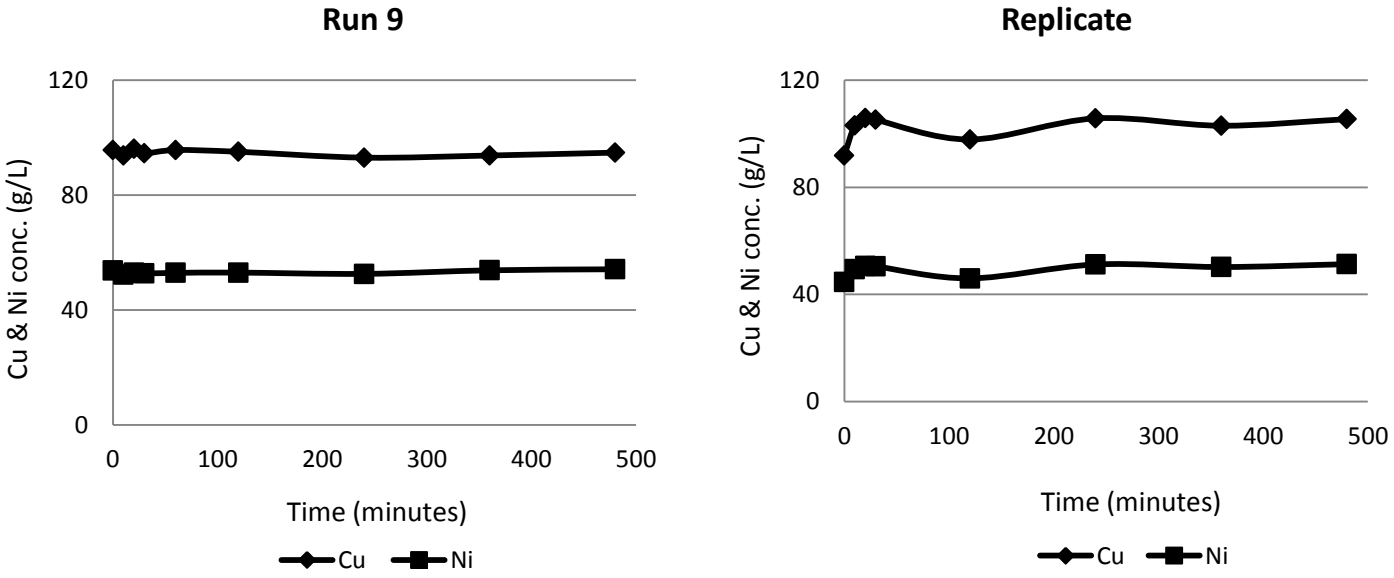

Figure 5.25: Comparing the base metals concentrations observed for #9 of the 3rd experimental method with those of the replicate.

Table 5.131: Evaluating percentage errors in measurements

Test(s)	x (%)	R1 (%)	|error|	% error (%)	y (%)	R2 (%)	|error|	% error(%)
T2	80.00	85.00	5.00	6.00	97.00	94.00	3.00	3.14
T4	91.00	93.00	2.00	2.17	93.33	96.00	2.70	1.42
T9	95.00	96.00	1.00	1.05	99.99	100.00	0.01	0.01

Where:

T2 represents the test performed at 65°C and 500 rpm agitation speed (5.8 cm^3/min SO_2 flow rate)

T4 represents the test performed at 65°C and 500 rpm agitation speed (4.4 cm^3/min SO_2 flow rate and 1 g/L copper powder addition)

T9 represents the test performed at 95°C and 250 rpm agitation speed (4.4 cm^3/min SO_2 flow rate and 1 g/L copper powder addition)

x represents the maximum Te precipitation achieved after the completion of the tests

R1 represents the maximum Te precipitation achieved for the replicates of the tests

y represents the maximum Se precipitation achieved after the completion of the tests

R2 represents the maximum Se precipitation achieved for the replicate of the tests

% error or difference = $|R1 - x|/(R1 + x)/2$ or $|R2-y|/(R2+y)/2$

Appendix H: Nomenclature

	Symbols	
Adj. R-squared	Adjusted R-squared	
ANOVA	Analysis of variation	
C	Final Te concentration in the solution used by (Shibasaki et al., 1992)	kg/m^3
Cf	Final Te concentration in the solution (used for this study) at a particular time	mg/L
Ci	Initial Te concentration in the solution (used for this study) at a particular time	mg/L
Co	Initial Te concentration in the solution used by (Shibasaki et al., 1992)	kg/m^3
C.V	Coefficient of variation	
d.f	Degree of freedom	
F	Gas flow rate	cm^3/min
H	Height of copper plate	mm
L	Length of copper plate	mm
m_{Fe}	Mass of iron in grams	g
Mw_{Fe}	Molecular weight or atomic mass of iron	g/mol
Mw_{Se}	Molecular weight of selenium	g/mol
m_{Se}	Mass of selenium species in the process solution	g
n_{Fe}	Amount of iron in the solution	mol
n_{SO2}	Amount of SO_2	mol
n_{Se}	Amount of selenium	mol
OPMs	Other Precious Metals	
PRESS	Prediction error sum of square	
Std Dev.	Standard deviation	
T	Time	min
V	Volume of SO_2 gas	cm^3
V_{soln}	Volume of process solution	L
W	Width of copper plate	mm
X_{Fe}	Iron concentration in process solution	g/L
X_{Se}	Selenium concentration in the process solution	g/L

Appendix I: Publications based on thesis

Refereed full length paper in the proceedings of an international conference

Bello, Y., and Dorfling, C., 2014. Tellurium precipitation from copper sulphate leach solutions. *Proceedings of The VI International Seminar on Process Hydrometallurgy – Hydroprocess 2014*, Vina del Mar, Chile, 23-25 July 2014

Presentations at national conferences

- Bello, Y., Dorfling, C., and Steenekamp, N., 2012. Tellurium precipitation from acidic copper sulphate leach solutions in the Se/Te removal section of a base metal refinery (BMR). *Mineral Processing 2012*, Western Cape Branch of SAIMM, Cape Town, South Africa, 5-6 August 2012 (poster presentation).
- Bello, Y., and Dorfling., C., 2013. Tellurium precipitation from copper sulphate leach solutions in the Se removal section of a base metal refinery. *Mineral Processing 2013*, Western Cape Branch of SAIMM, Cape Town, South Africa, 7 August 2013 (poster and short oral presentation). (Awarded Best Poster Prize)
- Bello, Y., and Dorfling., C., 2014. Tellurium precipitation from copper sulphate leach solutions in the Se/Te removal section of a base metal refinery. *Mineral Processing 2014*, Western Cape Branch of SAIMM, Cape Town, South Africa, 6 August 2014 (poster and short oral presentation). (Awarded Best Poster Prize)